

University of Alberta

Environmental Influences on Wood Structure and Water Transport in the
Model Tree *Populus*

by

Lenka Plavcová

A thesis submitted to the Faculty of Graduate Studies and Research
in partial fulfillment of the requirements for the degree of

Doctor of Philosophy
in
Forest Biology and Management

Department of Renewable Resources

©Lenka Plavcová
Fall 2012
Edmonton, Alberta

Permission is hereby granted to the University of Alberta Libraries to reproduce single copies of this thesis and to lend or sell such copies for private, scholarly or scientific research purposes only. Where the thesis is converted to, or otherwise made available in digital form, the University of Alberta will advise potential users of the thesis of these terms.

The author reserves all other publication and other rights in association with the copyright in the thesis and, except as herein before provided, neither the thesis nor any substantial portion thereof may be printed or otherwise reproduced in any material form whatsoever without the author's prior written permission.

To all beautiful trees

Abstract:

Variation in xylem structure and function has been extensively studied across different species with a wide taxonomic, geographical and ecological coverage. In contrast, our understanding of how xylem of a single species can adjust to different growing conditions remains limited. In this thesis, I studied phenotypic plasticity in xylem traits in hybrid poplar (*Populus trichocarpa* × *deltoides*). Clonally propagated saplings were grown under experimental drought, nitrogen fertilization and shade for >30 days. The hydraulic and anatomical traits of secondary xylem were subsequently examined. Substantial variation in the dimensions of xylem cells and wood density was observed. The changes in xylem structure were paralleled by differences in xylem hydraulic conductivity and vulnerability to drought-induced cavitation. In order to gain insights into the molecular underpinnings of different xylem phenotypes, I conducted a microarray analysis of gene expression in the developing xylem of plants receiving high versus low nitrogen (N) supply. I found 388 genes differentially expressed (fold change ± 1.5 , $P \leq 0.05$), including a number of genes putatively involved in nitrogen and carbohydrate metabolism and various aspects of xylem cell differentiation. The results of this study provide us with gene candidates potentially affecting xylem hydraulic and structural traits.

Furthermore, the results presented in this thesis enhance our knowledge of the mechanisms underlying xylem vulnerability to drought-induced cavitation. Using scanning and transmission electron microscopy, I studied the structure and chemical composition of pit membranes in saplings grown under shade and

control light conditions. I found that pit membranes in shade plants were thinner and showed an increased tendency for pore enlargement during membrane dehydration compared to control plants. This difference in pit membrane structure is consistent with greater xylem vulnerability in shade plants. I furthermore showed that pectic homogalacturonans are not abundant in the intervessel pit membranes of hybrid poplar. In a follow-up study, I corroborated this surprising result. Using immunolabeling and two specialized histological methods, I demonstrated that homogalacturonans and calcium are restricted only to a limited region around the edges of the membrane in four angiosperm species including poplar. This finding has important implications for our understanding of pit membranes.

Acknowledgement:

Foremost, I would like to express my great appreciation to my advisor, Dr. Uwe Hacke, for his invaluable guidance and support throughout the entire course of my PhD program. Uwe was always accessible and willing to help and share his knowledge with me. He kept me focused and taught me to use my time efficiently. Thanks to him, my journey to the Ph.D. has been smooth and rewarding.

My sincere gratitude goes to Prof. Vic Lieffers and Dr. Mike Deyholos, the members of my supervisory committee, for their kind support and valuable feedback on my work. I am very grateful to Prof. Carl Douglas, Dr. Eryang Li, Dr. Hua Bao (University of British Columbia, Vancouver) and Ms. Anne Haegert (Prostate Centre, Vancouver) for their guidance and assistance with the microarray analysis. I also thank to Prof. John Sperry (University of Utah, Salt Lake City) for his help with pit porosity modeling.

I am greatly indebted to Arlene Oatway, Dr. Ming H. Chen, George Braybrook, De-ann Rollings, and Randy Mandryk for their assistance with microscopy. Many of the nice images presented in my thesis would not have been possible without their help.

I would like to thank my colleagues in the lab, Adriana Almeida, Stefan Schreiber, and Joan Laur, for their help, encouragement and friendship. In particular, I would like to thank Adriana for her guidance throughout the molecular biology work and for having been a great companion. I am also very fortunate to have met Amanda Schoonmaker. Amanda was the first friend I made in Canada and it was her who helped me to get settled and start exploring this great country. She never said 'no' when I asked her for help or advice. My special thanks go to all my friends from the Triathlon club and the Fiera Race Club for helping me to stay relaxed, fit and healthy throughout the past four years.

Despite the geographical distance, I could constantly feel the support of my family. Thanks to my mom, my dad, my sisters and my grandparents for always being there for me. My heartiest thanks go to my husband Jan for his selfless love and support and for keeping me entertained and occasionally distracted from my research. I could not imagine having a better soulmate by my side.

Funding for the research presented in this thesis was provided by an Alberta Ingenuity New Faculty Award and an NSERC Discovery grant awarded to Dr. Hacke. I would also like to acknowledge financial support from the University of Alberta and the Czechoslovak Society of Arts and Sciences of Alberta.

Table of contents:

1. General Introduction.....	1
1.1 Water transport in trees – xylem structure and the cohesion-tension theory.....	1
1.2 The air-seeding mechanism of xylem cavitation and the role of pits.....	4
1.3 Vulnerability curves	6
1.4 Trade-offs in xylem structure and function.....	7
1.5 Interspecific vs. intraspecific variability in xylem traits	9
1.6 The scope of the thesis	10
1.7 Poplar as a model plant for my research	11
1.8 References	12
2. Phenotypic and developmental plasticity of xylem in hybrid poplar saplings subjected to experimental drought, nitrogen fertilization and shading.....	18
2.1 INTRODUCTION.....	18
2.2 METHODS.....	20
2.2.1 Plant material and experimental conditions	20
2.2.2 Sampling strategy.....	22
2.2.3 Xylem pressure	22
2.2.4 Growth measurements	22
2.2.5 Hydraulic measurements.....	23
2.2.6 Vessel diameter and wood density measurements.....	24
2.2.7 Statistical analyses	24
2.3 RESULTS.....	25
2.3.1 Plant growth.....	25
2.3.2 Leaf area, xylem area and stem hydraulic conductivity	26
2.3.3 Variation in stem morphology and xylem anatomy.....	26
2.3.4 Xylem-specific hydraulic conductivity.....	27
2.3.5 Xylem vulnerability to drought-induced cavitation	28
2.4 DISCUSSION	29
2.5 CONCLUSIONS.....	34
2.6 TABLES.....	35

2.7	FIGURES	38
2.8	REFERENCES.....	46
3.	Gene expression patterns underlying changes in xylem structure and function in response to increased nitrogen availability in hybrid poplar	51
3.1	INTRODUCTION.....	51
3.2	METHODS.....	53
3.2.1	Plant material	53
3.2.2	Xylem anatomy.....	54
3.2.3	Hydraulic measurements.....	55
3.2.4	Microarray analysis.....	55
3.2.5	Microarray qRT-PCR validation.....	56
3.3	RESULTS AND DISCUSSION	57
3.3.1	Nitrogen availability affects xylem structure and function in hybrid poplar	57
3.3.2	Nitrogen availability evokes transcriptional changes in developing xylem	58
3.4	CONCLUSIONS	66
3.5	TABLES	68
3.6	FIGURES	75
3.7	REFERENCES.....	80
4.	Linking irradiance-induced changes in pit membrane ultrastructure with xylem vulnerability to cavitation	87
4.1	INTRODUCTION.....	87
4.2	METHODS.....	90
4.2.1	Plant material and sampling strategy	90
4.2.2	Vulnerability to cavitation, xylem and leaf specific conductivity	90
4.2.3	Transmission electron microscopy (TEM) and immunolabeling of pectin epitopes	91
4.2.4	Scanning electron microscopy (SEM)	92
4.2.5	'Rare pit' model	93
4.2.6	Xylem anatomy.....	94
4.2.7	Wood density	95
4.2.8	Statistics	95

4.3	RESULTS.....	96
4.3.1	Plant growth.....	96
4.3.2	Xylem vulnerability and hydraulic conductivity	96
4.3.3	Pit membrane ultrastructure and immunolabeling.....	96
4.3.4	'Rare pit' model	97
4.3.5	Vessel and fiber anatomy.....	98
4.4	DISCUSSION	98
4.5	CONCLUSIONS.....	104
4.6	TABLES.....	105
4.7	FIGURES	108
4.8	REFERENCES.....	116

5. Heterogeneous distribution of pectin epitopes and calcium in different pit types of four angiosperm species..... 120

5.1	INTRODUCTION.....	120
5.2	METHODS.....	123
5.2.1	Plant material	123
5.2.2	Shifts in vulnerability to embolism.....	124
5.2.3	Scanning electron microscopy	124
5.2.4	Polysaccharide localization with transmission electron microcopy ..	125
5.2.5	Calcium localization	126
5.2.6	Statistical analysis.....	127
5.3	RESULTS.....	127
5.3.1	Shifts in xylem vulnerability to embolism.....	127
5.3.2	Scanning electron microcopy.....	128
5.3.3	Distribution of high and low methyl-esterified homogalacturonan ...	128
5.3.4	Calcium localization with TEM.....	130
5.3.5	Distribution of rhamnogalacturonan I and xyloglucan	130
5.4	DISCUSSION	131
5.5	CONCLUSIONS.....	135
5.6	TABLES.....	137
5.7	FIGURES	139
5.8	REFERENCES.....	147

6. General Discussion and Conclusions	153
6.1 The scope of the thesis	153
6.2 Variability in xylem traits in hybrid poplar saplings.....	154
6.3 Changes in gene expression underlying different xylem phenotypes ...	155
6.4 The role of intervessel pits in xylem vulnerability.....	156
6.4.1 Chemical properties of pit membranes	156
6.4.2 Structural properties of pits.....	159
6.5 Conclusion and outlook.....	161
6.6 References	162

List of Tables:

Table 2-1: Overview of the experimental design: the duration of experiments, the duration of treatments and a brief description of the treatment conditions for treated and control plants.	35
Table 2-2: Group means \pm standard error and t-test probability values for growth-related parameters of hybrid poplar saplings grown under drought, nitrogen fertilization, shade and control conditions.	36
Table 2-3: Analysis of variance results: variation in xylem structural and hydraulic parameters in response to treatments and between stem segment positions.	37
Table 3-1: List of qRT-PCR gene-specific primers.	68
Table 3-2: Growth characteristics of poplar saplings receiving 0.75 mM (low N) versus high 7.5 mM (high N) levels of ammonium nitrate.	69
Table 3-3: Xylem characteristics of poplar saplings receiving 0.75 mM (low N) versus 7.5 mM (high N) levels of ammonium nitrate.	70
Table 3-4: Genes differentially expressed (fold change ± 1.5 , P value ≤ 0.05) in developing xylem of hybrid poplar growing under high N versus low N availability.	71-74
Table 4.1: Growth characteristics of poplar saplings grown under shade and control light conditions.	105
Table 4-2: Fitted Weibull constants of empirical pit distributions and mean cavitation pressure from the ‘rare pit’ model for different pit pore diameter data.	106
Table 4-3: Properties of xylem cells and wood density of poplar saplings grown under shade or control light conditions.	107
Table 5-1: The intensity and localization of immunogold labeling for polysaccharide specific antibodies JIM5, JIM7, LM6 and LM15.	137
Table 5-2: Pit membrane diameter, annulus length and intensity of homogalacturonan labeling in the annulus in <i>Betula papyrifera</i> , <i>Populus balsamifera</i> , <i>Prunus virginiana</i> and <i>Amelanchier alnifolia</i>	138

List of Figures:

Figure 2-1: Relationship between supported leaf area and a stem’s capacity to transport water measured as xylem cross-sectional area and native hydraulic conductivity in hybrid poplar saplings grown under drought, nitrogen fertilization, shade, and control conditions.....38

Figure 2-2: Variation in xylem structure: xylem cross-sectional area, mean vessel diameter and wood density of basal and distal stem segments in hybrid poplar saplings grown under drought, nitrogen fertilization, shade, and control conditions.....39

Figure 2-3: Representative cross-sections of basal and distal stem segments from control plants.....40

Figure 2-4: Variation in xylem hydraulic function: xylem-specific hydraulic conductivity and the pressure at 50% loss of conductivity for basal and distal stem segments in hybrid poplar saplings grown under drought, nitrogen fertilization, shade, and control conditions.....41

Figure 2-5: Relationship between mean vessel diameter and xylem-specific hydraulic conductivity for basal and distal stem segments in hybrid poplar saplings grown under drought, nitrogen fertilization, shade, and control conditions.....42

Figure 2-6: Vulnerability curves and native values of percent loss of conductivity plotted against the native xylem pressure for basal and distal stem segments in saplings grown under drought and well-watered conditions, and under high and low nitrogen fertilization.....43

Figure 2-7: Relationships between the pressure at 50% loss of conductivity and wood density, xylem-specific hydraulic conductivity and mean vessel diameter for basal and distal stem segments in hybrid poplar saplings grown under drought, nitrogen fertilization, shade, and control conditions.....44

Figure 2-8: Cross-section of a distal stem segment perfused with safranin dye to visualize functional and embolised xylem conduits.45

Figure 3-1: Cross-sections of stem xylem from low N and high N plants.75

Figure 3-2: Frequency histograms of vessel and fiber lumen diameters for low N and high N plants.76

Figure 3-3: Frequency histograms of vessel element length, vessel length, and fiber length for low N and high N plants.77

Figure 3-4: Xylem-specific conductivity and the pressure at 50% loss of conductivity of stem segments from low N and high N plants.....	78
Figure 3-5: qRT-PCR validation of microarray results for nine selected genes...	79
Figure 4-1: Mean cavitation pressure, xylem-specific and leaf-specific conductivity of stem segments in poplar saplings grown under shade or control light conditions.....	108
Figure 4-2: Pit membrane and compound middle lamella thickness in plants grown in shade and control light conditions.	109
Figure 4-3: Immunogold localization of homogalacturonans in mature xylem with the monoclonal antibody JIM7 with transmission electron microscopy.	110
Figure 4-4: Scanning electron micrographs of exposed pit membranes.....	111
Figure 4-5: Scanning electron microscopy based measurements of pit membrane porosity: maximal pore diameter, average diameter of the 10% largest pores, and mean pore diameter measured per pit in water-dried or ethanol-dried SEM samples.....	112
Figure 4-6: Fitted cumulative frequency distribution for the air-seeding pressure of individual pits and pitted end-walls as calculated from the ‘rare pit’ model for ethanol-dried and water-dried samples. Closed and open circles show vulnerability curves from plants grown in shade and control light conditions, respectively.	113
Figure 4-7: Mean hydraulic vessel diameter, mean vessel length and mean vessel element length in shaded and control plants.	114
Figure 4-8: Secondary cell wall thickness in vessels measured from transmission electron micrographs and double vessel wall thickness measured with light microscopy.....	115
Figure 5-1: The effect of calcium removal on xylem vulnerability to embolism: vulnerability curves of <i>Betula papyrifera</i> , <i>Populus balsamifera</i> , <i>Prunus virginiana</i> and <i>Amelanchier alnifolia</i> in stems perfused with sodium phosphate solution at pH 10 or pH 4.	139
Figure 5-2: Relationship between vulnerability to cavitation and the magnitude of vulnerability shift (ΔP_{50}) in <i>Betula papyrifera</i> , <i>Populus balsamifera</i> , <i>Prunus virginiana</i> and <i>Amelanchier alnifolia</i>	140

Figure 5-3: Scanning electron micrographs of vessel-ray pits in stems of <i>Populus balsamifera</i> perfused with sodium phosphate solution at pH 4 and pH 10.	141
Figure 5-4: Transmission electron micrographs of the pit membrane annulus region showing the distribution of homogalacturonan and calcium precipitate as revealed by immunogold labeling and an antimonate precipitation technique, respectively.	142
Figure 5-5: Corresponding patterns of JIM5 immunolabeling and calcium localization in pseudotori and vessel-ray pits of <i>Amelanchier alnifolia</i> as observed with transmission electron microscopy.....	143
Figure 5-6: Ruthenium red staining of acidic pectin in the xylem of <i>Betula papyrifera</i> , <i>Populus balsamifera</i> and <i>Prunus virginiana</i>	145
Figure 5-7: Immunogold labeling of cell walls with anti-RG-I antibody LM6 and anti-xyloglucan antibody LM15.	146

List of Symbols and Abbreviations:

A_i	area of individual pit membranes
AIC	Akaike information criterion
A_L	leaf area
ANOVA	analysis of variance
A_p	total pit membrane area per vessel
A_X	stem cross-sectional area
cml	compound middle lamella
D_h	hydraulic vessel diameter
D_{max}	the diameter of the largest pore within a pit membrane
D_{mean}	mean diameter of all pores measured in a pit membrane
DNA	deoxyribonucleic acid
DR	drought treatment
DRC	control to the drought treatment, i.e., well-watered conditions
D_{stem}	stem diameter at 10 cm above the root collar
D_v	mean vessel diameter
d_w	wood density
DW _L	leaf dry weight
F	fertilization with 7.5 mM NH ₄ NO ₃ , i.e., high N treatment
FC	fertilization with 0.75 mM NH ₄ NO ₃ , i.e., low N treatment
$F_e(p)$	cumulative frequency distribution for the air-seeding pressure of pitted end-walls

$F_m(p)$	cumulative frequency distribution for the air-seeding pressure of individual pits
GalA	galacturonic acid
HG	homogalacturonans
K_{flush}	stem hydraulic conductivity after flushing
K_h	stem hydraulic conductivity
K_L	leaf-specific hydraulic conductivity
K_{max}	maximal hydraulic conductivity
K_{native}	native hydraulic conductivity
K_S	xylem-specific hydraulic conductivity
LWA	leaf weight to leaf area ratio
MCP	mean cavitation pressure
N	nitrogen
N-P-K	nitrogen-phosphorus-potassium
ns	non-significant
P	probability
P50	the pressure at 50% loss of hydraulic conductivity
PhAR	photosynthetic active radiation
PLC	percent loss of conductivity
pos	stem segment position
qRT-PCR	quantitative real-time polymerase chain reaction
RG-I	rhamnogalacturonan I
RIN	RNA integrity number

RNA	ribonucleic acid
<i>SD</i>	standard deviation
<i>SE</i>	standard error
SEM	scanning electron microscopy
SH	shade treatment ($70 \mu\text{mol m}^{-2} \text{s}^{-1}$ PhAR)
SHC	control to shade treatment ($350 \mu\text{mol m}^{-2} \text{s}^{-1}$ PhAR)
<i>T</i>	surface tension
TEM	transmission electron microscopy
t_{exp}	duration of experiment
t_{h}	double vessel wall thickness
<i>treat</i>	experimental treatment
t_{treat}	duration of treatment
α	contact angel
ΔP_{crit}	air-seeding inducing pressure difference
η	dynamic viscosity

1. General Introduction

In this thesis, I examine long-distance water transport in the ecologically and economically important genus *Populus*. I focus on variability in xylem anatomy and hydraulic function in response to growing conditions and I aim at better understanding the mechanism of drought-induced xylem dysfunction. Members of the genus *Populus*, commonly referred to as poplars, play a prominent role in the boreal forest and prairie parkland regions of Canada and in similar biomes across the Northern Hemisphere (Cooke & Rood, 2007). Poplars also provide a valuable source of wood, fiber and biomass for forest and bio-energy industries (Sannigrahi, Ragauskas & Tuskan, 2010, Balatinecz, Kretschmann & Leclercq, 2001).

The fast growth and high productivity of poplars depend on an ample water supply. In the last decade, large-scale drought-related mortality events occurred in stands of *Populus* across western North America (Hogg, Brandt & Michaelian, 2008, Michaelian, Hogg, Hall *et al.*, 2011, Rood, Mahoney, Reid *et al.*, 1995, Worrall, Egeland, Eager *et al.*, 2008), representing a significant concern for both forest conservation and the forest products industry. It has been shown that xylem dysfunction plays a prominent role during the decline of *Populus* stands (Anderegg, Berry, Smith *et al.*, 2012, Tyree, Kolb, Rood *et al.*, 1994). Therefore, a better understanding of how the hydraulic network operates and how it can adjust to changing environmental conditions, especially in terms of its resistance to drought, is highly desirable. In addition, studying variability in hydraulic function in a single genotype of poplar can conveniently complement previous studies at the interspecific level and enhance our understanding of long-distance transport in plants.

Before outlining the specific objectives of my research, I will start with providing background information on the basic principles of water ascent in trees and then elaborate in greater detail on the mechanism of xylem cavitation and its functional and ecological significance.

1.1 Water transport in trees – xylem structure and the cohesion-tension theory

The physiological mechanisms of water transport in plants are remarkable. Water can be extracted from the soil and lifted up to the leaves of a 100 m tall tree passively, along a gradient of decreasing water potential. From this point of view, plant water transport substantially differs from other transport systems known

from living organisms such as phloem transport in plants or circulation of blood in animals. These two processes depend on active ‘pumping’ mechanisms, requiring a constant supply of direct metabolic energy. The key to water transport in plants is that it couples the simple physical process of evaporation with an ingenious anatomical design of xylem conduits (Tyree & Zimmermann, 2002).

In order to effectively move water across large distances, a specialized low-resistance hydraulic system has evolved in vascular plants – the xylem. The xylem can be envisioned as an efficient, highly integrated network of pipelines. Xylem conduits consist of axially elongated cells that are at functional maturity dead and void of cellular content. In trees, shrubs, and even some herbs, a substantial volume of secondary xylem (i.e., wood) is produced by the activity of the vascular cambium (Evert, 2006). Besides its role in water conduction, wood performs other important functions in plants, such as the mechanical support of the plant body and storage of water, carbohydrates, nitrogen compounds and special defense metabolites.

Poplar exhibits a wood structure characteristic for many angiosperm species. The principal water-conducting cells in poplar are vessel elements that are embedded in a matrix of fibers and living parenchyma. Individual vessel elements are joined end-to-end. The end-walls between the vessel elements are completely hydrolyzed, thereby forming a long multicellular vessel. Vessels are further interconnected in a complex three-dimensional network via intervessel pitting. Intervessel pits are fascinating microstructures of paramount functional significance (Choat, Cobb & Jansen, 2008). The basic structure of pits involves two components – the pit membrane and the pit border. The pit membrane is a more or less porous and permeable interface between adjacent conduits and is derived from the compound middle lamella. The pit membrane is positioned in the center of a pit chamber; the chamber is created by an overarching secondary wall (pit border). The border is incomplete, leaving an aperture on both sides of the pit chamber (Evert, 2006). Poplars have homogenous pit membranes, i.e., the membrane is uniformly thick and microporous (as opposed to torus-margo pits which are characteristic for conifer wood).

The transport efficiency of xylem scales with the sum of conduit diameters (D) to the fourth power following the Hagen-Poiseuille equation:

$$K_h = \frac{\pi}{128\eta} \sum_{i=1}^n D_i^4$$

Eqn. 1-1

where K_h is the xylem hydraulic conductivity of a bundle of pipes of different diameters, η is the temperature-dependant dynamic viscosity of xylem sap and n is the number of conduits transporting water in parallel. The actual measured values of xylem hydraulic conductivity vary between 20% to 100% of the theoretical conductivity (Tyree & Ewers, 1991) because of additional resistances, such as those imposed by perforation plates and pitted end-walls. In poplars which have simple perforation plates, relatively long vessels and highly porous pit membranes, I found that the measured hydraulic conductivity represents 60-70% of the theoretical value (unpublished results).

Having described the basic structure of xylem, I will elaborate on the mechanism driving water uptake and transport in plants. The basic principles of sap ascent in plants are summarized by the cohesion-tension (C-T) theory. The C-T theory was formulated at the end of 19th century by Dixon and Joly (1894) and corroborated later by van den Honert (1948), Martin Zimmerman (1983) and others (Angeles, Bond, Boyer *et al.*, 2004, Sperry & Tyree, 1988, Tyree & Zimmermann, 2002). According to this well supported theory, evaporation from nanometer-scale cell wall pores in the leaf mesophyll generates capillary suction which is transmitted throughout continuous water columns in the xylem. This pulling force is ultimately transmitted to water in the soil. An important implication of the C-T theory is that the xylem sap is under negative (i.e., less than atmospheric) pressure (Tyree & Zimmermann, 2002). Under typical conditions, the xylem pressure of many well watered transpiring plants is around -1 MPa (Nobel, 1991). However, plants in drier regions experience more negative xylem pressures. Extremely negative xylem pressures below -10 MPa have been measured in some drought adapted species (Jacobsen, Esler, Pratt *et al.*, 2009).

The metastable state of water under tension raises an important challenge. Once the cohesive forces between the molecules are disrupted, an abrupt phase change from liquid to vapour occurs. This process is known as cavitation. The ultimate result of xylem cavitation is an air-filled (i.e., embolised) conduit that is permanently or temporarily blocked for water transport. Thus, xylem cavitation

represents a serious threat for plant performance (Fichot, Chamaillard, Depardieu *et al.*, 2011, Sperry, 2000) and in some cases even survival (Anderegg *et al.*, 2012, McDowell, Pockman, Allen *et al.*, 2008, Rood, Patino, Coombs *et al.*, 2000). Two common causes of xylem cavitation are freeze-thaw cycles of xylem sap and drought stress (Tyree & Sperry, 1989). In this thesis, I focus on drought-induced cavitation.

1.2 The air-seeding mechanism of xylem cavitation and the role of pits

Drought-induced xylem cavitation occurs when air is drawn into a water filled vessel as a result of increasingly negative xylem pressure. When soil desiccates, its water potential and hydraulic conductivity decline. In order to keep extracting water that is now more tightly bound to the soil particles (Sperry, Hacke, Oren *et al.*, 2002), the xylem pressure of a plant must drop below the soil water potential. As the xylem pressure becomes more negative, air can aspirate into a functional conduit from an adjacent air-filled conduit. The critical pressure difference between xylem sap and atmospheric pressure required to induce cavitation (ΔP_{crit}) is inversely proportional to the largest pore present in the conduit wall (D_p), following the equation

$$\Delta P_{crit} = \frac{4T \cos \alpha}{D_p}$$

Eqn.1-2

where T is the surface tension of xylem sap and α is the contact angle between sap and pore wall material, which is usually assumed to be zero (i.e., total wetting) for a hydrophilic cell wall.

Being the most porous part of the conduit wall, interconduit pits are the most likely sites for air-seeding to occur (Sperry & Tyree, 1988, Zimmermann, 1983). While the factors that influence pit permeability to air are not completely understood, a growing body of evidence suggests that it is a combination of the quantitative and qualitative parameters of pit membranes that determines the cavitation threshold.

Pit membranes are composed of modified primary cell walls and consist of an intricate meshwork of cellulose microfibrils embedded in an amorphous material that is often apparent at the membrane surface under a scanning electron microscope (SEM). The pit membranes of at least some species including poplar display resolvable pores (Jansen, Choat & Pletsers, 2009). However, it is not clear

if such conspicuous pores are present in vivo or if they are artifacts resulting from pit membrane dehydration during sample preparation (Jansen, Pletsers & Sano, 2008).

It has been suggested that cell wall matrix polysaccharides such as pectins fill in the space between the cellulose microfibrils, giving the native membranes a relatively non-porous appearance and properties of a hydrated gel (Nardini, Salleo & Jansen, 2011, Pesacreta, Groom & Rials, 2005, Zwieniecki, Melcher & Holbrook, 2001). Nevertheless, even such a gel is, to a certain degree, permeable to air. It is therefore likely that air will get into the vessel through spaces between the cellulose microfibrils, regardless of the existence of true physical pores or the presence of a gel-like matrix filling these pores. An additional question is how the pressure difference exerted on the pit membranes separating an air- and a water-filled vessel affects the pit membrane permeability to air. The mechanical properties of pit membranes may be critical for the air-seeding threshold because pores may enlarge and gel strength may weaken as the membrane stretches and deflects (Cochard, Herbette, Hernandez *et al.*, 2010).

An important tenet of the air-seeding hypothesis is that the cavitation threshold of a vessel is determined by the largest pore at the air-water interface. Thus, while many thousands of pit membranes are present in the wall of an average vessel, the vessel's cavitation threshold is determined by a single pit, the one containing the largest pore. Experimental data suggest that pores allowing air-seeding at physiological xylem pressures are rare (Choat, Ball, Luly *et al.*, 2003, Christman, Sperry & Adler, 2009, Jarbeau, Ewers & Davis, 1995). More specifically, the frequency of pits allowing air-seeding at a pressure close to the species-specific P_{50} has been predicted to be 0.01% in *Acer* and 7% in *Quercus* (Christman *et al.*, 2009, Christman, Sperry & Smith, 2012).

Based on substantial experimental evidence, it has been argued that a larger total area of intervessel pit membranes (or a higher number of pits) renders xylem more vulnerable to drought-induced cavitation, possibly because there is a higher probability for rare leaky pits to occur (Hargrave, Kolb, Ewers *et al.*, 1994, Wheeler, Sperry, Hacke *et al.*, 2005). This concept is known as the 'pit-area' or 'rare pit' hypothesis. Following the recommendation of Christman *et al.* (2009), I will hereafter use the term 'rare pit' hypothesis.

However, it is becoming increasingly obvious that the differences in pit area alone cannot fully explain the differences in xylem vulnerability observed

across species. Recent work using scanning and transmission electron microscopy has revealed that pit structural traits such as pit membrane thickness, porosity, and texture vary greatly across different angiosperm species (Jansen *et al.*, 2009, Lens, Sperry, Christman *et al.*, 2011, Schmitz, Jansen, Verheyden *et al.*, 2007). Such differences in pit properties can affect the likelihood of air-seeding independently from the total area of pit membranes. Therefore, the rare pit hypothesis needs to be coupled with detailed knowledge of pit membrane structure and chemistry in order to gain a better understanding of factors driving xylem vulnerability.

Studies linking differences in pit structure with cavitation resistance in angiosperms are rare but intriguing (Choat, Jansen, Zwieniecki *et al.*, 2004, Jansen *et al.*, 2009, Jarbeau *et al.*, 1995). In a survey of 26 hardwood species of wide taxonomic and geographical origin, more than a 25-fold variation in pit membrane thickness and porosity has been observed (Jansen *et al.*, 2009). Both pit thickness and porosity were correlated with a vessel air-seeding pressure. A highly vulnerable cottonwood *Populus fermentii* was included in this study and indeed showed very thin and extremely porous pit membranes. However, much remains to be learned about intervessel pits and their role in protecting xylem against cavitation. In particular, poor knowledge of their chemical composition impedes our understanding of pit functioning.

1.3 Vulnerability curves

Xylem vulnerability to drought-induced cavitation of stem and root segments can be assessed using vulnerability curves (Alder Pockman, Sperry *et al.*, 1997, Tyree & Sperry, 1989). Vulnerability curves show a decreasing xylem hydraulic conductivity as a function of increasingly negative xylem pressure. Xylem hydraulic conductivity is often expressed as a relative number representing percent loss of conductivity (PLC) due to cavitation. PLC-based vulnerability curves often have a sigmoidal shape, especially in conifer xylem which is made up of relatively homogeneous conduits (Hacke, Sperry, Ewers *et al.*, 2000). Curves that show a steep initial increase in PLC, and hence have an r-shape, are sometimes observed, especially in roots (Hacke *et al.*, 2000) and ring-porous species (Christman *et al.*, 2012, Hacke, Sperry, Wheeler *et al.*, 2006, Jacobsen & Pratt, 2012). The xylem pressure at which 50% of the maximal hydraulic conductivity is lost, referred to as P_{50} , can be derived from the vulnerability curves and is commonly used as a measure of xylem vulnerability to cavitation (e.g., Meinzer, Johnson, Lachenbruch *et al.*, 2009, Pockman & Sperry 2000).

Other coefficients, such as the air entry point (P_e) or the full embolism point (P_{max}), can be also obtained from the vulnerability curves and used to characterize the cavitation resistance of xylem (Domec & Gartner, 2001).

1.4 Trade-offs in xylem structure and function

In the last three decades, researchers have generated vulnerability curves for several hundred plant species growing in various types of environment. These measurements have revealed that plant species differ greatly in the magnitude of negative xylem pressure they can withstand before substantial cavitation occurs (Maherali, Pockman & Jackson, 2004). In general, species-specific P_{50} values tend to be more negative than the xylem pressures that typically develop (Meinzer *et al.*, 2009, Pockman & Sperry, 2000) indicating that a tree's hydraulic system is well adapted to prevent extensive 'run-away' cavitation in their natural habitat. A California chaparral shrub, *Ceanothus crassifolius*, with its P_{50} of -9 MPa, is one of the most resistant plants measured (Sperry, 2011). In contrast, poplars, and riparian cottonwoods in particular, are some of the most vulnerable species of woody angiosperms. Cottonwoods typically exhibit P_{50} close to -1.5 MPa (Hacke & Sauter, 1996, Pockman & Sperry, 2000, Tyree *et al.*, 1994), while aspen tends to be more resistant with P_{50} varying between -2 and -2.5 MPa (Schreiber, Hacke, Hamann *et al.*, 2011, Sperry, Perry & Sullivan, 1991).

While a number of strategies to cope with water shortage have evolved in plants, cavitation resistance is arguably a trait of paramount significance for drought tolerance in long lived woody plants (Maherali *et al.*, 2004, Sperry, 2003). In order to maintain sufficient water supply to the leaves, trees have to prevent excessive cavitation in their xylem. Even though stomatal closure (Brodribb, Holbrook, Edwards *et al.*, 2003), hydraulic redistribution (Nadezhdina, Steppe, De Pauw *et al.*, 2009) and the water storage capacitance of plant tissues (Meinzer *et al.*, 2009) can to a certain degree prevent catastrophic hydraulic failure, xylem pressures more negative than the cavitation threshold cannot be completely avoided. Thus, it would seem advantageous if all trees had xylem that can withstand highly negative pressures (e.g., -10 MPa) before cavitation occurs. In reality, however, cavitation resistance correlates well with the aridity of environment (Maherali *et al.*, 2004).

The fact that xylem is not overly resistant in environments with a plentiful water supply suggests that cavitation resistance comes at a certain cost. Significant carbon expenditures, which could be otherwise allocated towards

growth and reproduction, seem to be associated with high cavitation resistance. Conduits need strong mechanical support to prevent implosion under highly negative xylem pressure (Hacke, Sperry, Pockman *et al.*, 2001, Jacobsen, Ewers, Pratt *et al.*, 2005). More negative P_{50} values are indeed associated with greater conduit reinforcement and higher wood density (Hacke *et al.*, 2001, McCulloh, Johnson, Meinzer *et al.*, 2012, Pittermann, Sperry, Wheeler *et al.*, 2006). The strong correlation between wood density and xylem resistance to cavitation in angiosperms is rather surprising considering that wood density in angiosperms is mainly driven by fiber properties which are not directly involved in water conduction (Hacke *et al.*, 2001).

Previous studies showed that there is a trade-off between safety against drought-induced cavitation and efficiency of water transport (Hacke, Jacobsen & Pratt, 2009, Hacke *et al.*, 2006). The safety versus efficiency trade-off becomes apparent when comparing species that display contrasting water use strategies. For instance, many desert shrubs have xylem that is highly resistant to cavitation but also shows very low xylem-specific conductivity (Pockman & Sperry, 2000). The opposite situation (i.e., highly efficient but extremely vulnerable xylem) is typical for species adapted to moist, nutrition-rich environments. It has been proposed that the safety versus efficiency trade-off is a corollary of the rare pit hypothesis, because wide and long vessels, which are necessary to achieve high transport efficiency, have a large total pit membrane area (Hargrave *et al.*, 1994, Wheeler *et al.*, 2005). In support of this hypothesis, it has been observed that wider vessels embolize before the narrower ones within a single stem (Cai & Tyree, 2010, Hargrave *et al.*, 1994, LoGullo, Salleo, Piaceri *et al.*, 1995). The trade-off between safety and efficiency can be further enhanced at the level of pit structure as thin and porous pit membranes will provide low resistance to water flow but will be more prone to air-seeding (Wheeler *et al.*, 2005).

Taken together, xylem resistance to drought-induced cavitation is associated with high construction costs and reduction in transport efficiency. These trade-offs are apparent when a comprehensive dataset encompassing a high number of diverse species is examined. However, there is also considerable scatter around the global trends, reflecting the specificities of a particular xylem anatomy. Consequently, the trade-offs can appear weak or ambiguous when evaluated using a limited selection of species (Choat, Sack & Holbrook, 2007, Pratt, Jacobsen, Ewers *et al.*, 2007).

1.5 Interspecific vs. intraspecific variability in xylem traits

Most of the structure-function relationships in xylem, including the two above mentioned trade-offs, have been obtained from comparisons conducted across different species. These studies have taken advantage of the vast diversity of xylem structure and function that reflects the various ecological strategies and evolutionary histories of woody plants. The results from these surveys are valuable as they highlight the effective combinations of traits that passed through the sieve of natural selection over the course of evolution. However, xylem hydraulic and anatomical parameters vary to a certain extent even within a single species (Fichot *et al.*, 2011, Holste, Jerke & Matzner, 2006, Martinez-Vilalta, Cochard, Mencuccini *et al.*, 2009). Intraspecific variability in xylem traits has not been extensively studied, although there are several reasons why it is important to document and understand this type of variation.

Intraspecific variability of functional traits is closely coupled with a species' ability to cope with variable environments (Violle, Enquist, McGill *et al.*, 2012). In the next couple of decades, the Earth's climate will likely continue to change (IPCC, 2007). More frequent and more severe drought events are expected to occur in many parts of the world (IPCC, 2007, IPCC, 2012). Hence, hydraulic acclimation that involves adjustment in xylem properties might be critical to maintain stand productivity and prevent forest dieback under reduced moisture availability. While changes in stomatal aperture (Brodribb *et al.*, 2003) and root hydraulic conductance (Almeida-Rodriguez, Hacke & Laur, 2011) allow for dynamic adjustments of water flow through the plant, changes in xylem structure can become important over a longer period of time. Xylem transport efficiency and vulnerability to cavitation of a stem can be gradually changed by producing a new set of water-conducting cells. The developmental plasticity of xylem in response to environmental clues is exemplified by annual growth rings in trees. While traditional tree-ring variables such as ring width (e.g., Esper, Cook & Schweingruber, 2002) or the isotopic composition of xylem biomass (e.g., Kress, Saurer, Siegwolf *et al.*, 2010) have been used as powerful tools for reconstructing past climate, additional environmental information could be gained by conducting a finer-scale anatomical characterization of xylem cells (Fonti, von Arx, Garcia-Gonzalez *et al.*, 2010). However, a thorough understanding of developmental processes and detailed knowledge of how specific environmental clues influence xylogenesis is an essential prerequisite for the successful application of such techniques.

Studying variability in xylem traits observed at the intraspecific level might help to shed more light on the mechanisms driving the trade-offs in xylem structure and function that are apparent from interspecific comparisons. Testing for the presence of functional trade-offs within a single species, as opposed to a diverse array of species, is convenient because it eliminates the confounding effects arising from phylogenetic and ecological differences between diverse plant taxa. On the other hand, the narrower range of trait variation within a single species may make it challenging to detect clear patterns.

1.6 The scope of the thesis

In this thesis, I analyze phenotypic plasticity in xylem hydraulic and anatomical traits in hybrid poplar (*Populus trichocarpa* × *deltoides*, clone H11-11) (Chapter 2, Chapter 3, and Chapter 4). The same poplar genotype has previously been used in our laboratory (Hacke, Plavcová, Almeida-Rodriguez *et al.*, 2010) as well as in laboratories of other poplar researchers (Courtois-Moreau, Pesquet, Sjödin *et al.*, 2009, Pitre, Cooke & Mackay, 2007a) to study wood formation. This genotype exhibited substantial developmental plasticity in response to nitrogen availability (Hacke *et al.*, 2010, Pitre *et al.*, 2007a, Pitre, Pollet, Lafarguette *et al.*, 2007b,). In this thesis, I therefore examine the developmental plasticity of its xylem in response to nitrogen fertilization and two other environmental cues (drought, shading). I then use the observed variability in xylem traits to learn more about the air-seeding mechanism of drought-induced xylem cavitation. This interest in xylem cavitation led me to study pit membranes in greater detail (Chapter 4, Chapter 5). In the study on the chemical composition of pit membranes (Chapter 5), I use field-grown balsam poplar (*Populus balsamifera*) along with three other co-occurring hardwoods in order to confirm that the patterns observed in the young hybrid poplar saplings grown in a growth chamber are consistent with the situation occurring in mature individuals growing under field conditions.

The main objectives of my research were:

- a) to document the variability in xylem anatomy and hydraulic function in response to experimental drought, nitrogen fertilization and shading, and to discuss the potential functional significance of the observed changes under a given environmental constraint (Chapter 2, Chapter 3, Chapter 4)

- b) to study the molecular basis underlying different xylem phenotypes by analyzing changes in gene expression (Chapter 3)
- c) to gain a better understanding of the mechanisms underlying xylem vulnerability by analyzing relationships between vulnerability and other structural and functional xylem traits (Chapter 2) and by assessing the structural and chemical properties of pit membranes (Chapter 4, Chapter 5)

1.7 Poplar as a model plant for my research

Poplar represents a suitable model plant for studying wood structure and function and has been chosen for this research for several reasons. There are numerous practical benefits of using poplar to study xylem phenotypic plasticity. The natural ability of hybrid poplar to propagate vegetatively from rooted cuttings allowed me to generate genetically homogenous sets of plants for experiments, and thus to assess the true phenotypic plasticity of xylem traits (Chapter 2). In 2006, the genome of *Populus trichocarpa* was made publically available (Tuskan, DiFazio, Jansson *et al.*, 2006), greatly accelerating research on molecular aspects of wood formation. I took advantage of modern molecular tools to shed light on genes that are differentially expressed in xylem forming under contrasting environmental conditions in order to identify candidate genes that might underlie particular xylem traits (Chapter 3). In addition, poplar represents a suitable species for studying intervessel pits. Pit membranes in poplar are numerous, large in diameter and highly porous; and therefore, particularly convenient for electron microscopy observations (Chapter 4, Chapter 5).

Poplar was also chosen for this research because of its prominent role in the Canadian landscape and because of its significance for the Canadian forest products industry. An increased understanding of how poplar wood acclimates under different environmental conditions is valuable for future management and conservation of both natural and commercial poplar stands, especially in the light of climate change. In addition, better knowledge of wood anatomical properties is useful for the wood processing industry. For instance, fiber length governs the mechanical strength of pulp (Horn, 1978) and pits influence the penetration of liquids, preservatives and gases into wood (Comstock & Cote, 1968).

1.8 References

- Alder N.N., Pockman W.T., Sperry J.S. & Nuismer S. (1997) Use of centrifugal force in the study of xylem cavitation. *Journal of Experimental Botany*, **48**, 665-674.
- Almeida-Rodriguez A.M., Hacke U.G. & Laur J. (2011) Influence of evaporative demand on aquaporin expression and root hydraulics in hybrid poplar. *Plant, Cell & Environment*, **34**, 1318–1331.
- Anderegg W.R.L., Berry J.A., Smith D.D., Sperry J.S., Anderegg L.D.L. & Field C.B. (2012) The roles of hydraulic and carbon stress in a widespread climate-induced forest die-off. *Proceedings of the National Academy of Sciences of the United States of America*, **109**, 233-237.
- Angeles G., Bond B., Boyer J.S., Brodribb T., Brooks J.R., Burns M.J., Cavender-Bares J., Clearwater M., Cochard H., Comstock J., Davis S.D., Domec J.C., Donovan L., Ewers F., Gartner B., Hacke U., Hinckley T., Holbrook N.M., Jones H.G., Kavanagh K., Law B., Lopez-Portillo J., Lovisolo C., Martin T., Martinez-Vilalta J., Mayr S., Meinzer F.C., Melcher P., Mencuccini M., Mulkey S., Nardini A., Neufeld H.S., Passioura J., Pockman W.T., Pratt R.B., Rambal S., Richter H., Sack L., Salleo S., Schubert A., Schulte P., Sparks J.P., Sperry J., Teskey R. & Tyree M. (2004) The Cohesion-Tension theory. *New Phytologist*, **163**, 451-452.
- Balatinecz J.J., Kretschmann D.E. & Leclercq A. (2001) Achievements in the utilization of poplar wood - guideposts for the future. *Forestry Chronicle*, **77**, 265-269.
- Brodribb T.J., Holbrook N.M., Edwards E.J. & Gutierrez M.V. (2003) Relations between stomatal closure, leaf turgor and xylem vulnerability in eight tropical dry forest trees. *Plant Cell and Environment*, **26**, 443-450.
- Cai J. & Tyree M.T. (2010) The impact of vessel size on vulnerability curves: data and models for within-species variability in saplings of aspen, *Populus tremuloides* Michx. *Plant Cell and Environment*, **33**, 1059-1069.
- Choat B., Ball M., Luly J. & Holtum J. (2003) Pit membrane porosity and water stress-induced cavitation in four co-existing dry rainforest tree species. *Plant Physiology*, **131**, 41-48.
- Choat B., Cobb A.R. & Jansen S. (2008) Structure and function of bordered pits: new discoveries and impacts on whole-plant hydraulic function. *New Phytologist*, **177**, 608-625.
- Choat B., Jansen S., Zwieniecki M.A., Smets E. & Holbrook N.M. (2004) Changes in pit membrane porosity due to deflection and stretching: the role of vestured pits. *Journal of Experimental Botany*, **55**, 1569-1575.
- Choat B., Sack L. & Holbrook N.M. (2007) Diversity of hydraulic traits in nine *Cordia* species growing in tropical forests with contrasting precipitation. *New Phytologist*, **175**, 686-698.
- Christman M.A., Sperry J.S. & Adler F.R. (2009) Testing the 'rare pit' hypothesis for xylem cavitation resistance in three species of *Acer*. *New Phytologist*, **182**, 664-674.

- Christman M.A., Sperry J.S. & Smith D.D. (2012) Rare pits, large vessels and extreme vulnerability to cavitation in a ring-porous tree species. *New Phytologist*, **193**, 713-720.
- Cochard H., Herbette S., Hernandez E., Holtta T. & Mencuccini M. (2010) The effects of sap ionic composition on xylem vulnerability to cavitation. *Journal of Experimental Botany*, **61**, 275-285.
- Comstock G.L. & Cote W.A. (1968) Factors affecting permeability and pit aspiration in coniferous sapwood. *Wood Science and Technology*, **2**, 279-291.
- Cooke J.E.K. & Rood S.B. (2007) Trees of the people: the growing science of poplars in Canada and worldwide. *Canadian Journal of Botany*, **85**, 1103-1110.
- Dixon H.H. & Joly J. (1894) On the ascent of sap. *Philosophical Transactions of the Royal Society of London, Series B: Biological Sciences*, **186**, 563-576.
- Domec J.C. & Gartner B.L. (2001) Cavitation and water storage capacity in bole xylem segments of mature and young Douglas-fir trees. *Trees-Structure and Function*, **15**, 204-214.
- Esper J., Cook E.R. & Schweingruber F.H. (2002) Low-frequency signals in long tree-ring chronologies for reconstructing past temperature variability. *Science*, **295**, 2250-2253.
- Evert R.F. (2006) *Esau's plant anatomy: meristems, cells, and tissues of the plant body: their structure, function, and development*. (3rd ed.). John Wiley & Sons, Inc., New Jersey.
- Fichot R., Chamaillard S., Depardieu C., Le Thiec D., Cochard H., Barigah T.S. & Brignolas F. (2011) Hydraulic efficiency and coordination with xylem resistance to cavitation, leaf function, and growth performance among eight unrelated *Populus deltoides* x *Populus nigra* hybrids. *Journal of Experimental Botany*, **62**, 2093-2106.
- Fonti P., von Arx G., Garcia-Gonzalez I., Eilmann B., Sass-Klaassen U., Gaertner H. & Eckstein D. (2010) Studying global change through investigation of the plastic responses of xylem anatomy in tree rings. *New Phytologist*, **185**, 42-53.
- Hacke U. & Sauter J.J. (1996) Drought-induced xylem dysfunction in petioles, branches, and roots of *Populus balsamifera* L. and *Alnus glutinosa* (L.) Gaertn. *Plant Physiology*, **111**, 413-417.
- Hacke U.G., Jacobsen A.L. & Pratt R.B. (2009) Xylem function of arid-land shrubs from California, USA: an ecological and evolutionary analysis. *Plant Cell and Environment*, **32**, 1324-1333.
- Hacke U.G., Sperry J.S., Ewers B.E., Ellsworth D.S., Schäfer K.V.R. & Oren R. (2000) Influence of soil porosity on water use in *Pinus taeda*. *Oecologia*, **124**, 495-505.
- Hacke U.G., Sperry J.S., Pockman W.T., Davis S.D. & McCulloh K.A. (2001) Trends in wood density and structure are linked to prevention of xylem implosion by negative pressure. *Oecologia*, **126**, 457-461.
- Hacke U.G., Sperry J.S., Wheeler J.K. & Castro L. (2006) Scaling of angiosperm xylem structure with safety and efficiency. *Tree Physiology*, **26**, 689-701.

- Hargrave K.R., Kolb K.J., Ewers F.W. & Davis S.D. (1994) Conduit diameter and drought-induced embolism in *Salvia mellifera* Greene (Labiatae). *New Phytologist*, **126**, 695-705.
- Hogg E.H., Brandt J.P. & Michaellian M. (2008) Impacts of a regional drought on the productivity, dieback, and biomass of western Canadian aspen forests. *Canadian Journal of Forest Research*, **38**, 1373-1384.
- Holste E.K., Jerke M.J. & Matzner S.L. (2006) Long-term acclimatization of hydraulic properties, xylem conduit size, wall strength and cavitation resistance in *Phaseolus vulgaris* in response to different environmental effects. *Plant Cell and Environment*, **29**, 836-843.
- Horn R.A. (1978) *Morphology of pulp fiber from hardwoods and influence on paper strength*. USDA Forest Service. Research Paper FPL 312, Forest Products Laboratory, Madison, WI, USA.
- IPCC (2007) *Climate change 2007: synthesis report. Contribution of working groups I, II and III to the fourth assessment report of the Intergovernmental Panel on Climate Change* (eds. Core Writing Team, Pachauri, R.K and Reisinger, A.). IPCC, Geneva, Switzerland.
- IPCC (2012) *Managing the risks of extreme events and disasters to advance climate change adaptation. A special report of working groups I and II of the Intergovernmental Panel on Climate Change* (eds. Field, C.B., V. Barros, T.F. Stocker, D. Qin, D.J. Dokken, K.L. Ebi, M.D. Mastrandrea, K.J. Mach, G.-K. Plattner, S.K. Allen, M. Tignor, and P.M. Midgley). Cambridge University Press, Cambridge, UK, and New York, NY, USA.
- Jacobsen A.L., Esler K.J., Pratt R.B. & Ewers F.W. (2009) Water stress tolerance of shrubs in mediterranean-type climate regions: Convergence of fynbos and succulent karoo communities with California shrub communities. *American Journal of Botany*, **96**, 1445-1453.
- Jacobsen A.L., Ewers F.W., Pratt R.B., Paddock W.A. & Davis S.D. (2005) Do xylem fibers affect vessel cavitation resistance? *Plant Physiology*, **139**, 546-556.
- Jacobsen A.L. & Pratt R.B. (2012) No evidence for an open vessel effect in centrifuge-based vulnerability curves of a long-vesselled liana (*Vitis vinifera*). *New Phytologist*, **194**, 982-990.
- Jansen S., Choat B. & Pletsers A. (2009) Morphological variation of intervessel pit membranes and implications to xylem function in angiosperms. *American Journal of Botany*, **96**, 409-419.
- Jansen S., Pletsers A. & Sano Y. (2008) The effect of preparation techniques on SEM-imaging of pit membranes. *IAWA Journal*, **29**, 161-178.
- Jarbeau J.A., Ewers F.W. & Davis S.D. (1995) The mechanism of water-stress-induced embolism in two species of chaparral shrubs. *Plant Cell and Environment*, **18**, 189-196.
- Kress A., Saurer M., Siegwolf R.T.W., Frank D.C., Esper J. & Bugmann H. (2010) A 350 year drought reconstruction from Alpine tree ring stable isotopes. *Global Biogeochemical Cycles*, **24**.

- Lens F., Sperry J.S., Christman M.A., Choat B., Rabaey D. & Jansen S. (2011) Testing hypotheses that link wood anatomy to cavitation resistance and hydraulic conductivity in the genus *Acer*. *New Phytologist*, **190**, 709-723.
- LoGullo M.A., Salleo S., Piaceri E.C. & Rosso R. (1995) Relations between vulnerability to xylem embolism and xylem conduit dimensions in young trees of *Quercus cerris*. *Plant Cell and Environment*, **18**, 661-669.
- Maherali H., Pockman W.T. & Jackson R.B. (2004) Adaptive variation in the vulnerability of woody plants to xylem cavitation. *Ecology*, **85**, 2184-2199.
- Martinez-Vilalta J., Cochard H., Mencuccini M., Sterck F., Herrero A., Korhonen J.F.J., Llorens P., Nikinmaa E., Nole A., Poyatos R., Ripullone F., Sass-Klaassen U. & Zweifel R. (2009) Hydraulic adjustment of Scots pine across Europe. *New Phytologist*, **184**, 353-364.
- McCulloh K.A., Johnson D.M., Meinzer F.C., Voelker S.L., Lachenbruch B. & Domec J.-C. (2012) Hydraulic architecture of two species differing in wood density: opposing strategies in co-occurring tropical pioneer trees. *Plant Cell and Environment*, **35**, 116-125.
- McDowell N., Pockman W.T., Allen C.D., Breshears D.D., Cobb N., Kolb T., Plaut J., Sperry J., West A., Williams D.G. & Yezzer E.A. (2008) Mechanisms of plant survival and mortality during drought: why do some plants survive while others succumb to drought? *New Phytologist*, **178**, 719-739.
- Meinzer F.C., Johnson D.M., Lachenbruch B., McCulloh K.A. & Woodruff D.R. (2009) Xylem hydraulic safety margins in woody plants: coordination of stomatal control of xylem tension with hydraulic capacitance. *Functional Ecology*, **23**, 922-930.
- Michaelian M., Hogg E.H., Hall R.J. & Arsenault E. (2011) Massive mortality of aspen following severe drought along the southern edge of the Canadian boreal forest. *Global Change Biology*, **17**, 2084-2094.
- Nadezhdina N., Steppe K., De Pauw D.J.W., Bequet R., Čermák J. & Ceulemans R. (2009) Stem-mediated hydraulic redistribution in large roots on opposing sides of a Douglas-fir tree following localized irrigation. *New Phytologist*, **184**, 932-943.
- Nardini A., Salleo S. & Jansen S. (2011) More than just a vulnerable pipeline: xylem physiology in the light of ion-mediated regulation of plant water transport. *Journal of Experimental Botany*, **62**, 4701-4718.
- Nobel P.S. (1991) *Physicochemical and environmental plant physiology*. Academic Press, San Diego.
- Pesacreta T.C., Groom L.H. & Rials T.G. (2005) Atomic force microscopy of the intervessel pit membrane in the stem of *Sapium sebiferum* (Euphorbiaceae). *IAWA Journal*, **26**, 397-426.
- Pitre F.E., Cooke J.E.K. & Mackay J.J. (2007a) Short-term effects of nitrogen availability on wood formation and fibre properties in hybrid poplar. *Trees-Structure and Function*, **21**, 249-259.

- Pitre F.E., Pollet B., Lafarguette F., Cooke J.E.K., MacKay J.J. & Lapierre C. (2007b) Effects of increased nitrogen supply on the lignification of poplar wood. *Journal of Agricultural and Food Chemistry*, **55**, 10306-10314.
- Pittermann J., Sperry J.S., Wheeler J.K., Hacke U.G. & Sikkema E.H. (2006) Mechanical reinforcement of tracheids compromises the hydraulic efficiency of conifer xylem. *Plant, Cell and Environment*, **29**, 1618-1628.
- Pockman W.T. & Sperry J.S. (2000) Vulnerability to xylem cavitation and the distribution of Sonoran desert vegetation. *American Journal of Botany*, **87**, 1287-1299.
- Pratt R.B., Jacobsen A.L., Ewers F.W. & Davis S.D. (2007) Relationships among xylem transport, biomechanics and storage in stems and roots of nine Rhamnaceae species of the California chaparral. *New Phytologist*, **174**, 787-798.
- Rood S.B., Mahoney J.M., Reid D.E. & Zilm L. (1995) Instream flows and the decline of riparian cottonwoods along the St. Mary River, Alberta. *Canadian Journal of Botany*, **73**, 1250-1260.
- Rood S.B., Patino S., Coombs K. & Tyree M.T. (2000) Branch sacrifice: cavitation-associated drought adaptation of riparian cottonwoods. *Trees*, **14**, 248-257.
- Sannigrahi P., Ragauskas A.J. & Tuskan G.A. (2010) Poplar as a feedstock for biofuels: A review of compositional characteristics. *Biofuels Bioproducts & Biorefining-Biofpr*, **4**, 209-226.
- Schmitz N., Jansen S., Verheyden A., Kairo J.G., Beeckman H. & Koedam N. (2007) Comparative anatomy of intervessel pits in two mangrove species growing along a natural salinity gradient in Gazi Bay, Kenya. *Annals of Botany*, **100**, 271-281.
- Schreiber S.G., Hacke U.G., Hamann A. & Thomas B.R. (2011) Genetic variation of hydraulic and wood anatomical traits in hybrid poplar and trembling aspen. *New Phytologist*, **190**, 150-160.
- Sperry J.S. (2000) Hydraulic constraints on plant gas exchange. *Agricultural and Forest Meteorology*, **2831**, 1-11.
- Sperry J.S. (2003) Evolution of water transport and xylem structure. *International Journal of Plant Sciences*, **164**, S115-S127.
- Sperry J.S. (2011) Hydraulics of vascular water transport. In: *Mechanical Integration of Plant Cells and Plants* (ed P. Wojtaszek), pp. 303-327.
- Sperry J.S., Hacke U.G., Oren R. & Comstock J.P. (2002) Water deficits and hydraulic limits to leaf water supply. *Plant, Cell and Environment*, **25**, 251-263.
- Sperry J.S., Perry A.H. & Sullivan J.E.M. (1991) Pit membrane degradation and air-embolism formation in ageing xylem vessels of *Populus tremuloides* Michx. *Journal of Experimental Botany*, **42**, 1399-1406.
- Sperry J.S. & Tyree M.T. (1988) Mechanism of water stress-induced xylem embolism. *Plant Physiology*, **88**, 581-587.
- Tuskan G.A., DiFazio S., Jansson S., Bohlmann J., Grigoriev I., Hellsten U., Putnam N., Ralph S., Rombauts S., Salamov A., Schein J., Sterck L., Aerts A., Bhalerao R.R., Bhalerao R.P., Blaudez D., Boerjan W., Brun A.,

- Brunner A., Busov V., Campbell M., Carlson J., Chalot M., Chapman J., Chen G.-L., Cooper D., Coutinho P.M., Couturier J., Covert S., Cronk Q., Cunningham R., Davis J., Degroeve S., Dejardin A., dePamphilis C., Detter J., Dirks B., Dubchak I., Duplessis S., Ehlting J., Ellis B., Gendler K., Goodstein D., Gribskov M., Grimwood J., Groover A., Gunter L., Hamberger B., Heinze B., Helariutta Y., Henrissat B., Holligan D., Holt R., Huang W., Islam-Faridi N., Jones S., Jones-Rhoades M., Jorgensen R., Joshi C., Kangasjarvi J., Karlsson J., Kelleher C., Kirkpatrick R., Kirst M., Kohler A., Kalluri U., Larimer F., Leebens-Mack J., Leple J.-C., Locascio P., Lou Y., Lucas S., Martin F., Montanini B., Napoli C., Nelson D.R., Nelson C., Nieminen K., Nilsson O., Pereda V., Peter G., Philippe R., Pilate G., Poliakov A., Razumovskaya J., Richardson P., Rinaldi C., Ritland K., Rouze P., Ryaboy D., Schmutz J., Schrader J., Segerman B., Shin H., Siddiqui A., Sterky F., Terry A., Tsai C.-J., Uberbacher E., Unneberg P. (2006) The genome of black cottonwood, *Populus trichocarpa* (Torr. & Gray). *Science*, **313**, 1596-1604.
- Tyree M.T. & Ewers F.W. (1991) Tansley review no. 34: The hydraulic architecture of trees and other woody plants. *New Phytologist*, **119**, 345-360.
- Tyree M.T., Kolb K.J., Rood S.B. & Patino S. (1994) Vulnerability to drought-induced cavitation of riparian cottonwoods in Alberta: A possible factor in the decline of the ecosystem? *Tree Physiology*, **14**, 455-466.
- Tyree M.T. & Sperry J.S. (1989) Vulnerability of xylem to cavitation and embolism. *Annual Review of Plant Physiology and Molecular Biology*, **40**, 19-38.
- Tyree M.T. & Zimmermann M.H. (2002) *Xylem structure and the ascent of sap*. (2nd ed.). Springer Verlag, Berlin.
- van den Honert T.H. (1948) Water transport in plants as a catenary process. *Discussions of the Faraday Society*, 146-153.
- Violle C., Enquist B.J., McGill B.J., Jiang L., Albert C.H., Hulshof C., Jung V. & Messier J. (2012) The return of the variance: intraspecific variability in community ecology. *Trends in Ecology & Evolution*, **27**, 244-252.
- Wheeler J.K., Sperry J.S., Hacke U.G. & Hoang N. (2005) Inter-vessel pitting and cavitation in woody Rosaceae and other vesselled plants: a basis for a safety versus efficiency trade-off in xylem transport. *Plant, Cell and Environment*, **28**, 800-812.
- Worrall J.J., Egeland L., Eager T., Mask R.A., Johnson E.W., Kemp P.A. & Shepperd W.D. (2008) Rapid mortality of *Populus tremuloides* in southwestern Colorado, USA. *Forest Ecology and Management*, **255**, 686-696.
- Zimmermann M.H. (1983) *Xylem structure and the ascent of sap*. Springer-Verlag, Berlin.
- Zwieniecki M.A., Melcher P.J. & Holbrook N.M. (2001) Hydrogel control of xylem hydraulic resistance in plants. *Science*, **291**, 1059-1062.

2. Phenotypic and developmental plasticity of xylem in hybrid poplar saplings subjected to experimental drought, nitrogen fertilization and shading¹

2.1 INTRODUCTION

Light, nutrients and water are primary resources required by plants for their growth and reproduction (Larcher, 2003). Over the course of evolution, plant species have acquired a suite of traits allowing them to utilize these resources and persist under environmental conditions characteristic for their habitat. This process is known as adaptation (Lambers, Chapin & Pons, 1998). However, the availability of the resources can be rather variable during a plant's life time. For instance, periods of sufficient soil moisture supply can be interrupted by drought (Hogg, Brandt & Michaellian, 2008). Irradiance can rapidly increase when the surrounding vegetation is removed or decrease when a plant becomes shaded by faster-growing neighbors (Lieffers, Messier, Stadt *et al.*, 1999). The availability of inorganic nutrients such as nitrogen or phosphorous can become altered as a result of competition, flood pulse inundation or increased runoff from fertilized fields (Rennenberg, Wildhagen & Ehling, 2010). Plants are, to a certain extent, able to adjust to such changes because plant functional traits exhibit phenotypic plasticity. This adjustment of physiological and structural properties during a plant's life time in order to optimize life processes under new environmental constrains is known as acclimation (Lambers *et al.*, 1998).

Long-distance water transport in plants is a physiological process of paramount importance which is intimately linked with the acquisition and use of all three resources mentioned above. Both adaptive and acclimation processes can be seen in xylem structure and function. In the last decades, xylem structure and function has been studied in a wide range of different species (e.g., Carlquist, 1988, Carlquist, 2001, Wheeler, Baas & Rodgers, 2007) and vast adaptive variation has been demonstrated (e.g., Chave, Coomes, Jansen *et al.*, 2009, Maherali, Pockman & Jackson, 2004, McCulloh, Sperry, Lachenbruch *et al.*, 2010, Sperry, Hacke & Pittermann, 2006). Among the most important xylem hydraulic traits are xylem-specific conductivity and vulnerability to drought-

¹ A version of this chapter has been submitted for publication. Plavcová L & Hacke UG, 2012. Journal of Experimental Botany.

induced cavitation. While the former is a measure of xylem transport efficiency, the latter characterizes xylem safety. Both traits exhibit large interspecific variation. The xylem-specific hydraulic conductivity differs ~100 fold across diffuse porous angiosperms reflecting differences in the size and number of vessels (McCulloh *et al.*, 2010, Sperry *et al.*, 2006). The vulnerability to cavitation measured as the pressure at 50% loss of hydraulic conductivity (P50) spans from -1.25 MPa to -10 MPa reflecting the degree of aridity of a species' natural habitat (Sperry, 2011). Moreover, these two traits seem to be in a trade-off relationship, such that xylem of a given species cannot be both highly transport efficient and highly resistant to cavitation (Hacke, Sperry, Wheeler *et al.*, 2006, Maherali *et al.*, 2004). Wood density with values ranging from 0.1 to 1.2 g cm³ is another functionally important trait (Chave *et al.*, 2009). Wood density has been linked not only with wood mechanical strength (Niklas, 1992), but also with the resistance of xylem to cavitation (Hacke, Sperry, Pockman *et al.*, 2001a).

The structure and hydraulic function of xylem can also vary within a single species in response to growing conditions. The fact that xylem anatomy changes in response to environmental cues is well known and routinely used by paleoclimatologists, dendrochronologists and ecologists analyzing tree rings (for review see Fonti, von Arx, Garcia-Gonzalez *et al.*, 2010). Such studies often use the measurements of ring widths (Savva, Schweingruber, Vaganov *et al.*, 2003), conduit diameters (Gea-Izquierdo, Fonti, Cherubini *et al.*, 2012) or wood densities (Hogg, Hart & Lieffers, 2002) to reconstruct information about past environmental conditions and to infer the hydraulic function of xylem. While xylem anatomy can provide a good proxy of xylem function in some cases, solid knowledge of how specific growing conditions influence xylem anatomy and how patterns in xylem structure link with xylem function is an essential prerequisite for such approaches. Changes in xylem-specific hydraulic conductivity and vulnerability to cavitation in response to environmental conditions such as drought (Fichot, Barigah, Chamaillard *et al.*, 2010, Beikircher & Mayr, 2009), irradiance (Cochard, Lemoine & Dreyer, 1999), salinity (Stiller, 2009), nutrient availability (Hacke, Plavcová, Almeida-Rodriguez *et al.*, 2010, Harvey & van den Driessche, 1997), and soil type (Mayr, Beikircher, Obkircher *et al.*, 2010, Hacke, Sperry, Ewers *et al.*, 2000) have been shown. However, a broader range of species and environmental conditions should be tested in order to gain a better understanding of the acclimation potential of xylem.

In this study, we assessed phenotypic plasticity of xylem traits using clonally propagated saplings of hybrid poplar (*Populus trichocarpa* × *Populus deltoides*, clone H11-11). Given its parentage, we expected to find highly vulnerable and highly conductive xylem in this hybrid poplar. The xylem of riparian cottonwoods such as *P. trichocarpa* and *P. deltoides* is among the most vulnerable of all woody angiosperms studied so far (Sperry, 2011, Tyree, Kolb, Rood *et al.*, 1994). Cottonwood xylem is also highly efficient, which corresponds with its fast growth and high productivity (Bradshaw, Ceulemans, Davis *et al.*, 2000). These xylem characteristics are well suited for the exploitive ecological strategy of cottonwoods in their natural environment. Fluvial floodplains that represent their primary habitat are characterized by good availability of water, nutrients and light. Riverine floodplains are also a highly dynamic environment that is continuously modified by repeated disturbances (Braatne, Rood & Heilman, 1996). Therefore, we expected to find substantial phenotypic plasticity in our hybrid poplar in response to experimental drought, nitrogen fertilization and shading.

Variation in the anatomical and hydraulic parameters of xylem in response to treatments was assessed in stem segments sampled from two vertical positions along a plant's main axis. Based on the literature, we anticipated to find increased vulnerability to cavitation in saplings subjected to fertilization (Hacke *et al.*, 2010, Harvey & van den Driessche, 1997) and shade (Cochard *et al.*, 1999) and increased resistance in response to drought (Fichot *et al.*, 2010, Beikircher & Mayr, 2009). Xylem-specific hydraulic conductivity was expected to increase in fertilized plants (Hacke *et al.*, 2010) and decrease in drought-stressed (Beikircher & Mayr, 2009) and shaded (Schultz & Matthews, 1993) plants. Furthermore, we wanted to test whether the hydraulic and anatomical traits are coupled in a similar way as observed at the interspecific level. If so, we would expect to find correlations between vulnerability of xylem to cavitation and xylem transport efficiency as well as between vulnerability and wood density. Such a comparison of results at the interspecific and intraspecific levels may help to better understand the mechanisms that underlie xylem vulnerability to cavitation.

2.2 METHODS

2.2.1 Plant material and experimental conditions

Saplings of hybrid poplar (*Populus trichocarpa* × *Populus deltoides*, clone H11-11) were grown under drought (DR), nitrogen fertilization (F) and shading

(SH) in order to evaluate the effect of these treatments on growth and xylogenesis. Due to logistical concerns and a limited amount of space in our growth facility, the experimental treatments were imposed one at a time in three independent, temporally separated experiments. For each experiment, hybrid poplar saplings were produced from rooted cuttings and maintained in a growth chamber under the following standard growing conditions: 16/8 hour day/night cycle, 24/18 °C day/night temperature, ambient irradiance $350 \mu\text{mol m}^{-2} \text{s}^{-1}$. Saplings were grown in 6 L pots (1 plant per pot) filled with a commercial potting mix (Sunshine Mix LA4, Sun Gro Horticulture Canada Ltd., Vancouver, BC, Canada). Plants were kept well-watered and fertilized with a complete water soluble fertilizer (20-20-20 N-P-K, Plant Products, Brampton, ON, Canada) in 1 g/L dilution on a weekly basis. After a 7-9 week long period of sapling establishment, plants were randomly assigned to either a treatment (DR, F, SH) or a control (DRC, FC, SHC) group. At least 12 plants were grown per each group. Plants subjected to the DR treatment received 50-200 ml of water every other day. This limited irrigation resulted in repeated wilting but did not cause severe desiccation damage and extensive leaf die-off. In contrast, control plants (DRC) were kept well-watered at all times, receiving 500-1000 ml of water daily. Plants subjected to the F treatment were supplied with 400 ml of 7.5 mM NH_4NO_3 in 0.5 x Hocking's complete nutrient solution (Hocking, 1971) every other day while control plants (FC) received 0.75 mM NH_4NO_3 in 0.5 x Hocking's complete nutrient solution. These two fertilization protocols were previously shown to provide high (F) and low (FC) levels of nitrogen (N) for the growth of this hybrid poplar genotype (Hacke *et al.*, 2010, Pitre, Cooke & Mackay, 2007, Pitre, Pollet, Lafarguette *et al.*, 2007). In order to keep plants well watered, plants were irrigated with tap water on the days when the fertilizer solution was not applied. The SH treatment was imposed by enclosing plants in shade boxes made of gardening fabric. The shade boxes reduced ambient irradiation by 80%, from $350 \mu\text{mol m}^{-2} \text{s}^{-1}$ in control plants (SHC) to $70 \mu\text{mol m}^{-2} \text{s}^{-1}$ in shaded plants (SH). Experimental treatments were imposed for about 5 weeks. The exact duration of the three individual experiments (i.e., the period between planting the rooted cuttings and plant harvesting) and the duration of the experimental treatments (i.e., the period between the onset of a treatment and plant harvesting) are indicated in Table 2-1.

2.2.2 Sampling strategy

After measuring a plant's final height and stem diameter at a height of 10 cm above the root collar (D_{stem}), plants were cut at their base, placed in a dark plastic bag with a moist paper towel and immediately brought to the lab. Bags with the plant material were stored at 4 °C in a refrigerator until they were used for hydraulic measurements. For these measurements, stem segments 20-25 cm in length were sampled from two different positions along the plant's main stem. The first set of segments was sampled from a basal region of the stem at a fixed height of 5-30 cm above the root collar. These segments are hereafter referred to as 'basal'. The second set of segments was taken from a position closer to the apex of a plant, and hence these segments are referred to as 'distal'. The height at which the distal segments were collected differed among the three experiments, reflecting the different growth rates of plants exposed to different experimental treatments. Distal segments were located at ~60% of the final plant height. Hence, distal segments were sampled at a height of 40-60 cm above pots in DR, 60-85 cm in DRC, 95-120 cm in F, 85-110 cm in FC, and 65-90 cm in both SH and SHC plants. Distal segments underwent their entire growth and development under treatment conditions. Basal segments, by contrast, completed primary growth and initiated secondary growth under control conditions before experimental treatments began. Nevertheless, a significant portion of secondary xylem was formed after the onset of treatments.

2.2.3 Xylem pressure

Xylem pressure was measured using equilibrated mature leaves attached between the 5th and 8th node counted from the top of a plant. One leaf per plant was measured, from five plants per treatment group. Leaves were sealed in a plastic bag covered with aluminum foil the night before harvesting to inhibit transpiration and to ensure equilibration of water potentials. Immediately prior to harvesting, bagged leaves were excised and xylem pressure was measured using a Scholander-type pressure chamber (Model 1000; PMS Instrument Company, Albany, OR, USA). Xylem pressure measurements were conducted for F and DR experiments only.

2.2.4 Growth measurements

Final height and stem basal diameter (D_{stem}) of each sapling were assessed with a measuring tape and calipers, respectively. Leaf area (A_L) was measured with an area meter (LI-3100, Li-Cor, Lincoln, NE, USA). A plant's total A_L and

the A_L supported by basal stem segments were determined for each plant. The supported A_L was calculated as the sum of A_L distal to the segment and half of the A_L directly attached to the segment. All leaves of a plant were subsequently oven-dried at 70 °C for 3 days to determine the total leaf dry weight (DW_L) for each plant. The leaf weight to leaf area ratio (LWA) was calculated as DW_L divided by total A_L .

2.2.5 Hydraulic measurements

Segments used for hydraulic measurements were trimmed underwater to a final length of 14.2 cm. To measure native hydraulic conductivity (K_{native}), stem segments were fitted to a tubing apparatus and the gravity-induced water flow rate through the segments was recorded with an electronic balance (CP225 D; Sartorius, Göttingen, Germany) interfaced with a computer. A pressure head of 4-5 kPa was used to induce the flow. Stem hydraulic conductivity was then calculated as the flow rate for a given pressure gradient. Subsequently, segments were flushed with standard measuring solution (20 mM KCl + 1 mM CaCl₂ filtered at 0.2 µm) for 15-20 min at 50 kPa in order to remove native embolism. Conductivity measurements were repeated to determine hydraulic conductivity after flushing (K_{flush}). Stem segments were then attached in a custom-built centrifuge rotor and spun to progressively more negative pressures with the incremental steps of 0.25 or 0.5 MPa. Hydraulic conductivity was measured after each pressure increment until it dropped below 90% of the K_{flush} value. The percentage loss of hydraulic conductivity (PLC) relative to K_{flush} was plotted against the corresponding xylem pressure to generate vulnerability curves. Data points were fitted with a Weibull function and the xylem pressure corresponding to 50% loss of conductivity (P_{50}) was determined for each segment.

After hydraulic measurements were completed, stem segments were sectioned near the middle of their length. The exposed cross-sectional surface was captured with a digital camera attached to a stereomicroscope (MS5; Leica Microsystems, Wetzlar, Germany) at 10-16 x magnification. Xylem cross-sectional area (A_X) excluding pith and bark was measured with image analysis software (ImagePro Plus version 6.1, Media Cybernetics, Silver Spring, MD, USA). Xylem-specific hydraulic conductivity (K_S) was subsequently calculated as the maximal hydraulic conductivity (K_{max}) of a stem segment divided by the corresponding A_X . In the majority of stems, hydraulic conductivity increased after flushing. However, in few instances K_{flush} was slightly (i.e., less than 5%) lower

then K_{native} possibly due to a wounding response. Thus, the K_{max} of a stem was determined as either K_{flush} or K_{native} , whichever value was higher.

2.2.6 Vessel diameter and wood density measurements

The same stem segments previously used for measuring hydraulic conductivity and cavitation resistance were used for measuring vessel diameter and wood density. Stem cross-sections (~40-60 μm thick) were prepared from the middle portion of basal and distal segments using a sliding microtome (SM2400, Leica) or by hand with a fresh single-edge razor blade. Sections were stained with toluidine blue for 3 min to increase contrast, rinsed in water for 1 min, mounted on slides in glycerol and observed with a light microscope (DM3000, Leica). Images were captured at 100 x magnification using a digital camera (DFC420C, Leica). Vessel diameters were measured in complete radial sectors delimited by xylem rays spanning from the pith to the cambium. Between three to ten different sectors were selected for each stem providing a total of 300 to 500 vessel diameter measurements per stem. The average vessel diameter (D_v) per stem was subsequently calculated. Five to six stems were analyzed for each treatment and position.

For measuring wood density (d_w), samples 2 cm in length were excised from stem segments and split longitudinally into two subsamples. The bark was peeled off and the pith was carefully removed. Wood specimens were then submerged in a beaker filled with water placed on an electronic balance (CP224 S, Sartorius). The displaced water weight was recorded and converted into fresh wood volume. Specimens were then oven-dried at 70 °C for 2 days. d_w was calculated as the ratio between specimen dry weight and its fresh volume. The d_w of each stem segment was finally determined by averaging the values of the two subsamples. Five to eight stems were analyzed for each treatment and position.

2.2.7 Statistical analyses

Since the three experimental treatments were imposed as three independent and temporally separated experiments, the effects of treatments were statistically evaluated by comparing treated plants with their controls within a single experiment. In order to evaluate the effect of treatments on plant growth parameters, independent two sample t-tests were performed. Analysis of variance was carried out in order to dissect the effect of treatment and stem segment position on xylem hydraulic and structural parameters (A_x , D_v , d_w , K_S and P50). The following linear model was used to fit the measured data:

$$var = f[treat + pos + (treat \times pos)]$$

where *var* represents the tested variable, *treat* and *pos* are the fixed effect factors ‘treatment’ and ‘position’, and *treat* × *pos* is the interaction term. In preliminary analyses, a more complex linear regression model, which included a random effect factor ‘plant’ in which the fixed effect factor ‘position’ was nested, was used for the F and SH experiments because in these two experiments basal and distal segments were sampled from the same plant. However, based on an Akaike information criterion (AIC) comparison (Šmilauer, 2007), introducing the random effect factor ‘plant’ did not substantially improve the model fits in comparison with a simple linear model and hence, this factor was removed. Planned comparisons between means of treated versus control plants within the same stem segment position (i.e., either basal or distal) and between means of basal and distal stem segments within either treated or control plant groups were carried out using the least significance difference procedure (Sokal & Rohlf, 1995). In addition to the formal statistical analysis, box plots are presented for each variable tested with ANOVA in order to provide more detailed information on the magnitude of differences and variability within and between groups. Lastly, to elucidate potential relationships between selected growth, hydraulic and anatomical parameters, we tested for significant linear correlations between the group means across all three experiments. The results of all statistical analyses were deemed significant at $P \leq 0.05$. Probability (*P*) values for the planned comparisons were adjusted to 0.0125 using the Bonferroni correction procedure for multiple comparisons (Sokal & Rholf, 1995). The statistical software package R 2.10.1 (R Development CoreTeam 2009, Auckland, NewZealand) was used to perform the analyses. Throughout this chapter, group means are cited with their standard errors.

2.3 RESULTS

2.3.1 Plant growth

The growth characteristics of hybrid poplar saplings differed between treated and control plants as well as between experiments (Table 2-2). The average final height ranged from 77.1 ± 0.7 cm to 171.3 ± 2.2 cm in DR and F plants, respectively. Similarly, the stem basal diameter (D_{stem}) was smallest in DR (6.3 ± 0.1 mm) and largest in F (9.5 ± 0.1 mm). Furthermore, total leaf area (total A_L) exhibited substantial differences ranging from 0.27 ± 0.01 m² to $0.99 \pm$

0.03 m². The total A_L co-varied with total leaf dry weight (DW_L) as indicated by a relatively constant leaf weight per area ratio (LWA). LWA ranged from 0.043±0.001 to 0.054 ± 0.001 kg m⁻² with the exception of a substantially lower LWA (0.025 ± 0.0004 kg m⁻²) in SH plants. As for the effect of treatments, DR plants exhibited reduced growth in height and girth and had smaller A_L and DW_L as well as slightly lower LWA compared with controls. The opposite trend in growth was observed in F relative to FC plants although their LWA ratios were not different from each other. The height growth increment was higher in SH, while their radial growth was reduced in comparison with controls. Although there were no significant differences in the A_L of SH and SHC plants, DW_L was significantly lower in SH plants, resulting in substantially lower LWA in SH plants.

2.3.2 Leaf area, xylem area and stem hydraulic conductivity

The supported A_L scaled linearly with A_X across all plant groups ($R^2=0.933$, $P=0.002$) (Fig. 2-1a). A_X was tightly correlated with a stem's maximal hydraulic conductivity (K_{max}) ($R^2=0.976$, $P<0.001$). The level of native embolism was low in most basal stem segments; therefore, their K_{max} corresponded well with their native hydraulic conductivity (K_{native}). As a result, the supported A_L was positively correlated with both K_{native} ($R^2=0.921$, $P=0.002$) (Fig. 2-1b) and K_{max} ($R^2=0.921$, $P=0.002$).

2.3.3 Variation in stem morphology and xylem anatomy

The structure and the amount of xylem differed between treated and control plants and between the two stem segment positions (Table 2-3, Fig. 2-2, Fig. 2-3). Variation in A_X in response to treatments reflected changes in plant radial growth (Fig. 2-2a-c). In basal segments, A_X decreased in DR and SH plants and increased in F plants in comparison with their controls. Similar patterns in xylem formation were observed in distal segments although there was no significant difference in A_X between SH and SHC plants. The A_X of distal segments was 45-60% smaller compared with basal segments, even though the external stem diameters of distal and basal segments were often similar. The difference in A_X was mainly caused by a substantially larger pith area in distal segments compared with their basal counterparts (Fig. 2-3). Furthermore, the vascular cylinder in distal segments had an irregular (rather than more or less cylindrical) shape and the patterns associated with primary growth were still apparent in stem cross-sections. For instance, clusters of primary xylem could be

readily distinguished adjacent to the vertices of the pentagonal pith (arrowheads in Fig. 2-3b). Despite these signs of juvenility, the transition from primary to secondary growth was clearly completed and a substantial amount of secondary xylem was produced along the entire length of distal segments.

Differences in overall xylem morphology were paralleled by differences in xylem anatomy. In basal segments, mean vessel diameters (D_v) ranged between $35.2 \pm 0.3 \mu\text{m}$ and $43.4 \pm 0.3 \mu\text{m}$ in SHC and DRC plants, respectively (Fig. 2-2d-f). In basal segments, D_v decreased in DR while it increased in F plants when compared with their controls. D_v was not significantly different between SH and SHC plants. In distal segments, D_v showed even more variation in response to treatments. The smallest ($30.1 \pm 0.5 \mu\text{m}$) and the largest D_v ($48.6 \pm 0.5 \mu\text{m}$) were measured in DR and F plants, respectively. The relative changes in D_v in response to treatments were consistent with the trends observed in basal segments. With the exception of DR plants, distal segments exhibited substantially wider vessels than their basal counterparts.

Large differences were also observed in wood density (d_w) with values ranging from $0.244 \pm 0.006 \text{ g cm}^{-3}$ in the distal segments of F plants to $0.404 \pm 0.004 \text{ g cm}^{-3}$ in the basal segments of SHC plants (Fig. 2-2g-i). Basal segments typically showed higher d_w than the corresponding distal segments. In basal segments, d_w was significantly lower in F and SH plants in comparison with their respective controls, while it did not substantially differ between DR and DRC plants. In distal segments, d_w was lower in F and SH segments relative to their controls, following the same pattern as in basal segments. In contrast, the distal segments in DR exhibited denser wood than DRC plants.

2.3.4 Xylem-specific hydraulic conductivity

Changes in xylem structure were paralleled by differences in xylem hydraulic parameters (Table 2-3, Fig. 2-4). Xylem-specific hydraulic conductivity (K_S), which represents a measure of xylem transport efficiency, varied ~3-fold, from $2.7 \pm 0.1 \text{ kg m}^{-1} \text{ s}^{-1} \text{ MPa}^{-1}$ to $8.3 \pm 0.3 \text{ kg m}^{-1} \text{ s}^{-1} \text{ MPa}^{-1}$ in DR and F plants, respectively (Fig. 2-4a-c). In basal segments, K_S was lower in DR and SH plants in comparison with their controls. K_S tended to be higher in F than in FC plants; however, the difference was not statistically significant. The K_S of basal segments scaled with their D_v ($R^2 = 0.803$, $P = 0.016$) (Fig. 2-5). In distal segments, K_S was higher in SH and did not substantially differ in DR and F plants with respect to their respective controls (Fig. 2-4a-c). The K_S of distal segments was not

significantly linearly correlated with their D_v as observed in basal segments although there was a tendency for lower conductivity in segments with narrower vessels. In addition, the K_S of distal segments tended to be lower than in basal segments with comparable D_v , indicating that other factors aside from vessel diameter alone had a significant effect on the transport efficiency of the distal segments (Fig. 2-5).

2.3.5 Xylem vulnerability to drought-induced cavitation

Cavitation resistance varied profoundly in response to experimental treatments and segment location (Fig. 2-4d-f). The P50 of basal segments differed less than 0.5 MPa across all three treatments, ranging from -1.14 MPa in both SH and F plants to -1.53 MPa in SHC. While the vulnerability of basal stem segments did not significantly change in response to the DR treatment, stems of SH and F plants were more vulnerable than their controls. In distal segments, P50 values exhibited a large variation of 1.5 MPa between the most vulnerable (F plants, -0.15 ± 0.03 MPa) and the most resistant plants (DR plants, -1.71 ± 0.09 MPa). With the exception of the DR treatment, distal segments were more vulnerable than their basal counterparts. In fact, distal segments of DR plants had the most resistant xylem across all the plant groups and segment positions tested in this study.

The differences in P50 between basal and distal segments were associated with a marked change in the shape of their vulnerability curves. While all basal segments showed typical sigmoidal-shaped vulnerability curves, the shape of the curves of distal segments varied from sigmoidal through linear to r-shaped depending on the treatment (Fig. 2-6). The distal segments of F plants were extremely vulnerable. These segments exhibited 75% PLC at a modest xylem pressure of -0.25 MPa, resulting in an r-shaped vulnerability curve (Fig. 2-6c). In distal segments of DR plants, by contrast, embolism did not exceed 20% at xylem pressures less negative than -1.25 MPa (Fig. 2-6a). Vulnerability curves generated by our centrifuge method were in good agreement with the native PLC values plotted against the native xylem pressures measured in the F and DR experiments (square symbols in Fig. 2-6). Xylem pressure was not measured for the SH experiment.

P50s of both basal and distal segments scaled tightly with d_w (basal: $R^2=0.928$, $P=0.002$ distal: $R^2=0.925$, $P=0.002$) (Fig. 2-7a). In contrast, P50 was not correlated with K_S (Fig. 2-7b). P50 was significantly correlated with D_v in distal

segments (distal: $R^2 = 0.766$, $P = 0.023$); however, this correlation was mainly driven by the two extremely different distal segments in DR and F plants (Fig. 2-7c).

2.4 DISCUSSION

Plant growth and development were greatly affected when saplings of hybrid poplar were grown under experimental drought (DR), shade (SH) or nitrogen fertilization (F) for >30 days (Table 2-1, Fig. 2-1). This study particularly focused on changes in xylem anatomy and hydraulic function. Across all treatments, the A_X was tightly correlated with the supported A_L (Fig. 2-1a). Since A_X represents the principal anatomical basis of a stem's capacity to transport water, the allometric relationship between A_X and A_L translates into tight scaling between A_L and a stem's hydraulic conductivity (K_{native}) (Fig. 2-1b). These relationships, reflecting a well-established allometric relationship between stem basal diameter and leaf area (e.g., Harrington & Fownes, 1993, McCulloh, Johnson, Meinzer *et al.*, 2012), arguably help to maintain an adequate supply of water from roots to transpiring leaves (Shinozaki, Yoda, Hozumi *et al.*, 1964).

A tight correlation between A_L and A_X would in principle not be required if a plant could radically change the hydraulic parameters of its xylem. For instance, if the xylem could become much more efficient for water transport, a smaller A_X per unit A_L would be sufficient to provide an adequate water supply. Such a situation has been documented in a recent study (Hacke *et al.*, 2010). Using the same hybrid poplar clone and similar experimental conditions, we previously observed that stems with a comparable A_X could support almost twice as much A_L in plants receiving high versus low N fertilization. This difference was attributed to a higher xylem-specific hydraulic conductivity (K_S) exhibited by high N plants. Despite an almost 2-fold variation in K_S values across the basal segments in the current dataset, these differences in transport efficiency did not significantly alter the overall linear relationship between A_L and A_X across the experimental group averages. However, it is possible that the relative importance of changes in xylem transport efficiency would increase over a longer period of acclimation or when evaluated within a single treatment with a broader within-group variation as in Hacke *et al.* (2010).

The changes in K_S observed in response to individual experimental treatments were largely consistent with our initial hypotheses. In basal segments, K_S values were lower in resource-limited DR and SH plants in which the requirements for water transport were reduced due to drought-induced stomatal closure and lower evaporative demand. In contrast, the highest value of K_S was found in basal segments of F plants that received copious amounts of nitrogen and were kept well irrigated. These findings are in agreement with changes in K_S observed in other studies in response to low water availability (Beikircher & Mayr, 2009), shade (Raimondo, Trifilo, Lo Gullo *et al.*, 2009) and high nutrient supply (Hacke *et al.*, 2010).

For basal segments, the values of K_S showed a significant positive correlation with the mean vessel diameter (D_v) (Fig. 2-5). Such a relationship is expected based on the Hagen-Poiseuille equation and is consistent with results from interspecific comparisons (Hacke, Jacobsen & Pratt, 2009, Sperry *et al.*, 2006). The relationship between K_S and D_v was more variable in distal segments. In addition, distal segments generally showed lower K_S values than basal segments although their vessels diameters were comparable or even larger (with the exception of DR plants) than those of basal segments. Thus, it seems that other factors such as vessel density, vessel length, pit properties, overall xylem network connectivity and stem taper may have affected the K_S of the more juvenile distal segments.

In agreement with our initial hypothesis, xylem vulnerability to drought-induced cavitation changed in response to experimental treatments. More vulnerable xylem in comparison with controls was found in both basal and distal segments of SH and F plants. Cavitation resistant xylem requires significant carbon investments (Hacke *et al.*, 2001a) and F and SH plants preferentially allocated their carbon resources into growth and light inception. These findings are in line with results obtained in other species in response to similar environmental cues (Barigah, Ibrahim, Bogard *et al.*, 2006, Cochard *et al.*, 1999, Harvey & van den Driessche, 1999). P50 was not substantially different between DR and DRC plants in basal segments; however, the cavitation resistance increased in distal segments of DR saplings. As growth was significantly reduced in DR plants, the amount of xylem produced under treatment conditions was small in basal segments, and hence did not affect the overall vulnerability of the bulk xylem tissue. However, the increased resistance in distal segments of DR plants indicates that their xylem adjusted to sustain lower xylem pressures and

prevent excessive cavitation. An increase in cavitation resistance in response to low water availability has been previously documented in several species, including poplar, exposed to various levels of drought severity (Awad, Barigah, Badel *et al.*, 2010, Beikircher & Mayr, 2009, Fichot *et al.*, 2010), while only a limited change has been found in three willow clones (Wikberg & Ögren, 2007).

Across the three experiments conducted in the current study, the average difference in P50 between treated and control plants was 0.3 MPa and 0.6 MPa for basal and distal segments, respectively. Even a relatively subtle change in P50 may have important implications for plant hydraulic performance because the loss of conductivity due to embolism increases very steeply around the P50 value. The smaller variation in P50 observed in basal segments in comparison with distal segments is not surprising given the experimental design. The basal segments completed their primary growth and started their secondary growth under the same conditions prior to the commencement of treatment. In distal segments, by contrast, the entire growth and development took place under treatment conditions.

With the exception of DR plants, distal segments were more vulnerable than their basal counterparts. The difference between basal and distal segments across the treatment groups was on average 0.6 MPa with the largest difference of almost 1 MPa found in F plants. Age-related differences in xylem vulnerability have been previously studied using branches of field-grown trees. While some studies found that younger branches and roots were more vulnerable to cavitation (Choat, Lahr, Melcher *et al.*, 2005, Sperry & Ikeda, 1997), others studies do not support this trend (Hacke & Sauter, 1996, Sperry & Saliendra, 1994). Based on the vulnerability segmentation hypothesis (Tyree & Ewers, 1991, Zimmermann, 1983) it has been proposed that more distal organs such as leaf petioles and terminal branches should be more vulnerable than trunk xylem in mature trees. Distal plant parts are arguably expendable; their sacrifice can help to maintain favorable plant water balance by reducing the total transpiring surface (Rood, Patino, Coombs *et al.*, 2000). This strategy might be particularly vital in poplar, which is well-known for its ability to regenerate by root suckering and re-sprouting from auxiliary buds (Galvez & Tyree, 2009, Lu, Equiza, Deng *et al.*, 2010). Nevertheless, it is questionable if such reasoning is relevant to the relatively young saplings measured in this current study.

The increased vulnerability of the distal segments could be potentially linked with their juvenility. In distal segments, primary xylem represented a

substantial proportion of the bulk xylem. Primary xylem has been shown to be more vulnerable than secondary xylem in one-year old branches of sugar maple (Choat *et al.*, 2005). However, we found little evidence for increased vulnerability of primary xylem in hybrid poplar in the current study. When native and artificially induced embolism was visualized by perfusing distal stem segments with safranin dye, more embolised vessels were detected in secondary xylem while the clusters of primary xylem vessels were largely functional (Fig. 2-8). Thus, the increased proportion of primary xylem in distal segments cannot explain their increased vulnerability.

The distal segments of F plants appeared particularly vulnerable as indicated by their r-shaped vulnerability curve (Fig. 2-6c). r-shaped vulnerability curves have been sometimes regarded as measurement artifacts (Choat, Drayton, Brodersen *et al.*, 2010, Cochard, Herbette, Barigah *et al.*, 2010). However, it now becomes obvious that such curves are valid and that they are associated with the presence of extremely vulnerable vessels that embolize at near-atmospheric pressures (Christman, Sperry & Smith, 2012, Jacobsen & Pratt, 2012, Sperry, Christman, Torres-Ruiz *et al.*, 2012). r-shaped curves have been typically measured in large-vesseled plants such as oaks and grapevine (Jacobsen & Pratt, 2012, Taneda & Sperry, 2008); however, similar curves have been observed in poplar under distinct conditions of cavitation fatigue (Hacke, Stiller, Sperry *et al.*, 2001b) and xylem senescence (Sperry, Perry & Sullivan, 1991). In the current study, native PLC measured in distal segments of F plants plotted against the values of native xylem pressure corresponded well with the vulnerability curves (Fig. 2-6c), providing support that these curves are valid. According to the air-seeding hypothesis, the population of particularly vulnerable vessels is characterized by extremely leaky pits. Thus, the pit membranes in distal segments of F plants might have been inherently more porous or more susceptible to pore enlargement during pit membrane deflection. Alternatively, it is possible that the low mechanical reinforcement of vessels, as evidenced by low wood density, resulted in an irreversible damage to some of the pit membranes rendering them extremely permeable for air.

In fact, the correlation between wood density (d_w) and P50 was remarkably strong across all basal and distal segments measured in this study (Fig. 2-7a). Hence, it can be argued that the probability that pit membranes will be leaky to air is proportional to the mechanical reinforcement of xylem cells. This finding agrees with previous studies that identified a trade-off between

vulnerability and xylem construction cost at the interspecific level (Hacke *et al.*, 2001a, Jacobsen, Ewers, Pratt *et al.*, 2005, Pratt, Jacobsen, Ewers *et al.*, 2007). Results from intraspecific comparisons are less conclusive regarding this trade-off. No relationship between d_w and P50 was found in a recent study comparing eight different genotypes of *Populus deltoides* \times *Populus nigra* grown under two levels of irrigation (Fichot *et al.*, 2010). However, a significant correlation between P50 and another parameter related to xylem mechanical strength, the double vessel wall thickness, was found in the same study. Similarly, Awad *et al.* (2010) found that increased vulnerability scaled with decreasing cell wall thickness and vessel thickness-to-span ratio in plants of a single *Populus tremula* \times *Populus alba* clone grown under three contrasting water regimes, while no significant correlation was found between P50 and d_w . In the current study, saplings were maintained in a controlled environment with their stems secured to supporting stakes. In plants supported by stakes, wood density may strongly reflect demands arising from cohesion-driven water transport while the mechanical function of xylem is likely to be less important than in plants growing in a natural environment. This might have contributed to the tight correlation observed between P50 and d_w in this study.

The mean values of K_S and P50 across all basal segments were $6.7 \text{ kg m}^{-1} \text{ s}^{-1} \text{ MPa}^{-1}$ and -1.3 MPa , respectively, which ranks hybrid poplar among diffuse-porous species that are relatively transport efficient in water transport but vulnerable to cavitation. Thus, these data support the notion that xylem cannot be superior in both cavitation resistance and transport efficiency (Hacke *et al.*, 2006, Lens, Sperry, Christman *et al.*, 2011, Maherali *et al.*, 2004). However, within our dataset, there was no significant correlation between P50 and K_S in either basal or distal stem segments (Fig. 2-7b). A correlation between D_v and P50, which can also be regarded as an indicator of a safety versus efficiency trade-off, was significant only in distal segments, and this trend was mainly driven by two extreme data points (Fig. 2-7c). Thus, these findings indicate that increased resistance to cavitation is not necessarily associated with reduced transport efficiency. This is good news for tree breeders because it suggests that there is some limited room for simultaneous improvement of both hydraulic efficiency and drought resistance. In the current dataset, the basal segments were closer to this optimum than the distal ones (Fig. 2-7). Interestingly, basal segments under treatments in which either water or light resources were severely limited (i.e., DR and SH plants) appeared less hydraulically optimized compared with the basal segments of F and all three control plant groups.

2.5 CONCLUSIONS

Hybrid poplar used in this study inherited a genetic blueprint from the riparian cottonwoods *Populus trichocarpa* and *Populus deltoides*, which defines the general characteristics of its anatomy, morphology and physiology. This study has specifically focused on the anatomy and hydraulic function of xylem. Our data show that the xylem of hybrid poplar is efficient and highly vulnerable to drought-induced cavitation, as expected given its parentage. While these general properties of xylem cannot be radically changed, our data demonstrate that the xylem structure and function is, to a certain extent, variable. Differences in xylem cross-sectional area, mean vessel diameter, wood density, xylem-specific hydraulic conductivity, and vulnerability to cavitation were detected not only in response to experimental treatments (drought, nitrogen fertilization and shade), but also in stem segments sampled from different vertical positions along a plant's main axis (basal and distal segments). Such developmental and phenotypic plasticity in xylem traits can be potentially used to cope with different and changing environmental conditions. However, it is difficult to predict what xylem phenotypes would be produced under field conditions.

Our results also provide insights into xylem structure-function trade-offs and can help to elucidate mechanistic underpinnings of some of these patterns. The close correlation between wood density and P50 observed in this study is intriguing and suggests that there might have been a true functional link between these two traits in this study. It is likely that stronger cell walls helped to stabilize the pit fields thereby protecting pit membranes from mechanically induced damage. More research is necessary to show if this situation is unique to this highly vulnerable hybrid poplar clone grown with stems structurally supported by stakes or if it can be extrapolated to a broader array of species and growing conditions. In contrast, we did not find a correlation between P50 and K_S across our dataset, indicating that the safety versus efficiency trade-off is not, within certain bounds, inevitable.

2.6 TABLES

Table 2-1: An overview of the experimental design. Saplings of hybrid poplar (*Populus trichocarpa* × *deltoides*, clone H11-11) were grown under three experimental treatments – drought, nitrogen fertilization and shading. Three independent, temporally separated experiments were conducted. For each experiment, plants were randomly assigned to an experimental treatment, while a second group of plants was maintained as control. Thus, three pairs of treated versus control plants were generated (DR– plants subjected to drought treatment, DRC–control well-watered plants; F – plants receiving high levels of N fertilization, FC – control plants receiving low levels of N fertilization; SH – plants grown under low light conditions, SHC – control plants growing under sufficient irradiance). Treatments were imposed after the initial period of sapling establishment during which plants were grown under the same reference conditions. The duration of experiments (t_{exp} , i.e., the number of days from the date when rooted cuttings were planted to the date of sapling harvesting), the duration of treatments (t_{treat} , i.e., the number of days from the onset of treatment to sapling harvesting) and a brief description of the treatment conditions for treated (DR, F, SH) and control (DRC, FC, SHC) plants are indicated.

experiment	t_{exp} (days)	t_{treat} (days)	treatment	treatment conditions
Drought	87	37	DR	175 -700 ml water per week
			DRC	1750 - 3500 ml water per week
Fertilization	101	33	F	7.5 mM NH_4NO_3 in 0.5x Hocking solution
			FC	0.75 mM NH_4NO_3 in 0.5x Hocking solution
Shade	96	40	SH	$70 \mu\text{mol m}^{-2} \text{s}^{-1}$ PhAR
			SHC	$350 \mu\text{mol m}^{-2} \text{s}^{-1}$ PhAR

Table 2-2: Group means \pm SE and t-test probability (*P*) values for growth-related parameters of hybrid poplar saplings grown under drought (DR), nitrogen fertilization (F), shade (SH) and control conditions (DRC, FC, SHC).

	Drought			Fertilization			Shade		
	DR	DRC	<i>P</i> value	F	FC	<i>P</i> value	SH	SHC	<i>P</i> value
height (cm)	77.1 \pm 0.7	116.6 \pm 1.1	<0.001	171.3 \pm 2.2	160.0 \pm 2.3	0.003	118.0 \pm 2.2	109.3 \pm 1.3	0.007
D _{stem} (mm)	6.3 \pm 0.1	8.3 \pm 0.1	<0.001	9.5 \pm 0.1	8.9 \pm 0.2	0.016	6.8 \pm 0.1	8.1 \pm 0.1	<0.001
total A _L (m ²)	0.27 \pm 0.01	0.60 \pm 0.01	<0.001	0.99 \pm 0.03	0.63 \pm 0.03	<0.001	0.47 \pm 0.02	0.49 \pm 0.01	ns
DW _L (g)	12.4 \pm 1.7	30.1 \pm 2.0	<0.001	42.8 \pm 6.1	28.6 \pm 4.2	<0.001	11.7 \pm 1.5	26.3 \pm 1.0	<0.001
LWA (kg m ⁻²)	0.046 \pm 0.001	0.050 \pm 0.001	0.029	0.043 \pm 0.001	0.046 \pm 0.002	ns	0.025 \pm 0.000	0.054 \pm 0.001	<0.001

Abbreviations: height – sapling final height measured from the root-collar, D_{stem} – stem basal diameter measured at 10 cm above the root collar, total A_L – plant total leaf area, DW_L – plant total leaf dry weight, LWA – leaf weight to leaf area ratio, ns – non-significant result (*P*>0.05)

Table 2-3: Analysis of variance (ANOVA) results. Variation in xylem structural and hydraulic parameters in response to treatment (treat) and stem segment position (pos) was evaluated.

	Drought			Fertilization			Shade		
	treat	pos	treat x pos	treat	pos	treat x pos	treat	pos	treat x pos
A_X (mm ²)	<0.001	<0.001	<0.001	<0.001	<0.001	ns	0.012	<0.001	<0.001
D_V (μm)	<0.001	<0.001	<0.001	<0.001	<0.001	ns	ns	<0.001	0.023
d_w (g cm ⁻³)	ns	<0.001	<0.001	<0.001	<0.001	0.039	<0.001	<0.001	<0.001
K_S (kg m ⁻¹ s ⁻¹ MPa ⁻¹)	<0.001	<0.001	0.002	ns	ns	0.006	ns	<0.001	<0.001
P50 (MPa)	0.011	ns	<0.001	<0.001	<0.001	<0.001	<0.001	<0.001	ns

Abbreviations: A_X – xylem cross-sectional area, D_V – mean vessel diameter, d_w – wood density, K_S – xylem-specific hydraulic conductivity, P50 – the pressure at 50% loss of hydraulic conductivity

2.7 FIGURES

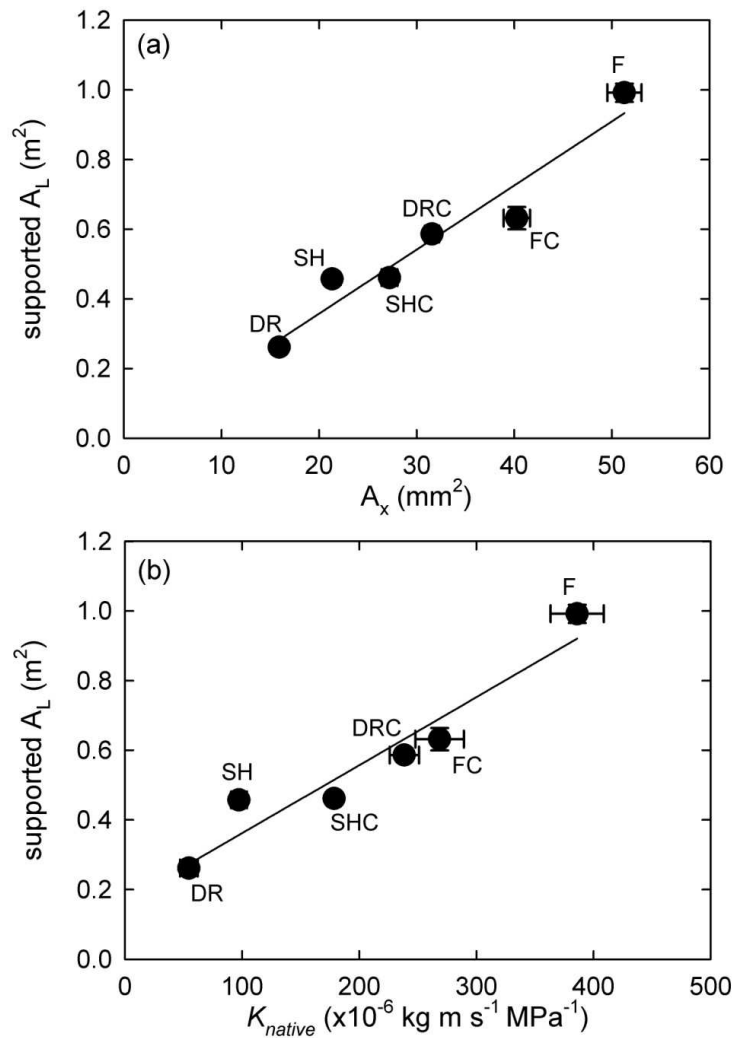


Figure 2-1: Relationship between supported leaf area (A_L) and a stem's capacity to transport water measured as (a) xylem cross-sectional area (A_X) and (b) native hydraulic conductivity (K_{native}) in hybrid poplar saplings grown under drought (DR), nitrogen fertilization (F), shade (SH) and control conditions (DRC, FC, SHC).

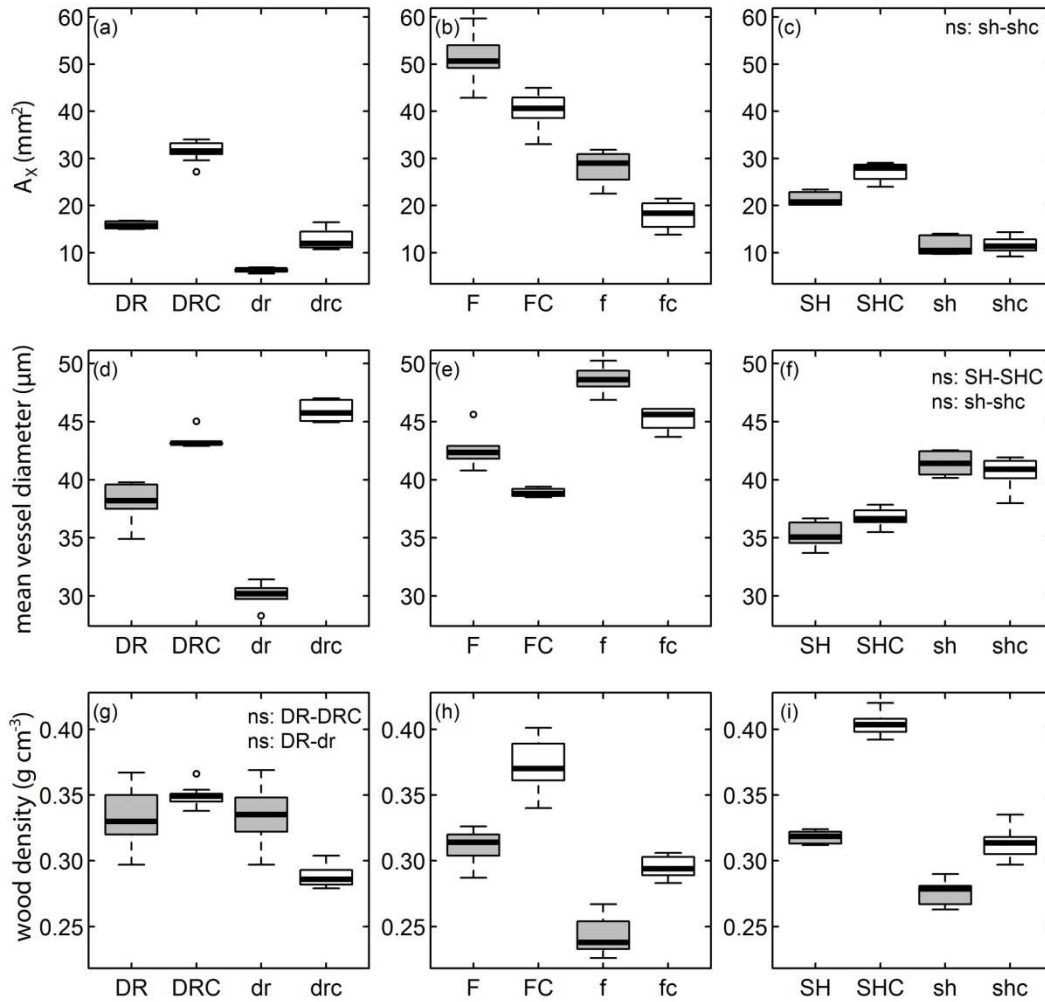


Figure 2-2: Variation in xylem structure: (a-c) xylem cross-sectional area (A_x), (d-f) mean vessel diameter and (g-i) wood density of basal (capital letters) and distal (lower case letters) stem segments in hybrid poplar saplings grown under drought (DR, dr), nitrogen fertilization (F, f), shade (SH, sh) and control conditions (DRC, drc; FC, fc; SHC, shc). In each box plot, the median (50th percentile) is represented with a heavy line inside of the central box. The horizontal borders of the box represent the 25th and 75th percentiles. Whiskers indicate the 10th and 90th percentiles with outliers shown as circles. Non-significant (ns) results for a specified comparison of means are indicated. $n=5-8$.

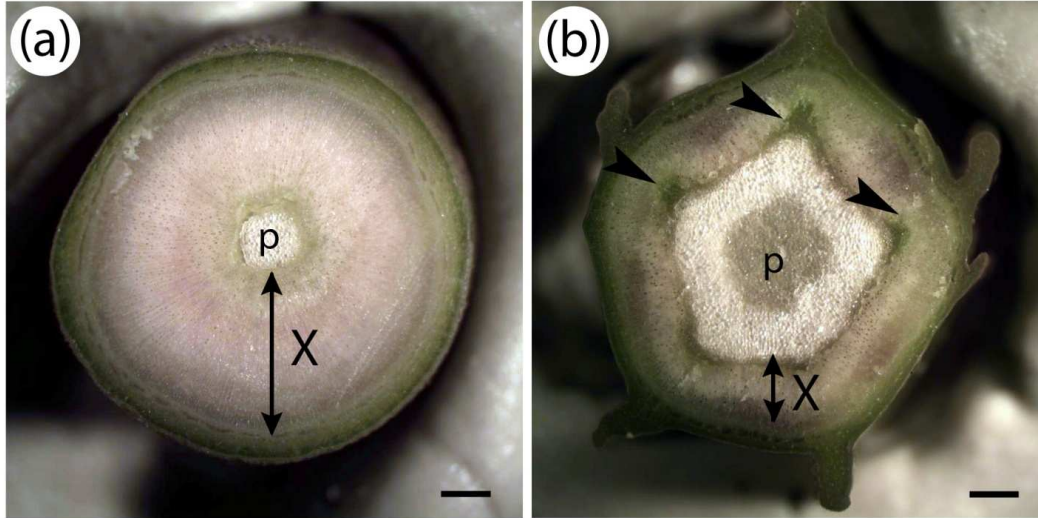


Figure 2-3: Representative cross-sections of (a) basal and (b) distal stem segments from one of the control plants (FC). In the basal segment (a), secondary xylem (X) represents the majority of stem cross-sectional area, while the area of pith (p) is relatively small. In contrast, a large pentagonal pith is surrounded by a relatively narrow layer of secondary xylem in the distal segment (b). Signs of juvenility are apparent in the distal segment. Clusters of primary xylem and secondary xylem formed early after the transition to secondary growth are apparent in the distal segment cross-section (arrowheads). Scale bars = 1 mm

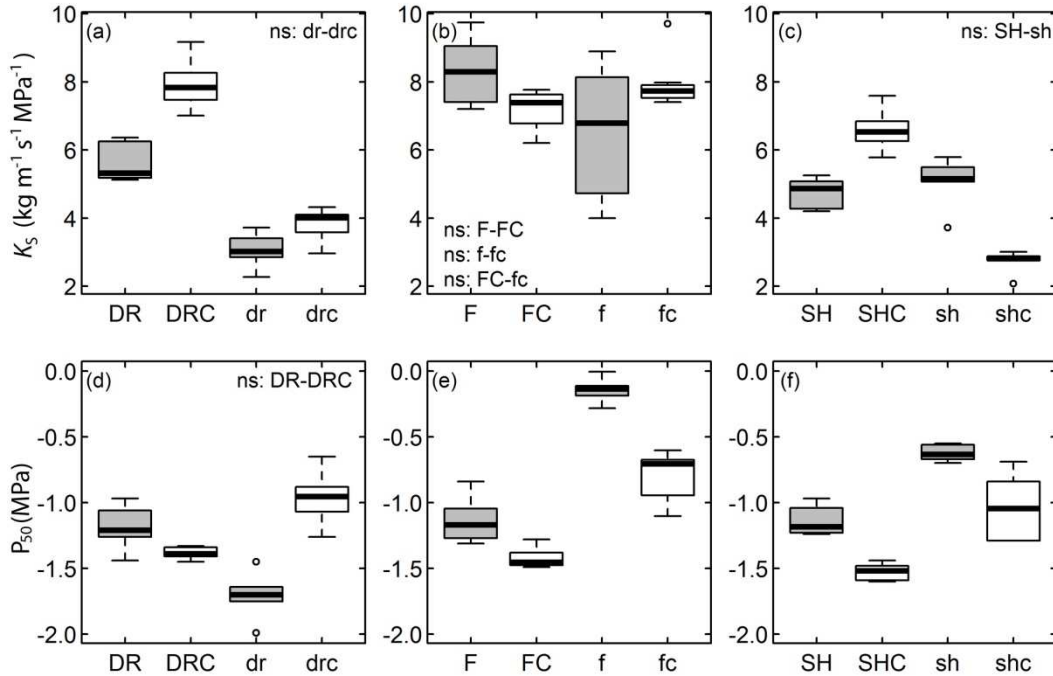


Figure 2-4: Variation in xylem hydraulic function: (a-c) xylem-specific hydraulic conductivity (K_S) and (d-f) the pressure at 50% loss of conductivity (P_{50}) of basal (capital letters) and distal (lower case letters) stem segments in hybrid poplar saplings grown under drought (DR, dr), nitrogen fertilization (F, f), shade (SH, sh), and control conditions (DRC, drc; FC, fc; SHC, shc). In each box plot, the median (50th percentile) is represented with a heavy line inside of the central box. The horizontal borders of the box represent the 25th and 75th percentiles. Whiskers indicate the 10th and 90th percentiles with outliers shown as circles. Non-significant (ns) results for a specified comparison of means are indicated. $n=5-8$.

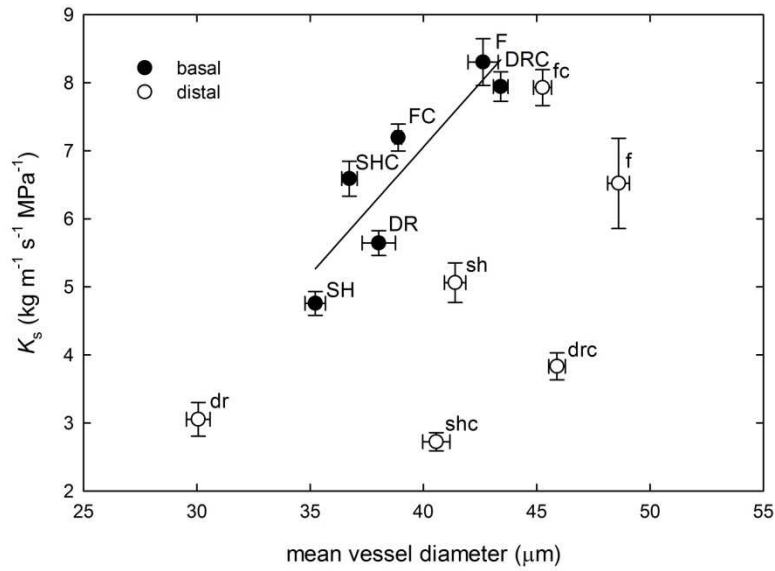


Figure 2-5: Relationship between mean vessel diameter and xylem-specific hydraulic conductivity (K_S) for basal (filled circles, capital letters) and distal (open circles, lower case letters) stem segments in hybrid poplar saplings grown under drought (DR, dr), nitrogen fertilization (F, f), shade (SH, sh) and control conditions (DRC, drc; FC, fc; SHC, shc). Means \pm SE.

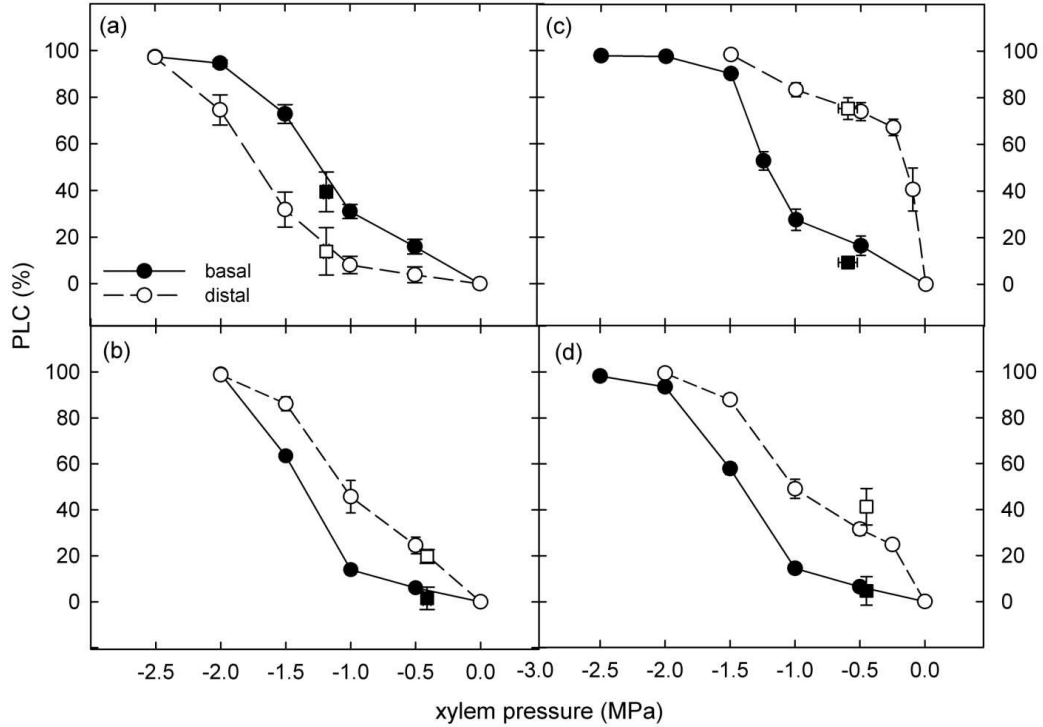


Figure 2-6: Vulnerability curves (circles) and native values of percent loss of conductivity (PLC) plotted against the native xylem pressure (squares) for basal (filled symbols) and distal (open symbols) stem segments in saplings grown under (a) drought (DR) and (b) well-watered conditions (DRC), and under (c) high N (F) and (d) low N (FC) fertilization. Note the profoundly different shape of the vulnerability curves in distal segments (open circles), ranging from (a) sigmoidal through (b,d) linear to (c) r-shaped.

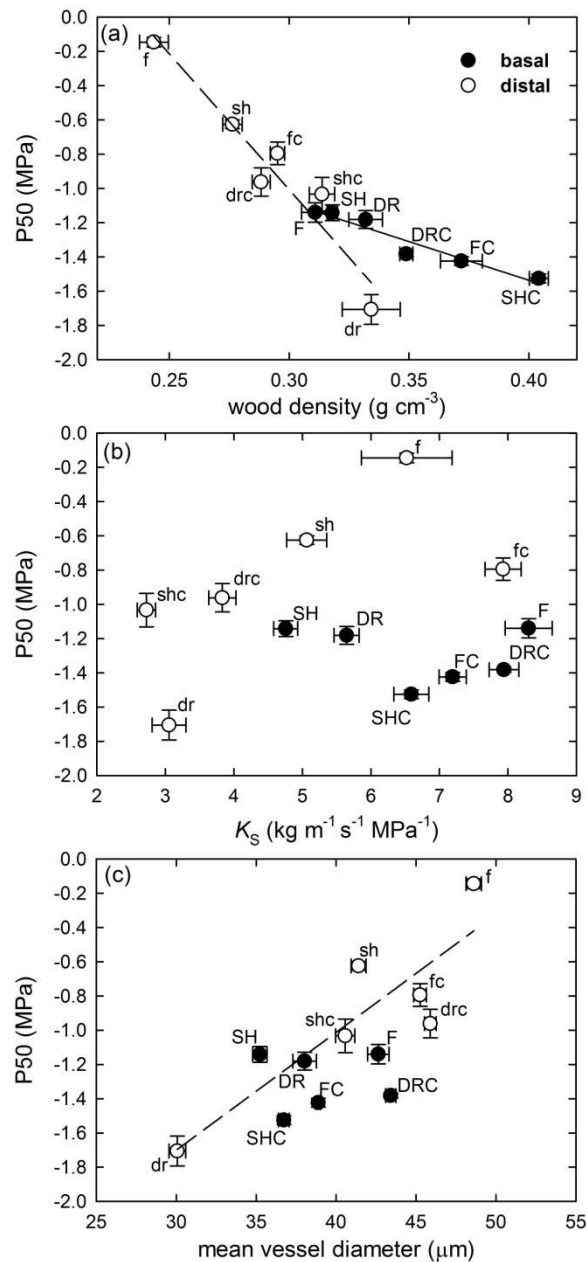


Figure 2-7: Relationship between P50 and (a) wood density, (b) xylem-specific hydraulic conductivity (K_s) and (c) mean vessel diameter for basal (filled circles, capital letters) and distal (open circles, lower case letters) stem segments in hybrid poplar saplings grown under drought (DR, dr), nitrogen fertilization (F, f), shade (SH, sh) and control conditions (DRC, drc; FC, fc; SHC, shc). Means \pm SE. Solid and dashed lines represent significant linear correlations for basal and distal segments, respectively.

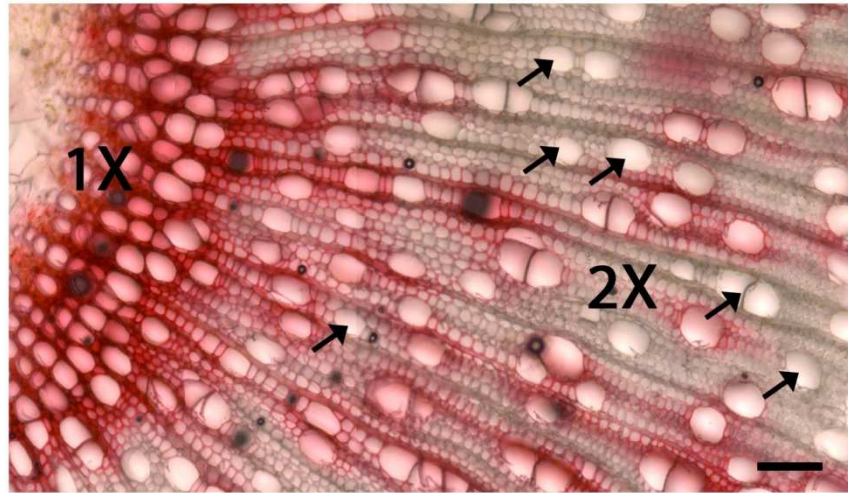


Figure 2-8: Cross-section of a distal stem segment perfused with safranin dye to visualize functional and embolised xylem conduits. A number of non-stained, presumably embolised, vessels (arrows) occurs in the secondary xylem region (2X), while primary xylem (1X) vessels appear mostly functional. Scale bar = 100 μm .

2.8 REFERENCES

- Awad H., Barigah T., Badel E., Cochard H. & Herbette S. (2010) Poplar vulnerability to xylem cavitation acclimates to drier soil conditions. *Physiologia Plantarum*, **139**, 280-288.
- Barigah T.S., Ibrahim T., Bogard A., Faivre-Vuillin B., Lagneau L.A., Montpied P. & Dreyer E. (2006) Irradiance-induced plasticity in the hydraulic properties of saplings of different temperate broad-leaved forest tree species. *Tree Physiology*, **26**, 1505-1516.
- Beikircher B. & Mayr S. (2009) Intraspecific differences in drought tolerance and acclimation in hydraulics of *Ligustrum vulgare* and *Viburnum lantana*. *Tree Physiology*, **29**, 765-775.
- Braatne J., Rood S. & Heilman P. (1996) Life history, ecology, and conservation of riparian cottonwoods in North America. In: *Biology of Populus and its implications for management and conservation* (eds R. Stettler, H.J. Bradshaw, P. Heilman, & T. Hinckley), pp. 57-85. NRC Research Press, Ottawa, ON, Canada.
- Bradshaw H.D., Ceulemans R., Davis J. & Stettler R. (2000) Emerging model systems in plant biology: Poplar (*Populus*) as a model forest tree. *Journal of Plant Growth Regulation*, **19**, 306-313.
- Carlquist S. (1988) *Comparative wood anatomy*. Springer-Verlag, Berlin.
- Carlquist S. (2001) *Comparative wood anatomy: systematic, ecological, and evolutionary aspects of dicotyledon wood*. (2nd ed.). Springer Verlag, Berlin.
- Chave J., Coomes D., Jansen S., Lewis S.L., Swenson N.G. & Zanne A.E. (2009) Towards a worldwide wood economics spectrum. *Ecology Letters*, **12**, 351-366.
- Choat B., Drayton W.M., Brodersen C., Matthews M.A., Shackel K.A., Wada H. & McElrone A.J. (2010) Measurement of vulnerability to water stress-induced cavitation in grapevine: a comparison of four techniques applied to a long-vesseled species. *Plant Cell and Environment*, **33**, 1502-1512.
- Choat B., Lahr E.C., Melcher P.J., Zwieniecki M.A. & Holbrook N.M. (2005) The spatial pattern of air seeding thresholds in mature sugar maple trees. *Plant Cell and Environment*, **28**, 1082-1089.
- Christman M.A., Sperry J.S. & Smith D.D. (2012) Rare pits, large vessels and extreme vulnerability to cavitation in a ring-porous tree species. *New Phytologist*, **193**, 713-720.
- Cochard H., Herbette S., Barigah T., Badel E., Ennajeh M. & Vilagrosa A. (2010) Does sample length influence the shape of xylem embolism vulnerability curves? A test with the Cavitron spinning technique. *Plant Cell and Environment*, **33**, 1543-1552.
- Cochard H., Lemoine D. & Dreyer E. (1999) The effects of acclimation to sunlight on the xylem vulnerability to embolism in *Fagus sylvatica* L. *Plant Cell and Environment*, **22**, 101-108.
- Fichot R., Barigah T.S., Chamaillard S., Le Thiec D., Laurans F., Cochard H. & Brignolas F. (2010) Common trade-offs between xylem resistance to cavitation and other physiological traits do not hold among unrelated

- Populus deltoides* x *Populus nigra* hybrids. *Plant, Cell and Environment*, **33**, 1553-1568.
- Fonti P., von Arx G., Garcia-Gonzalez I., Eilmann B., Sass-Klaassen U., Gaertner H. & Eckstein D. (2010) Studying global change through investigation of the plastic responses of xylem anatomy in tree rings. *New Phytologist*, **185**, 42-53.
- Galvez D.A. & Tyree M.T. (2009) Impact of simulated herbivory on water relations of aspen (*Populus tremuloides*) seedlings: the role of new tissue in the hydraulic conductivity recovery cycle. *Oecologia*, **161**, 665-671.
- Gea-Izquierdo G., Fonti P., Cherubini P., Martin-Benito D., Chaar H. & Canellas I. (2012) Xylem hydraulic adjustment and growth response of *Quercus canariensis* Willd. to climatic variability. *Tree Physiology*, **32**, 401-413.
- Hacke U. & Sauter J.J. (1996) Drought-induced xylem dysfunction in petioles, branches, and roots of *Populus balsamifera* L. and *Alnus glutinosa* (L.) Gaertn. *Plant Physiology*, **111**, 413-417.
- Hacke U.G., Jacobsen A.L. & Pratt R.B. (2009) Xylem function of arid-land shrubs from California, USA: an ecological and evolutionary analysis. *Plant Cell and Environment*, **32**, 1324-1333.
- Hacke U.G., Plavcová L., Almeida-Rodriguez A., King-Jones S., Zhou W. & Cooke J.E.K. (2010) Influence of nitrogen fertilization on xylem traits and aquaporin expression in stems of hybrid poplar. *Tree Physiology*, **30**, 1016-1025.
- Hacke U.G., Sperry J.S., Ewers B.E., Ellsworth D.S., Schäfer K.V.R. & Oren R. (2000) Influence of soil porosity on water use in *Pinus taeda*. *Oecologia*, **124**, 495-505.
- Hacke U.G., Sperry J.S., Pockman W.T., Davis S.D. & McCulloh K.A. (2001a) Trends in wood density and structure are linked to prevention of xylem implosion by negative pressure. *Oecologia*, **126**, 457-461.
- Hacke U.G., Sperry J.S., Wheeler J.K. & Castro L. (2006) Scaling of angiosperm xylem structure with safety and efficiency. *Tree Physiology*, **26**, 689-701.
- Hacke U.G., Stiller V., Sperry J.S., Pittermann J. & McCulloh K.A. (2001b) Cavitation fatigue. Embolism and refilling cycles can weaken the cavitation resistance of xylem. *Plant Physiology*, **125**, 779-786.
- Harrington R.A. & Fownes J.H. (1993) Allometry and growth of planted versus coppice stands of four fast-growing tropical tree species. *Forest Ecology and Management*, **56**, 315-327.
- Harvey H.P. & van den Driessche R. (1997) Nutrition, xylem cavitation and drought resistance in hybrid poplar. *Tree Physiology*, **17**, 647-654.
- Harvey H.P. & van den Driessche R. (1999) Nitrogen and potassium effects on xylem cavitation and water-use efficiency in poplars. *Tree Physiology*, **19**, 943-950.
- Hocking D. (1971) Preparation and use of a nutrient solution for culturing seedlings of lodgepole pine and white spruce, with selected bibliography. Northern Forest Research Centre Information Report Nor-XI. Canadian Forest Service, Department of the Environment, Edmonton, Canada.

- Hogg E.H., Brandt J.P. & Michaellian M. (2008) Impacts of a regional drought on the productivity, dieback, and biomass of western Canadian aspen forests. *Canadian Journal of Forest Research*, **38**, 1373-1384.
- Hogg E.H., Hart M. & Lieffers V.J. (2002) White tree rings formed in trembling aspen saplings following experimental defoliation. *Canadian Journal of Forest Research*, **32**, 1929-1934.
- Jacobsen A.L., Ewers F.W., Pratt R.B., Paddock W.A. & Davis S.D. (2005) Do xylem fibers affect vessel cavitation resistance? *Plant Physiology*, **139**, 546-556.
- Jacobsen A.L. & Pratt R.B. (2012) No evidence for an open vessel effect in centrifuge-based vulnerability curves of a long-vesselled liana (*Vitis vinifera*). *New Phytologist*, **194**, 982-990.
- Lambers H., Chapin F.S. & Pons T.L. (1998) *Plant physiological ecology*. Springer-Verlag, New York.
- Larcher W. (2003) *Physiological plant ecology*. Springer-Verlag Berlin Heidelberg New York
- Lens F., Sperry J.S., Christman M.A., Choat B., Rabaey D. & Jansen S. (2011) Testing hypotheses that link wood anatomy to cavitation resistance and hydraulic conductivity in the genus *Acer*. *New Phytologist*, **190**, 709-723.
- Lieffers V.J., Messier C., Stadt K.J., Gendron F. & Comeau P.G. (1999) Predicting and managing light in the understory of boreal forests. *Canadian Journal of Forest Research*, **29**, 796-811.
- Lu Y., Equiza M.A., Deng X. & Tyree M.T. (2010) Recovery of *Populus tremuloides* seedlings following severe drought causing total leaf mortality and extreme stem embolism. *Physiologia Plantarum*, **140**, 246-257.
- Maherali H., Pockman W.T. & Jackson R.B. (2004) Adaptive variation in the vulnerability of woody plants to xylem cavitation. *Ecology*, **85**, 2184-2199.
- Mayr S., Beikircher B., Obkircher M.-A. & Schmid P. (2010) Hydraulic plasticity and limitations of alpine Rhododendron species. *Oecologia*, **164**, 321-330.
- McCulloh K., Sperry J.S., Lachenbruch B., Meinzer F.C., Reich P.B. & Voelker S. (2010) Moving water well: comparing hydraulic efficiency in twigs and trunks of coniferous, ring-porous, and diffuse-porous saplings from temperate and tropical forests. *New Phytologist*, **186**, 439-450.
- McCulloh K.A., Johnson D.M., Meinzer F.C., Voelker S.L., Lachenbruch B. & Domec J.-C. (2012) Hydraulic architecture of two species differing in wood density: opposing strategies in co-occurring tropical pioneer trees. *Plant Cell and Environment*, **35**, 116-125.
- Niklas K.J. (1992) *Plant Biomechanics*. University of Chicago Press, Chicago.
- Pitre F.E., Cooke J.E.K. & Mackay J.J. (2007a) Short-term effects of nitrogen availability on wood formation and fibre properties in hybrid poplar. *Trees-Structure and Function*, **21**, 249-259.
- Pitre F.E., Pollet B., Lafarguette F., Cooke J.E.K., MacKay J.J. & Lapierre C. (2007b) Effects of increased nitrogen supply on the lignification of poplar wood. *Journal of Agricultural and Food Chemistry*, **55**, 10306-10314.

- Pratt R.B., Jacobsen A.L., Ewers F.W. & Davis S.D. (2007) Relationships among xylem transport, biomechanics and storage in stems and roots of nine Rhamnaceae species of the California chaparral. *New Phytologist*, **174**, 787-798.
- Raimondo F., Trifilo P., Lo Gullo M.A., Buffa R., Nardini A. & Salleo S. (2009) Effects of reduced irradiance on hydraulic architecture and water relations of two olive clones with different growth potentials. *Environmental and Experimental Botany*, **66**, 249-256.
- Rennenberg H., Wildhagen H. & Ehling B. (2010) Nitrogen nutrition of poplar trees. *Plant Biology*, **12**, 275-291.
- Rood S.B., Patino S., Coombs K. & Tyree M.T. (2000) Branch sacrifice: cavitation-associated drought adaptation of riparian cottonwoods. *Trees*, **14**, 248-257.
- Savva Y.V., Schweingruber F.H., Vaganov E.A. & Milyutin L.I. (2003) Influence of climate changes on tree-ring characteristics of scots pine provenances in southern Siberia (forest-steppe). *IAWA Journal*, **24**, 371-383.
- Schultz H.R. & Matthews M.A. (1993) Xylem development and hydraulic conductance in sun and shade shoots of grapevine (*Vitis vinifera* L) - Evidence that low-light uncouples water transport capacity from leaf area. *Planta*, **190**, 393-406.
- Shinozaki K., Yoda K., Hozumi K. & Kira T. (1964) A quantitative analysis of plant form-the pipe model theory: I. Basic analysis. *Japanese Journal of Ecology*, **14**, 97-105.
- Šmilauer P. (2007) *Moderní regresní metody (Modern regression methods)*. Faculty of Biological Sciences, University of South Bohemia, the Czech Republic.
- Sokal R.R. & Rohlf F. (1995) *Biometry: the principles and practice of statistics in biological research*. W.H. Freeman & Company, New York, NY, USA.
- Sperry J.S. (2011) Hydraulics of vascular water transport. In: *Mechanical integration of plant cells and plants* (ed P. Wojtaszek), pp. 303-327.
- Sperry J.S., Christman M.A., Torres-Ruiz J.M., Taneda H. & Smith D.D. (2012) Vulnerability curves by centrifugation: is there an open vessel artefact, and are 'r' shaped curves necessarily invalid? *Plant Cell and Environment*, **35**, 601-610.
- Sperry J.S., Hacke U.G. & Pittermann J. (2006) Size and function in conifer tracheids and angiosperm vessels. *American Journal of Botany*, **93**, 1490-1500.
- Sperry J.S. & Ikeda T. (1997) Xylem cavitation in roots and stems of Douglas-fir and white fir. *Tree Physiology*, **17**, 275-280.
- Sperry J.S., Perry A.H. & Sullivan J.E.M. (1991) Pit membrane degradation and air-embolism formation in ageing xylem vessels of *Populus tremuloides* Michx. *Journal of Experimental Botany*, **42**, 1399-1406.
- Sperry J.S. & Saliendra N.Z. (1994) Intra-and inter-plant variation in xylem cavitation in *Betula occidentalis*. *Plant, Cell and Environment*, **17**, 1233-1241.

- Stiller V. (2009) Soil salinity and drought alter wood density and vulnerability to xylem cavitation of baldcypress (*Taxodium distichum* (L.) Rich.) seedlings. *Environmental and Experimental Botany*, **67**, 164-171.
- Taneda H. & Sperry J.S. (2008) A case-study of water transport in co-occurring ring- versus diffuse-porous trees: contrasts in water-status, conducting capacity, cavitation and vessel refilling. *Tree Physiology*, **28**, 1641-1651.
- Tyree M.T. & Ewers F.W. (1991) Tansley review no. 34: The hydraulic architecture of trees and other woody plants. *New Phytologist*, **119**, 345-360.
- Tyree M.T., Kolb K.J., Rood S.B. & Patino S. (1994) Vulnerability to drought-induced cavitation of riparian cottonwoods in Alberta: A possible factor in the decline of the ecosystem? *Tree Physiology*, **14**, 455-466.
- Wheeler E.A., Baas P. & Rodgers S. (2007) Variations in dicot wood anatomy: a global analysis based on the insidewood database. *IAWA Journal*, **28**, 229-258.
- Wikberg J. & Ögren E. (2007) Variation in drought resistance, drought acclimation and water conservation in four willow cultivars used for biomass production. *Tree Physiology*, **27**, 1339-1346.
- Zimmermann M.H. (1983) *Xylem structure and the ascent of sap*. Springer-Verlag, Berlin.

3. Gene expression patterns underlying changes in xylem structure and function in response to increased nitrogen availability in hybrid poplar²

3.1 INTRODUCTION

Wood (i.e., secondary xylem produced by cambial activity) of poplars represents an important raw material of great economic value (Balatinecz, Kretschmann & Leclercq, 2001). In the last few decades, the importance of poplars further increased as their biomass provides a promising bioenergy feedstock that could help to reduce our dependency on fossil fuels (Sannigrahi, Ragauskas & Tuskan, 2010). From a biological perspective, wood serves three main functions that are fundamental for plant growth. These functions are 1) long distance transport of water and nutrients from roots to transpiring leaves, 2) providing mechanical support to the plant body, and 3) storage of carbohydrates, water and various other specialized compounds. In a typical hardwood such as poplar, these three functions are divided among three different cell types – vessel elements, fibers and living parenchyma, respectively.

Vessel elements and fibers represent 85-90% (vol/vol) of mature wood in poplar (Mellerowicz, Baucher, Sundberg *et al.*, 2001). Hydraulic and mechanical properties of wood are closely associated with the physical structure of these cells. For instance, xylem hydraulic conductivity is proportional to the vessel diameter to the fourth power as predicted by the Hagen-Poiseuille equation (Tyree & Zimmermann, 2002), and mechanical parameters such as modulus of rupture have been linked with wood density and fiber lumen diameters (Onoda, Richards & Westoby, 2010, Pratt, Jacobsen, Ewers *et al.*, 2007, Woodrum, Ewers & Telewski, 2003). Moreover, hydraulic and mechanical functions appear to be closely integrated as strong mechanical support is required to prevent implosion of xylem conduits under high xylem tension (Hacke, Sperry, Pockman *et al.*, 2001, Jacobsen, Ewers, Pratt *et al.*, 2005, Pittermann, Sperry, Wheeler *et al.*, 2006). Furthermore, wood density and fiber length together with the chemical composition of wood are critical factors that determine its material properties and hence its suitability for a specific end use in the wood processing industry.

² A version of this chapter has been accepted for publication. Plavcová L, Hacke UG, Almeida-Rodriguez AM, Li Eryang & Douglas CJ 2012. *Plant, Cell & Environment*.

Wood structure is established during xylogenesis as a result of cambial activity. Wood is formed through a series of precisely regulated developmental steps that include cell division, cell expansion, secondary cell wall deposition and programmed cell death (Samuels, Kaneda & Rensing, 2006). Many genes influencing xylem differentiation in poplar have been recently identified, including several key regulatory and structural genes (e.g., Aspeborg, Schrader, Coutinho *et al.*, 2005, Groover, Nieminen, Helariutta *et al.*, 2010, Zhong, McCarthy, Lee *et al.*, 2011). The process of xylogenesis and the resulting xylem phenotype are strongly affected by environmental conditions such as water (Arend & Fromm, 2007), nutrient (Hacke, Plavcová, Almeida-Rodriguez *et al.*, 2010, Lautner, Ehlting, Windeisen *et al.*, 2007) and light availability (Plavcová, Hacke & Sperry, 2011). The developmental program giving rise to specific physiological and anatomical xylem phenotypes is underpinned by changes in gene expression as demonstrated by recent studies describing transcriptional changes in developing xylem of poplars subjected to drought (Berta, Giovannelli, Sebastiani *et al.*, 2010) and high salinity (Janz, Lautner, Wildhagen *et al.*, 2012). However, more research is needed to better understand the molecular mechanisms underlying xylem phenotypic plasticity as it is likely that expression of different genes is altered by different environmental triggers.

In this study, we used nitrogen (N) fertilization to perturb the xylem phenotype of hybrid poplar (*Populus trichocarpa* × *deltoides*, clone H11-11) saplings and investigated corresponding changes in gene expression. Nitrogen fertilization has a profound effect on poplar growth and development including xylogenesis (Hacke *et al.*, 2010, Harvey & van den Driessche, 1999, Pitre, Cooke & Mackay, 2007a, Pitre, Pollet, Lafarguette *et al.*, 2007b). The influence of nitrogen supply on the expression of selected genes has been evaluated in poplar leaves, roots, phloem and bulk xylem (Cooke, Brown, Wu *et al.*, 2003, Cooke, Martin & Davis, 2005, Ehlting, Dluzniewska, Dietrich *et al.*, 2007, Hacke *et al.*, 2010). To our knowledge, there is only one genome-wide study focused on the expression of nitrogen availability-related genes in the cambial region of poplar (Pitre, Lafarguette, Boyle *et al.*, 2010), and this study was specifically designed to compare the effects of nitrogen fertilization and stem leaning on wood formation. In contrast, our study was designed to explore changes in gene expression that may underlie traits related to xylem water transport. Our goal was to identify candidate genes that may be linked with increased radial growth, wide vessel diameters and decreased wood density that we expected to be differentially expressed in poplars growing under high N availability.

3.2 METHODS

3.2.1 Plant material

Saplings of hybrid poplar (*Populus trichocarpa* × *deltoides*, clone H11-11) were produced from rooted cuttings and maintained in a growth chamber under the following conditions: 16/8 hour day/night cycle, 24/18 °C day/night temperature, ca. 75% daytime relative humidity, photon flux density of ca. 400 $\mu\text{mol m}^{-2} \text{s}^{-1}$. During the initial phase of sapling establishment, plants were kept in 6 L pots filled with a commercial potting mix (Sunshine Mix LA4, Sun Gro Horticulture Canada Ltd., Vancouver, BC, Canada) and fertilized once a week with 500 ml of N-P-K: 20-20-20 fertilizer (1 g/L dilution) (Plant Product Brampton, Ontario, Canada). After 6 weeks, when the saplings were ca. 70 cm in height, plants were randomly assigned to either low or high nitrogen (N) treatment. The fertilizer was applied every other day as either 0.75 mM or 7.5 mM NH_4NO_3 in 0.5 x Hocking's complete nutrient solution (Hocking, 1971) for low and high N plants, respectively. To avoid drought stress, plants were irrigated with tap water on the days when the fertilizer was not applied. The fertilization treatment was applied for 33 days after which plants were harvested. Final height and stem basal diameter (D_{stem}) of each sapling were assessed with a measuring tape and calipers, respectively. Leaf area (A_L) was measured with an area meter (LI-3100, Li-Cor, Lincoln, NE, USA). Stem segments ca. 25 cm in length were excised 5 cm above the root collar, placed in a dark plastic bag with a wet paper towel and stored at 4 °C until hydraulic measurements were conducted. The same stem segments were later used for anatomical measurements. For RNA extraction, developing xylem tissue was collected from 50 cm long stem segments distally adjacent to the segments used for hydraulic and anatomical measurements. In both treatments, the secondary xylem was well developed and no obvious differences in stem maturation were apparent in this region of the stem. To collect the tissue, the bark was peeled from the stem and discarded. Subsequently, the exposed secondary xylem tissue was scraped using a fresh razor blade until resistance could be felt and the color of the scraping changed, indicating that fully mature xylem cells were reached. The tissue was immediately frozen in liquid nitrogen and stored at -80 °C. Careful preliminary observations using a light microscope revealed that the bark separates from the stem in the cambial region. Thus, the tissue scraped from the outermost layer of the exposed xylem contained newly formed expanding xylem cells and cells that underwent

secondary wall thickening. Although this sampling method did not allow sampling specific developmental stages, it has been widely used to analyze transcript and protein levels in developing secondary xylem (Berta *et al.*, 2010, Gray-Mitsumune, Mellerowicz, Abe *et al.*, 2004, Song, Xi, Shen *et al.*, 2011).

3.2.2 Xylem anatomy

Xylem anatomy was analyzed using light microscopy as described previously (Plavcová *et al.*, 2011). Five or six individual stems were measured for each treatment. Exposed cross-sectional surface of stems was captured with a digital camera attached to a stereomicroscope (MS5; Leica Microsystems, Wetzlar, Germany) at 10-16 x magnification. Xylem cross-sectional area (A_x), excluding pith and bark, was measured with an image analysis software (ImagePro Plus version 6.1, Media Cybernetics, Silver Spring, MD, USA). Vessel lumen diameters were measured in two radial sectors on stem cross-sections prepared with a sliding microtome and stained with toluidine blue. Between 300-400 vessels observed at 200 x magnification were measured from each stem. Since fibers are much narrower than vessels, resin embedded samples and 400 x magnification were used to produce reliable measurements of fiber lumen diameters. 200-300 fibers from at least 3 different randomly selected areas were measured for each stem. In addition, measurements of fiber double wall thickness were conducted on at least 80 fiber pairs. Only fibers that did not have a conspicuous gelatinous layer were selected for measurements of lumen diameters and double wall thickness. Vessel element and fiber length measurements were conducted on macerated xylem tissue. At least 100 individual cells were photographed under 100 x magnification and measured for each stem. Vessel length was assessed using the silicone injection method (Sperry, Hacke & Wheeler, 2005). Finally, wood density was measured by the water displacement method. Debarked stem segments ca. 2 cm in length were longitudinally split with a razor blade and the pith was removed. Samples were submersed in a beaker of water on a balance to measure the wood fresh volume. Samples were then oven-dried at 70 °C for 48 hours and weighed. Wood density was expressed as a dry weight per fresh volume. For statistical analysis, an independent two sample t-test was used to compare the differences in means between the treatments. Prior to the analysis, normality and homogeneity of variances were graphically checked.

3.2.3 Hydraulic measurements

Stem hydraulic conductivity and vulnerability to cavitation were measured following the standard methodology described in detail in Hacke et al. (2010). Stem segments 14.2 cm in length were flushed with standard measuring solution (20 mM KCl +1 mM CaCl₂ filtered at 0.2 μm) for 20 min at 50 kPa. Subsequently, the gravity-driven flow through the segments was recorded using an electronic balance (CP225, Sartorius, Göttingen, Germany) interfaced with a computer. The value of maximal conductivity was normalized by xylem cross-sectional area (A_X) to calculate the xylem-specific hydraulic conductivity (K_S). After measuring maximal conductivity, stem segments were fixed into a custom-built centrifuge rotor and spun to progressively more negative pressures with the incremental steps of 0.25 or 0.5 MPa. Hydraulic conductivity was measured after each pressure increment. The percentage loss of hydraulic conductivity was plotted against the corresponding xylem pressure to generate vulnerability curves. Data points were fitted with a Weibull function and the xylem pressure corresponding to 50% loss of conductivity (P_{50}) was calculated for each segment.

3.2.4 Microarray analysis

Total RNA was extracted from six individual poplar saplings per treatment using the hexadecyltrimethylammonium bromide (CTAB) extraction protocol of Chang et al. (1993). Total RNA quality for each individual sample was assessed with an Agilent 2100 bioanalyzer prior to microarray analysis. Samples with a RNA integrity number (RIN) value of greater than or equal to 8.0 were deemed to be acceptable for microarray analysis. Samples were prepared following NimbleGen's Arrays User Guide (Gene Expression Analysis version 3.2). 10 μg of each total RNA was converted to double stranded (ds) cDNA with the Invitrogen SuperScript Double-Stranded cDNA Synthesis Kit, 1 μg of each ds cDNA was fluorescently labeled using the NimbleGen One-Color DNA Labeling Kit, and 4 μg of each Cy3-labeled sample was hybridized on Roche NimbleGen poplar gene expression microarrays (Design Name Populus 135K EXP HX12 090828). These arrays target 55,794 gene models predicted in the *Populus trichocarpa* genome with each gene model represented by 3 unique 60mer probes. Arrays were scanned at a 5 μm resolution with a Molecular Devices GenePix 4200AL scanner. NimbleScan version 2.5 was used for quantitation and robust multichip average (RMA) normalization of data which included quantile normalization and background subtraction. Agilent's GeneSpring 7.3.1 was used to analyze the normalized data. To find significantly differentially regulated

genes, fold changes between the compared groups and *P* values gained from t-tests between the same groups were calculated. The *P* values were further corrected for multiple testing (MTC) using the method of Benjamini and Hochberg (1995). The t-tests were performed on normalized data that had been log-transformed and the variances were not assumed to be equal between sample groups. The genes with MTC *P* value ≤ 0.05 and fold change ± 1.5 were considered to be significantly differentially regulated. The robustness of the selected cut-off criteria was validated with quantitative real time-PCR (qRT-PCR) analysis. The gene model names and annotation is based on the Phytozome v2.2 version of the *Populus* genome (ftp://ftp.jgi-psf.org/pub/JGI_data/phytozome/v7.0/Trichocarpa/annotation/).

3.2.5 Microarray qRT-PCR validation

One microgram of total RNA was treated with DNase I (Invitrogen, Burlington, ON, Canada) and used for first strand cDNA synthesis using oligo(dT)23VN (IDT, Coralville, IA, USA) and SuperScript II reverse transcriptase (Invitrogen) according to the manufacturer's protocols. Four potential reference genes were identified by screening the microarray data for cDNAs whose signals remained apparently unchanged (fold-difference ratios between 0.97 and 1.05). Eight candidate genes were also selected in the microarray and included in the validation assay. Gene-specific qRT-PCR primers were designed mainly in the 3' untranslated (UTR)-region using Primer Express v3 (Applied Biosystems, Foster City, CA, USA) (Table 3-1). For each gene, PCR efficiency (*E*) was determined from a four point cDNA serial dilution, according to: $E = 10^{-1/\text{slope}}$. The stability of the gene expression profile of the four potential reference genes was evaluated in three biological replicates for each of the two fertilization treatments. The two most stable reference genes were selected for the qRT-PCR assay (*Protein phosphatase 2A (PP2A)*, *POPTR_0010s13760*; and *Yellow-leaf-specific gene 8 (YLS8)*, *POPTR_0007s07660*). Real-Time PCR was performed on a 7900 HT Fast Real-Time PCR system (Applied Biosystems). Assays were carried out in 384-well plates. Three biological replicates, each with three technical replicates, were assayed for high N and low N nitrogen treatments. A negative control (no cDNA template) was included for every gene. PCR was carried out in a final volume of 10 μl including a final concentration of 20 ng of cDNA, 0.4 μM of each primer (IDT), 1 x master mix containing 0.2 mM dNTPs, 0.3 U Platinum Taq polymerase (Invitrogen), 0.25 x SYBR Green and 0.1 x ROX. PCR conditions were as

previously described (Almeida-Rodriguez, Cooke, Yeh *et al.*, 2010). Samples were subjected to auto Ct (cycle threshold) for analysis, and dissociation curves were verified for each of the genes. Changes in gene expression of nine target genes (including *YLS8*) were calculated according to Pfaffl (2001), relative to the reference gene *PP2A*.

3.3 RESULTS AND DISCUSSION

3.3.1 Nitrogen availability affects xylem structure and function in hybrid poplar

We exposed clonally propagated hybrid poplar ramets (*Populus trichocarpa* × *deltooides*, clone H11-11) to either low or high levels of ammonium nitrate. As expected, nitrogen fertilization enhanced growth of poplar saplings in both height and girth (Table 3-2). High N availability influenced not only the amount but also the structure of the secondary xylem produced. Substantial differences in xylem cell dimensions and wall reinforcement were identified when low versus high N plants were compared (Table 3-2, Fig. 3-1). More specifically, vessel and fiber lumens were significantly wider (Fig. 3-2) and the average vessel element length was higher in high N plants (Table 3-3). In contrast, the mean vessel length was not significantly different (Table 3-3), although a slight tendency towards longer vessels was identified in high N plants (Fig. 3-3). Similarly, the average fiber length did not significantly differ between the treatments (Table 3-3); however, a decrease in the proportion of fibers longer than 700 μm was apparent in high N plants (Fig. 3-3). Lower fiber length in high N-treated plants has been previously reported as one of the hallmarks of nitrogen fertilization in this hybrid poplar genotype (Pitre *et al.*, 2007a, Pitre *et al.*, 2010). These studies have also reported the increased occurrence of fibers with thick secondary cell walls resembling a gelatinous layer typical for the reaction wood in high N-treated plants of this genotype. While we noticed the gelatinous fibers in our plant material as well, we found such layers in plants treated with both high N and low N. Furthermore, the gelatinous fibers were found only in certain regions of cross-sections usually forming a distinct band around the stem. In regions where fibers lacked the gelatinous layer, the regular secondary cell wall was thinner in high N in comparison with low N plants (Fig. 3-1, Table 3-3). In agreement with these results, lower secondary cell wall thickness has been reported in three poplar species subjected to nitrogen fertilization (Luo,

Langenfeld-Heyser, Calfapietra *et al.*, 2005). Thus, while nitrogen fertilization may stimulate gelatinous layer production (Pitre *et al.*, 2007a, Pitre *et al.*, 2010), it also negatively affects the deposition of the regular secondary cell wall. Increased vessel and fiber lumen diameters and lower wall reinforcement in fibers translated into lower wood density in high N plants (Table 3-3).

The changes in xylem structure were paralleled by differences in hydraulic properties, which have important implications for plant water use. High N plants with larger vessel diameters transported water more efficiently, as measured by average xylem-specific conductivity (Fig. 3-4a), than low N plants with narrower vessel diameters. More efficient water transport is correlated with the necessity to sustain the larger areas of transpiring leaves in high N treated plants (Table 3-2). However, high N plants were more vulnerable to cavitation than low N plants, as shown by the less negative P_{50} values in high N plants (Fig. 3-4b). Thus, although more efficient, water transport in high N plants was more prone to dysfunction under drought conditions. This finding is in agreement with previous work (Hacke *et al.*, 2010, Harvey & van den Driessche, 1999).

3.3.2 Nitrogen availability evokes transcriptional changes in developing xylem

To investigate the molecular basis for the developmental changes leading to the xylem phenotypes described above, we carried out gene expression profiling of developing xylem isolated from high N and low N treated plants. RNA was isolated from developing secondary xylem, exposed by peeling bark from stem segments adjacent to segments used for hydraulic and anatomical measurements, and hybridized to NimbleGen poplar full genome microarrays. Six biological replicates per treatment were analyzed. Expression of 49,476 gene models was detected; of those 388 non-redundant genes showed statistically significant ($P \leq 0.05$) 1.5-fold or greater changes in transcript abundance between the treatments. Out of these genes, 243 were up- and 145 down-regulated. We used quantitative qRT-PCR to independently assay expression of nine selected genes, which confirmed the reliability of the microarray analysis (Fig. 3-5).

Microarray results suggest that extensive remodeling of the poplar transcriptome accompanies changes in xylem development and secondary cell wall deposition associated with increased nitrogen availability. The potential functional roles played by differentially regulated genes in xylem development were further analyzed based on the annotations of the differentially regulated

poplar genes or their presumed *Arabidopsis* orthologs. Genes of particular interest that might be associated with various aspects of stem growth and development including xylem and secondary wall development are presented in Table 3-4 and discussed below.

Nitrogen metabolism: Several poplar genes with a putative function as amino acid transporters were differentially regulated in this study. Amino acids and amides represent the principal long-distance transport form of organic nitrogen. They are abundant in phloem and xylem sap of woody plants (Sauter & Van Cleve, 1992, Weber, Stoermer, Gessler *et al.*, 1998), from which they can be translocated radially into the cambial zone where they are required for protein and lignin biosynthesis. Among the differentially regulated genes encoding amino acid transporters were an uncharacterized amino acid transporter, a homolog of *Arabidopsis* amino acid exporter *GLUTAMINE DUMPER 3 (GDU3)* and a homolog of *BIDIRECTIONAL AMINO ACID TRANSPORTER 1 (BAT1)*. The importance of *GDU3* and *BAT1* genes in vascular tissue physiology is reinforced by the fact that they are highly expressed in the *Arabidopsis* vasculature (Dundar, 2009, Pratelli, Voll, Horst *et al.*, 2010). Two other amino acid transporter genes, namely genes homologous to *Arabidopsis* *LYSINE HISTIDINE TRANSPORTER 1 (LHT1)* and *AMINO ACID PERMEASE 3 (AAP3)*, were down regulated in high N plants. The specific role of the differentially regulated transporters cannot be elucidated from this study; nonetheless, these genes represent interesting candidates for future research on xylogenesis and nitrogen metabolism in poplar. Increased expression during secondary xylem formation in poplar has been already demonstrated for the *GDU3* and *AAP3* homologs (Dharmawardhana, Brunner & Strauss, 2010).

Furthermore, we found several genes involved in organic acid metabolism up-regulated in high N plants. Organic acids such as malate, citrate, and α -oxoglutarate are required as carbon skeletons for amino acid synthesis. The genes up-regulated in this study included two genes encoding glucose-6-phosphate dehydrogenase of the pentose phosphate pathway, and several other enzymes (phosphoenolpyruvate carboxylase, phosphoenolpyruvate carboxykinase, alanin aminotransferase and NADP-malic enzyme) related to organic acid metabolism. In agreement with our findings, an increased nitrate supply has been previously shown to induce genes involved in the synthesis of organic acids in *Arabidopsis* (Scheible, Gonzalez-Fontes, Lauerer *et al.*, 1997, Stitt, 1999). The observed patterns in gene expression suggest that due to an increased need for nitrogen

assimilation and amino acid synthesis, relatively more carbon is channeled towards the synthesis of organic acids in high N plants relative to controls, potentially leaving less carbon for polysaccharide biosynthesis. Organic acid metabolism hence represents an important intersection between nitrogen and carbon metabolism with possible implications for cell wall formation.

Carbohydrate metabolism: The microarray analysis revealed extensive changes in the transcription of genes involved in carbohydrate metabolism. Sucrose synthase (*Pt-SUS2.2*) and plant neutral invertase genes were up-regulated in high N plants. These enzymes break down sucrose into fructose and glucose monomers (Koch, 2004) and are important in carbon partitioning into cellulose biosynthesis during secondary wall development (Coleman, Yan & Mansfield, 2009, Hauch & Magel, 1998). Furthermore, a gene encoding hexokinase (*Pt-HXK1.1*), an enzyme required for activation of non-phosphorylated sugar monomers, was up-regulated. Thus, these three enzymes could act together to provide free phosphorylated sugar monomers for the biosynthesis of cellulose and/or hemicellulose. Enhanced expression of enzymes involved in sucrose metabolism is expected in fast growing high N plants (Table 3-2), considering that the developing xylem acts as a major carbon sink and carbohydrates for the production of new cells are delivered from photosynthetic source organs via the phloem, mainly in the form of sucrose.

Simple sugars such as hexoses originating from sucrose cleavage represent effective signaling molecules, and a pivotal role of sugar-mediated signaling during many developmental processes has been recognized (Rolland, Baena-Gonzalez & Sheen, 2006). Aside from its enzymatic activity, hexokinase acts as a glucose sensor, evoking changes in a variety of regulatory networks including several important hormone-related pathways (Jang, Leon, Zhou *et al.*, 1997). Similarly, trehalose has been implicated as a novel signaling molecule, and links between hexokinase and trehalose signaling pathways have been established (Smeeckens, Ma, Hanson *et al.*, 2010). Three trehalose-phosphatase genes showed increased expression in high N plants. Up-regulation of genes involved in trehalose metabolism in response to increased nitrate availability was previously reported in *Arabidopsis* (Scheible, Morcuende, Czechowski *et al.*, 2004, Wang, Okamoto, Xing *et al.*, 2003), and it has been suggested that trehalose could act as a regulator of the pentose phosphate pathway (Wang *et al.*, 2003). To our knowledge, the role of sugar sensing and signaling during xylogenesis has not yet been investigated. Nevertheless, it might provide a promising avenue for future

research considering the complex dynamics of sugars (Schrader & Sauter, 2002), hormones (Tuominen, Puech, Fink *et al.*, 1997) and transcription factors (Du & Groover, 2010) and their interplay that occurs in the cambial zone of trees.

The poplar genes potentially involved in metabolism of cell wall polysaccharides have been previously studied (Aspeborg *et al.*, 2005); however, the specific functions of many of them still remain elusive. Only a few genes encoding polysaccharide synthases and glycosyl transferases, enzymes responsible for cell wall polysaccharide synthesis, were differentially expressed in our dataset. Among them, two closely related cellulose synthase-like D genes (*Pt-ATCSLD5.1*, *Pt-ATCSLD5.2*) both showed more than 2-fold up-regulation in high N plants. These genes are likely involved in the biosynthesis of xylan (Aspeborg *et al.*, 2005, Bernal, Jensen, Harholt *et al.*, 2007), which represents a hemicellulosic polysaccharide that is abundantly present in poplar wood. Furthermore, two putative UDP-glycosyl transferase genes and a homolog to an *Arabidopsis* gene encoding plant glycogenin-like starch initiation protein 1 (*PGSIP1*) were down-regulated in high N plants. The protein encoded by poplar *PGSIP1* may have a priming function for cell wall polysaccharides (Aspeborg *et al.*, 2005). The fact that only a few polysaccharide biosynthetic genes, and especially no genes related to cellulose synthesis, were down-regulated in high N plants is surprising, considering the thin cell wall phenotype of high N plants. However, the faster radial growth in high N plants (Table 3-2) could lead to thinner cell walls even under constant biosynthetic activity. Alternatively, other processes such as polysaccharide remodeling or alternations in lignin metabolism can drive the lower cell wall thickness in high N versus low N plants.

Up-regulation of a plethora of glycoside hydrolase (GH) genes in high N plants was one of the most apparent patterns revealed in this study. Five 1,3- β -D-glucan endohydrolases (GH17 family), two α -galactosidase, three endo-1,4- β -D-glucanase (GH9 family, cellulase), α -xylosidase, β -glucosidase and xyloglucan endotransglucosylase/hydrolase all showed increased transcript abundance in high N plants. High activity of GH enzymes is typical for growing and expanding tissue (Cosgrove, 2005). The wide lumen diameters of vessels and fibers in high N plants (Fig. 3-2) indicate that more intensive cell expansion took place in the cambial region of high N treated plants. Thus, a role of at least some of these genes in primary cell wall loosening conferring increased cell wall extensibility can be implied. Three α -L-arabinofuranosidases, two glycosyl hydrolases with a putative function of endo- β -mannanases and one endo-1,4- β -D-glucanase (GH9)

showed lower expression levels in high N plants. α -L-arabinofuranosidases are most likely involved in the modification of the carbohydrate moieties of arabinogalactan proteins (AGPs) (Geisler-Lee, Geisler, Coutinho *et al.*, 2006, Kotake, Tsuchiya, Aohara *et al.*, 2006). AGPs in turn are involved in a number of developmental processes and their importance during secondary cell wall deposition has been reported in poplar (Dharmawardhana *et al.*, 2010) and pine (Zhang, Brown, Whetten *et al.*, 2003). In our dataset, two genes encoding fasciclin-like AGPs (FLAs) were differentially expressed, one up- and the other down-regulated. Several *FLAs* have been previously shown to be involved in tension wood formation (Andersson-Gunneras, Mellerowicz, Love *et al.*, 2006, Lafarguette, Leple, Dejardin *et al.*, 2004). Gelatinous layer formation is affected by nitrogen fertilization (Pitre *et al.*, 2007a); hence, it is possible that the two genes differentially expressed in this study are involved in this process.

Substantial changes in pectin composition occur during xylogenesis (Guglielmino, Liberman, Jauneau *et al.*, 1997a, Hafren, Daniel & Westermarck, 2000). We found two pectin methyl esterase (*PME*) genes up-regulated and one rhamnogalacturonate lyase gene down-regulated in high N plants. *PMEs* catalyze de-esterification of pectin molecules. In the cambial zone of poplar, *PME* activity has been localized predominantly in cell corners (Guglielmino, Liberman, Catesson *et al.*, 1997b) and a role of *PMEs* in xylem cell expansion and fiber elongation has been demonstrated (Siedlecka, Wiklund, Peronne *et al.*, 2008). Previous studies have shown that nitrogen fertilization results in shorter length of fibers in this hybrid poplar (Pitre *et al.*, 2007a, Pitre *et al.*, 2010). Our results also suggest changes in fiber intrusive growth (Fig. 3.3). Thus, it is possible that the increased activity of *PME* resulting from up-regulation of the two *PME* genes leads to calcium-mediated stiffening of the intercellular matrix and inhibited the intrusive growth of fiber tips. Alternatively, some of the genes encoding *GH* and *PME* enzymes may play a role in the secondary cell wall deposition or production of gelatinous fibers as extensive remodeling involving carbohydrate hydrolysis occurs during the secondary cell wall biosynthesis as well.

Lignin-related genes: Surprisingly, only a few genes with a predicted function in secondary cell wall lignification were differentially regulated in this study. Among the few were three laccase (*LAC*) genes that were down-regulated in high N plants. These included two homologs of *Arabidopsis LAC17* and a closely related homolog of *LAC2*. *LAC17* is known to be directly involved in lignin monomer polymerization, and *lac17* mutants have reduced lignin

deposition (Berthet, Demont-Caulet, Pollet *et al.*, 2011). Thus, a major mechanism underlying reduced lignin deposition in high N treated plants (Pitre *et al.*, 2007b) may be reduced polymerization activity.

Transcription factors: A number of transcription factors were differentially expressed in high N versus low N plants indicating extensive changes in regulation of gene transcription in response to fertilization. A gene homologous to *LATERAL ORGAN BOUNDARY DOMAIN 38* (*AtLBD38*) showed 3.2-fold up-regulation in high N plants. Expression of *AtLBD38* is strongly induced by nitrate addition in *Arabidopsis* and an important regulatory role for this and two other closely related genes (*AtLBD37*, *AtLBD39*) in response to nitrate availability has been reported (Rubin, Tohge, Matsuda *et al.*, 2009). These three LBD transcription factors act as repressors of many N-responsive genes such as nuclear factor Y subunit A-10 (*NF-YA10*) (Rubin *et al.*, 2009). In agreement, we found two poplar genes homologous to *AtNF-YA10* strongly down-regulated in high N plants. At least some members of the LBD family of transcription factors have been recently identified as regulators of secondary growth in poplar (Yordanov, Regan & Busov, 2010). A homolog of *AtLBD15* that was down-regulated in high N plants in this study could fulfill such function as its paralog has been recently characterized to be part of the transcriptional network involved in secondary xylem patterning (Zhong *et al.*, 2011).

Furthermore, three genes encoding NAC domain transcription factors, PtrNAC157, PtrNAC105, and PtrNAC150, and, a zinc finger transcription factor PtrZF1 were down-regulated in high N plants. These genes have been implicated as intermediate regulators in a transcriptional network governing secondary cell wall biosynthesis in poplar (Zhong *et al.*, 2011). Thus, their lower transcript abundance could be correlated with the significantly thinner secondary cell walls observed in fibers of high N plants. Work in *Arabidopsis* and poplar showed that expression of many regulatory and structural genes related to xylem differentiation, including several genes differentially expressed in this study, is under the control of NAC domain transcription factor master regulators such as SND1, NST1, VND6 and VND7 (Kubo, Udagawa, Nishikubo *et al.*, 2005, Yamaguchi, Mitsuda, Ohtani *et al.*, 2011) and their homologs in poplar (Ohtani, Nishikubo, Xu *et al.*, 2011, Zhong *et al.*, 2011). These regulators are characterized by the ability to ectopically activate secondary cell wall biosynthesis and deposition in vessels, fibers, and other secondarily thickened cells (Ohtani *et al.*, 2011, Yamaguchi, Goue, Igarashi *et al.*, 2010). Five genes

encoding these master regulators, namely *PtVNS01/PtrWND5A*, *PtVNS03/PtrWND4A*, *PtVNS04/PtrWND4B*, *PtVNS06/PtrWND3B*, *PtVNS10/PtrWND2B* (gene names according to Ohtani *et al.*, 2011, Zhong *et al.*, 2011) showed more than 1.5-fold down-regulation in high N plants, but did not meet our criteria for significance ($P \leq 0.05$). Nevertheless, it is reasonable to expect that even such potentially subtle changes in their expression are biologically significant, considering the central position of these transcription factors in the regulatory cascade controlling secondary cell wall biosynthesis. Also down-regulated in high N plants was the poplar homolog of *Arabidopsis WRKY21*, a gene of undefined function that is regulated by *Arabidopsis VND7* in transgenic poplar (Ohtani *et al.*, 2011). A homolog of the *Arabidopsis KNOTTED-like* gene *KNAT3* was also down-regulated in high N plants. While the function of *KNAT3* is unknown, this poplar gene is up-regulated in response to osmotic stress treatments (Bae, Lee, Lee *et al.*, 2010), suggesting that it could play a role in adjustment of xylem to water stress.

Cell division, expansion, and death: The processes of cell division, cell expansion, and programmed cell death and their dynamics are important during xylem development. The increased radial stem growth of high N plants suggests that increased cell proliferation may have occurred in the cambial region, leading to more cambial derivatives. Transcription of several genes encoding important cell cycle regulators was elevated in high N plants. Two cyclin (*CYC*) genes were strongly up-regulated. In addition, two more *CYC* and two cyclin-dependent kinase (*CDK*) genes showed more than a 2-fold higher transcript abundance in high relative to low N plants, although this difference was not significant according to our criteria ($P \sim 0.075$). At least some poplar *CYC* and *CDK* genes have been previously shown to have specific expression maxima on the xylem side of the cambium; and hence, have been linked with xylem cell proliferation (Schrader, Nilsson, Mellerowicz *et al.*, 2004).

Another gene strongly up-regulated in high N plants was an apyrase (*Pt-APY1.2*). Apyrases displaying nucleoside triphosphate diphosphohydrolytic activity are involved in cell growth regulation and are highly expressed in rapidly growing tissues and/or tissues that accumulate auxin at high levels (Clark & Roux, 2011). Interestingly, we also found three genes encoding acid phosphatases strongly up-regulated in high N plants. While acid phosphates are involved in a variety of physiological functions, they are also involved in xylem development. Their specific functions during xylem differentiation are not clear, but putative

roles in secretion and resorption of sugars, secondary cell wall deposition (Charvat & Esau, 1975), and/or degradation of cellular content (Gahan, 1978) have been proposed.

Water uptake is essential to drive cell expansion. Three genes encoding aquaporins of the tonoplast intrinsic protein (TIP) class were up-regulated in high N plants, *PtTIP1;3*, *PtTIP1;4* and *PtTIP2;1*. In contrast, three other aquaporin genes were down-regulated, a plasma membrane intrinsic protein *PtPIP1;4*, a small basic intrinsic protein *PtSIP1;2* and a nodulin-like intrinsic protein *PtNIP3;3* (gene names according to Gupta & Sankararamakrishnan, 2009). Expression of *PtTIP2;1* and *PtSIP1;2* in response to high N availability was previously studied in the bulk xylem of poplar stems (Hacke *et al.*, 2010) and the change in expression was in the same direction as in the present study. Expression of several aquaporin genes has been shown to peak in the radial expansion zone of poplar cambium (Schrader *et al.*, 2004) and it has been speculated that aquaporins may play a role in xylogenesis by facilitating the flow of water into the zone of expanding cells (Groover *et al.*, 2010, Hacke *et al.*, 2010). Following this hypothesis, the up-regulation of the three TIPs observed in this study may be linked with the wider vessels in high N plants. Many TIPs and PIPs have been functionally characterized as water channels (Almeida-Rodriguez, 2009, Chaumont, Barrieu, Herman *et al.*, 1998, Sade, Vinocur, Diber *et al.*, 2009, Secchi, Maciver, Zeidel *et al.*, 2009). In a recent study, an elevated hydraulic conductance of root tips was associated with a decreased expression of *PtPIP1;4* suggesting that the *PtPIP1;4* may not be a water channel (Almeida-Rodriguez, Hacke & Laur, 2011). Similarly, NIPs usually display low water permeability but are permeable to small solutes such as urea and glycerol (Gomes, Agasse, Thiébaud *et al.*, 2009) and the transport specificity of SIPs is largely unknown. Thus, it is reasonable to expect that the down-regulated aquaporins may fulfill roles other than water transport within the developing xylem region.

Programmed cell death (PCD) is a crucial process during xylogenesis, as xylem vessels and fibers are dead and hollow at maturity. Two genes homologous to *Arabidopsis* *XYLEM SERINE PEPTIDASE 1* (*XSP1*) and a homolog of *XYLEM CYSTEIN PEPTIDASE 2* (*AXCP2*), known to be involved in PCD during xylem differentiation in *Arabidopsis* (Funk, Kositsup, Zhao *et al.*, 2002) showed significantly lower expression in high N plants. In addition, two other PCD-related genes, homologs of *Arabidopsis* *SERINE CARBOXYPEPTIDASE-LIKE 45* and *49* (*SCPL45* and *49*), were down-regulated in high N plants indicating that

cell maturation and death were suppressed. The down-regulation of genes involved in PCD in high N plants supports previous findings that nitrogen fertilization results in wood with more juvenile characteristics (Pitre *et al.*, 2007b) and supports a recent notion that PCD and secondary cell wall formation are correlated and governed by common regulatory mechanisms involving PtVNS/PtWND transcription factors (Bollhöner, Prestele & Tuominen, 2012).

3.4 CONCLUSIONS

In this study, we showed that fertilization with ammonium nitrate evokes changes in growth, anatomy, and hydraulic properties of secondary xylem in hybrid poplar stems. These anatomical and physiological differences were underpinned by changes in transcription of hundreds of genes in the developing xylem region. Our results revealed that several transcriptional patterns previously observed in *Arabidopsis* roots and shoots in response to high nitrate availability are also elicited in the developing secondary xylem of poplar. An example of such common responses is increased expression of genes encoding the transcription factor *LBD38* and enzymes involved in organic acid and trehalose metabolism. Such comparisons between a short lived annual herb and a relatively long lived perennial tree as well as between the different types of tissues suggest that metabolic and regulatory pathways controlled by the corresponding proteins may represent evolutionarily conserved aspects of plant responses to high N availability. However, future studies are needed to confirm this finding in a broader range of species and experimental conditions and to better understand the specific roles of these genes and processes in plant responses to high N.

Furthermore, the data presented in this study shed light on molecular mechanisms that underlie the phenotypic plasticity of xylem hydraulic and structural traits. We identified gene candidates that may affect xylem cell dimensions and cell wall thickness, although detailed functional characterization of these genes in poplar is required to corroborate the proposed function. Based on our results, wider lumens of vessels and fibers in high N plants might be linked with increased expression levels of genes encoding cell wall loosening enzymes, such as various glycoside hydrolases and genes encoding aquaporins that may facilitate increased water uptake into expanding xylem cells. Our results also suggest that the changes in xylem development and secondary wall deposition in response to N availability may, at least in part, be mediated by the differential

expression of several transcription factors that are part of a core transcriptional cascade governed by the recently characterized master regulators of xylem cell differentiation, the NAC domain transcription factors (PtVNS/PtrWND). Future research will reveal if the same genes that were identified in this study underlie changes in xylem phenotype under different environmental conditions, or if distinctly different suites of genes are regulated by various environmental clues, yet result in a similar xylem phenotype.

3.5 TABLES

Table 3-1: List of qRT-PCR gene-specific primers used in this study. Gene names were given according to annotation. Gene models correspond to the Phytozome database (<http://www.phytozome.net/search.php>).

Given name	Gene model ID	Forward primer	Reverse primer	TAIR best hit	Annotation
<i>CSLD5</i>	POPTR_0014s12000	GTGTAGCTTTTGTGTAAGCAGATGAAG	AGAAAAGCGATGAAACTAAACAGTGA	AT1G02730	Cellulose synthase-like D5
<i>GH9C2</i>	POPTR_0003s13940	ACGAGCCTACGAGTGCTTTCTT	TTGCAGATACATCACAATCCAAAA	AT1G64390	Glycosyl hydrolase 9C2
<i>XSP1</i>	POPTR_0002s15330	AAGGTTGTGGTCAAGGCAAAA	CATACGAGTGAACCTGACAACATTT	AT4G00230	Xylem serine peptidase 1
<i>NAC150</i>	POPTR_0018s06790	CCTTTCTATAAGAGAACCAAGAGATCATC	CCCCAGCCCAAGAGAAAATAA	AT4G29230	NAC domain containing protein 75
<i>WND2B</i>	POPTR_0002s17950	AACAACCTGGGTTGCCCTTGA	AGGTTTCAGCCTGGCCATT	AT2G46770	No apical meristem (NAM) protein
<i>MYB26</i>	POPTR_0005s06410	CAAGGAGATCATGGAGGTCAAGT	TCCCCACACCAAGAAAGTCTATAAA	AT4G33450	Myb-like binding domain
<i>LBD15</i>	POPTR_0013s15220	CCGTGTCCATTTCAACACCAT	CTGAAGGAGGAGGTGGTTGTG	AT2G40470	LOB domain-containing protein 15
<i>BNF1</i>	POPTR_0011s04430	TCATGAAACGCATTGCTCAAG	CCCCAAAAATCCGATTCAAGA	AT1G11190	Bifunctional nuclease I
<i>YLS8</i>	POPTR_0007s07660	GGTGCCCTGGTTAATTCAAAATC	TCCAAAGCATGGAAGTGGTTATC	AT5G08290	Yellow-leaf-specific gene 8
<i>PP2A</i>	POPTR_0008s19590	ACGCTGCTTACTCTACCCTGA	TTTCTGCAAGGATGCAACAC	AT1G59830	Serine/threonine protein phosphatase 2A

Table 3-2: Growth characteristics of poplar saplings receiving 0.75 mM (low N) versus 7.5 mM (high N) levels of ammonium nitrate.

	low N	high N
height (cm)	160 ± 2.3	171.3 ± 2.2**
D _{stem} (mm)	8.9 ± 0.2	9.5 ± 0.1*
A _X (mm ²)	40.3 ± 1.3	51.3 ± 1.8**
A _L (m ²)	0.63 ± 0.03	0.99 ± 0.03**

Abbreviations: height - final height of saplings, D_{stem} - stem diameter at 10 cm above the root collar, A_X - xylem cross-sectional area at ~10 cm above the root collar, A_L - plant total leaf area. Mean ± SE (*n*=8). Results of independent two-sample t-tests, testing for differences between low and high N plants, are indicated (**P* ≤ 0.05, ***P* ≤ 0.01).

Table 3-3: Xylem characteristics of poplar saplings receiving 0.75 mM (low N) versus 7.5 mM (high N) levels of ammonium nitrate.

	low N	high N
vessel lumen D (μm)	38.9 \pm 0.2	42.6 \pm 0.7**
vessel element length (μm)	234 \pm 2	255 \pm 4**
vessel length (cm)	5.2 \pm 0.2	5.8 \pm 0.2 ns
fiber lumen D (μm)	9.5 \pm 0.4	11.2 \pm 0.5*
fiber length (μm)	579 \pm 9	561 \pm 7 ns
fiber double wall thickness (μm)	3.3 \pm 0.1	2.7 \pm 0.2*
wood density (g/cm^3)	0.37 \pm 0.01	0.31 \pm 0.01**

Mean \pm SE ($n=5-6$). Results of independent two-sample t-tests, testing for differences between low and high N plants, are indicated (* $P \leq 0.05$, ** $P \leq 0.01$), ns – non-significant result ($P > 0.05$).

Table 3-4: Genes differentially expressed in the developing xylem of hybrid poplar growing under high N versus low N availability. The poplar gene names indicated in the brackets were obtained from 1- Phytozome (ftp://ftp.jgi-psf.org/pub/JGI_data/phytozome/v7.0/Ptrichocarpa/annotation/), 2- Zhong et al. (2011), 3- Gupta and Sankararamakrishnan (2009). Fold change values represent a ratio between the normalized averaged values of high N relative to low N plants. Multiple testing corrections adjusted *P* values of t-tests comparing low and high N plants are indicated.

<i>Populus trichocarpa</i> Phytozome v2.0 gene name	<i>Arabidopsis thaliana</i> homologous gene	TAIR Description	Fold change	<i>P</i> value
amino acid transport				
POPTR_0008s03620	At2g39130	Transmembrane amino acid transporter family protein	4.75	0.014
POPTR_0006s18790	At5g57685 (<i>GDU3</i>)	glutamine dumper 3	2.35	0.021
POPTR_0008s12400	At2g01170 (<i>BAT1</i>)	bidirectional amino acid transporter 1	1.69	0.031
POPTR_0001s36330 (<i>Pt-LHT1.2</i>) [†]	At5g40780 (<i>LHT1</i>)	lysine histidine transporter 1	-1.87	0.037
POPTR_0002s07960 (<i>PtAAP5</i>) [†]	At1g77380 (<i>AAP3</i>)	amino acid permease 3	-3.10	0.041
organic acid metabolism				
POPTR_0008s11330	At1g68750 (<i>PPC4</i>)	phosphoenolpyruvate carboxylase 4	2.52	0.015
POPTR_0001s13510 (<i>Pt-G6PD.2</i>) [†]	At5g13110 (<i>G6PD2</i>)	glucose-6-phosphate dehydrogenase 2	2.51	0.032
POPTR_0001s16300 (<i>Pt-ALAAT1.1</i>) [†]	At1g72330 (<i>ALAAT2</i>)	alanine aminotransferase 2	1.82	0.037
POPTR_0013s00660	At1g09420 (<i>G6PD4</i>)	glucose-6-phosphate dehydrogenase 4	1.69	0.028
POPTR_0007s14250	At4g37870 (<i>PCK1</i>)	phosphoenolpyruvate carboxykinase 1	1.68	0.047
POPTR_0006s25280	At5g25880 (<i>NADP-ME3</i>)	NADP-malic enzyme 3	1.57	0.032
carbohydrate metabolism				
POPTR_0006s06460	At5g20250 (<i>DIN10</i>)	Raffinose synthase family protein	5.21	0.018
POPTR_0011s00480	At1g11580 (<i>PMEPCRA</i>)	methylesterase PCR A	3.84	0.017
POPTR_0007s05670	At5g65140	Haloacid dehalogenase-like hydrolase (HAD) superfamily protein / trehalose-phosphatase family protein	3.42	0.029
POPTR_0014s12000 (<i>Pt-ATCSLD5.1</i>) [†]	At1g02730 (<i>CSLD5</i>)	cellulose synthase-like D5	2.88	0.015
POPTR_0002s21700	At2g05790	O-Glycosyl hydrolases family 17 protein	2.74	0.030
POPTR_0002s20130 (<i>Pt-ATCSLD5.2</i>) [†]	At1g02730 (<i>CSLD5</i>)	cellulose synthase-like D5	2.46	0.045

Table 3-4 (Continued)

<i>Populus trichocarpa</i> Phytozome v2.0 gene name	<i>Arabidopsis thaliana</i> homologous gene	TAIR Description	Fold change	P value
POPTR_0009s01210 (<i>Pt-XTR8.1</i>) [†]	At2g36870 (<i>XTH32</i>)	xyloglucan endotransglucosylase/hydrolase 32	2.46	0.023
POPTR_0008s20870	At5g18670 (<i>BMY3</i>)	beta-amylase 3	2.42	0.029
POPTR_0008s13200 (<i>Pt-CEL1.3</i>) [†]	At1g70710 (<i>GH9B1</i>)	glycosyl hydrolase 9B1	2.07	0.042
POPTR_0008s09380 (<i>Pt-HIUHASE.1</i>) [†]	At1g26560 (<i>BGLU40</i>)	beta glucosidase 40	2.06	0.023
POPTR_0003s07040 (<i>Pt-PE3.4</i>) [†]	At3g14310 (<i>PME3</i>)	pectin methylesterase 3	2.05	0.033
POPTR_0004s03830	At5g08370 (<i>AGAL2</i>)	alpha-galactosidase 2	2.01	0.019
POPTR_0006s08030	At5g58090	O-Glycosyl hydrolases family 17 protein	1.99	0.023
POPTR_0010s13560 (<i>Pt-XYL1.1</i>) [†]	At1g68560 (<i>XYL1</i>)	alpha-xylosidase 1	1.98	0.011
POPTR_0011s09660	At5g55180	O-Glycosyl hydrolases family 17 protein	1.94	0.048
POPTR_0019s09740	At1g71380 (<i>CEL3</i>)	cellulase 3	1.86	0.032
POPTR_0002s20340 (<i>Pt-SUS2.2</i>) [†]	At4g02280 (<i>SUS3</i>)	sucrose synthase 3	1.79	0.049
POPTR_0010s26170	At5g08380 (<i>AGAL1</i>)	alpha-galactosidase 1	1.75	0.046
POPTR_0002s09450	At1g78060	Glycosyl hydrolase family protein	1.73	0.022
POPTR_0008s10090	At3g06500	Plant neutral invertase family protein	1.69	0.043
POPTR_0018s09560 (<i>Pt-HXK1.1</i>) [†]	At4g29130 (<i>HXK1</i>)	hexokinase 1	1.69	0.014
POPTR_0018s14730	At5g58090	O-Glycosyl hydrolases family 17 protein	1.65	0.041
POPTR_0013s05620	At1g64760	O-Glycosyl hydrolases family 17 protein	1.61	0.021
POPTR_0010s11510	At1g68020 (<i>ATTPS6</i>)	UDP-Glycosyltransferase / trehalose-phosphatase family protein	1.58	0.015
POPTR_0008s13590	At1g68020 (<i>ATTPS6</i>)	UDP-Glycosyltransferase / trehalose-phosphatase family protein	1.56	0.042
POPTR_0003s13940	At1g64390 (<i>GH9C2</i>)	glycosyl hydrolase 9C2	1.50	0.033
POPTR_0005s06280	At3g18660 (<i>PGSIP1</i>)	plant glycogenin-like starch initiation protein 1	-1.55	0.023
POPTR_0004s06840	At3g16520 (<i>UGT88A1</i>)	UDP-glucosyl transferase 88A1	-1.62	0.023
POPTR_0006s11040	At5g01930 (<i>MAN6</i>)	Glycosyl hydrolase superfamily protein	-1.76	0.029
POPTR_0004s06910	At3g16520 (<i>UGT88A1</i>)	UDP-glucosyl transferase 88A1	-1.79	0.009
POPTR_0016s02640	At3g10740 (<i>ASD1</i>)	alpha-L-arabinofuranosidase 1	-1.79	0.009
POPTR_0016s14550	At5g01930 (<i>MAN6</i>)	Glycosyl hydrolase superfamily protein	-1.85	0.023
POPTR_0002s11090	At1g09890	Rhamnogalacturonate lyase family protein	-1.95	0.041

Table 3-4 (Continued)

<i>Populus trichocarpa</i> Phytozome v2.0 gene name	<i>Arabidopsis thaliana</i> homologous gene	TAIR Description	Fold change	P value
POPTR_0016s02620	At3g10740 (<i>ASD1</i>)	alpha-L-arabinofuranosidase 1	-1.95	0.040
POPTR_0001s08750	At1g11260 (<i>STP1</i>)	sugar transporter 1	-2.02	0.025
POPTR_0002s02550	At1g19940 (<i>GH9B5</i>)	glycosyl hydrolase 9B5	-2.02	0.025
POPTR_0016s02690	At3g10740 (<i>ASD1</i>)	alpha-L-arabinofuranosidase 1	-2.04	0.011
POPTR_0005s27680	At4g35300 (<i>TMT2</i>)	tonoplast monosaccharide transporter2	-2.07	0.047
fasciclin-like arabinogalactan				
POPTR_0014s16610	At4g12730 (<i>FLA2</i>)	FASCICLIN-like arabinogalactan 2	2.07	0.010
POPTR_0073s00210	At5g06390 (<i>FLA17</i>)	FASCICLIN-like arabinogalactan protein 17 precursor	-1.67	0.047
laccase				
POPTR_0004s16370	At5g03260 (<i>LAC11</i>)	laccase 11	2.65	0.026
POPTR_0011s12090	At5g60020 (<i>LAC17</i>)	laccase 17	-1.67	0.045
POPTR_0011s12100	At5g60020 (<i>LAC17</i>)	laccase 17	-1.91	0.040
POPTR_0009s03940	At2g29130 (<i>LAC2</i>)	laccase 2	-4.98	0.045
transcription factor				
POPTR_0009s01110	At5g22920	CHY-type/CTCHY-type/RING-type Zinc finger protein	3.37	0.035
POPTR_0009s09270	At3g49940 (<i>LBD38</i>)	LOB domain-containing protein 38	3.21	0.019
POPTR_0003s12240	At1g63100	GRAS family transcription factor	2.52	0.028
POPTR_0001s08850	At1g63100	GRAS family transcription factor	2.5	0.009
POPTR_0017s06590	At4g26400	RING/U-box superfamily protein	2.38	0.011
POPTR_0018s10510	At5g57660 (<i>COL5</i>)	CONSTANS-like 5	2.35	0.036
POPTR_0014s11940	At5g49300 (<i>GATA16</i>)	GATA transcription factor 16	1.82	0.029
POPTR_0005s05470 (<i>Pt-BZO2.3</i>) ¹	At5g28770 (<i>BZO2H3</i>)	bZIP transcription factor family protein	1.69	0.040
POPTR_0005s20890 (<i>Pt-SCL1.1</i>) ¹	At1g21450 (<i>SCL1</i>)	SCARECROW-like 1	-1.61	0.021
POPTR_0017s12740 (<i>PtrZF1</i>) ²	At1g26610	C2H2-like zinc finger protein	-1.63	0.041
POPTR_0018s06790 (<i>PtrNAC150</i>) ²	At4g29230 (<i>NAC075</i>)	NAC domain containing protein 75	-1.65	0.028
POPTR_0006s27570	At5g25220 (<i>KNAT3</i>)	KNOTTED1-like homeobox gene 3	-1.68	0.032
POPTR_0011s05740 (<i>PtrNAC105</i>) ²	At4g28500 (<i>NAC073</i>)	NAC domain containing protein 73	-1.72	0.023
POPTR_0003s11120	At2g30590 (<i>WRKY21</i>)	WRKY DNA-binding protein 21	-1.73	0.022
POPTR_0006s04770 (<i>Pt-HSFB3.1</i>) ¹	At2g41690 (<i>HSFB3</i>)	heat shock transcription factor B3	-1.73	0.011

Table 3-4 (Continued)

<i>Populus trichocarpa</i> Phytozome v2.0 gene name	<i>Arabidopsis thaliana</i> homologous gene	TAIR Description	Fold change	P value
<i>POPTR_0010s22320</i>	<i>At2g28550 (RAP2.7)</i>	related to AP2.7	-1.83	0.017
<i>POPTR_0013s08040</i>	<i>At2g40470 (LBD15)</i>	LOB domain-containing protein 15	-1.83	0.041
<i>POPTR_0009s16590</i>	<i>At1g08320 (TGA9)</i>	bZIP transcription factor family protein	-1.89	0.041
<i>POPTR_0004s04900 (PtrNAC157)²</i>	<i>At4g28500 (NAC073)</i>	NAC domain containing protein 73	-1.91	0.033
<i>POPTR_0005s14860</i>	<i>At2g01275</i>	RING/FYVE/PHD zinc finger superfamily protein	-2.01	0.018
<i>POPTR_0009s03240 (Pt-MYB111.1)¹</i>	<i>At3g46130 (MYB48)</i>	myb domain protein 48	-2.28	0.038
<i>POPTR_0006s21640</i>	<i>At5g06510 (NF-YA10)</i>	nuclear factor Y, subunit A10	-2.91	0.010
<i>POPTR_0016s06860</i>	<i>At5g06510 (NF-YA10)</i>	nuclear factor Y, subunit A10	-4.12	0.022
cell cycle				
<i>POPTR_0001s27890</i>	<i>At2g26760 (CYCB1;4)</i>	Cyclin B1;4	3.26	0.041
<i>POPTR_0009s16730</i>	<i>At1g76310 (CYCB2;4)</i>	Cyclin B2;4	2.87	0.047
phosphatases				
<i>POPTR_0019s04670 (Pt-APY1.2)¹</i>	<i>At5g18280 (APY2)</i>	apyrase 2	5.97	0.023
<i>POPTR_0001s19180</i>	<i>At4g25150</i>	HAD superfamily, subfamily IIIB acid phosphatase	5.22	0.020
<i>POPTR_0012s09940 (Pt-PPD3.2)¹</i>	<i>At5g50400 (PAP27)</i>	purple acid phosphatase 27	3.82	0.023
<i>POPTR_0004s16720 (Pt-PAP.2)¹</i>	<i>At2g16430 (PAP10)</i>	purple acid phosphatase 10	1.64	0.018
aquaporins				
<i>POPTR_0010s21700 (PtTIP1;3)³</i>	<i>At4g01470 (TIP1;3)</i>	tonoplast intrinsic protein 1;3	2.26	0.047
<i>POPTR_0008s05050 (PtTIP1;4)³</i>	<i>At4g01470 (TIP1;3)</i>	tonoplast intrinsic protein 1;3	2.25	0.041
<i>POPTR_0001s18730 (PtTIP2;1)³</i>	<i>At3g16240 (DELTA-TIP)</i>	delta tonoplast integral protein	1.87	0.029
<i>POPTR_0019s04640 (PtSIP1;2)³</i>	<i>At3g04090 (SIP1A)</i>	small and basic intrinsic protein 1A	-1.70	0.033
<i>POPTR_0001s45920 (PtNIP3;3)³</i>	<i>At4g10380 (NIP5;1)</i>	NOD26-like intrinsic protein 5;1	-1.80	0.040
<i>POPTR_0006s09920 (PtPIP1;4)³</i>	<i>At4g00430 (PIP1;4)</i>	plasma membrane intrinsic protein 1;4	-3.27	0.040
programmed cell death				
<i>POPTR_0008s03480</i>	<i>At3g10410 (SCPL49)</i>	serine carboxypeptidase-like 49	-1.53	0.032
<i>POPTR_0002s00720</i>	<i>At1g20850 (XCP2)</i>	xylem cysteine peptidase 2	-1.69	0.043
<i>POPTR_0014s07050</i>	<i>At4g00230 (XSP1)</i>	xylem serine peptidase 1	-1.85	0.030
<i>POPTR_0001s13140</i>	<i>At1g28110 (SCPL45)</i>	serine carboxypeptidase-like 45	-1.99	0.040
<i>POPTR_0002s15330</i>	<i>At4g00230 (XSP1)</i>	xylem serine peptidase 1	-2.56	0.023

3.6 FIGURES

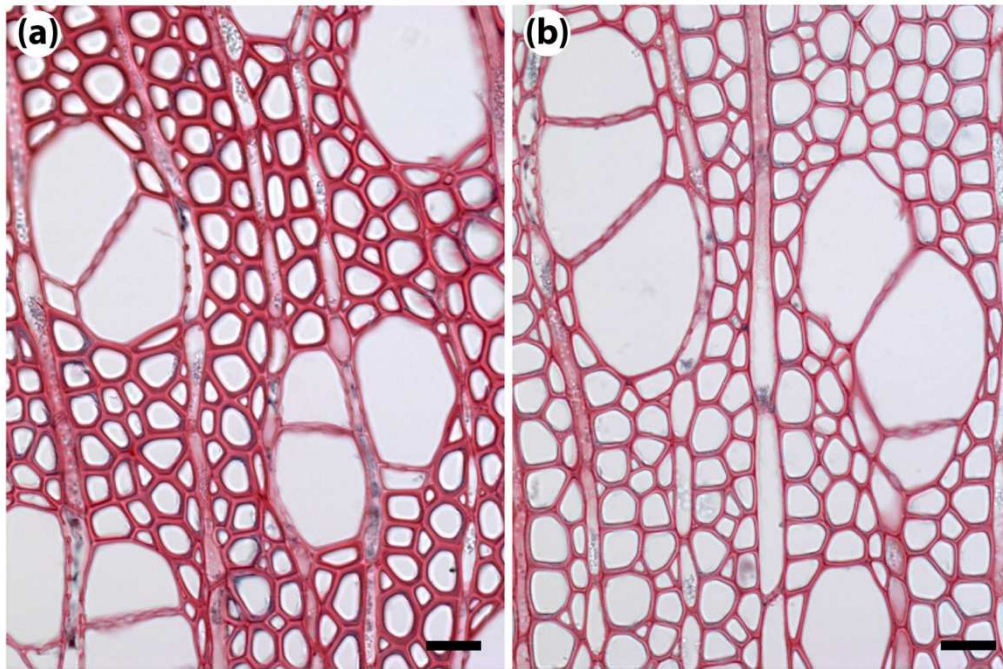


Figure 3-1: Cross-sections of stem xylem from (a) low N and (b) high N plants. High N plants had wider fibers and vessels and thinner fiber walls than low N plants. Scale bars = 20 μm .

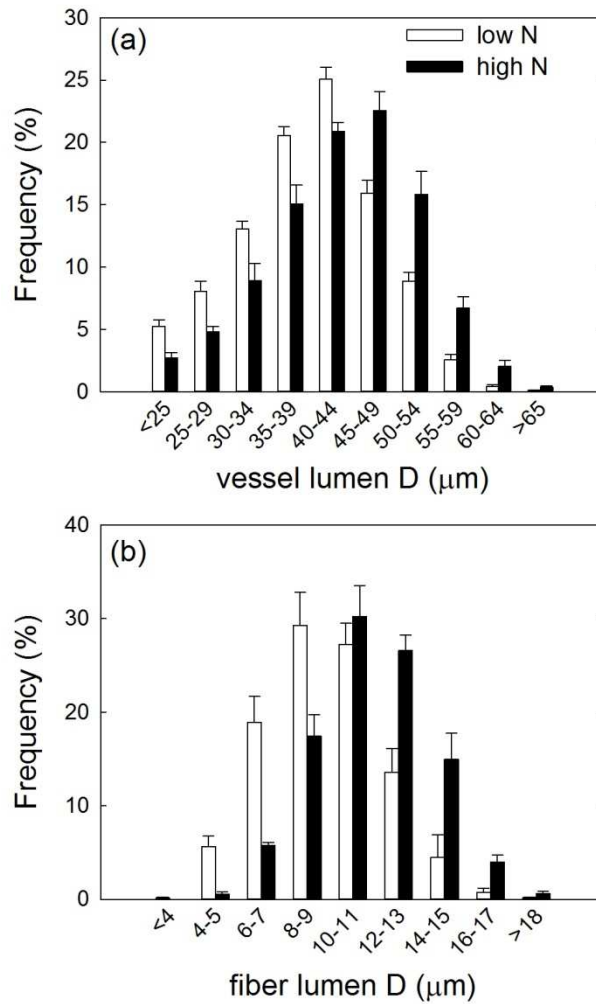


Figure 3-2: Frequency histograms of (a) vessel and (b) fiber lumen diameters for low N (open bars) and high N (black bars) plants. Means and SE ($n=5-6$).

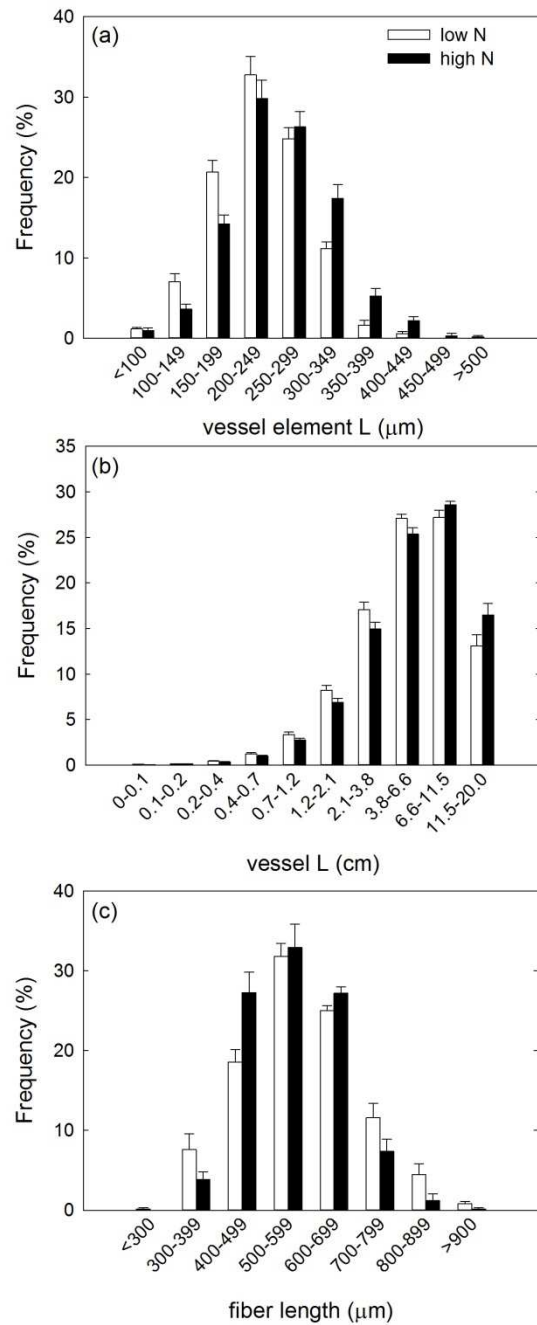


Figure 3-3: Frequency histograms of (a) vessel element length, (b) vessel length, and (c) fiber length for low N (open bars) and high N (black bars) plants. Means and SE ($n=6$).

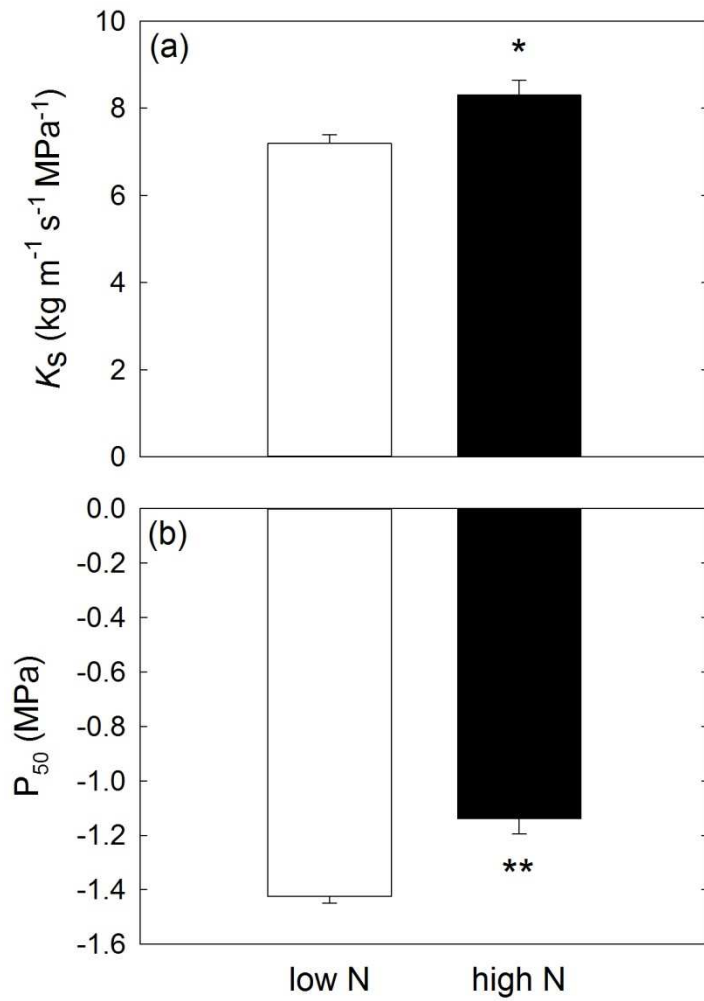


Figure 3-4: Average (a) xylem-specific conductivity (K_s) and (b) xylem pressure causing 50% loss of conductivity (P_{50}) of stem segments from low N (open bars) and high N (black bars) plants. Error bars are SE ($n=8$). * indicates the means are significantly different at $P \leq 0.05$; ** indicates significant differences at $P \leq 0.01$ (independent two-sample t-test).

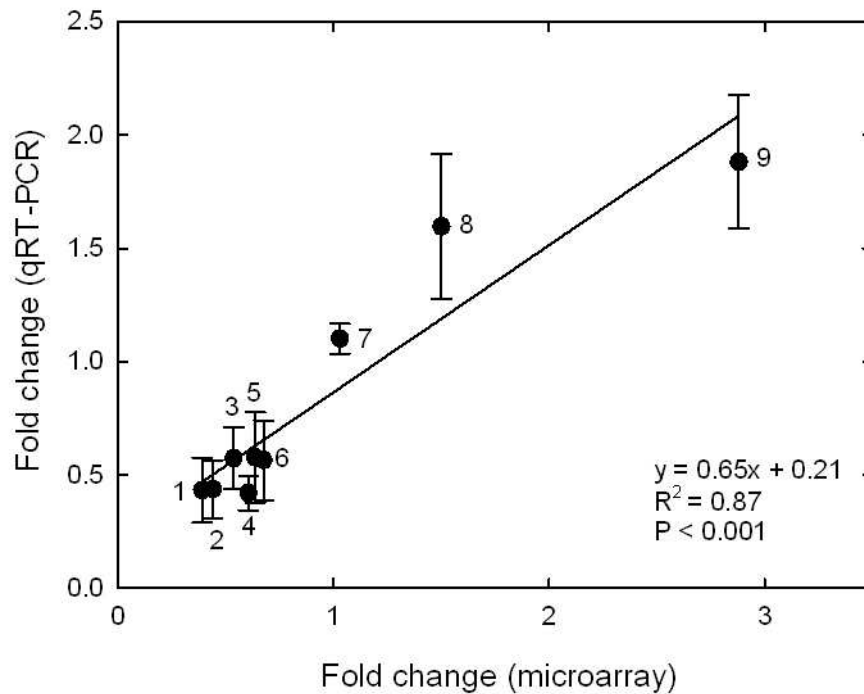


Figure 3-5: qRT-PCR validation of microarray results for nine selected genes: (1) Xylem serine peptidase 1 (*XSPI*, POPTR_0014s12000), (2) LOB domain-containing protein 15 (*LBD15*, POPTR_0013s15220), (3) Bifunctional nuclease I (*BFNI*, POPTR_0011s04430), (4) NAC domain containing protein 75 (*NAC150*, POPTR_0018s06790), (5) No apical meristem (NAM) protein (*WND2B*, POPTR_0002s17950), (6) Myb-like binding domain (*MYB26*, POPTR_0005s06410), (7) Yellow-leaf-specific gene 8 (*YSL8*, POPTR_0007s07660), (8) Glycosyl hydrolase 9C2 (*GH9C2*, POPTR_0003s13940), and (9) Cellulose synthase-like D5 (*CSLD5*, POPTR_0014s12000).

3.7 REFERENCES

- Almeida-Rodriguez A.M. (2009) *Aquaporins in poplars: characterization, transcript profiling and drought stress*. Dissertation, University of Alberta.
- Almeida-Rodriguez A.M., Cooke J.E.K., Yeh F. & Zwiazek J.J. (2010) Functional characterization of drought-responsive aquaporins in *Populus balsamifera* and *Populus simonii* × *balsamifera* clones with different drought resistance strategies. *Physiologia Plantarum*, **140**, 321-333.
- Almeida-Rodriguez A.M., Hacke U.G. & Laur J. (2011) Influence of evaporative demand on aquaporin expression and root hydraulics in hybrid poplar. *Plant, Cell & Environment*, **34**, 1318–1331.
- Andersson-Gunneras S., Mellerowicz E.J., Love J., Segerman B., Ohmiya Y., Coutinho P.M., Nilsson P., Henrissat B., Moritz T. & Sundberg B. (2006) Biosynthesis of cellulose-enriched tension wood in *Populus*: global analysis of transcripts and metabolites identifies biochemical and developmental regulators in secondary wall biosynthesis. *Plant Journal*, **45**, 144-165.
- Arend M. & Fromm J. (2007) Seasonal change in the drought response of wood cell development in poplar. *Tree Physiology*, **27**, 985-992.
- Aspeborg H., Schrader J., Coutinho P.M., Stam M., Kallas A., Djerbi S., Nilsson P., Denman S., Amini B., Sterky F., Master E., Sandberg G., Mellerowicz E., Sundberg B., Henrissat B. & Teeri T.T. (2005) Carbohydrate-active enzymes involved in the secondary cell wall biogenesis in hybrid aspen. *Plant Physiology*, **137**, 983-997.
- Bae E.-K., Lee H., Lee J.-S. & Noh E.-W. (2010) Isolation and characterization of osmotic stress-induced genes in poplar cells by suppression subtractive hybridization and cDNA microarray analysis. *Plant Physiology and Biochemistry*, **48**, 136-141.
- Balatinecz J.J., Kretschmann D.E. & Leclercq A. (2001) Achievements in the utilization of poplar wood - guideposts for the future. *Forestry Chronicle*, **77**, 265-269.
- Benjamini Y. & Hochberg Y. (1995) Controlling the false discovery rate - a practical and powerful approach to multiple testing *Journal of the Royal Statistical Society Series B-Methodological*, **57**, 289-300.
- Bernal A.J., Jensen J.K., Harholt J., Sorensen S., Moller I., Blaukopf C., Johansen B., de Lotto R., Pauly M., Scheller H.V. & Willats W.G.T. (2007) Disruption of ATCSLD5 results in reduced growth, reduced xylan and homogalacturonan synthase activity and altered xylan occurrence in *Arabidopsis*. *Plant Journal*, **52**, 791-802.
- Berta M., Giovannelli A., Sebastiani F., Camussi A. & Racchi M.L. (2010) Transcriptome changes in the cambial region of poplar (*Populus alba* L.) in response to water deficit. *Plant Biology*, **12**, 341-354.
- Berthet S., Demont-Caulet N., Pollet B., Bidzinski P., Cezard L., Le Bris P., Borrega N., Herve J., Blondet E., Balzergue S., Lapierre C. & Jouanin L. (2011) Disruption of *LACCASE4* and *17* results in tissue-specific

- alterations to lignification of *Arabidopsis thaliana* stems. *Plant Cell*, **23**, 1124-1137.
- Bollhöner B., Prestele J. & Tuominen H. (2012) Xylem cell death: emerging understanding of regulation and function. *Journal of Experimental Botany*, **63**, 1081-1094.
- Chang S.J., Puryear J. & Cairney J. (1993) A simple and efficient method for isolating RNA from pine trees. *Plant Molecular Biology Reporter*, **11**, 113-116.
- Charvat I. & Esau K. (1975) Ultrastructural study of acid phosphatase localization in *Phaseolus vulgaris* xylem by use of an azo dye method. *Journal of Cell Science*, **19**, 543-561.
- Chaumont F., Barrieu F., Herman E.M. & Chrispeels M.J. (1998) Characterization of a maize tonoplast aquaporin expressed in zones of cell division and elongation. *Plant Physiology*, **117**, 1143-1152.
- Clark G. & Roux S.J. (2011) Apyrases, extracellular ATP and the regulation of growth. *Current Opinion in Plant Biology*, **14**, 700-706.
- Coleman H.D., Yan J. & Mansfield S.D. (2009) Sucrose synthase affects carbon partitioning to increase cellulose production and altered cell wall ultrastructure. *Proceedings of the National Academy of Sciences of the United States of America*, **106**, 13118-13123.
- Cooke J.E.K., Brown K.A., Wu R. & Davis J.M. (2003) Gene expression associated with N-induced shifts in resource allocation in poplar. *Plant Cell and Environment*, **26**, 757-770.
- Cooke J.E.K., Martin T.A. & Davis J.M. (2005) Short-term physiological and developmental responses to nitrogen availability in hybrid poplar. *New Phytologist*, **167**, 41-52.
- Courtois-Moreau C.L., Pesquet E., Sjödin A., Muñoz L., Bollhöner B., Kaneda M., Samuels L., Jansson S, and Tuominen H (2009): A unique program for cell death in xylem fibers of *Populus* stem. *Plant Journal*, **58**, 260-274.
- Cosgrove D.J. (2005) Growth of the plant cell wall. *Nature Reviews Molecular Cell Biology*, **6**, 850-861.
- Dharmawardhana P., Brunner A.M. & Strauss S.H. (2010) Genome-wide transcriptome analysis of the transition from primary to secondary stem development in *Populus trichocarpa*. *BMC Genomics*, **11**.
- Du J. & Groover A. (2010) Transcriptional Regulation of Secondary Growth and Wood Formation. *Journal of Integrative Plant Biology*, **52**, 17-27.
- Dundar E. (2009) Multiple GUS expression patterns of a single *Arabidopsis* gene. *Annals of Applied Biology*, **154**, 33-41.
- Ehltling B., Dluzniewska P., Dietrich H., Selle A., Teuber M., Haensch R., Nehls U., Polle A., Schnitzler J.P., Rennenberg H. & Gessler A. (2007) Interaction of nitrogen nutrition and salinity in Grey poplar (*Populus tremula* x *alba*). *Plant Cell and Environment*, **30**, 796-811.
- Funk V., Kositsup B., Zhao C.S. & Beers E.P. (2002) The *Arabidopsis* xylem peptidase XCP1 is a tracheary element vacuolar protein that may be a papain ortholog. *Plant Physiology*, **128**, 84-94.

- Gahan P.B. (1978) A re-interpretation of cytochemical evidence for acid phosphatase activity during cell death in xylem differentiation. *Annals of Botany*, **42**, 755-757.
- Geisler-Lee J., Geisler M., Coutinho P.M., Segerman B., Nishikubo N., Takahashi J., Aspeborg H., Djerbi S., Master E., Andersson-Gunneras S., Sundberg B., Karpinski S., Teeri T.T., Kleczkowski L.A., Henrissat B. & Mellerowicz E.J. (2006) Poplar carbohydrate-active enzymes. Gene identification and expression analyses. *Plant Physiology*, **140**, 946-962.
- Gomes D., Agasse A., Thiébaud P., Delrot S., Gerós H. & Chaumont F. (2009) Aquaporins are multifunctional water and solute transporters highly divergent in living organisms. *Biochimica et Biophysica Acta (BBA) - Biomembranes*, **1788**, 1213-1228.
- Gray-Mitsumune M., Mellerowicz E.J., Abe H., Schrader J., Winzell A., Sterky F., Blomqvist K., McQueen-Mason S., Teeri T.T. & Sundberg B. (2004) Expansins abundant in secondary xylem belong to subgroup a of the alpha-expansin gene family. *Plant Physiology*, **135**, 1552-1564.
- Groover A.T., Nieminen K., Helariutta Y. & Mansfield S.D. (2010) Wood Formation in *Populus*. In: *Genetics and Genomics of Populus* (eds S. Jansson, R.P. Bhalerao, & A.T. Groover), Springer, New York, NY, USA, pp. 201-224.
- Guglielmino N., Liberman M., Catesson A.M., Mareck A., Prat R., Mutaftschiev S. & Goldberg R. (1997a) Pectin methylesterases from poplar cambium and inner bark: Localization, properties and seasonal changes. *Planta*, **202**, 70-75.
- Guglielmino N., Liberman M., Jauneau A., Vian B., Catesson A.M. & Goldberg R. (1997b) Pectin immunolocalization and calcium visualization in differentiating derivatives from poplar cambium. *Protoplasma*, **199**, 151-160.
- Gupta A.B. & Sankararamakrishnan R. (2009) Genome-wide analysis of major intrinsic proteins in the tree plant *Populus trichocarpa*: Characterization of XIP subfamily of aquaporins from evolutionary perspective. *BMC Plant Biology*, **9**.
- Hacke U.G., Plavcová L., Almeida-Rodriguez A., King-Jones S., Zhou W. & Cooke J.E.K. (2010) Influence of nitrogen fertilization on xylem traits and aquaporin expression in stems of hybrid poplar. *Tree Physiology*, **30**, 1016-1025.
- Hacke U.G., Sperry J.S., Pockman W.T., Davis S.D. & McCulloh K.A. (2001) Trends in wood density and structure are linked to prevention of xylem implosion by negative pressure. *Oecologia*, **126**, 457-461.
- Hafren J., Daniel G. & Westermark U. (2000) The distribution of acidic and esterified pectin in cambium, developing xylem and mature xylem of *Pinus sylvestris*. *IAWA Journal*, **21**, 157-168.
- Harvey H.P. & van den Driessche R. (1999) Nitrogen and potassium effects on xylem cavitation and water-use efficiency in poplars. *Tree Physiology*, **19**, 943-950.
- Hauch S. & Magel E. (1998) Extractable activities and protein content of sucrose-phosphate synthase, sucrose synthase and neutral invertase in trunk tissues

- of *Robinia pseudoacacia* L. are related to cambial wood production and heartwood formation. *Planta*, **207**, 266-274.
- Hocking D. (1971) Preparation and use of a nutrient solution for culturing seedlings of lodgepole pine and white spruce, with selected bibliography. Northern Forest Research Centre Information Report Nor-XI. Canadian Forest Service, Department of the Environment, Edmonton, Canada.
- Jacobsen A.L., Ewers F.W., Pratt R.B., Paddock W.A. & Davis S.D. (2005) Do xylem fibers affect vessel cavitation resistance? *Plant Physiology*, **139**, 546-556.
- Jang J.C., Leon P., Zhou L. & Sheen J. (1997) Hexokinase as a sugar sensor in higher plants. *Plant Cell*, **9**, 5-19.
- Janz D., Lautner S., Wildhagen H., Behnke K., Schnitzler J.-P., Rennenberg H., Fromm J. & Polle A. (2012) Salt stress induces the formation of a novel type of 'pressure wood' in two *Populus* species. *New Phytologist*, **194**, 129-141.
- Koch K. (2004) Sucrose metabolism: regulatory mechanisms and pivotal roles in sugar sensing and plant development. *Current Opinion in Plant Biology*, **7**, 235-246.
- Kotake T., Tsuchiya K., Aohara T., Konishi T., Kaneko S., Igarashi K., Samejima M. & Tsumuraya Y. (2006) An alpha-L-arabinofuranosidase/beta-D-xylosidase from immature seeds of radish (*Raphanus sativus* L.). *Journal of Experimental Botany*, **57**, 2353-2362.
- Kubo M., Udagawa M., Nishikubo N., Horiguchi G., Yamaguchi M., Ito J., Mimura T., Fukuda H. & Demura T. (2005) Transcription switches for protoxylem and metaxylem vessel formation. *Genes & Development*, **19**, 1855-1860.
- Lafarguette F., Leple J.C., Dejardin A., Laurans F., Costa G., Lesage-Descauses M.C. & Pilate G. (2004) Poplar genes encoding fasciclin-like arabinogalactan proteins are highly expressed in tension wood. *New Phytologist*, **164**, 107-121.
- Lautner S., Ehling B., Windeisen E., Rennenberg H., Matyssek R. & Fromm J. (2007) Calcium nutrition has a significant influence on wood formation in poplar. *New Phytologist*, **173**, 743-752.
- Luo Z.B., Langenfeld-Heyser R., Calfapietra C. & Polle A. (2005) Influence of free air CO₂ enrichment (EUROFACE) and nitrogen fertilisation on the anatomy of juvenile wood of three poplar species after coppicing. *Trees-Structure and Function*, **19**, 109-118.
- Mellerowicz E.J., Baucher M., Sundberg B. & Boerjan W. (2001) Unravelling cell wall formation in the woody dicot stem. *Plant Molecular Biology*, **47**, 239-274.
- Ohtani M., Nishikubo N., Xu B., Yamaguchi M., Mitsuda N., Goue N., Shi F., Ohme-Takagi M. & Demura T. (2011) A NAC domain protein family contributing to the regulation of wood formation in poplar. *Plant Journal*, **67**, 499-512.

- Onoda Y., Richards A.E. & Westoby M. (2010) The relationship between stem biomechanics and wood density is modified by rainfall in 32 Australian woody plant species. *New Phytologist*, **185**, 493-501.
- Pfaffl M.W. (2001) A new mathematical model for relative quantification in real-time RT-PCR. *Nucleic Acids Research*, **29**.
- Pitre F.E., Cooke J.E.K. & Mackay J.J. (2007a) Short-term effects of nitrogen availability on wood formation and fibre properties in hybrid poplar. *Trees-Structure and Function*, **21**, 249-259.
- Pitre F.E., Lafarguette F., Boyle B., Pavy N., Caron S., Dallaire N., Poulin P.L., Ouellet M., Morency M.J., Wiebe N., Lim E.L., Urbain A., Mouille G., Cooke J.E.K. & Mackay J.J. (2010) High nitrogen fertilization and stem leaning have overlapping effects on wood formation in poplar but invoke largely distinct molecular pathways. *Tree Physiology*, **30**, 1273-1289.
- Pitre F.E., Pollet B., Lafarguette F., Cooke J.E.K., MacKay J.J. & Lapierre C. (2007b) Effects of increased nitrogen supply on the lignification of poplar wood. *Journal of Agricultural and Food Chemistry*, **55**, 10306-10314.
- Pittermann J., Sperry J.S., Wheeler J.K., Hacke U.G. & Sikkema E.H. (2006) Mechanical reinforcement of tracheids compromises the hydraulic efficiency of conifer xylem. *Plant, Cell and Environment*, **29**, 1618-1628.
- Plavcová L., Hacke U.G. & Sperry J.S. (2011) Linking irradiance-induced changes in pit membrane ultrastructure with xylem vulnerability to cavitation. *Plant, Cell and Environment*, **34**, 501-513.
- Pratelli R., Voll L.M., Horst R.J., Frommer W.B. & Pilot G. (2010) Stimulation of nonselective amino acid export by glutamine dumper proteins. *Plant Physiology*, **152**, 762-773.
- Pratt R.B., Jacobsen A.L., Ewers F.W. & Davis S.D. (2007) Relationships among xylem transport, biomechanics and storage in stems and roots of nine Rhamnaceae species of the California chaparral. *New Phytologist*, **174**, 787-798.
- Rolland F., Baena-Gonzalez E. & Sheen J. (2006) Sugar sensing and signaling in plants: Conserved and novel mechanisms. In: *Annual Review of Plant Biology*, **57**, pp. 675-709.
- Rubin G., Tohge T., Matsuda F., Saito K. & Scheible W.-R. (2009) Members of the LBD family of transcription factors repress anthocyanin synthesis and affect additional nitrogen responses in *Arabidopsis*. *Plant Cell*, **21**, 3567-3584.
- Sade N., Vinocur B.J., Diber A., Shatil A., Ronen G., Nissan H., Wallach R., Karchi H. & Moshelion M. (2009) Improving plant stress tolerance and yield production: is the tonoplast aquaporin SITIP2;2 a key to isohydric to anisohydric conversion? *New Phytologist*, **181**, 651-661.
- Samuels A.L., Kaneda M. & Rensing K.H. (2006) The cell biology of wood formation: from cambial divisions to mature secondary xylem. *Canadian Journal of Botany*, **84**, 631-639.
- Sannigrahi P., Ragauskas A.J. & Tuskan G.A. (2010) Poplar as a feedstock for biofuels: A review of compositional characteristics. *Biofuels Bioproducts & Biorefining-Biofpr*, **4**, 209-226.

- Sauter J.J. & Van Cleve B. (1992) Seasonal variation of amino acids in the xylem sap of "*Populus x canadensis*" and its relation to protein body mobilization. *Trees-Structure and Function*, **7**, 26-32.
- Scheible W.R., Gonzalez-Fontes A., Lauerer M., Muller-Rober B., Caboche M. & Stitt M. (1997) Nitrate acts as a signal to induce organic acid metabolism and repress starch metabolism in tobacco. *Plant Cell*, **9**, 783-798.
- Scheible W.R., Morcuende R., Czechowski T., Fritz C., Osuna D., Palacios-Rojas N., Schindelasch D., Thimm O., Udvardi M.K. & Stitt M. (2004) Genome-wide reprogramming of primary and secondary metabolism, protein synthesis, cellular growth processes, and the regulatory infrastructure of *Arabidopsis* in response to nitrogen. *Plant Physiology*, **136**, 2483-2499.
- Schrader J., Nilsson J., Mellerowicz E., Berglund A., Nilsson P., Hertzberg M. & Sandberg G. (2004) A high-resolution transcript profile across the wood-forming meristem of poplar identifies potential regulators of cambial stem cell identity. *Plant Cell*, **16**, 2278-2292.
- Schrader S. & Sauter J.J. (2002) Seasonal changes of sucrose-phosphate synthase and sucrose synthase activities in poplar wood (*Populus x canadensis* Moench < robusta >) and their possible role in carbohydrate metabolism. *Journal of Plant Physiology*, **159**, 833-843.
- Secchi F., Maciver B., Zeidel M.L. & Zwieniecki M.A. (2009) Functional analysis of putative genes encoding the PIP2 water channel subfamily in *Populus trichocarpa*. *Tree Physiology*, **29**, 1467-1477.
- Siedlecka A., Wiklund S., Peronne M.A., Micheli F., Lesniewska J., Sethson I., Edlund U., Richard L., Sundberg B. & Mellerowicz E.J. (2008) Pectin methyl esterase inhibits intrusive and symplastic cell growth in developing wood cells of *Populus*. *Plant Physiology*, **146**, 554-565.
- Smeeckens S., Ma J.K., Hanson J. & Rolland F. (2010) Sugar signals and molecular networks controlling plant growth. *Current Opinion in Plant Biology*, **13**, 274-279.
- Song D.L., Xi W., Shen J.H., Bi T. & Li L.G. (2011) Characterization of the plasma membrane proteins and receptor-like kinases associated with secondary vascular differentiation in poplar. *Plant Molecular Biology*, **76**, 97-115.
- Sperry J.S., Hacke U.G. & Wheeler J.K. (2005) Comparative analysis of end wall resistivity in xylem conduits. *Plant, Cell and Environment*, **28**, 456-465.
- Stitt M. (1999) Nitrate regulation of metabolism and growth. *Current Opinion in Plant Biology*, **2**, 178-186.
- Tuominen H., Puech L., Fink S. & Sundberg B. (1997) A radial concentration gradient of indole-3-acetic acid is related to secondary xylem development in hybrid aspen. *Plant Physiology*, **115**, 577-585.
- Tyree M.T. & Zimmermann M.H. (2002) *Xylem structure and the ascent of sap*. (2nd ed.). Springer Verlag, Berlin.
- Wang R.C., Okamoto M., Xing X.J. & Crawford N.M. (2003) Microarray analysis of the nitrate response in *Arabidopsis* roots and shoots reveals over 1,000 rapidly responding genes and new linkages to glucose,

- trehalose-6-phosphate, iron, and sulfate metabolism. *Plant Physiology*, **132**, 556-567.
- Weber P., Stoermer H., Gessler A., Schneider S., Von Sengbusch D., Hanemann U. & Rennenberg H. (1998) Metabolic responses of Norway spruce (*Picea abies*) trees to long-term forest management practices and acute $(\text{NH}_4)_2\text{SO}_4$ fertilization: Transport of soluble non-protein nitrogen compounds in xylem and phloem. *New Phytologist. Nov.*, **140**, 461-475.
- Woodrum C.L., Ewers F.W. & Telewski F.W. (2003) Hydraulic, biomechanical, and anatomical interactions of xylem from five species of *Acer* (Aceraceae). *American Journal of Botany*, **90**, 693-699.
- Yamaguchi M., Goue N., Igarashi H., Ohtani M., Nakano Y., Mortimer J.C., Nishikubo N., Kubo M., Katayama Y., Kakegawa K., Dupree P. & Demura T. (2010) VASCULAR-RELATED NAC-DOMAIN6 and VASCULAR-RELATED NAC-DOMAIN7 effectively induce transdifferentiation into xylem vessel elements under control of an induction system. *Plant Physiology*, **153**, 906-914.
- Yamaguchi M., Mitsuda N., Ohtani M., Ohme-Takagi M., Kato K. & Demura T. (2011) VASCULAR-RELATED NAC-DOMAIN 7 directly regulates the expression of a broad range of genes for xylem vessel formation. *Plant Journal*, **66**, 579-590.
- Yordanov Y.S., Regan S. & Busov V. (2010) Members of the LATERAL ORGAN BOUNDARIES DOMAIN transcription factor family are involved in the regulation of secondary growth in *Populus*. *Plant Cell*, **22**, 3662-3677.
- Zhang Y., Brown G., Whetten R., Loopstra C.A., Neale D., Kieliszewski M.J. & Sederoff R.R. (2003) An arabinogalactan protein associated with secondary cell wall formation in differentiating xylem of loblolly pine. *Plant Molecular Biology*, **52**, 91-102.
- Zhong R., McCarthy R.L., Lee C. & Ye Z.-H. (2011) Dissection of the transcriptional program regulating secondary wall biosynthesis during wood formation in poplar. *Plant Physiology*, **157**, 1452-1468.

4. Linking irradiance-induced changes in pit membrane ultrastructure with xylem vulnerability to cavitation³

4.1 INTRODUCTION

In the majority of terrestrial plants, a large amount of water is lost by transpiration as stomata open to facilitate CO₂ uptake. The ability of plants to acquire and transport water to leaves is therefore an important factor which often limits their productivity and survival (McDowell, Pockman, Allen *et al.*, 2008, Sperry, 2000). Water transport in the xylem is driven by a gradient in negative pressure. Water columns are in a metastable state and are prone to being disrupted by the phenomenon of cavitation. Cavitation results in an embolized (air-filled) conduit which is no longer available for water transport. According to the air-seeding hypothesis, cavitation occurs when air outside a water-filled conduit is aspirated into the conduit through pores in the cell wall. The pores will retain an air-water meniscus until the difference between the air pressure (P_a) and xylem pressure (P_x) exceeds a critical pressure difference (ΔP_{crit}), according to:

$$\Delta P_{crit} = \frac{4T \cos \alpha}{D_p}$$

Eqn. 4-1

where $\Delta P = P_a - P_x$, T is the surface tension of xylem sap and α is the contact angle between sap and pore wall material, which is usually assumed to be zero (i.e., total wetting). The value of ΔP_{crit} is inversely related to the pore diameter (D_p). The largest pores in conduit walls appear to be located in the pit membranes that permit water flow between conduits (Cochard, Cruiziat & Tyree, 1992, Sperry, Saliendra, Pockman *et al.*, 1996, Sperry & Tyree, 1988). The air-seeding threshold is therefore determined by the structure of pit membranes, and pits represent a weak link in the protection of the transpiration stream against air entry (Choat, Cobb & Jansen, 2008).

Cavitation resistance can vary even within a species or genotype in response to factors such as water status (e.g., Stiller, 2009), nitrogen fertilization (Hacke, Plavcová, Almeida-Rodriguez *et al.*, 2010), and shading (Cochard, Lemoine & Dreyer, 1999). Lower irradiance is usually associated with lower

³ A version of this chapter has been published. Plavcová L, Hacke UG & Sperry JS 2011. *Plant, Cell & Environment*. 34:501-513.

evaporative demand and stomatal conductance, which is paralleled by a decreased need for water transport. Hence, xylem-specific and leaf-specific conductivity tend to be lower in shade (Caquet, Barigah, Cochard *et al.*, 2009, Shumway, Steiner & Kolb, 1993). The risk of drought-induced embolism is also usually lower in shade environments, implying reduced requirements for xylem safety. As a result, the xylem might be more vulnerable since the safety features are costly and shaded plants have limited carbon resources which are preferentially allocated to promote light capture (Schoonmaker, Hacke, Landhausser *et al.*, 2010). Indeed, the majority of studies found increased vulnerability as a result of shading (Barigah, Ibrahim, Bogard *et al.*, 2006, Cochard *et al.*, 1999, Schoonmaker *et al.*, 2010). However, others found no change (Raimondo, Trifilo, Lo Gullo *et al.*, 2009) or increased resistance (Holste, Jerke & Matzner, 2006) in shaded plants. Thus, there is still some ambiguity in the effect of light on cavitation resistance.

The main objective of this study was to evaluate the effect of contrasting light availability on cavitation resistance and on the ultrastructure of intervessel pits in poplar xylem. Based on previous findings (see above) and considering the potential of poplar xylem for phenotypic plasticity (Hacke *et al.*, 2010) we expected that shaded plants will be more vulnerable to cavitation. Given the central role of intervessel pits in determining cavitation resistance, we expected to find larger pores in the pit membranes of shaded plants. Observations of homogeneous pit membranes in angiosperm species showed significant variation in their structure (Jansen, Choat & Pletsers, 2009), and correlations between ΔP_{crit} and pore size as well as pit membrane thickness have been observed. However, the potential for structural acclimation at the pit membrane level within a single angiosperm species or genotype remains to be evaluated. A certain degree of phenotypic plasticity in the structure and function of inter-vessel pits can be expected as acclimation at the pit level has already been described in conifers (Domec, Lachenbruch, Meinzer *et al.*, 2008, Schoonmaker *et al.*, 2010).

In order to test our hypothesis, we used scanning (SEM) and transmission (TEM) electron microscopy. Both methods have often been used to study pit membrane ultrastructure (e.g., Jansen *et al.*, 2009, Sano, 2005, Schmid & Machado, 1968) even though there are valid concerns that artifacts due to sample preparation may occur. This is especially true for SEM during which the delicate pit membranes are not supported by any embedding medium (Jansen, Pletsers & Sano, 2008). Previous studies relating measured pit membrane pore sizes to the corresponding air-seeding pressure have reinforced these concerns. In at least two

cases, membrane pores were much smaller than pores that would allow air-seeding at realistic xylem pressures (Choat, Ball, Luly *et al.*, 2003, Shane, McCully & Canny, 2000). It has been proposed that the large pores that allow air-seeding are very rare and therefore not likely to be detected with SEM (Choat *et al.*, 2008, Hargrave, Kolb, Ewers *et al.*, 1994, Wheeler, Sperry, Hacke *et al.*, 2005). This concept is also known as the ‘rare pit’ hypothesis. Recently, Christman *et al.* (2009) developed a model that allows prediction of the frequency of pits with a certain porosity based on stem-level air-seeding experiments. Here we used this model to test how pit porosity data observed with SEM agree with measured proxies of cavitation resistance. The pit membrane structure of poplars is particularly suitable for this approach, because membranes bear many large, easily resolvable pores (Jansen *et al.*, 2009).

Pit membranes may also differ in their chemical composition. It is difficult to elucidate what chemical compounds are present in the pit membrane considering the small size of pit membranes and the fact that their surface is usually obscured by an overarching secondary cell wall. It is generally assumed that their chemical nature is similar to that of the primary cell wall from which the pit membranes are derived. Pectins, and specifically their subgroup homogalacturonans (HG), are believed to be important components of pit membranes (Cochard, Herbette, Hernandez *et al.*, 2010, Zwieniecki, Melcher & Holbrook, 2001). HG can differ in the degree of methyl-esterification, which has consequences for the flexibility and extensibility of the primary cell wall (Goldberg, Morvan & Roland, 1986, Guglielmino, Liberman, Jauneau *et al.*, 1997, Willats, McCartney, Mackie *et al.*, 2001). The flexibility of pit membranes might influence the vulnerability to cavitation as pores may enlarge when pit membranes deflect during the process of air-seeding (Choat, Jansen, Zwieniecki *et al.*, 2004, Cochard *et al.*, 2010). We therefore asked whether plants growing under contrasting light levels differed in the abundance of pectins and/or the degree of their esterification by using monoclonal antibodies, JIM5 and JIM7, which recognize HG with low and high degrees of methyl-esterification, respectively (Knox, Linstead, King *et al.*, 1990).

Saplings of hybrid poplar were grown under contrasting irradiance for 40 days. The resulting changes in xylem traits were assessed with light and electron microscopy as well as physiological measurements. Our main hypothesis was that shaded saplings will exhibit increased vulnerability to cavitation along with larger pores in their pit membranes. Differences in light level can have a profound effect

on other aspects of hydraulic architecture, including conduit size and transport efficiency (Schoonmaker *et al.*, 2010). Our second hypothesis was that decreased evaporative demands will correspond with narrower vessels and lower xylem-specific and leaf-specific conductivities in shaded plants. Since carbon resources tend to be more limited in shaded plants, we finally expected that xylem cells of shaded plants will exhibit thinner cell walls and lower wood density than in plants growing at higher light level.

4.2 METHODS

4.2.1 Plant material and sampling strategy

Saplings of hybrid poplar (*Populus trichocarpa* × *deltoides*, clone H11-11) were produced from rooted cuttings. The saplings were maintained in a growth chamber from December 2008 to February 2009 under a 16/8 hour day/night cycle, 24/18 °C day/night temperature, and a daytime relative humidity of 75%. Plants were kept in 6 L pots filled with a commercial potting mix Sunshine Mix LA4 (Sun Gro Horticulture Canada Ltd., Vancouver, BC, Canada) and fertilized once a week with 500 ml of a complete water soluble fertilizer (20-20-20 N-P-K, Plant Products, Brampton, ON, Canada) in 1 g/L dilution. After 8 weeks of sapling establishment, shading structures were built over 11 randomly selected plants. The shading resulted in 80% reduction in irradiance from 350 $\mu\text{mol m}^{-2} \text{s}^{-1}$ (control, C) to 70 $\mu\text{mol m}^{-2} \text{s}^{-1}$ (shade, SH). Plants were harvested 40 days after the beginning of the shade treatment. Hydraulic measurements and silicone injections for vessel length measurements were conducted within 4 days after harvesting. For these measurements 25 cm long stem segments were cut from the basal part of the plant (5 cm above the root collar). After the hydraulic measurements were completed, stem segments were stored at -4 °C and later used for vessel diameter and wood density measurements.

4.2.2 Vulnerability to cavitation, xylem and leaf specific conductivity

Stem segments trimmed to a final length of 14.2 cm were used to generate vulnerability curves. The hydraulic conductivity of the stems was measured using a method originally described in Alder *et al.* (1997). Briefly, a filtered (0.2 μm) measuring solution (20 mM KCl + 1 mM CaCl_2) was perfused through stem segments under a pressure head of 4-5 kPa. Flow through the segments was

recorded with an electronic balance (CP225D, Sartorius, Göttingen, Germany), which was interfaced with a computer. Maximum hydraulic conductivity (K_{max}) was determined after flushing the segments for 15 min at 50 kPa. Xylem-specific conductivity (K_S) and leaf-specific conductivity (K_L) were calculated by dividing K_{max} by cross-sectional xylem area and leaf area distal to the measured segment, respectively (Tyree & Zimmermann, 2002). Vulnerability curves were generated by spinning segments in a centrifuge to progressively more negative pressure and measuring the loss of hydraulic conductivity at each pressure. After fitting the curves to a Weibull function, cavitation resistance was expressed as the mean cavitation pressure (MCP). The MCP is the mean of the Weibull probability density function. In perfectly sigmoidal curves, the MCP equals the xylem pressure associated with 50% loss of hydraulic conductivity (P50). Six stems per group were measured for each light treatment.

4.2.3 Transmission electron microscopy (TEM) and immunolabeling of pectin epitopes

TEM was used to study the effect of light level on pit membrane thickness, cell wall thickness and on the presence and distribution of homogalacturonans (HG) in cell walls and pit membranes. For the regular TEM, small blocks of xylem tissue (1x1x2 mm) were fixed overnight at room temperature in a fixative containing 2% paraformaldehyde and 2.5% glutaraldehyde in 0.05M phosphate buffer. The following day, samples were repeatedly buffer-washed, postfixed in osmium tetroxide for 2 hours, 3x buffer-washed and dehydrated in a graded ethanol series (20-30-40-60-80-90-100-100% for 15 min each). The dehydrated samples were embedded in Spurr resin. Ultrathin sections (80 nm) were sectioned with an ultramicrotome (Ultracut E, Reichert-Jung, Vienna, Austria), collected on copper grids and contrasted in uranyl acetate and lead citrate.

Immunolabelling with JIM5 and JIM7 antibodies, kindly donated by Prof. J. P. Knox (University of Leeds, UK), was used to detect pectic HG in xylem samples. JIM5 and JIM7 are well-characterized monoclonal antibodies that have been previously used to detect differently-esterified HG in various plant tissues (Guglielmino *et al.*, 1997, Guillemin, Guillon, Bonnin *et al.*, 2005, Hafren & Westermarck, 2001). Typically, JIM5 binds to HG with few or no esters, whereas JIM7 recognizes highly methyl-esterified pectin epitopes (Knox *et al.*, 1990). In our experiment, we followed a preparation procedure described by Micheli *et al.* (2002). After fixation in 4% paraformaldehyde and 1.25% glutaraldehyde in

0.05 M phosphate buffer for 1.5 hour at room temperature, samples were dehydrated in an ethanol series as described above. Samples were then embedded in LR White resin. Ultrathin sections collected on nickel grids were immunolabeled by floating the grids on drops of successively changing solutions as described below. Sections were preincubated for 10 min on a drop of 0.05 M Tris-buffered saline (pH= 7.6) with 0.1% Tween 20 and 0.1% bovine serum albumin, blocked for 20 min with goat serum (Sigma-Aldrich Corp., St. Louis, MO, USA) diluted 1:30 (v/v) in the same buffer, treated with the primary antibody JIM5 or JIM7 (diluted 1:45) for 4 hours, four times buffer-washed and stained with a secondary antibody, goat-anti rat IgG conjugated with 10 nm gold particles (Sigma-Aldrich Corp., St. Louis, MO, USA) for 1 hour. The grids were then extensively washed with buffer and filtered water and finally contrasted with 1% uranylacetate for 25 min. All these steps were conducted at room temperature.

Regular and immunolabeled samples were examined under a transmission electron microscope (Morgagni 268, Fei Company, Hillsboro, OR, USA). About 20 individual pit membranes from five individual stems were photographed at 20,000-45,000 x magnification and used for pit membrane thickness measurements in both light treatments. For cell wall thickness measurements, a region of a vessel and a fiber adjacent to each other was randomly selected and photographed. The thickness of the electron dense compound middle lamella (a layer composed of the middle lamella and primary cell walls of two adjacent cells) was measured together with the thickness of the less electron dense secondary cell wall of fibers and vessels. Five different vessel-fiber regions were measured in each stem; five stems were measured in total for each light treatment. Three grids were prepared for immunostaining with each antibody for both SH and C samples.

4.2.4 Scanning electron microscopy (SEM)

Two sample preparation procedures were used to generate samples for SEM. Initially, fresh stem segments 1.5 cm in length were air-dried on a bench for several weeks. Samples were split longitudinally with a razor blade and mounted on aluminum stubs using conductive silver paste. The split was made about 1 mm from the surface of the stem to expose pits that developed under treatment conditions. Although air-drying without any chemical treatment was recently recommended for observing pit membranes (Jansen *et al.*, 2008), we experienced difficulties finding undamaged pits in our plant material. We attributed this to the capillary forces caused by the high surface tension of water. Therefore, we

gradually exchanged water for pure ethanol (with low surface tension) before air drying the samples. Frozen stem samples were thawed and soaked for 5 days in distilled water. Samples were subsequently dehydrated through an ethanol series (30-50-70-90%) for 30 min in each solution, immersed in 100% ethanol overnight, and finally air-dried. Splitting and mounting was conducted as described above. Samples were sputter coated with chromium and carbon. The thickness of the coating was approximately 5-10 nm. Samples were observed with a field-emission scanning electron microscope (6301F, JEOL, Tokyo, Japan) under 2 kV accelerating voltage. Pictures of pit membranes were taken at 8,000-15,000 x magnification. In shade samples prepared by air drying from water it was difficult to find undamaged exposed membranes. Therefore, about 15% of pictures were taken through the aperture in the secondary cell wall in these samples. In the rest of the images, at least half of the fully exposed membrane area was analyzed to provide a reliable estimate of pit membrane porosity. Pore size was measured using image analysis software (ImagePro Plus version 6.1, Media Cybernetics, Silver Spring, MD, USA). Pore areas were converted into diameters assuming a circular shape of pores. Pores smaller than 20 nm in diameter could not be accurately distinguished from random pixel noise and were excluded. Maximum (D_{\max}) and average pore size (D_{mean}) was determined for each pit membrane. About 100 individual pit membranes from at least 30 different pit fields were measured for each light treatment and each preparation technique. Individual pit-level measurements were averaged for each stem segment analyzed.

4.2.5 ‘Rare pit’ model

Details of the model have been described previously (Christman *et al.*, 2009). According to the air-seeding hypothesis, the cavitation threshold for a given vessel is determined by the size of the largest pore that can be present in any of the pits in the vessel. An assumption of the rare pit hypothesis is that there are few pits with large pores and with relatively low air-seeding pressure, compared with the majority of ‘air-tight’ pits. A cumulative distribution function (cdf) $F_m(p)$ can be used to describe the cumulative frequency of intervessel pits that air seed at progressively greater pressure difference (p). Assuming that pits are independently distributed among vessel endwalls, the $F_m(p)$ can be used to calculate the cumulative frequency of vessel end walls that air seed at increasing pressure differences (end wall cdf, $F_e(p)$):

$$F_e(p) = 1 - [1 - F_m(p)]^u$$

(Eqn. 4-2)

where u is the number of intervessel pits per vessel. The $F_e(p)$ cdf can be converted into the corresponding probability density function (pdf). The mean pressure of this distribution represents the mean end wall air-seeding pressure (MCP_e). This value should be a proxy for the MCP of the xylem.

From SEM porosity measurements, we obtained empirical $F_m(p)$ distributions. First, the Young-Laplace equation (Eqn. 4-1) was used to convert the D_{\max} of individual pits to the corresponding air-seeding pressure (P_a). Second, the empirical data were fitted with a Weibull cdf

$$F_m(p) = 1 - e^{-\left(\frac{p}{b}\right)^c} \quad (\text{Eqn. 4-3})$$

where b is the scale, and c is the shape fitting parameter of the Weibull distribution. Then, we used the fitted distribution $F_m(p)$ in Eqn. 4-2 to calculate MCP_e . Initial calculations based on D_{\max} yielded high (less negative) MCP_e in comparison to the measured MCP . It is likely that dehydration of the membranes resulted in enlargement of the pit pores from their native state because of shrinkage of the membrane matrix. To account for this, we also represented the D_{\max} per pit by averaging the top percentile of pore diameters per pit, and finding the percentile that provided the best fit of MCP_e to MCP .

4.2.6 Xylem anatomy

Stem cross-sections were prepared with a sliding microtome (SM2400, Leica Microsystems, Wetzlar, Germany) from the center of segments previously used for hydraulic measurements. The sections were stained with toluidine blue for 3 minutes, rinsed in water, mounted on slides and observed with a light microscope (DM3000, Leica). Three radial transects were selected in a cross-section. Images were captured with a digital camera (DFC420C, Leica). The diameters (D) of vessels in each radial sector were measured using image analysis software (ImagePro). The hydraulic diameter (D_h) was then calculated as $D_h = (\sum D^5) / (\sum D^4)$. A total of 300 to 500 vessel diameters was measured per stem; six stems were analyzed for each light treatment. The vessel double wall thickness (t_h) was measured on vessel pairs in which at least one of the vessels fell within $\pm 3 \mu\text{m}$ of D_h . A total of 15 vessel pairs was measured per stem; six stems were analyzed for each light treatment.

Vessel length was measured using the silicone injection method (Sperry, Hacke & Wheeler, 2005). Stems 14 cm in length were flushed for 15 min at 50 kPa. Silicone (Rhodorsil RTV-141, Bluestar Silicones, distributed by Skycon, Toronto, ON, Canada) was mixed with a fluorescent whitening agent (Uvitex OB, Ciba Specialty Chemicals, Tarrytown, NY, USA), and injected into the stems at a pressure of 50 kPa for 24 hours. The silicone did not penetrate vessel end walls. Therefore, a progressively decreasing number of vessels was filled with silicone as the distance from the injection surface increased. This relationship can be fitted with an exponential decay function, and the vessel length distribution can be estimated. The mean of log-transformed vessel length data was used to represent the vessel length distribution of a stem. Five to six stems per light treatment were analyzed. Vessel element length as well as the length and diameter of wood fibers were measured on macerated wood tissue, using a light microscope and image analysis software. At least 100 cells were measured from each individual stem; six stems were analyzed for each light treatment. The number of pits per vessel, the u parameter of the rare pit model, was calculated as the total pit membrane area per vessel (A_p) divided by the area of individual pit membranes (A_i). To measure A_i longitudinal sections of stem xylem were prepared and observed under 1000 x magnification. The A_p was estimated as the product of average vessel area (A_v), contact fraction and pitfield fraction (see details in Wheeler *et al.*, 2005).

4.2.7 Wood density

Wood density (d_w) was determined on six segments per group by water displacement. Debarked stem segments approximately 2 cm in length were split longitudinally and the pit was removed. Samples were submersed in a beaker of water on a balance to determine the fresh volume of wood. Samples were then oven-dried at 70 °C for 48 hours. Wood density of each sample was calculated as $d_w = \text{dry weight} / \text{fresh volume}$.

4.2.8 Statistics

Prior to the analysis, normality and homogeneity of variance were graphically checked. Independent two sample t-tests were used to compare the differences in means between SH and C. Two-way ANOVA and Tukey's HSD post hoc comparison tests were used to dissect the effect of light treatment and sample preparation technique on porosity data. The statistical software package R 2.10.1 was used to perform the analysis.

4.3 RESULTS

4.3.1 Plant growth

Hybrid poplar is a fast growing tree with a high demand for light. When shaded, the saplings exhibited a typical response of shade avoiders. They enhanced shoot elongation and developed thinner leaves in order to increase light interception (Table 4-1). Average daily height increments were 2.2 ± 0.1 and 2.0 ± 0.1 cm (mean \pm SD), leading to a final height of 118 ± 5.3 and 109.3 ± 3.2 cm in SH and C plants, respectively. The radial growth of SH plants was reduced, which resulted in thinner stems in this plant group ($D_{\text{stem}} = 6.8 \pm 0.3$ vs. 8.1 ± 0.2 mm in SH and C plants, respectively). Total leaf area (A_L) was the same, but leaf dry weight was much larger in C plants implying a strong difference in leaf weight per unit leaf area (LWA). For the stem segments used for hydraulic measurements, the ratio between supported leaf area and cross-sectional xylem area (A_L/A_X) was significantly higher in SH plants.

4.3.2 Xylem vulnerability and hydraulic conductivity

Differences in light level had an effect on vulnerability of stems to cavitation (Fig. 4-1a). SH plants were more vulnerable with a *MCP* of -1.13 ± 0.10 MPa, compared with -1.51 ± 0.06 MPa in C stems. In addition to being more resistant to cavitation, stems of C plants showed higher transport efficiency than those of SH plants. The specific conductivity values (K_S) were 6.6 ± 0.6 and 4.7 ± 0.4 kg s⁻¹ m⁻¹ MPa⁻¹ in C and SH stems, respectively (Fig. 4-1b). Leaf-specific conductivity was almost twice as high in C plants (Fig. 4-1c).

4.3.3 Pit membrane ultrastructure and immunolabeling

TEM micrographs revealed that intervessel pit membranes in SH plants were thinner (162.1 ± 20.3 nm) than in C plants (229.5 ± 28.8 nm) (Fig. 4-2a). Differences in pit membrane thickness were paralleled by a similar trend in compound middle lamella thickness (Fig. 4-2b). Pit membranes appeared granular and less electron-dense than the adjacent compound middle lamella layer (cml). The annulus (the periphery of the pit membrane) was usually more electron-dense than the rest of the pit membrane, and could clearly be distinguished at the transition between primary cell wall and the actual pit membrane (Fig. 4-3b).

The immunolocalization pattern for both antibodies, JIM5 and JIM7, was similar in SH and C xylem. JIM7 provided a slightly stronger signal than JIM5. The distribution of immunogold particles indicated that HG were present in the compound middle lamella. The strongest labeling was found in cell corners (Fig. 4-3a). Most importantly, neither JIM5 nor JIM7 labeling were evident in the pit membranes, with an exception of the annulus which often showed stronger labeling than seen in compound middle lamella (Fig. 4-3b).

In SEM micrographs, resolvable pores were observed in the vast majority of pit membranes, but their number and size varied substantially. Measurements of membrane porosity gave contrasting results depending on the sample preparation method. In water-dried samples (air-dried from water), pores appeared to be larger than in ethanol-dried samples (air-dried from pure ethanol). Drying from water tended to produce a high number of pit membranes with a non-microfibrilous texture and large, round, and well-defined pores (Fig. 4-4a). In contrast, the surface of ethanol-dried pit membranes usually displayed an extensive meshwork of randomly oriented microfibrils connected with amorphous filling material. The pores were generally smaller and not as clearly distinguishable as in water-dried samples (Fig. 4-4b). In a few instances, pit membranes with no visible pores were observed and such membranes also lacked a resolvable microfibrilous texture. In some cases, a gelatinous layer was observed. This layer seemed to be detached along the edges of the pit membrane, thereby forming a distinct white ring (Fig. 4-4c).

The influence of the drying method on pore size was more pronounced in the thinner pit membranes of SH samples (Fig. 4-5). The maximal pore diameter per pit (D_{\max}), the mean diameter of the largest 10% of pores per pit ($D_{10\%}$), and the mean pore diameter per pit (D_{mean}) were all significantly larger in water-dried samples than in ethanol-dried SH samples (compare black and grey bars on the left hand side of Fig. 4-5a-c). In water-dried samples, all measures of pore size tended to be larger in SH than in C plants. By contrast, in ethanol-dried samples, pore size did not vary in response to light level (Fig. 4-5, compare grey bars).

4.3.4 ‘Rare pit’ model

Given the fact that the different preparation techniques had a larger effect on pit porosity than the light treatments, we pooled SH and C data while distinguishing between ethanol- and water-dried samples when calculating the expected mean cavitation pressure (MCP_e) using the rare pit model. For both

preparation methods, the predicted MCP_e was substantially higher (less negative) than the value obtained from vulnerability curves when D_{max} was used (Fig. 4-6a-b, solid thick curves). In ethanol-dried samples, a reasonable agreement between modeled and measured MCP was found when averages of the largest 7.5% of pores were used instead of the single largest pore diameters (Fig. 4-6a, dashed curve). In water-dried samples, the best agreement between modeled and measured MCP was achieved when the average of the largest 50% of pores was used (Fig. 4-6b). The Weibull parameters for cumulative pit frequency distributions and the corresponding MCP_e predicted by the model for various pit porosity data are presented in Table 4-2.

4.3.5 Vessel and fiber anatomy

Shading resulted in significant changes in the dimensions of xylem cells. Vessels in SH stems were narrower (Fig. 4-7a) and longer (Fig. 4-7b) than in C stems. Hydraulic vessel diameters (D_h) were 41.1 ± 1.2 and 43.1 ± 1.4 μm in SH and C plants, respectively. Mean vessel lengths were 3.9 ± 0.4 cm in SH and 3.1 ± 0.2 cm in C stems. The increased length of vessels in SH plants was in agreement with a higher average vessel element length (238.5 ± 10.8 μm in SH vs. 226.3 ± 7.2 μm in C) (Fig 4-7c). Secondary cell wall thickness of vessels measured from TEM micrographs did not significantly differ between SH and C plants although the wall tended to be thinner in SH plants (Fig. 4-8a). The double vessel wall thickness measured with light microscopy was significantly lower in SH than in C plants (Fig. 4-8b). While fiber diameters did not change in response to light level, fiber length was significantly reduced in SH plants (Table 4-3). Analysis of TEM images showed that shading also resulted in significantly thinner secondary cell walls in fibers, a trend that was paralleled by lower wood densities in stems of SH plants (Table 4-3).

4.4 DISCUSSION

In agreement with our main hypothesis, hybrid poplar saplings exhibited increased xylem vulnerability when grown under shade (Fig. 4-1a). This finding is consistent with previous results on other tree species (Barigah *et al.*, 2006, Cochard *et al.*, 1999, Schoonmaker *et al.*, 2010). Increased vulnerability was associated with thinner pit membranes. This finding agrees with a recent study on angiosperm species, which found correlations between pit membrane thickness and membrane porosity as well as vulnerability to cavitation (Jansen *et al.*, 2009).

Species with thinner, more porous membranes should be more vulnerable than species with thicker membranes (Jansen *et al.*, 2009), and such interspecific correlations may also occur within a single genotype. Thinner pit membranes in SH plants (Fig. 4-2a) probably represented a weaker barrier between air and water-filled vessels, and allowed air-seeding at lower ΔP_{crit} than in C plants with thicker pit membranes. The link between membrane porosity and thickness remained somewhat ambiguous in our study (Fig. 4-5), which may be due to artifacts resulting from sample preparation (as discussed below). Several experiments have also suggested that pores become enlarged when the membrane deflects during air-seeding (Choat *et al.*, 2004, Cochard *et al.*, 2010). Such enlargement would presumably be more pronounced in the thinner membranes of SH plants and would contribute to the lower air-seeding threshold observed in SH plants, despite similar porosity under relaxed conditions. In any case, pit membrane thickness appears to be an important characteristic influencing cavitation resistance.

The factors determining pit membrane thickness are not fully understood. In this study, reduced pit membrane thickness in SH samples was paralleled by a thinner primary cell wall and middle lamella layer (Fig. 4-2b). Since pit membranes are derived from this compound middle lamella, such a correlation is not unexpected. In shaded samples, there was no significant difference between the compound middle lamella and pit membrane thickness. In control samples, pit membranes were on average 50 nm thicker than the compound middle lamella. It is possible that some material is deposited on the pit membrane surface as suggested by the observation that pit membranes were almost twice as thick as the compound middle lamella in some angiosperm species (Jansen *et al.*, 2009).

The SEM-based measurements of pit porosity in SH and C samples produced different results depending on the sample preparation method (compare Fig. 4-4a-b, Fig. 4-5). When samples were water-dried (air-dried from water), pores appeared larger in SH than in C plants, which was in agreement with our initial hypothesis. However, there was no significant difference in pore sizes between SH and C when ethanol-drying was used. Consistent with the rare pit hypothesis, the vast majority (95%) of pores detected with SEM were smaller than the pore size allowing air-seeding at the *MCP*. This result is in agreement with previous SEM work (Choat *et al.*, 2003). However, when we used the pit porosity data in the 'rare pit' model to predict *MCP*, the results suggested that pore sizes measured from SEM images overestimate real porosity (Table 4-2, Fig.

4-6), especially in the water-dried samples. There could be several possible reasons for this finding, and most likely a combination of them contributed to this result. First, sample dehydration may have resulted in a general enlargement of pores as the gelatinous material filling the space between the microfibrils shrank. It is possible that the effect of such shrinkage was more dramatic in thinner pit membranes, which might explain the larger porosity of water-dried samples in SH plants. Second, some of the large pores that we measured were probably artifacts or resulted from local damages to the membrane that were caused as some of the microfibrils ruptured during the desiccation process. Occasionally, some pores in an individual pit membrane were suspiciously larger than the rest of the pores, similar to the pattern found by Sano (2005, his Fig. 8). However, it was difficult to draw a distinct line between pores that could be considered real and those resulting from artificial damage. The fact that model predictions based on the averages from 7.5% of the largest pores already provided a reasonable agreement with the measured *MCP* in ethanol-dried samples (Table 4-2) is encouraging since it indicates that the porosity measurements are relatively close to expected reality. Nonetheless, the exact magnitude of pore enlargement due to the sample dehydration method is difficult to quantify because of the inherent difficulty of locating the rare pits with the largest pores, thus measuring the real range of D_{max} values.

Based on our results from poplar xylem, ethanol dehydration seems to be a better alternative for preparing pit membrane samples for SEM-imaging in comparison to air-drying, as it produced a higher number of intact pit membranes with more reasonable porosity. Air-drying from pure ethanol was presumably less disruptive than air-drying from water and hence, preserved pit membrane structure closer to its natural state. This finding contrasts with conclusions of Jansen et al. (2008) who got better results with water-drying of samples prior to SEM observations. It is possible that some preparation techniques are more suitable for certain species. Notably, Jansen et al. used species with thicker pit membranes than those found in poplar. Thicker membranes are probably more resistant to the negative effects of air-drying from water.

Although ethanol-drying provided better results, it was probably far from being free of artifacts. In a few instances, we observed a layer that tended to detach around the perimeter of the pit membrane, creating an apparent white ring as the edges of the layer rolled up (Fig. 4-4c). In several angiosperm species (e.g., *Goniorrhachis*, *Salix*, *Betula*), pit membranes were shown to consist of multiple

layers of microfibrils that can be peeled off during the sample preparation (Jansen *et al.*, 2009, Sano, 2005, Schmid & Machado, 1968). In contrast to these SEM studies, in our case this upper layer appeared amorphous with no visible fibrils. In addition, we observed several pits that displayed a homogenous surface texture with no resolvable pores and microfibrils. In a pioneering study using atomic force microscopy for investigating the structural properties of pit membranes, Pesacreta *et al.* (2005) found a microfibrillar coating at the surface of pit membranes of *Sapium sebiferum*. The coating was homogeneously thick when non-dried samples were observed, while air-dried samples showed variability in the thickness of this coating. The coating was on average thinner when compared with non-dried samples. Thus, it is possible that the layer shown in Fig. 4-4c represents a similar coating. Although the chemical nature of this coating is not known, Pesacreta *et al.* (2005) suggested that polyphenolics or pectins might be present.

Strikingly, our TEM immunolabeling procedure using the antibodies JIM5 and JIM7 failed to detect homogalacturonans (HG) in poplar pit membranes with a notable exception of the annulus region (Fig. 4.3a-b). These results should be verified in naturally grown mature poplar trees since it is possible that the young age of the saplings influenced the chemical composition of the pit membranes and compound middle lamella. Nevertheless, the overall pattern of labeling in the compound middle lamella in our experiment was similar to the pattern found in mature wood of Scots pine (Hafren, Daniel & Westermarck, 2000). However, in the case of pine, the torus of the pit membrane was labeled as well. In poplar, the labeling suggests that HG were removed or modified when the compound middle lamella developed into a pit membrane. It has been suggested that non-cellulosic polysaccharides are hydrolyzed in the pit membranes of *Salix* (O'Brien, 1970). In a recent study, Herbette and Cochard (2010) showed that removal of calcium from the conduit cell wall resulted in increased xylem vulnerability in eleven tree species while no effect of calcium removal was found in *Salix* and *Betula*. The effect of calcium removal on vulnerability was attributed to the disruption of the supermolecular structure of HG polymers present in the pit membranes, allowing air-seeding under less negative pressure. The absence of an effect of calcium removal on cavitation resistance in *Salix* and *Betula* suggests that HG might not be present in the pit membranes of these highly vulnerable species. In further support of our results, Nardini *et al.* (2007) did not find any differences in the ion-mediated effect on stem hydraulic conductivity in tobacco plants with reduced HG content when compared to control plants with unaltered composition. We

suggest that the current paradigm about the general presence of HG in mature pit membranes needs to be reconsidered. To date, there is no *direct* evidence that pectins are present in mature angiosperm pit membranes (Choat *et al.*, 2008), even though there is clear evidence for the occurrence of pectins in pit membranes of conifers (Hafren *et al.*, 2000).

Some kind of filling material in which cellulosic microfibrils are embedded is clearly present but the question about its chemical nature remains unresolved. Given the dramatically different appearance of pit membranes in different species (Jansen *et al.*, 2009), variability in their chemical composition may be expected. While HG may be present in the pit membranes of some species (Perez-Donoso, Sun, Roper *et al.*, 2010), they may be absent or masked in other species like poplar, willow or birch. Hemicelluloses and two other groups of pectin (rhamnogalacturonan I and II) are commonly present in primary cell walls (Fry, 2004), and are probably also present in pit membranes. In addition, Schmitz *et al.* (2008) reported a low but detectable lignin content in pit membranes of two mangrove species. The presence of hydrophobic substances such as lignin in pit membrane would have an important effect on xylem vulnerability as a non-zero contact angle in Eqn. 4-1 would result in lower cavitation pressure for a given pore size (Meyra, Kuz & Zarragoicoechea, 2007). More research addressing pit membrane chemistry is clearly required for a better understanding of intervessel pit functioning.

The xylem of SH grown poplars was not only more vulnerable, but also exhibited lower transport efficiency (Fig. 4-1b). These observations are in line with earlier results (Lemoine, Jacquemin & Granier, 2002, Raimondo *et al.*, 2009). Lower K_S can be explained by significantly narrower vessels found in SH plants (Fig. 4-7a). However, the vessels in SH plants were also longer (Fig. 4-7b) which should result in smaller end wall resistance as xylem sap crosses fewer end walls in series. This decrease in end wall resistance was probably not big enough to compensate for the effect of narrower vessels. The xylem of SH plants therefore appears less optimized from a hydraulic standpoint. This study also reinforces the point that higher xylem vulnerability is not always associated with increased xylem transport efficiency; especially when looking at the intraspecific level (Fichot, Barigah, Chamaillard *et al.*, 2010, Martinez-Vilalta, Cochard, Mencuccini *et al.*, 2009).

Despite smaller xylem areas and lower xylem transport efficiency, the total leaf area was comparable between SH and C plants (Table 4-1). This implies

that K_L was lower in SH plants compared with their C counterparts (Fig. 4-1c). Lower K_L in plants growing under shade has been previously reported from both controlled and field conditions (Caquet *et al.*, 2009, Schoonmaker *et al.*, 2010, Schultz & Matthews, 1993). In shade conditions, the vapor pressure difference between the leaf and ambient atmosphere is usually low. Well-watered plants can maintain large leaf areas even though their xylem transport is less efficient. A large leaf area in shade is desirable as it helps to capture more light which represents the main limiting factor in such an environment. However, low K_L can represent a risk to the plant under high evaporative demands as insufficient water supply to the leaves may result in stomatal closure and/or xylem cavitation.

As is obvious from the lower wood densities and thinner cell walls in both vessels and fibers (Fig. 4-8a-b, Table 4-3), the mechanical function of xylem was suppressed in SH plants, probably due to limiting carbon availability. The lower wood density in SH plants was driven mainly by the lower fiber cell wall thickness, because the diameter of fibers as well as vessel density were not significantly different between SH and C plants. It is also worth noticing that the fiber length was lower in SH plants (Table 4-2), which contrasts with the pattern found with vessel and vessel element length. During xylogenesis, the future vessel elements and fibers have the same length until an intensive intrusive growth of fiber tips is initiated (Siedlecka, Wiklund, Peronne *et al.*, 2008). Hence, our data suggest that the intrusive growth of fibers was inhibited in SH plants relative to C. Consistent with our results, lower wood density (Hacke, Sperry, Pockman *et al.*, 2001) and decreased double wall thickness (Cochard, Barigah, Kleinhentz *et al.*, 2008) are often associated with increased xylem vulnerability. The link between these characteristics and xylem safety has been viewed as indirect and based on the fact that strong mechanical reinforcement is required in cavitation-resistant conduits to prevent their collapse when they are subjected to highly negative xylem pressure (Hacke *et al.*, 2001). However, there may be a coordination between compound middle lamella (and hence pit membrane) thickness and overall cell wall thickness which could influence wood density as suggested by Jansen *et al.* (2009). The results presented in this study (Fig. 4-2) are in agreement with their hypothesis. However, more research is required to further verify this proposed link between wood density and xylem vulnerability.

4.5 CONCLUSIONS

This study provides new insights into homogenous pit membrane functioning. The results presented here indicate that the structure of homogenous pit membranes in poplar is affected by growing conditions. The thinner pit membranes that developed in SH plants served as a weaker protection against air-seeding resulting in more vulnerable xylem. By using the empirical pit porosity data in conjunction with the 'rare pit' model, we were able to evaluate how SEM-based porosity estimates compared with the porosity expected based on the air-seeding theory. To the best of our knowledge, this is the first study using carbohydrate-specific antibodies to dissect inter-vessel pit membrane chemistry in poplar. Pectic HG are believed to be responsible for many physiological processes associated with pit functioning such as the ion-mediated changes in hydraulic conductivity or calcium-dependant changes in xylem vulnerability. Our finding that HG are not universally present in all angiosperm pit membranes highlights the need for a better characterization of pit membrane structure and function.

4.6 TABLES

Table 4-1: Growth characteristics of poplar saplings grown under shade (SH) or control light conditions (C).

	SH	C	<i>P</i> value
height (cm)	118.0 ± 5.3	109.3 ± 3.2	0.007
D _{stem} (mm)	6.8 ± 0.3	8.1 ± 0.2	< 10 ⁻³
total A _L (m ²)	0.47 ± 0.04	0.49 ± 0.02	ns
DWL (g)	11.7 ± 1.5	26.3 ± 1.0	< 10 ⁻³
LWA (g/m ²)	24.7 ± 1.1	53.6 ± 2.9	< 10 ⁻³
A _L /A _X (cm ² /mm ²)	214.0 ± 9.8	170.3 ± 15.7	< 10 ⁻³

Abbreviations: height - sapling final height, D_{stem} - stem diameter at 10 cm above the root collar, A_L - total leaf area, DW_L - total leaf dry weight, LWA - leaf weight per unit leaf area and A_L/A_X - supported leaf area to xylem area ratio of the measured stem segment. Means ± SD, *n* = 6. *P* values show results of independent two-sample t-tests, testing for differences between the two light treatments; ns = non-significant difference (*P* > 0.05).

Table 4-2: Fitted Weibull constants of empirical pit distributions and mean cavitation pressure from the ‘rare pit’ model for different pit pore diameter data. The *D data* column indicates what data was assumed as an empirical pit distribution (max-the largest pore from an individual pit or the average from the indicated percentage of the largest pores per individual pit). *b* and *c* represent the Weibull parameters providing the best fit of Eqn. 4-3 to empirical pit distribution data. MCP_e is mean end wall air seeding pressure predicted by the model.

	<i>D data</i>	Weibull parameters		MCP_e (MPa)
		<i>b</i>	<i>c</i>	
Ethanol-dried	max	4.08	3.14	-0.43
	1%	4.27	4.12	-0.73
	2.5%	4.59	4.76	-0.98
	5%	4.95	5.16	-1.18
	7.5%	5.21	5.61	-1.38
	10%	5.44	5.84	-1.52
Water-dried	max	3.04	2.84	-0.27
	1%	3.19	3.23	-0.37
	10%	4.17	3.81	-0.63
	15%	4.48	3.99	-0.72
	30%	5.21	4.40	-0.98
	50%	5.99	4.83	-1.29

Table 4-3: Properties of xylem cells and wood density of poplar saplings grown under shade (SH) or control light conditions (C). Diameter and length of fibers (measured from macerations, grand means of $n = 6$ stems), thickness of secondary cell wall of fibers (measured from TEM micrographs, grand means of $n = 5$ stems), and wood density ($n = 6$). Means \pm SD. P values show results of independent two-sample t-tests; ns = non-significant difference.

	SH	C	P value
Fiber diameter (mm)	19.5 ± 0.9	19.8 ± 0.8	ns
Fiber length (mm)	531.1 ± 23.3	580.7 ± 15.7	0.001
Secondary cell wall thickness of fibers (nm)	762.5 ± 65.3	1031.6 ± 163.2	< 0.01
Wood density (g cm^{-3})	0.32 ± 0.01	0.40 ± 0.01	$< 10^{-3}$

4.7 FIGURES

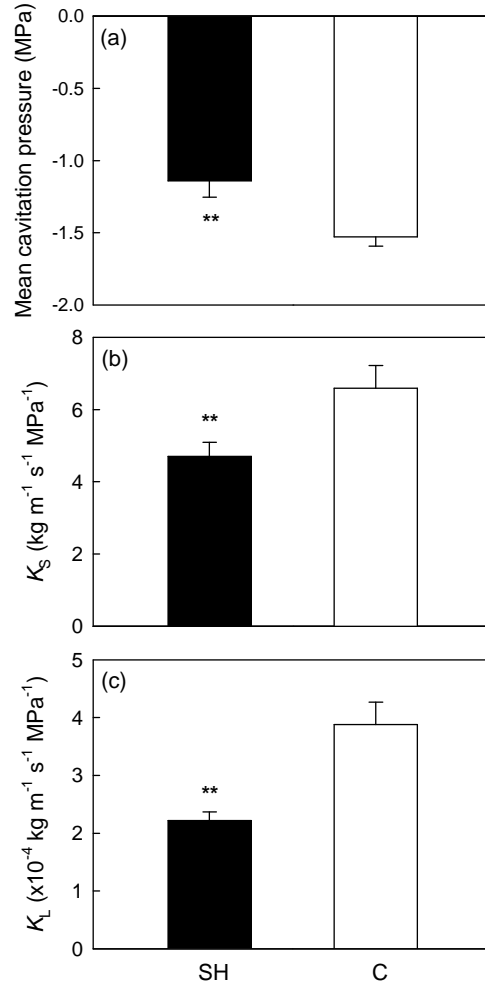


Figure 4-1: The (a) mean cavitation pressure, (b) xylem-specific and (c) leaf-specific conductivity of stem segments of poplar saplings grown under shade (SH, black bars) or control light conditions (C, open bars). Error bars show SD ($n=6$). ** indicates significant differences at $P \leq 0.01$ (independent two-sample t-test).

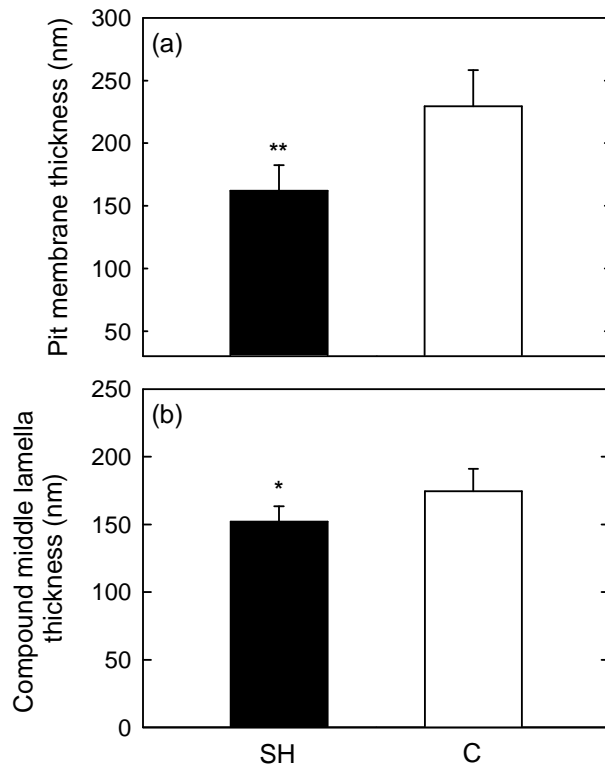


Figure 4-2: (a) pit membrane and (b) compound middle lamella thickness in plants grown in shade (SH, black bars) or control light conditions (C, open bars). The bars represent grand means \pm SD ($n=5$). * and ** indicate significant differences at $P \leq 0.05$ and 0.01 , respectively (independent two-sample t-test).

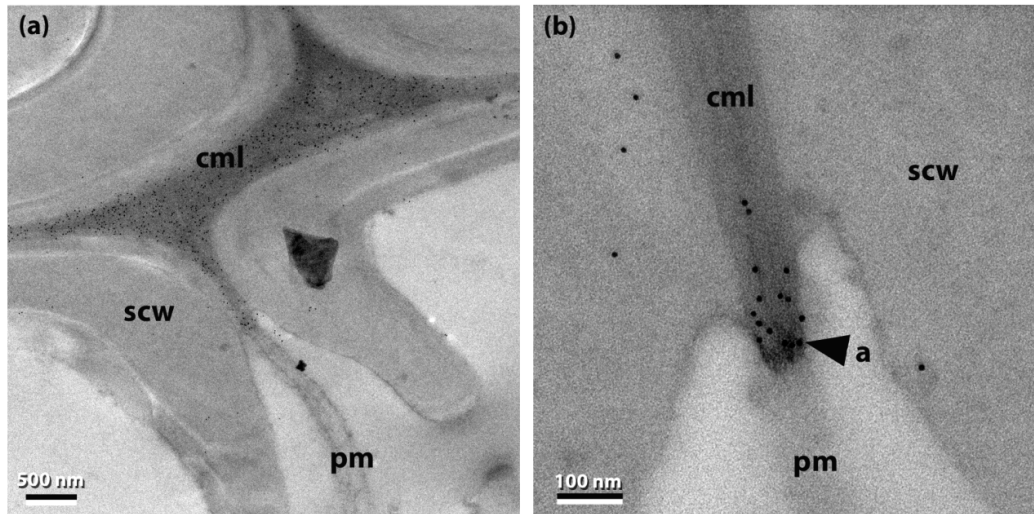


Figure 4-3: Immunogold localization of homogalacturonans in mature xylem with the monoclonal antibody JIM7 with transmission electron microscopy. (a) JIM7 labeled the compound middle lamella (cml), but not the mature pit membrane (pm), suggesting that homogalacturonans were not present in the pm. (b) Gold particles were frequently located in the pit membrane annulus (arrowhead marked 'a'). Plants were grown in (a) shade and (b) control light conditions. scw- secondary cell wall

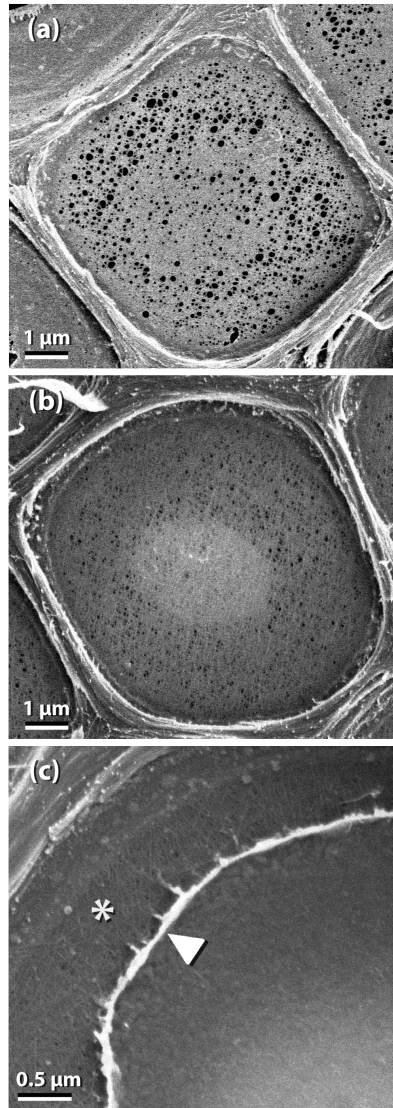


Figure 4-4: Scanning electron micrographs of exposed pit membranes. Porosity and texture of the pit membranes differed depending on the drying method used for sample preparation. (a) Pit membranes from water-dried (i.e., air-dried from the fully hydrated state) samples displayed large clearly resolvable pores and no visible microfibrils. (b) Pit membranes from ethanol-dried samples showed smaller pores embedded in a readily visible meshwork of randomly oriented microfibrils. The outline of the pit aperture is apparent as a lighter area in the center of the pit membrane. (c) Close-up view of the pit membrane showing amorphous material (arrowhead) being detached from the edges of the pit membrane revealing a layer with visible pores and microfibrils (asterisk). The pictures were taken in samples from (a, b) shaded plants and (c) plants grown under control light conditions.

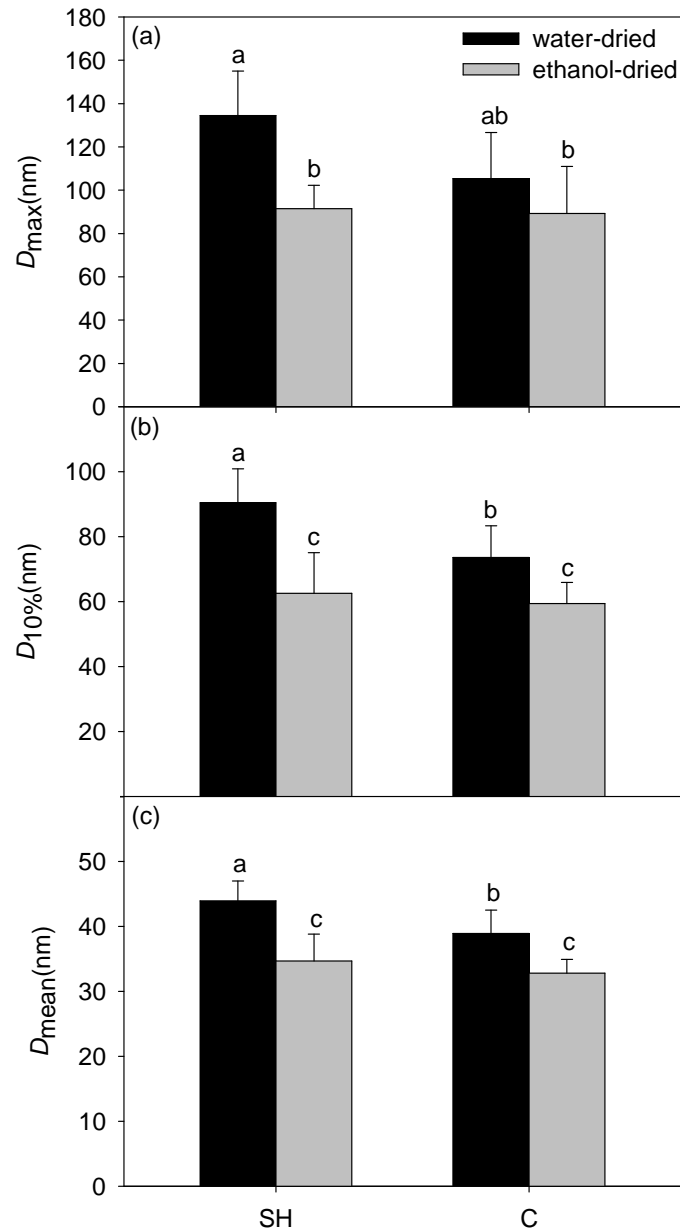


Figure 4-5: Scanning electron microscopy based measurements of pit membrane porosity. (a) maximal pore diameter D_{max} , (b) average diameter of the 10% largest pores $D_{10\%}$, and (c) mean pore diameter D_{mean} measured per pit in water-dried (black bars) or ethanol-dried (gray bars) SEM samples. The bars represent grand means \pm SD from six individual stems. Bars with no letters in common were statistically different at $P \leq 0.05$ (two-way ANOVA and Tukey HSD test).

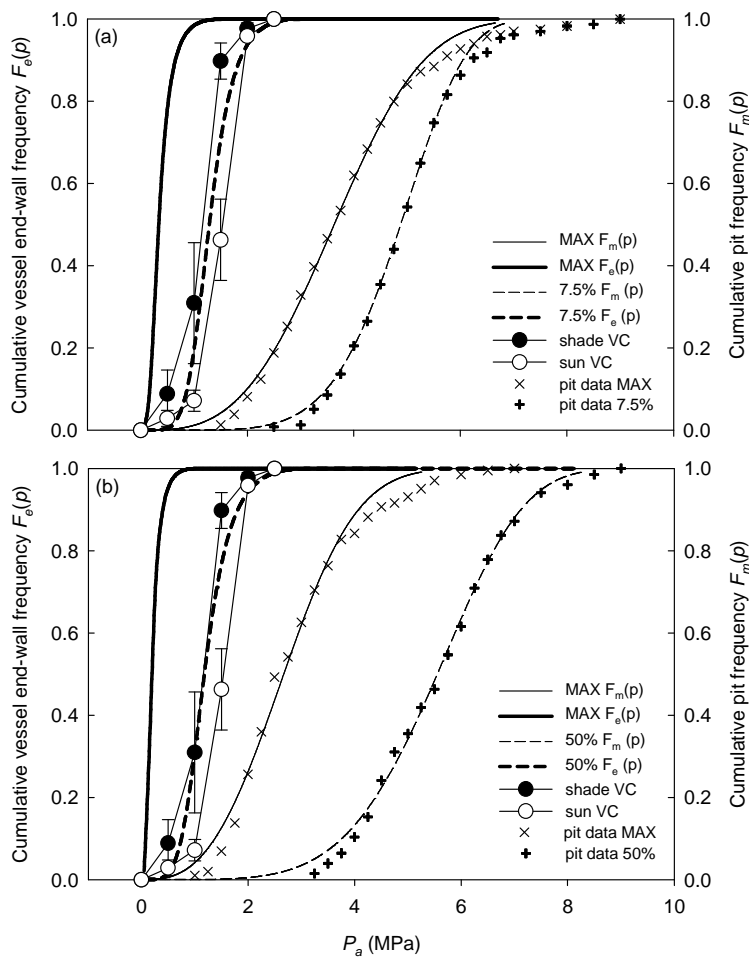


Figure 4-6: Fitted cumulative frequency distribution for the air-seeding pressure (P_a) of individual pits ($F_m(p)$) and pitted end-walls ($F_e(p)$) as calculated from the ‘rare pit’ model for (a) ethanol-dried and (b) water-dried samples. The mean of the $F_e(p)$ distribution provides an estimate of the mean cavitation pressure (MCP). Results obtained when maximal pore diameter per individual pit was used to generate cumulative pit frequency distribution are shown together with the results providing reasonable agreement with measured MCP . This occurred when the average from 7.5% and 50% of the largest pore diameters per pit were used to generate $F_m(p)$ for ethanol- and water-dried samples, respectively. Closed and open circles show vulnerability curves from plants grown in shade and control light conditions, respectively.

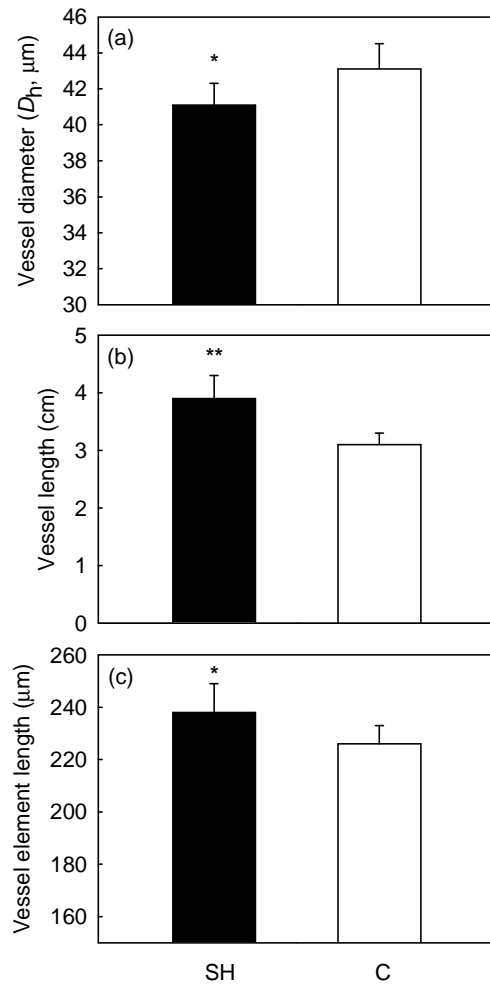


Figure 4-7: (a) mean hydraulic vessel diameter, (b) mean vessel length and (c) mean vessel element length in shaded (SH, black bars) and control plants (C, open bars). The bars represent grand means \pm SD from five to six individual stems. * and ** indicate significant differences at $P \leq 0.05$ and 0.01, respectively (independent two-sample t-test).

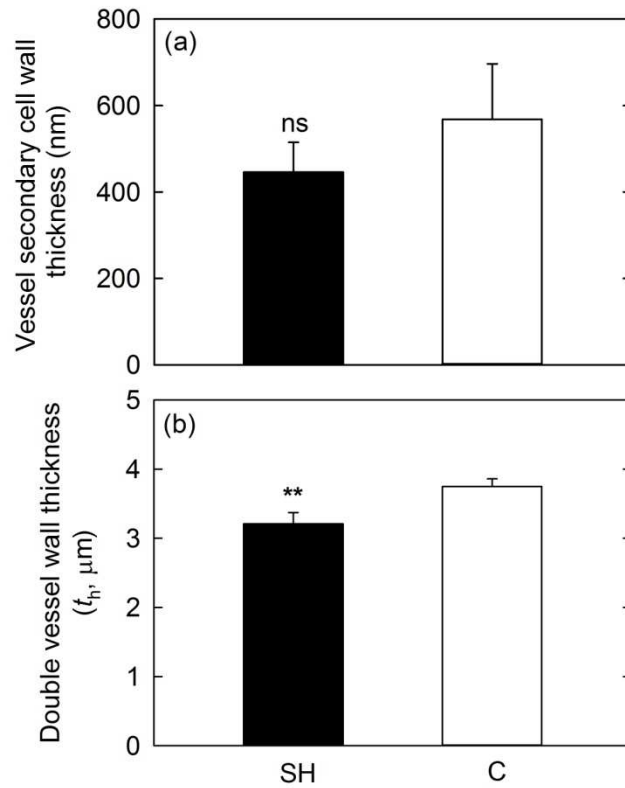


Figure 4-8: Secondary cell wall thickness in vessel measured from (a) TEM micrographs and (b) double vessel wall thickness measured with light microscopy. The bars represent grand means \pm SD ($n=5-6$). ** indicates significant differences at $P \leq 0.01$ while 'ns' indicates non-significant difference (independent two-sample t-test).

4.8 REFERENCES

- Alder N.N., Pockman W.T., Sperry J.S. & Nuismer S. (1997) Use of centrifugal force in the study of xylem cavitation. *Journal of Experimental Botany*, **48**, 665-674.
- Barigah T.S., Ibrahim T., Bogard A., Faivre-Vuillin B., Lagneau L.A., Montpied P. & Dreyer E. (2006) Irradiance-induced plasticity in the hydraulic properties of saplings of different temperate broad-leaved forest tree species. *Tree Physiology*, **26**, 1505-1516.
- Caquet B., Barigah T.S., Cochard H., Montpied P., Collet C., Dreyer E. & Epron D. (2009) Hydraulic properties of naturally regenerated beech saplings respond to canopy opening. *Tree Physiology*, **29**, 1395-1405.
- Choat B., Ball M., Luly J. & Holtum J. (2003) Pit membrane porosity and water stress-induced cavitation in four co-existing dry rainforest tree species. *Plant Physiology*, **131**, 41-48.
- Choat B., Cobb A.R. & Jansen S. (2008) Structure and function of bordered pits: new discoveries and impacts on whole-plant hydraulic function. *New Phytologist*, **177**, 608-625.
- Choat B., Jansen S., Zwieniecki M.A., Smets E. & Holbrook N.M. (2004) Changes in pit membrane porosity due to deflection and stretching: the role of vested pits. *Journal of Experimental Botany*, **55**, 1569-1575.
- Christman M.A., Sperry J.S. & Adler F.R. (2009) Testing the 'rare pit' hypothesis for xylem cavitation resistance in three species of *Acer*. *New Phytologist*, **182**, 664-674.
- Cochard H., Barigah S.T., Kleinhentz M. & Eshel A. (2008) Is xylem cavitation resistance a relevant criterion for screening drought resistance among *Prunus* species? *Journal of Plant Physiology*, **165**, 976-982.
- Cochard H., Cruiziat P. & Tyree M.T. (1992) Use of positive pressures to establish vulnerability curves: Further support for the air-seeding hypothesis and implications for pressure-volume analysis. *Plant Physiology*, **100**, 205-209.
- Cochard H., Herbette S., Hernandez E., Holtta T. & Mencuccini M. (2010) The effects of sap ionic composition on xylem vulnerability to cavitation. *Journal of Experimental Botany*, **61**, 275-285.
- Cochard H., Lemoine D. & Dreyer E. (1999) The effects of acclimation to sunlight on the xylem vulnerability to embolism in *Fagus sylvatica* L. *Plant Cell and Environment*, **22**, 101-108.
- Domec J.C., Lachenbruch B., Meinzer F.C., Woodruff D.R., Warren J.M. & McCulloh K.A. (2008) Maximum height in a conifer is associated with conflicting requirements for xylem design. *Proceedings of the National Academy of Sciences of the United States of America*, **105**, 12069-12074.
- Fichot R., Barigah T.S., Chamaillard S., Le Thiec D., Laurans F., Cochard H. & Brignolas F. (2010) Common trade-offs between xylem resistance to cavitation and other physiological traits do not hold among unrelated *Populus deltoides* x *Populus nigra* hybrids. *Plant, Cell and Environment*, **33**, 1553-1568.

- Fry S.C. (2004) Primary cell wall metabolism: tracking the careers of wall polymers in living plant cells. *New Phytologist*, **161**, 641-675.
- Goldberg R., Morvan C. & Roland J.C. (1986) Composition, properties and localization of pectins in young and mature cells of the mung bean hypocotyl *Plant and Cell Physiology*, **27**, 417-429.
- Guglielmino N., Liberman M., Jauneau A., Vian B., Catesson A.M. & Goldberg R. (1997) Pectin immunolocalization and calcium visualization in differentiating derivatives from poplar cambium. *Protoplasma*, **199**, 151-160.
- Guillemain F., Guillon F., Bonnin E., Devaux M.F., Chevalier T., Knox J.P., Liners F. & Thibault J.F. (2005) Distribution of pectic epitopes in cell walls of the sugar beet root. *Planta*, **222**, 355-371.
- Hacke U.G., Plavcová L., Almeida-Rodriguez A., King-Jones S., Zhou W. & Cooke J.E.K. (2010) Influence of nitrogen fertilization on xylem traits and aquaporin expression in stems of hybrid poplar. *Tree Physiology*, **30**, 1016-1025.
- Hacke U.G., Sperry J.S., Pockman W.T., Davis S.D. & McCulloh K.A. (2001) Trends in wood density and structure are linked to prevention of xylem implosion by negative pressure. *Oecologia*, **126**, 457-461.
- Hafren J., Daniel G. & Westermark U. (2000) The distribution of acidic and esterified pectin in cambium, developing xylem and mature xylem of *Pinus sylvestris*. *IAWA Journal*, **21**, 157-168.
- Hafren J. & Westermark U. (2001) Distribution of acidic and esterified polygalacturonans in sapwood of spruce, birch and aspen. *Nordic Pulp & Paper Research Journal*, **16**, 284-290.
- Hargrave K.R., Kolb K.J., Ewers F.W. & Davis S.D. (1994) Conduit diameter and drought-induced embolism in *Salvia mellifera* Greene (Labiatae). *New Phytologist*, **126**, 695-705.
- Herbette S. & Cochard H. (2010) Calcium is a major determinant of xylem vulnerability to cavitation. *Plant Physiology*, **153**, 1932-1939.
- Holste E.K., Jerke M.J. & Matzner S.L. (2006) Long-term acclimatization of hydraulic properties, xylem conduit size, wall strength and cavitation resistance in *Phaseolus vulgaris* in response to different environmental effects. *Plant Cell and Environment*, **29**, 836-843.
- Jansen S., Choat B. & Pletsers A. (2009) Morphological variation of intervessel pit membranes and implications to xylem function in angiosperms. *American Journal of Botany*, **96**, 409-419.
- Jansen S., Pletsers A. & Sano Y. (2008) The effect of preparation techniques on SEM-imaging of pit membranes. *IAWA Journal*, **29**, 161-178.
- Knox J.P., Linstead P.J., King J., Cooper C. & Roberts K. (1990) Pectin esterification is spatially regulated both within cell walls and between developing tissues of root apices. *Planta*, **181**, 512-521.
- Lemoine D., Jacquemin S. & Granier A. (2002) Beech (*Fagus sylvatica* L.) branches show acclimation of xylem anatomy and hydraulic properties to increased light after thinning. *Annals of Forest Science*, **59**, 761-766.

- Martinez-Vilalta J., Cochard H., Mencuccini M., Sterck F., Herrero A., Korhonen J.F.J., Llorens P., Nikinmaa E., Nole A., Poyatos R., Ripullone F., Sass-Klaassen U. & Zweifel R. (2009) Hydraulic adjustment of Scots pine across Europe. *New Phytologist*, **184**, 353-364.
- McDowell N., Pockman W.T., Allen C.D., Breshears D.D., Cobb N., Kolb T., Plaut J., Sperry J., West A., Williams D.G. & Yepez E.A. (2008) Mechanisms of plant survival and mortality during drought: why do some plants survive while others succumb to drought? *New Phytologist*, **178**, 719-739.
- Meyra A.G., Kuz V.A. & Zarragoicoechea G.J. (2007) Geometrical and physicochemical considerations of the pit membrane in relation to air seeding: the pit membrane as a capillary valve. *Tree Physiology*, **27**, 1401-1405.
- Micheli F., Ermel F.F., Bordenave M., Richard L. & Goldberg R. (2002) Cell walls of woody tissues: cytochemical, biochemical and molecular analysis of pectins and pectin methylesterases. In: *Wood formation in trees: cell and molecular biology techniques* (ed N.J. Chaffey), pp. 179-200. Taylor & Francis, London.
- Nardini A., Gasco A., Cervone F. & Salleo S. (2007) Reduced content of homogalacturonan does not alter the ion-mediated increase in xylem hydraulic conductivity in tobacco. *Plant Physiology*, **143**, 1975-1981.
- O'Brien T.P. (1970) Further observations on hydrolysis of the cell wall in the xylem. *Protoplasma*, **69**, 1-14.
- Perez-Donoso A.G., Sun Q., Roper M.C., Greve L.C., Kirkpatrick B. & Labavitch J.M. (2010) Cell wall-degrading enzymes enlarge the pore size of intervessel pit membranes in healthy and *Xylella fastidiosa*-infected grapevines. *Plant Physiology*, **152**, 1748-1759.
- Pesacreta T.C., Groom L.H. & Rials T.G. (2005) Atomic force microscopy of the intervessel pit membrane in the stem of *Sapium sebiferum* (Euphorbiaceae). *IAWA Journal*, **26**, 397-426.
- Raimondo F., Trifilo P., Lo Gullo M.A., Buffa R., Nardini A. & Salleo S. (2009) Effects of reduced irradiance on hydraulic architecture and water relations of two olive clones with different growth potentials. *Environmental and Experimental Botany*, **66**, 249-256.
- Sano Y. (2005) Inter- and intraspecific structural variations among intervessel pit membranes as revealed by field-emission scanning electron microscopy. *American Journal of Botany*, **92**, 1077-1084.
- Schmid R. & Machado R.D. (1968) Pit membranes in hardwoods - Fine structure and development. *Protoplasma*, **66**, 185-204.
- Schmitz N., Koch G., Schmitt U., Beeckman H. & Koedam N. (2008) Intervessel pit structure and histochemistry of two mangrove species as revealed by cellular UV microspectrophotometry and electron microscopy: Intraspecific variation and functional significance. *Microscopy and Microanalysis*, **14**, 387-397.

- Schoonmaker A.L., Hacke U.G., Landhausser S.M., Lieffers V.J. & Tyree M.T. (2010) Hydraulic acclimation to shading in boreal conifers of varying shade tolerance. *Plant Cell and Environment*, **33**, 382-393.
- Schultz H.R. & Matthews M.A. (1993) Xylem development and hydraulic conductance in sun and shade shoots of grapevine (*Vitis vinifera* L) - Evidence that low-light uncouples water transport capacity from leaf area. *Planta*, **190**, 393-406.
- Shane M.W., McCully M.E. & Canny M.J. (2000) Architecture of branch-root junctions in maize: structure of the connecting xylem and the porosity of pit membranes. *Annals of Botany*, **85**, 613-624.
- Shumway D.L., Steiner K.C. & Kolb T.E. (1993) Variation in seedling hydraulic architecture as a function of species and environment. *Tree Physiology*, **12**, 41-54.
- Siedlecka A., Wiklund S., Peronne M.A., Micheli F., Lesniewska J., Sethson I., Edlund U., Richard L., Sundberg B. & Mellerowicz E.J. (2008) Pectin methyl esterase inhibits intrusive and symplastic cell growth in developing wood cells of *Populus*. *Plant Physiology*, **146**, 554-565.
- Sperry J.S. (2000) Hydraulic constraints on plant gas exchange. *Agricultural and Forest Meteorology*, **2831**, 1-11.
- Sperry J.S., Hacke U.G. & Wheeler J.K. (2005) Comparative analysis of end wall resistivity in xylem conduits. *Plant, Cell and Environment*, **28**, 456-465.
- Sperry J.S., Saliendra N.Z., Pockman W.T., Cochard H., Cruiziat P., Davis S.D., Ewers F.W. & Tyree M.T. (1996) New evidence for large negative xylem pressures and their measurement by the pressure chamber method. *Plant, Cell and Environment*, **19**, 427-436.
- Sperry J.S. & Tyree M.T. (1988) Mechanism of water stress-induced xylem embolism. *Plant Physiology*, **88**, 581-587.
- Stiller V. (2009) Soil salinity and drought alter wood density and vulnerability to xylem cavitation of baldcypress (*Taxodium distichum* (L.) Rich.) seedlings. *Environmental and Experimental Botany*, **67**, 164-171.
- Tyree M.T. & Zimmermann M.H. (2002) *Xylem structure and the ascent of sap*. (2nd ed.). Springer Verlag, Berlin.
- Wheeler J.K., Sperry J.S., Hacke U.G. & Hoang N. (2005) Inter-vessel pitting and cavitation in woody Rosaceae and other vesselled plants: a basis for a safety versus efficiency trade-off in xylem transport. *Plant, Cell and Environment*, **28**, 800-812.
- Willats W.G.T., McCartney L., Mackie W. & Knox J.P. (2001) Pectin: cell biology and prospects for functional analysis. *Plant Molecular Biology*, **47**, 9-27.
- Zwieniecki M.A., Melcher P.J. & Holbrook N.M. (2001) Hydrogel control of xylem hydraulic resistance in plants. *Science*, **291**, 1059-1062.

5. Heterogeneous distribution of pectin epitopes and calcium in different pit types of four angiosperm species⁴

5.1 INTRODUCTION

Water and nutrients move through a complex network of xylem conduits that, when mature, are dead and void of cellular content. Water movement is driven by a gradient in negative pressure that is a result of evaporation from the tiny menisci localized in the cell walls of leaf parenchyma. Consequently, xylem sap is in a metastable state and hydraulic failure can readily occur (Tyree & Zimmermann, 2002). As the xylem pressure decreases due to increased evaporative demand or lack of soil moisture, there is a higher risk of water columns essentially ‘breaking’ and xylem conduits becoming air-filled (i.e., embolized). Embolized conduits are temporarily or permanently disconnected from the transpiration stream and hydraulic conductivity (K_h) decreases.

Interconduit pits connect adjacent conduits to permit water flow while preventing the spread of air from embolized conduits to adjacent functional ones (Choat, Cobb & Jansen, 2008, Sperry & Hacke, 2004, Sperry & Tyree, 1988). According to the air-seeding hypothesis, microporous pit membranes will support an air-water interface until the pressure difference across the membrane overcomes the capillary forces (Sperry, Saliendra, Pockman *et al.*, 1996). The air-seeding threshold is inversely related to the pore diameter, such that higher pit membrane porosity will result in more vulnerable xylem (Choat *et al.*, 2008, Jarbeau, Ewers & Davis, 1995). A consequence of the role of interconduit pits as safety valves is that they provide a significant constraint to water flow. In both conifer tracheids and angiosperm vessels, interconduit pits contributed on average more than half of the total conduit resistivity (Hacke, Sperry, Wheeler *et al.*, 2006, Pittermann, Sperry, Hacke *et al.*, 2005).

Pits are also found between (axial and ray) parenchyma cells and xylem conduits, thus providing an interface between the living and dead components of the xylem. Controlled fluxes of various solutes including ions (De Boer & Volkov, 2003, Nardini, Grego, Trifilo *et al.*, 2010), sugars (Salleo, Trifilo, Esposito *et al.*, 2009, Sauter, Iten & Zimmermann, 1973), and amino acids (Sauter

⁴ A version of this chapter has been published. Plavcová L & Hacke UG 2011. *New Phytologist*. 192: 885-897.

& Van Cleve, 1992) occur between ray cells and vessels. These exchange processes are most likely influenced by the properties of vessel-ray pit membranes. In addition, vessel-ray pits may play a role in embolism refilling as water appears to enter refilling vessels through this interface (Braun, 1970, Brodersen, McElrone, Choat *et al.*, 2010).

The permeability of pit membranes in both intervessel and vessel-ray pits is critical for their function. The porosity and permeability of pit membranes are likely to be affected by the chemical composition of the membrane. However, our knowledge of pit membrane chemistry is limited. Pit membranes develop from the compound middle lamella (cml) (Evert, 2006), and it is usually assumed that their chemical composition resembles that of a typical primary cell wall. However, this assumption awaits further testing because of the extensive remodeling and hydrolysis of the original primary wall that takes place during pit membrane differentiation (Morrow & Dute, 1998, O'Brien, 1970, Schmid & Machado, 1968). According to the current paradigm, pit membranes are composed of multiple layers of cellulose microfibrils embedded in a matrix of hemicellulose and pectins (Choat *et al.*, 2008). Structural proteins that are common in the primary cell wall (Cassab, 1998, Valentin, Cerclier, Geneix *et al.*, 2010) may also occur in pit membranes (Harrak, Chamberland, Plante *et al.*, 1999).

Experimental evidence suggests that pectins play important roles in pit membrane functioning (Boyce, Zwieniecki, Cody *et al.*, 2004, Cochard, Herbette, Hernandez *et al.*, 2010, Nardini *et al.*, 2010, van Ieperen, 2007, Wisniewski, Davis & Arora, 1991, Zwieniecki, Melcher & Holbrook, 2001). Pectins are a highly complex and heterogeneous group of polysaccharides rich in galacturonic acid (GalA). Different domains of pectins can be distinguished based on their biochemical properties; namely homogalacturonan (HG), rhamnogalacturonan-I (RG-I), and rhamnogalacturonan-II (Willats, McCartney, Mackie *et al.*, 2001). HG are linear polymers of 1,4-linked α -D-GalA and are the most abundant pectic domain in the primary cell wall comprising up to 60% of total pectin (O'Neill & William, 2003). The pectic polymers extensively interact with each other as well as with the other cell wall components (MacDougall, Brett, Morris *et al.*, 2001a, Ryden, MacDougall, Tibbits *et al.*, 2000, Valentin *et al.*, 2010), but the complexity of these connections is not fully understood.

Due to the presence of numerous carboxyl groups, pectins exhibit properties of polyelectrolytes and have an overall negative charge (Valentin *et al.*, 2010). Calcium pectin gels tend to swell when there is an imbalance in the

distribution of mobile counterions between the gel and surrounding solution, which results from the Donnan effect (MacDougall *et al.*, 2001a). Crosslinking of the polymer network constrains the swelling tendencies (MacDougall *et al.*, 2001a). The hydrogel behavior of pectins has been used to explain why the K_h of stem segments is higher when measured with salt solution (typically 10-100 mM KCl solution) compared with perfusion with distilled water (Gasco, Nardini, Gortan *et al.*, 2006, Lopez-Portillo, Ewers & Angeles, 2005, van Ieperen, 2007, Zwieniecki *et al.*, 2001).

In addition to the ionic effect, calcium-mediated cross-links between pectins have been proposed to influence the vulnerability of xylem to embolism (Sperry & Tyree, 1988). Perfusion of stems with oxalic acid and calcium solution induced greater vulnerability in sugar maple, perhaps by disrupting calcium-mediated cross-links in the pectins of the pit membrane, which could make the membrane more flexible and allow for transient pore widening (Sperry & Tyree, 1988). Herbette and Cochard (2010) also found that embolism vulnerability increased after perfusing stems with a calcium chelating solution. In the presence of >10 consecutive unmethyl-esterified GalA residues, calcium may interact with the negative charges of the GalA residues to form stable gels based on the 'egg-box' model (Caffall & Mohnen, 2009). While other linkages exist in the pectin network, calcium cross-linking of HG is known to contribute to wall strength (Caffall & Mohnen, 2009, MacDougall *et al.*, 2001a, Micheli, 2001). The presence of low methyl-esterified HG in intervessel pit membranes may therefore be associated with shifts in vulnerability to embolism and may even explain differences in vulnerability between various species (Herbette & Cochard, 2010).

Both the ionic effect and the magnitude of the shift in vulnerability vary greatly among species (Cochard *et al.*, 2010, Herbette & Cochard, 2010, Jansen, Gortan, Lens *et al.*, 2011). While the factors influencing the ionic effect have been previously investigated (Gortan, Nardini, Salleo *et al.*, 2011, Jansen *et al.*, 2011), the factors affecting the magnitude of the vulnerability shift after calcium removal are poorly understood. Herbette and Cochard (2010) noted that the shift was greater in more embolism-resistant species. Of the thirteen species tested in their study, two (*Salix alba* and *Betula pendula*) remained unaffected by the treatments. It seems possible that pectins were not present in the intervessel pit membranes of these species. Alternatively, if pectins were present, they may not have been capable of forming calcium mediated cross-links, possibly due to a high degree of esterification. The fact that monoclonal antibodies did not

recognize HG in intervessel pit membranes of hybrid poplar saplings (Plavcová, Hacke & Sperry, 2011) supports the hypothesis that some highly vulnerable species do not possess pectinaceous intervessel pit membranes. The absence of HG would also prevent an increase in vulnerability after calcium removal. To test this hypothesis, we measured the shift in vulnerability in two relatively vulnerable species, *Betula papyrifera* and *Populus balsamifera*, and two more resistant species, *Prunus virginiana* and *Amelanchier alnifolia*. We hypothesized that HG will be absent in the intervessel pit membranes of the two vulnerable species, and that the vulnerability of these species will therefore remain unaffected by calcium removal. We expected the opposite pattern in the two resistant species.

One of the most powerful ways to study pectin in its physiological context is by using anti-pectin antibody probes (Willats *et al.*, 2001, Wisniewski & Davis, 1995). However, this tool has rarely been used on intervessel pit membranes of woody angiosperms. In this present study, we used immunogold labeling with monoclonal antibodies raised against primary cell wall polysaccharides (HG, RG-I, and xyloglucan) to probe the chemical composition of pit membranes. We asked if the pattern of HG labeling corresponded with the presence of calcium in pit membranes. To do this, we used an antimonate precipitation technique and compared the distribution of HG and calcium at the transmission electron microscopy level. Our final objective was to compare the structure and chemistry of different pit types. Although intervessel and vessel-ray pits may occur in the same vessel element, they have very different functions and may therefore differ in their chemical composition.

5.2 METHODS

5.2.1 Plant material

Branches (approx. 1 cm in diameter) of *Betula papyrifera* Marsh., *Populus balsamifera* L., *Prunus virginiana* L., and *Amelanchier alnifolia* Nutt. were collected in the vicinity of the University of Alberta campus in Edmonton (53°50'N 113°52'W). These species were selected to cover a wide range of xylem vulnerability. The trees used for sampling were mature individuals growing in a river valley. For the measurements of vulnerability to embolism, branches were sampled from different randomly selected individuals. The plant material was used immediately or wrapped in plastic bags with wet paper towels and stored at 4°C for no longer than 3 days before the measurements were carried out.

For electron microscopy work, xylem samples were collected from the same trees used for the hydraulic measurements. In this case, samples were processed immediately. Samples for hydraulic measurements and TEM immunolabeling were collected in October and November 2010, samples for SEM observations and TEM calcium localization were collected in February 2011, and samples for ruthenium red staining were taken in May 2011. In addition, a limited set of hydraulic measurements was carried out in February to verify that vulnerability to embolism did not undergo seasonal shifts.

5.2.2 Shifts in vulnerability to embolism

To evaluate the effect of calcium removal on vulnerability to embolism, vulnerability curves were obtained for control stems and stems perfused with a calcium chelating sodium phosphate solution (Herbette & Cochard, 2010). Stem segments were trimmed under water to a length of 14.2 cm. Segments were flushed with the treatment (pH 10) or control (pH 4) 10 mM NaPO₄ solution for 30-40 min at 20 kPa. At least 5 ml of solution were perfused through each stem. At pH 10, the phosphate occurs mainly in the form of HPO₄²⁻ anions that readily precipitate Ca²⁺ cations. In contrast, at pH 4 the predominant ionic form of phosphate is H₂PO₄⁻, which does not bind calcium. The same solutions used for flushing were used during the K_h measurements. After flushing, stem segments were fitted to a tubing apparatus and the maximal hydraulic conductivity (K_{max}) was measured as the flow rate per pressure gradient (Plavcová *et al.*, 2011). The standard centrifuge method (Alder, Pockman, Sperry *et al.*, 1997, Li, Sperry, Taneda *et al.*, 2008) was used to generate vulnerability curves. Curves were constructed by plotting the negative xylem pressure against the percent loss of conductivity as described previously (Plavcová *et al.*, 2011). Curves were fitted with a Weibull function and the xylem pressure corresponding to 50% loss of conductivity (P_{50}) was calculated for each stem segment. Six stems per species were measured for each NaPO₄ solution.

5.2.3 Scanning electron microscopy

Scanning electron microscopy (SEM) was used to evaluate whether perfusion with the calcium chelating solution caused changes in pit membrane structure. To prepare the samples for SEM observation, stem segments 5 cm in length were perfused with the treatment (pH 10) or control (pH 4) NaPO₄ solution at a pressure of 20 kPa for 1 h. Then, samples were soaked in the same solution for 24 h at room temperature. Subsequently, segments were rinsed with distilled

water and dehydrated through a gradual ethanol series 30-50-70-90% (30 min each) and placed in 100% ethanol overnight. Finally, segments were air-dried for 24 h, split with a razor blade and mounted on aluminum stubs using conductive silver paste. Samples were sputter-coated with chromium and carbon and observed with a field-emission scanning electron microscope (6301F, JOEL, Tokyo, Japan) using 2 kV acceleration voltage. Four different stems of *P. balsamifera* were observed for each NaPO₄ solution (pH 4 and 10, respectively). *P. balsamifera* was selected for these SEM observations, because both intervessel and vessel-ray pits were relatively easy to find on a tangential surface plane in comparison with the other three species studied. A semi-quantitative elemental analysis via SEM coupled X-ray spectrometry (Princeton Gamma-Tech Inc, Princeton, NJ, USA) was used to assess the chemical composition of conspicuous particles that were abundant in the specimens treated with NaPO₄ at pH 10. An acceleration voltage of 50 kV was used for this analysis.

5.2.4 Polysaccharide localization with transmission electron microscopy

For immunolabeling, blocks of xylem tissue 1 mm³ in size sampled from the outer part of the stems were fixed in a mixture of 0.2% glutaraldehyde and 3.7% paraformaldehyde in 25 mM piperazine-N, N'-bis (2-ethanesulfonic acid) (PIPES) for 4.5 h at room temperature. Specimens were then buffer washed, dehydrated and embedded in LR White resin (London Resin Co., London, UK). Our embedding procedure closely followed the steps previously described by Chaffey (2002), with the modification that we used heat polymerization at 60°C for 24 h. Ultrathin sections (70-90 nm) were cut using an ultramicrotome (Ultracut E, Reichert-Jung, Vienna, Austria) equipped with a diamond knife. Sections were collected on pioloform-coated nickel grids and immunolabeled. Four monoclonal antibodies (JIM5, JIM7, LM6 and LM15, PlantProbes, Leeds, UK) raised against different cell wall polysaccharide epitopes were used in this study. JIM5 and JIM7 bind to HG with low and high degree of methyl-esterification, respectively (Guillemin, Guillon, Bonnin *et al.*, 2005, Knox, Linstead, King *et al.*, 1990, Willats *et al.*, 2001). LM6 recognizes arabinan side chains of RG-I (Ermel, Follet-Gueye, Cibert *et al.*, 2000, Guillemin *et al.*, 2005, Willats *et al.*, 2001). LM15 is targeted against the XXXG motif of xyloglucan (Marcus, Verhertbruggen, Herve *et al.*, 2008). Immunolabeling was performed by floating the grids on drops of successively changing solutions. Sections were preincubated for 10 min on a drop of 0.05 M Tris-buffered saline (pH 7.6) with 0.1% Tween 20 and 0.1% bovine serum albumin, blocked for 20 min with goat

serum (Sigma-Aldrich Corp., St. Louis, MO, USA) diluted 1:30 (v/v) in the same buffer, treated with the primary antibody (JIM5, JIM7, and LM6 diluted 1:4, LM15 diluted 1:3) overnight at 4 °C, four times buffer-washed and stained with a secondary antibody, goat-anti rat IgG conjugated with 10 nm gold particles (Sigma-Aldrich) for 1 h. The grids were then extensively washed with buffer and filtered water and finally contrasted with 4% uranyl acetate for 25 min and with Reynolds' lead citrate for 2 min. Sections were examined under a transmission electron microscope (Morgagni 268, Fei Company, Hillsboro, OR, USA).

The immunolabeling experiment was conceived as a qualitative study aiming to describe the pit membrane chemical composition as well as differences between species. Given our interest in the occurrence of HG in pit membranes, we assessed the labeling density of JIM5 and JIM7 antibodies in the pit membrane annulus. We counted the gold particles in this region. The labeling density in pit membrane annuli was estimated based on six to 15 pits per species and antibody. In addition, the length of the annulus was measured as the distance from the edge of the pit (following the plane of the cml) to the area where the annulus transitioned into the main portion of the pit membrane. This transition zone could be clearly identified based on the difference in the electron density of the membrane. In addition to these measurements, pit membrane diameter was calculated from the pit area assessed in tangential sections with a light microscope at 1000 x magnification assuming a circular shape of pit membranes.

To verify the immunolocalization pattern, a histological detection of pectins was performed via ruthenium red staining based on methods described previously (Gortan *et al.*, 2011, Micheli, Ermel, Bordenave *et al.*, 2002). Xylem tissue was fixed in Karnovsky's fixative containing 0.1% (w/v) ruthenium red for 1.5 h and post-fixated in 1% buffered osmium tetroxide with 0.1% ruthenium red for 1.5 h at room temperature. Subsequently, samples were dehydrated and embedded in Spurr's resin. As osmium tetroxide post-fixation provides some contrast to the tissue, control samples were prepared using the same solutions without ruthenium red. Sections were mounted on coated copper grids and examined without further staining.

5.2.5 Calcium localization

Calcium was localized within the wood tissue using an antimonate precipitation technique (Slocum & Roux, 1982, Wick & Hepler, 1980). This method has been successfully used to localize cell wall bound calcium in the

cambial zone of poplar (Baier, Goldberg, Catesson *et al.*, 1994, Guglielmino, Liberman, Jauneau *et al.*, 1997) and European ash (Funada & Catesson, 1991). In this study, small blocks (1 mm³) of mature xylem were fixed in a mixture of 2% glutaraldehyde, 2.5% formaldehyde, 0.1% tannic acid, and 2% potassium antimonate in 0.1 M potassium phosphate buffer at pH 7.6 for 6 h at room temperature in the dark. Specimens were then washed two times for 15 min in antimonate buffer (2% K₂Sb(OH)₆ in 0.1 M potassium phosphate at pH 8), postfixed in 1% OsO₄ in antimonate buffer for 2 h, three times buffer washed for 10 min, washed for 30 min in 0.01 M potassium phosphate buffer without antimonate at pH 7.6, and finally gradually dehydrated and embedded in Spurr's resin. Ultrathin sections were collected on coated copper grids and observed without further staining.

5.2.6 Statistical analysis

The statistical environment R (R Development Core Team, 2009) was used to perform the statistical analysis. Analysis of variance followed by Tukey's HSD post hoc comparison test was conducted to evaluate differences among the species and perfusion solutions. For all tests, differences were considered statistically significant at $P \leq 0.05$.

5.3 RESULTS

5.3.1 Shifts in xylem vulnerability to embolism

Vulnerability to embolism was significantly higher in stems perfused with NaPO₄ solution at pH 10 in comparison with the same solution at pH 4 in three out of four species studied ($P \leq 0.05$) (Fig. 5-1). The P₅₀ values at pH 4 did not differ from values previously measured in our laboratory for these species using a regular measuring solution (20 mM KCl and 1 mM CaCl₂) instead of NaPO₄ (data not shown). Therefore, perfusion with NaPO₄ at pH 4 does not affect xylem vulnerability and the P₅₀ at pH 4 reflects the 'native' xylem vulnerability. The difference in P₅₀ (ΔP_{50}) in stems infiltrated with solutions of different pH was largest in the most resistant species, *A. alnifolia* ($\Delta P_{50} = 2.12 \pm 0.16$ MPa). The magnitude of the shift in P₅₀ was proportional to the native vulnerability of species, with more resistant species shifting more (Fig. 5-2). Although their P₅₀ values at pH 4 did not differ ($P = 0.945$), *P. balsamifera* exhibited a significant shift in vulnerability ($P=0.020$) while *B. papyrifera* did not ($P=0.998$). The

correlation between ΔP_{50} and the P_{50} at pH 4 closely followed the relationship observed by Herbette and Cochard (2010), although we used different species and a different centrifuge method to measure the vulnerability curves.

5.3.2 Scanning electron microscopy

SEM was used to test if perfusion with calcium chelating solution caused visible changes in pit membrane structure. Spherical particles were often found in the vessel lumens of samples treated with NaPO_4 at pH 10, but were rare in samples treated with NaPO_4 solution at pH 4 (Fig. 5-3). Semi-quantitative elemental analysis with an X-ray analysis system coupled with the SEM microscope revealed that the particles were rich in phosphorus, calcium, sodium and magnesium. At pH 10, but not at pH 4, these particles were consistently found in high concentrations on the surface of vessel-ray pit membranes (Fig. 5-3b). At pH 10, precipitate was occasionally found on the surface of intervessel pit membranes (images not shown). However, compared with vessel-ray pit membranes, intervessel pit membranes had far fewer particles, and precipitate was only sporadically observed in different samples. The distribution of these particles within the intervessel pit membrane seemed fairly random. However, in several instances more particles were found around the periphery of the pit membrane, i.e., the annulus region.

5.3.3 Distribution of high and low methyl-esterified homogalacturonan

None of the antibodies used in this study showed a strong signal in the entire pit membrane of interconduit pits. Nevertheless, several labeling patterns could be distinguished (Table 5-1). JIM7 labeling was more or less evenly distributed in the cml (Fig. 5-4a). In contrast, the JIM5 epitope was only rarely found in the cml between two cells, but was more frequently present in the cml of cell corners. This pattern indicates that the HG in the cml was largely esterified. Pit membranes of all species showed a distinct annulus, i.e., an electron dense area near the periphery of the pit membrane. The annulus was substantially shorter in *B. papyrifera* in comparison with the other species. Importantly, this region was strongly labeled with both JIM5 and JIM7 (Fig. 5-4a-c). Whereas JIM7 labeling was usually evident throughout the entire annulus region (Fig. 5-4a), the JIM5 epitope was often confined to the tip of the annulus (Fig. 5-4b,c). The number of gold particles per annulus for JIM5 and JIM7 varied on average from five to 15 between the species (Table 5-2). These counts provide an estimate

of the ratio between low and high methyl-esterified HG in the annulus. This ratio was highest in *B. papyrifera*.

The pit annuli of imperforate tracheary elements in *P. virginiana*, *A. alnifolia* and *B. papyrifera* showed the same HG labeling pattern that was observed in intervessel pits (Fig. 5-5a). We use the term ‘imperforate tracheary element’ in the all-inclusive sense outlined by Carlquist (1986). Pits of imperforate tracheary elements in *P. virginiana* and *A. alnifolia* were distinct in that they often had pseudotori thickenings. The attachment of the cap-like thickenings to the membrane varied. Sometimes the pads were closely attached to the membrane. In those cases, strong labeling with JIM7 was found throughout the inner membrane layer, i.e., the part of the membrane located between the pads (images not shown). In other cases, the thickenings were somewhat disconnected and formed hollow horseshoe- or cap-like structures that overarched the membrane (Fig. 5-5a). Strong labeling with both JIM5 and JIM7 was seen on the inner surface of the cap-like thickenings (Fig. 5-5a, arrows).

In contrast to intervessel pit membranes, the membranes of vessel-ray pits consistently exhibited strong labeling for both JIM5 and JIM7 (Fig. 5-5c). JIM5 was localized closer to the surface of the membrane facing the vessel lumen (Fig. 5-5c), whereas the density of JIM7 labeling was more homogenous across the pit membrane. JIM5 and JIM7 labeling was also detected in the amorphous cell wall layer of ray parenchyma cells. In *A. alnifolia*, JIM5 labeling was enriched in a darker band that traversed the amorphous layer (Fig. 5-5c).

The HG distribution patterns as detected with antibodies were verified using ruthenium red staining. Electron dense regions indicated a positive staining reaction with ruthenium red. In agreement with the immunolabeling results, staining was consistently observed in the annulus of intervessel pits (Fig. 5-6a,b), vessel-ray pit membranes, the amorphous layer (Fig. 5-6c), and in pseudotori (Fig. 5-6d). The pattern described above was not found in control samples prepared without ruthenium red, indicating that osmium tetroxide alone was not responsible for the differential contrast. The main part of intervessel pit membranes could be distinguished in samples of all species as a very faint, almost electron-transparent granular layer. No increase in electron density of the main part of intervessel pit membranes was apparent in samples stained in ruthenium red.

5.3.4 Calcium localization with TEM

The antimonate technique was used to localize electron dense calcium precipitate in TEM-samples. In agreement with the calcium chelating experiments described above (Fig. 5-3b), the precipitates often formed a thin layer of clumps along the inner vessel walls. In contrast, precipitates were less common in fiber lumens. A distinct layer of precipitate was consistently observed in the annulus region of interconduit pits (Fig. 5-4d, Fig. 5-5b). This pattern matched the labeling with JIM5. The distribution of calcium precipitate also matched the JIM5 labeling patterns found in pseudotori (compare Fig. 5-5a,b). Precipitate was consistently found on the surface of vessel-ray pit membranes (Fig. 5-5d, arrows). While the distribution of calcium precipitate closely matched the distinct JIM5 labeling patterns described above, there was less agreement with JIM7 labeling. Calcium precipitate was not found throughout the entire annulus or the entire vessel-ray pit membrane. Instead, the precipitate often formed a lining around the annulus (Fig. 5-4d) and was restricted to the surface of vessel-ray pit membranes (Fig. 5-5d).

5.3.5 Distribution of rhamnogalacturonan I and xyloglucan

The signal for the other antibodies, LM6 and LM15, tended to be weaker and more variable than the patterns seen for JIM5 and JIM7. Nevertheless, both antibodies were localized in the cml. Weak labeling of anti-RG-I LM6 occurred in vessel-ray pit membranes. The LM6 epitope was most abundant in the amorphous layer of ray cells (Fig. 5-7a), where it provided a strong signal in all species. While LM6 labeled pseudotori (Fig. 5-7c), the LM6 signal was not enriched in annuli. Intervessel pit membranes of *P. virginiana* showed weak labeling with LM6, but this pattern could not be confirmed in the other species.

The LM15 xyloglucan epitope was consistently found in the cml (Fig. 5-7b) and in the outer layer of cell corners (Fig. 5-7d). Weak labeling was also found in intervessel pit membranes of *P. virginiana* and *A. alnifolia* (Fig. 5-7b, dark grey arrow). LM15 labeling was not observed in pseudotori, vessel-ray pit membranes, and in the amorphous layer (Table 5-1).

5.4 DISCUSSION

A significant increase in xylem vulnerability after perfusion with calcium chelating solution was found in three out of four species studied (Fig. 5-1). The magnitude of the shift was proportional to the native vulnerability of the species with the more resistant species showing larger shifts (Fig. 5-2). These results are in agreement with previous findings of Herbette and Cochard (2010). In addition, our data indicate that at least some highly vulnerable species can become even more vulnerable after calcium removal, as evidenced by the 0.6 MPa shift seen in *P. balsamifera*. The shift in vulnerability after calcium removal was highly reproducible, suggesting that it was caused by a 'controlled' change in pit membrane properties rather than a complete loss of integrity of the pit membranes. Sperry & Tyree (1988) and Herbette & Cochard (2010) suggested that the shift in vulnerability is caused by disruptions of calcium-HG crosslinks in intervessel pit membranes that would change the rigidity and stretching properties of the membranes.

The pectin localization experiments conducted in this study showed that the main part of intervessel pit membranes in all four species contained very little or no HG. Thus, our original hypothesis that there is a link between the presence or absence of HG in the pit membrane and the magnitude of the vulnerability shift was not supported. The only portion of the membrane that was rich in HG was the marginal annulus region. The pit membrane annulus is a conspicuous feature of the pit membrane and has often been noted by wood anatomists. A distinct annulus occurs both in interconduit pits of angiosperms (Gortan *et al.*, 2011, Jansen, Choat & Pletsers, 2009, Schmid, 1965, Schmid & Machado, 1968) as well as in torus-margo pits of gymnosperms (Dute, Hagler & Black, 2008, Liese, 1965, Pittermann, Choat, Jansen *et al.*, 2010). Under the TEM, the annulus typically appears more electron-dense than the rest of the membrane. However, the opposite pattern has also been found in a few species (Gortan *et al.*, 2011, Jansen *et al.*, 2009, Schmitz, Jansen, Verheyden *et al.*, 2007). To the best of our knowledge, it is not known whether the annulus plays a physiological role or if it simply relates to pit development (e.g., the enzymes that remodel the pit membrane may have restricted access to the marginal membrane region).

A high HG content in the annulus was consistently observed in all four species studied and agrees with our previous observations on hybrid poplar saplings (Plavcová *et al.*, 2011) as well as earlier reports (O'Brien, 1970).

Furthermore, the anti-RG-I antibody did not display an increased labeling density in the annulus, indicating that it is specifically the HG domain of pectins that is enriched in the annulus. HG are known for their calcium binding capacity (MacDougall, Rigby, Ryden *et al.*, 2001b, Proseus & Boyer, 2008) and this premise was confirmed by our calcium localization experiment. Hence, it is possible that the effect of calcium removal on xylem vulnerability is realized through the disruption of the HG-calcium superstructure within the annulus. The fact that the magnitude of the shift in the four species studied was proportional to the length of the annulus further supports this hypothesis.

Based on our findings, we propose that the pit membrane should not be viewed as an isotropic material. Instead, there are two chemically and structurally distinct domains (the pit membrane annulus and the main part of the membrane) that likely exhibit different mechanical properties. A growing body of evidence suggests that the large pressure difference that is exerted on the pit membrane prior to air seeding results in pit membrane stretching, and that the extent of membrane deflection influences the cavitation threshold. Features that minimize pit membrane deflection such as vestures (Choat, Jansen, Zwieniecki *et al.*, 2004) or shallow pit chambers (Hacke & Jansen, 2009, Lens, Sperry, Christman *et al.*, 2011) were found in embolism-resistant xylem. Although calcium crosslinks can substantially enhance cell wall strength (Cybulska, Zdunek & Konstankiewicz, 2011, Parre & Geitmann, 2005), cellulose microfibrils most likely represent the main load-bearing component of pit membranes and limit the degree of membrane deformation (Petty, 1972, Sperry & Hacke, 2004). The orientation of microfibrils is critical for mechanical properties. The wall is more pliable in the direction perpendicular to the prevailing orientation of the microfibrils. In the pit membrane, the microfibrils seem to be oriented randomly. However, it is not clear whether the same pattern of microfibril orientation is maintained in the annulus. Observations of developing pits suggest that microfibrils are deposited in a circular fashion near the pit border (Chaffey, Barnett & Barlow, 1997, Imamura & Harada, 1973, Wardrop, 1954). This deposition pattern is usually interpreted as an initial step in the formation of the pit border. However, Imamura (1973) states: "...the circularly oriented microfibrils have been laid down making the periphery of the pit area, called the pit annulus".

If microfibrils in the annulus are oriented in a circular fashion, the annulus would extend more than the rest of the membrane during air seeding as the cellulose microfibrils would move apart. When stems were perfused with the

calcium chelating agent, the annulus region may have become looser and even more extensible. Thus, it is possible that calcium removal led to the formation of small pores or micro-cracks within the annulus or the annulus-membrane interface through which air could penetrate and cause embolism. Alternatively, calcium removal from the annulus may allow for increased pit membrane deflection, which in turn would lead to a widening of membrane pores. A more extensible annulus would allow the pit membrane to deflect further and aspirate sooner against the pit border. As the membrane continues to deflect through the pit aperture, the pores will start to enlarge even more and air seeding will occur at less negative xylem pressure (Sperry & Hacke, 2004).

B. papyrifera was the only species in this study that did not show a shift in vulnerability after calcium removal. Although HG and calcium were present in the pit membrane annulus, annuli of *B. papyrifera* were significantly shorter than those of the other three species. This may explain why the effect of calcium removal was less pronounced in *B. papyrifera*. In addition, intervessel pits of *B. papyrifera* were much smaller than those of the other species. With all other parameters being equal, smaller pits should show less membrane deflection than larger ones (see Eqn.8 in Sperry & Hacke, 2004). Membrane deflection in *B. papyrifera* may therefore be minimal. On the other hand, pit membrane diameter alone does not have a strong effect on xylem vulnerability (Jansen *et al.*, 2009, Lens *et al.*, 2011). Pit membrane thickness can also play a role. More detailed knowledge of the overall pit geometry and mechanical properties is necessary to decipher if and how pit membrane deflection influences the air seeding threshold. Our results also indicate that HG in annuli of *B. papyrifera* exhibited a relatively low degree of methyl-esterification (Table 5-2). Low esterified HG bind calcium more tightly in comparison with high methoxyl pectin (Tibbits, MacDougall & Ring, 1998). It is possible that calcium was less susceptible to sequestration in *B. papyrifera* and that the annulus consequently retained its original strength. However, the data on labeling density shown in Table 5-2 should be interpreted with caution as they originate from only one or two independent immunolabeling experiments per species.

The proposed hypothesis that changes in the extensibility of the annulus can induce increased vulnerability is speculative. An alternative explanation would be that a low amount of HG and calcium is present in interconduit pit membranes, and that this small amount was not detected by the methods employed in this study. Following this argument, one would expect that HG and

calcium were completely removed during pit development in *B. papyrifera* (which did not shift), but not in the other species, which did shift. This seems unlikely and none of our data supported this view. The different methods employed in this study all indicated that the annulus is the region of the pit membrane with the highest HG and calcium content. It seems improbable that the treatment with calcium chelating agents would not have any effect on it.

Our results highlight the differences in interconduit and vessel-ray pit membrane chemistry. In contrast to intervessel pits, the entire surface of vessel-ray pit membranes was rich in pectins (Fig. 5-5c, Fig. 5-6c) and calcium (Fig. 5-3, Fig. 5-5d). Vessel-ray pit membranes lacked an annulus. The transitional region between cml and pit membrane did not show enhanced HG-labeling, further supporting that the annulus might have a specific role in interconduit pit functioning. Pectins were previously found in vessel-ray pit membranes of *Prunus persica* (Wisniewski & Davis, 1995). It has been suggested that pectinaceous vessel-ray pit membranes effectively isolate intracellular water from extracellular ice, thereby conferring the ability of the tissue to undergo supercooling.

This study also provides information on pseudotori. The function, if any, of these peculiar structures is unknown. Pseudotori occur in tracheary elements of several woody taxa including Rosaceae, Ericaceae, and Oleaceae (Jansen, Sano, Choat *et al.*, 2007, Rabaey, Lens, Huysmans *et al.*, 2008). Pseudotori develop as secondary thickenings following the formation of plasmodesmata-associated primary thickenings. Later in development, autolytic enzymes remove the primary thickenings leaving the pseudotori intact, and the tracheary cell undergoes programmed cell death (Rabaey *et al.*, 2008). Our immunolabeling experiments complement this description with some chemistry data. We often observed a non-hydrolyzed portion of the pit membrane that was protected by pseudotorus caps. This finding further highlights the substantial remodeling and hydrolysis that affects most of the non-cellulosic components during the development of interconduit pit membranes (Czaninski, Y, 1972, O'Brien, 1970). In addition, the co-localization of HG and calcium (Fig. 5-5a,b) demonstrates that calcium abundantly occurs in association with HG in the xylem.

A different pattern in pectin distribution was recently found in pit membranes of four Lauraceae species (Gortan *et al.*, 2011). In these species, intervessel pit membranes strongly reacted with ruthenium red, while annuli and vessel-ray pit membranes showed a negative reaction. Pectins were also present in the pit membranes of grapevine (Sun, Greve & Labavitch, 2011) and conifers

(Hafren, Daniel & Westermarck, 2000). Thus, it is obvious that substantial variability in pit membrane chemistry exists across different plant taxa. Future research will likely highlight the functional and ecological significance of these differences in pit chemistry. A comparative study using angiosperm species with high and low pectin content in their pit membranes would provide further insights into the role of pectins in pit membrane functioning. For instance, it would be helpful to see whether a similar shift in vulnerability after calcium removal occurs in Lauraceae species and whether the high pectin content in pit membranes of Lauraceae is associated with high pit resistance and with the ability to trap solutes within refilling vessels (Hacke & Sperry, 2003, Nardini, Lo Gullo & Salleo, 2011).

In addition, the relationship between shifts in vulnerability and the ion-mediated increase in hydraulic conductivity (Gasco *et al.*, 2006, Zwieniecki *et al.*, 2001) needs to be evaluated as both phenomena are attributed to the presence of HG in the pit membranes. However, there are also distinct differences that may partially uncouple these two phenomena. For instance, a broader spectrum of pectin types can be responsible for the ionic effect while only the long linear stretches of GalA that are typical for the HG domain are capable of substantial calcium cross-linking. All four species in this study showed a relatively weak ionic effect between 5 to 16% (data not shown). The magnitude of the ionic effect did not correspond with ΔP_{50} . It is not clear whether the hydrogel behavior of pectins in the annulus could influence K_h . However, it is possible that the tension of the annulus as determined by the ionic interactions transmits to the cellulosic matrix of the pit membrane, thereby stretching and relaxing the membrane pores.

5.5 CONCLUSIONS

This study enhances our knowledge of the chemical composition of pit membranes, which is a prerequisite for a better understanding of the role of these micro-valves in xylem functioning. Our results suggest that there is no link between the general presence or absence of HG in intervessel pit membranes and the shift in vulnerability after calcium removal. We provide evidence that pectic HG are not homogeneously distributed in intervessel pit membranes. In the four species studied, the main part of the membrane contained very little or no pectins whereas the annulus showed substantial enrichment in HG-labeling. Calcium precipitation experiments confirmed that calcium co-localizes with HG in the

annulus. We therefore hypothesize that the disruption of HG-calcium crosslinks within the annulus can lead to increased vulnerability to cavitation. Our results also highlight differences in chemical composition between interconduit and vessel-ray pit membranes. Observed differences in chemistry likely reflect the different biological functions of these pit types. While intervessel pits facilitate water flow, vessel-ray pits may be designed to provide a selective barrier between living ray cells and dead vessel elements.

5.6 TABLES

Table 5-1: The intensity and localization of immunogold labeling for polysaccharide specific antibodies JIM5, JIM7, LM6 and LM15.

antibody epitope	JIM5 low methyl-esterified/ non-esterified HG	JIM7 methyl-esterified HG	LM6 (1-5)- α -L-arabinan of RG-I	LM15 XXXG motif of XG
Intervessel pit membrane	-	-	-/+	-/+
Annulus	++	++	-/+	-/+
Vessel-ray pit membrane	++	++	+	-/+
Amorphous layer of ray cells	++	++	++	-/+
cml-between two cells	-/+	+	+	+
cml-cell corners	+	+	+	+
Pseudotori	-	-/+	++	-
Membrane under pseudotorus	++	++	-/+	-

Abbreviations: ++ strong signal/enrichment in labeling; + weak signal; - no signal; cml-compound middle lamella; HG-homogalacturonan; RG-I-rhamnogalacturonan I; XG-xyloglucan.

Table 5-2: Pit membrane diameter (D_m), annulus length and intensity of homogalacturonan labeling in the annulus in *B. papyrifera* (*Bp*), *P. balsamifera* (*Pb*), *P. virginiana* (*Pv*) and *A. alnifolia* (*Aa*). The intensity of the labeling was assessed by counting the number of gold particles localized in the annulus. The JIM5/JIM7 ratio is indicative of the ratio of low methyl esterified to high methyl esterified homogalacturonans. Values represent means \pm SE, the number of individual pits and annuli used for these measurements is indicated in brackets. Different letters indicates that the means were significantly different between the species, one-way ANOVA followed by Tukey HSD test ($P < 0.05$).

species	D_m (um)	annulus length (nm)	number of gold particles		
			JIM5	JIM7	JIM5/JIM7
<i>Bp</i>	2.3 ± 0.03 (86) ^a	141 ± 8 (24) ^a	12 ± 1 (13) ^a	5 ± 1 (13) ^a	2.49
<i>Pb</i>	6.8 ± 0.06 (85) ^b	275 ± 24 (20) ^b	9 ± 2 (16) ^{ab}	10 ± 2 (6) ^{ab}	0.82
<i>Pv</i>	4.6 ± 0.05 (87) ^c	331 ± 27 (20) ^b	5 ± 0 (6) ^b	10 ± 2 (15) ^b	0.48
<i>Aa</i>	4.8 ± 0.05 (76) ^c	351 ± 23 (20) ^b	6 ± 1 (15) ^b	15 ± 1 (9) ^b	0.44

5.7 FIGURES

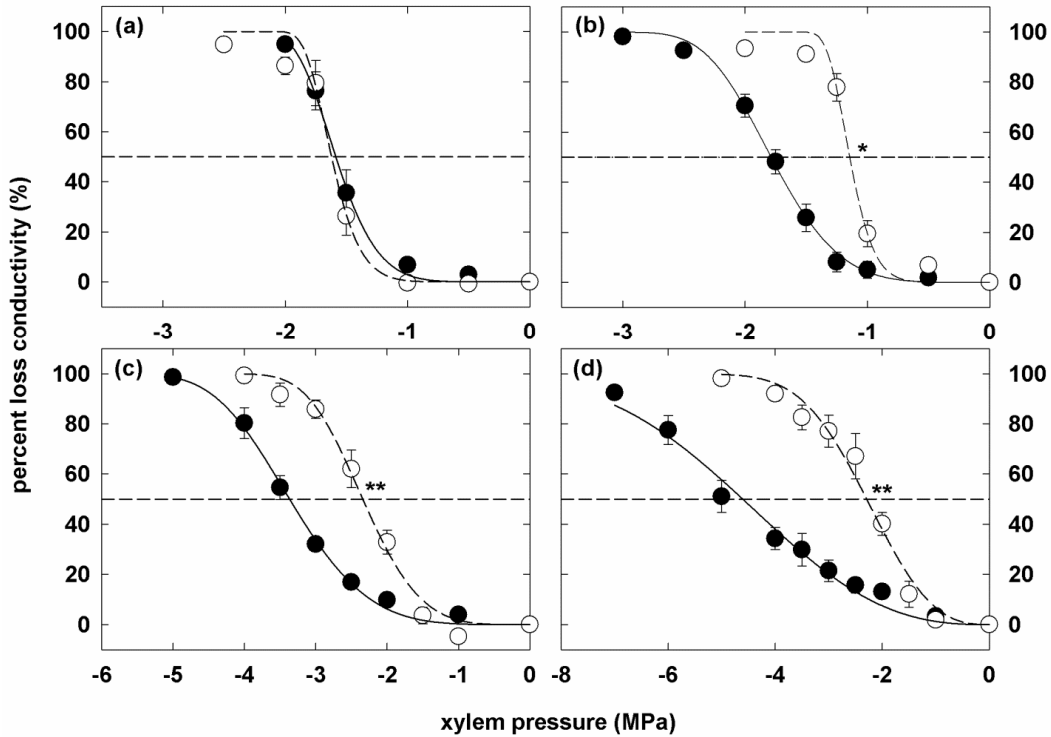


Figure 5-1: The effect of calcium removal on xylem vulnerability to embolism. Vulnerability curves of (a) *Betula papyrifera*, (b) *Populus balsamifera*, (c) *Prunus virginiana* and (d) *Amelanchier alnifolia* in stems perfused with sodium phosphate solution at pH 10 (open circles) or pH 4 (closed circles). The phosphate solution at pH 10 is capable of chelating calcium, while the solution at pH 4 is a non-chelating control. Error bars show standard error of mean (n=6). * and ** indicates that the xylem pressure at which stems showed 50% loss of conductivity (P_{50}) differed at $P \leq 0.05$ and $P \leq 0.001$, respectively, between stems perfused with treatment *versus* control phosphate solution (Tukey HSD test).

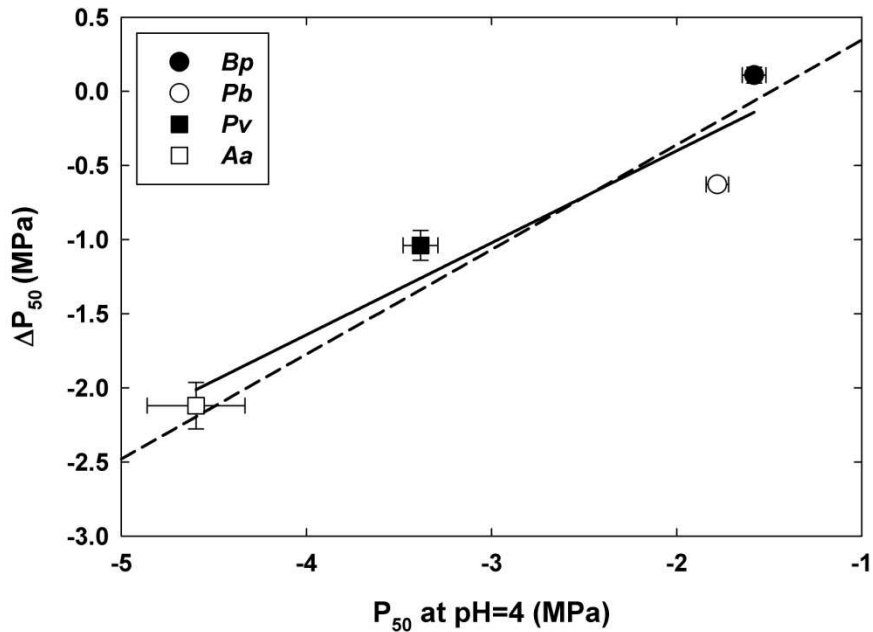


Figure 5-2: Relationship between vulnerability to cavitation and the magnitude of vulnerability shift (ΔP_{50}) in four angiosperm species. The xylem pressure at which stems showed 50% loss of conductivity (P_{50}) measured in stems perfused with sodium phosphate solution at pH 4 represents the ‘native’ xylem resistance. The ΔP_{50} was calculated as the difference between the P_{50} measured at pH 10 and pH 4. Data points are means \pm SE for *Betula papyrifera* (Bp), *Populus balsamifera* (Pb), *Prunus virginiana* (Pv) and *Amelanchier alnifolia* (Aa). The solid line shows a linear regression through data points ($r=0.95$, $P\leq 0.05$). The dashed line is the regression line obtained by Herbette and Cochard (2010) and demonstrates the close correspondence between our data with their dataset.

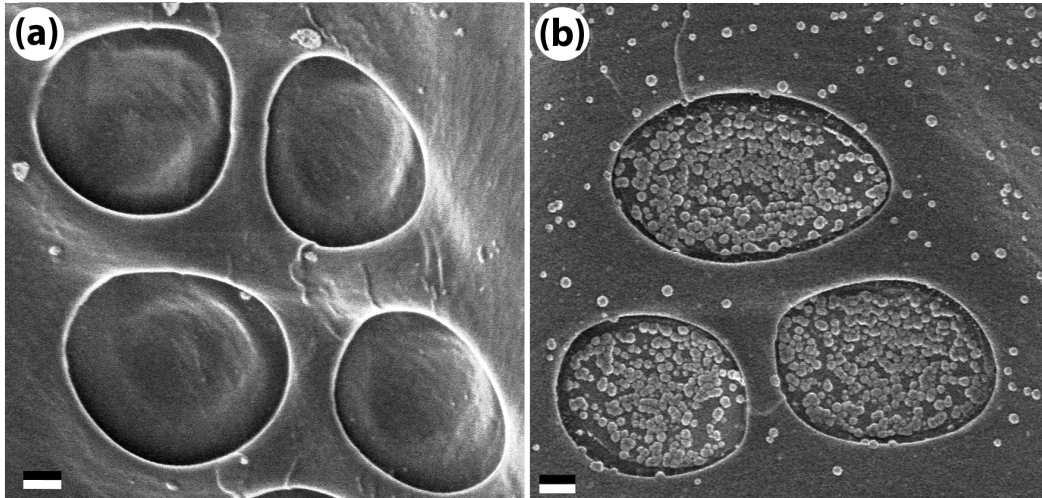


Figure 5-3: Scanning electron micrographs of vessel-ray pits in stems of *Populus balsamifera* perfused with sodium phosphate solution at (a) pH 4 or (b) pH 10. Pit membranes are viewed from the vessel lumen through wide apertures in the secondary cell wall. Conspicuous spherical particles were often found in the vessel lumen of samples perfused with the solution at pH 10 and were especially abundant on the surface of vessel-ray pit membranes. These particles were rich in phosphorus, calcium, magnesium and sodium as revealed with a semi-quantitative elemental analysis. Scale bars = 1 μ m.

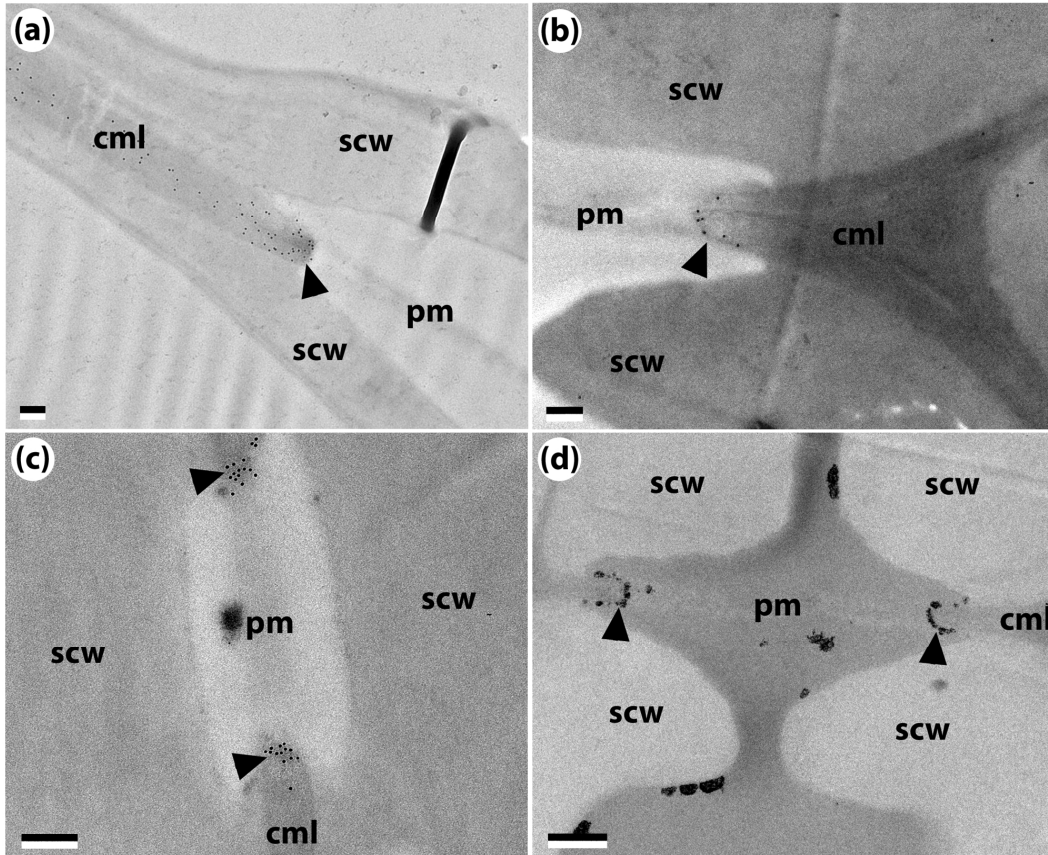


Figure 5-4: Transmission electron micrographs of the pit membrane annulus region showing the distribution of (a, b, c) homogalacturonan (HG) and (d) calcium precipitate as revealed by (a, b, c) immunogold labeling and (d) an antimonate precipitation technique. (a) JIM7 labeling is indicative of high methyl-esterified HG and was evident throughout the entire annulus region. (b, c) JIM5 labeling shows the distribution of low methyl-esterified HG and was often restricted to the tip of the annulus. (d) Electron dense calcium precipitates in the annulus closely resembled the JIM5 labeling pattern (compare b and d). Micrographs show pits of (a) *P. balsamifera* labeled with JIM7, (b) *P. virginiana* labeled with JIM5, (c) *B. papyrifera* labeled with JIM5, and (d) *A. alnifolia* after antimonate precipitation. Arrow heads point to annuli; cml = compound middle lamella; pm = pit membrane; scw = secondary cell wall. Scale bars represent 0.2 μm in (a), (b), (c) and 0.5 μm in (d).

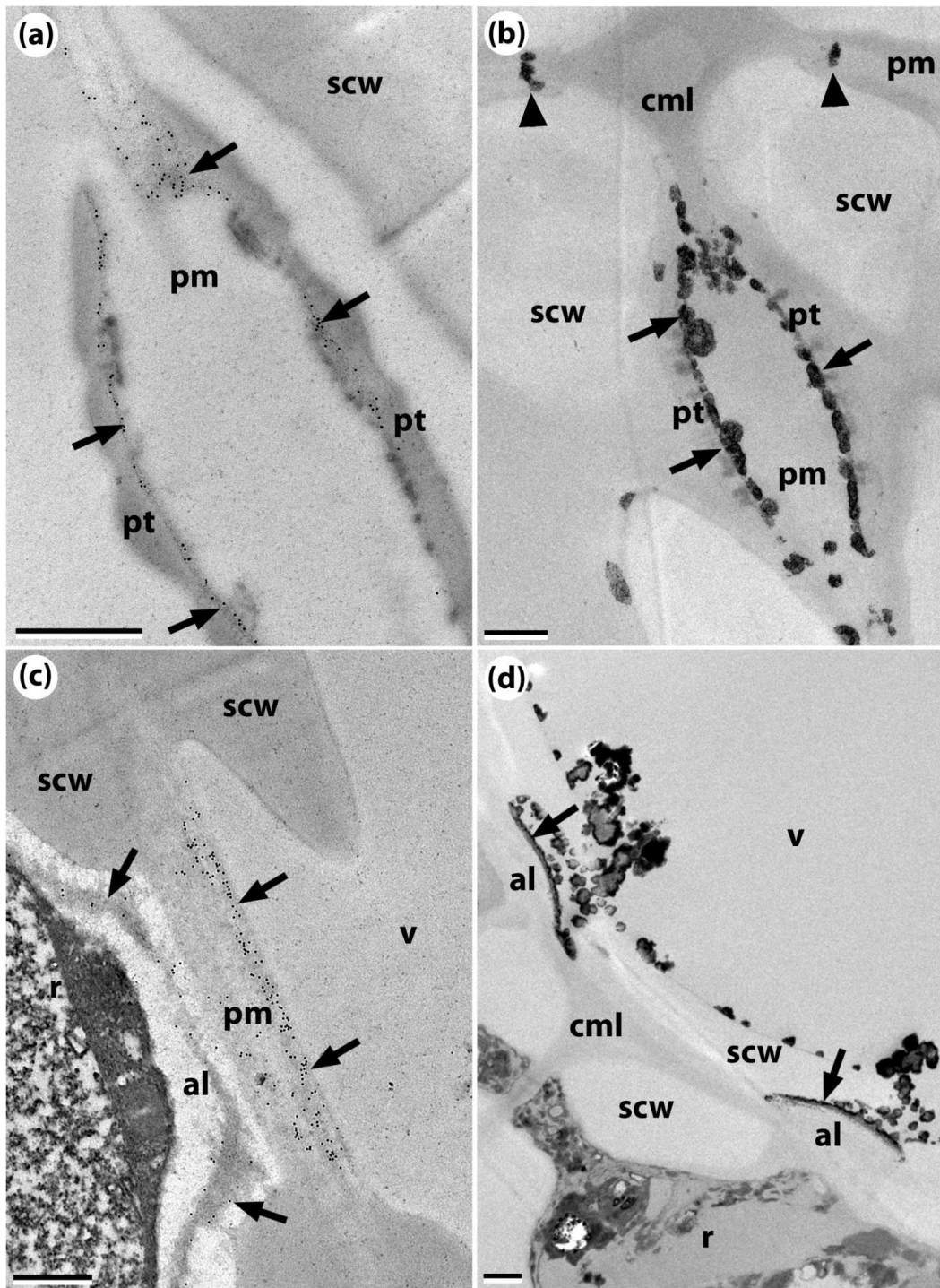


Figure 5-5: Corresponding patterns of (a, c) JIM5 immunolabeling and (b, d) calcium localization in (a, b) pseudotorii and (c, d) vessel-ray pits of *A. alnifolia* as observed with transmission electron microscopy. Gold particles and calcium precipitate were localized on the inner surface of pseudotorii (arrows in a, b) of imperforate tracheary elements. Precipitates were also evident in the annulus

(arrowheads in b). JIM5 epitopes were abundant in the vessel-ray pit membrane (pm in c) and in the amorphous layer (al) of ray cells (c). The highest labeling density within the vessel-ray pit membrane was found close to the surface of the membrane, near the vessel lumen (v, arrows). Correspondingly, a distinct layer of precipitates was observed lining the outer vessel-ray pit membrane surface in samples treated with antimonate (d). Precipitates were also found around the periphery of the vessel lumen. al = amorphous layer; cml = compound middle lamella; pm= pit membrane; pt = pseudotorus; r = ray cell; scw = secondary cell wall; v = vessel lumen. The scale bars represent 0.5 μm .

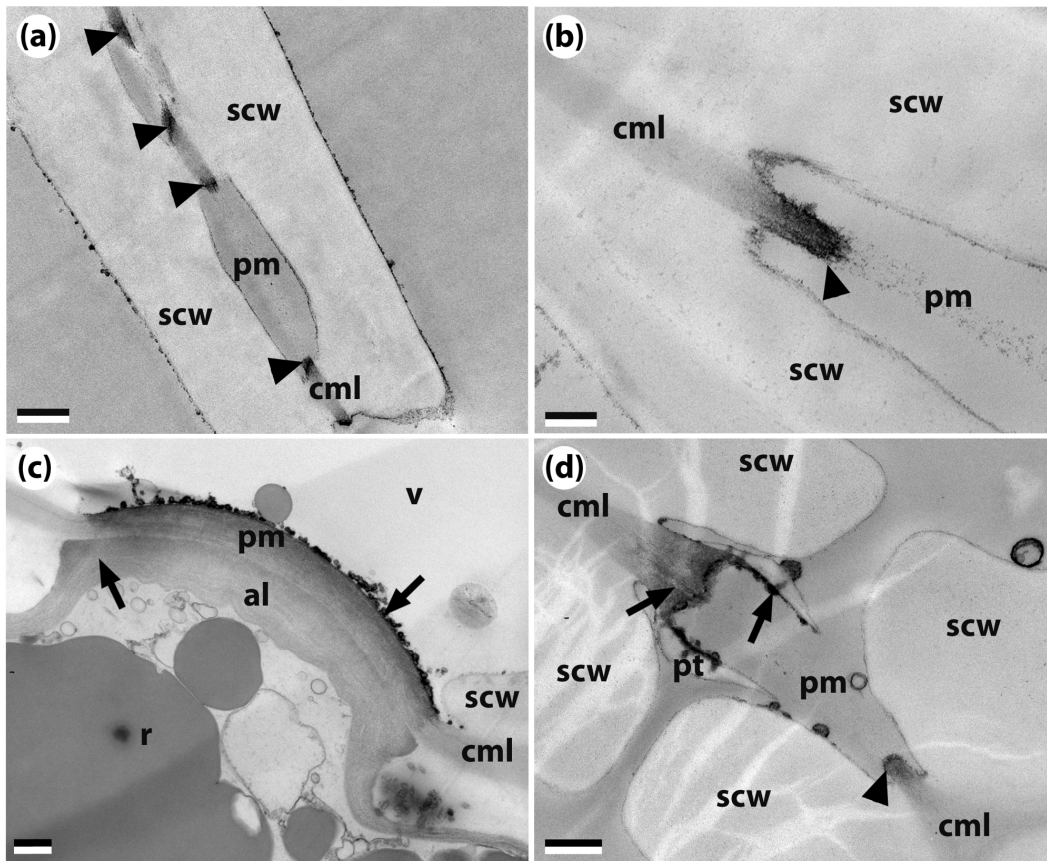


Figure 5-6: Ruthenium red staining of acidic pectin in the xylem of (a) *Betula papyrifera*, (b, c) *Populus balsamifera* and (d) *Prunus virginiana*. Dark, electron-dense regions (arrowheads, arrows) show a positive staining reaction. Ruthenium red staining was apparent in the pit membrane annulus (arrowheads in a, b and d), in the vessel-ray pit membrane (pm), the amorphous layer (al) (arrows in c), as well as the inner surface of pseudotori (pt, arrows in d). There was a very close correspondence between ruthenium red staining and JIM5 immunolabeling (compare this figure with Figs. 3 and 4). al = amorphous layer; cml = compound middle lamella; pm = pit membrane; pt = pseudotorus; r = ray cell; scw = secondary cell wall, v = vessel lumen. The scale bars are 0.5 μm in (a), (c), (d) and 0.2 μm in (b).

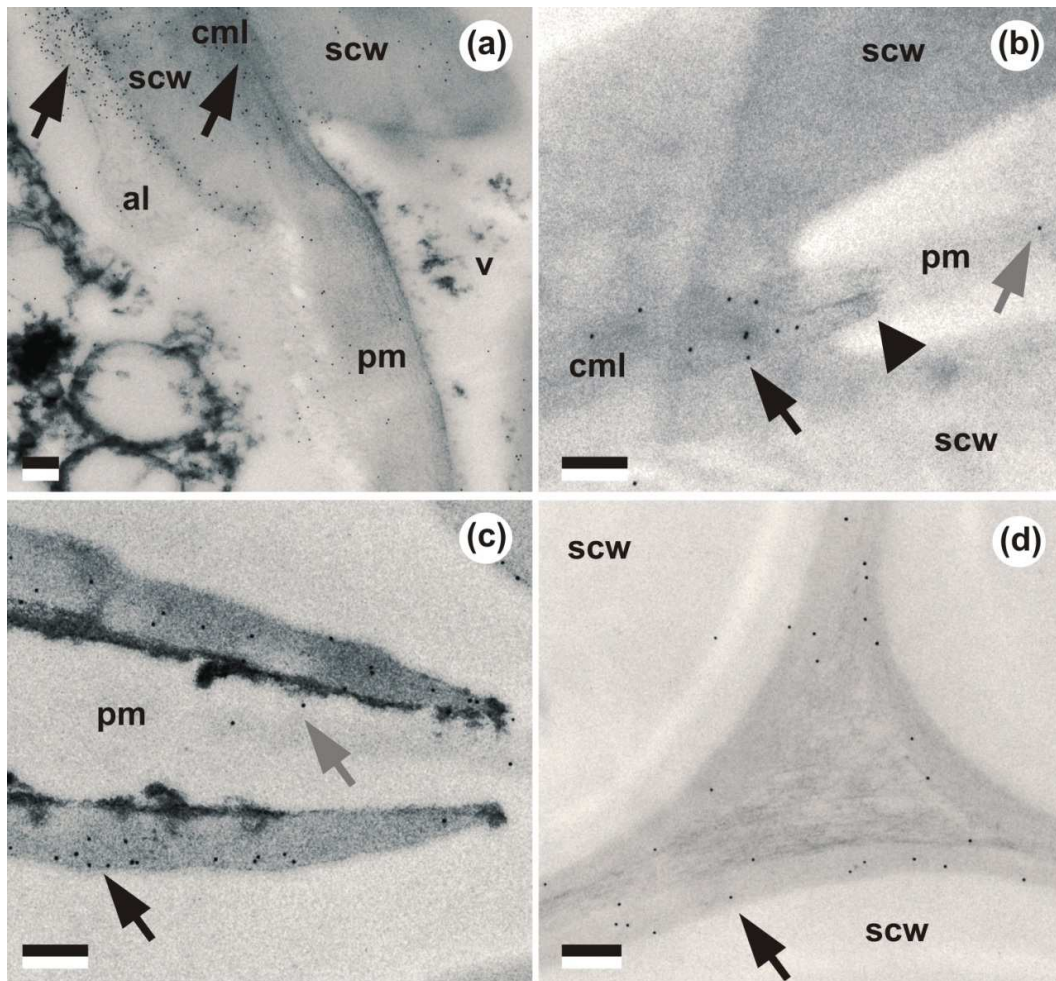


Figure 5-7 Immunogold labeling of cell walls with (a, c) anti-RG-I antibody LM6 and (b, d) anti-xyloglucan antibody LM15. (a) Vessel-ray pit of *A. alnifolia*. LM6 epitopes were abundant in a dark band which was part of the amorphous layer (al, arrow) near the edge of the pit. A strong LM6 signal was also evident in the compound middle lamella near the pit (cml, arrow). (b) Periphery of an intervessel pit in *P. virginiana*. LM15 epitopes were present in the compound middle lamella (arrow); weak labeling was observed in the pit membrane (pm, dark grey arrow), but not in the annulus (arrow head). (c) Pseudotorus in *A. alnifolia* labeled with LM6. Labeling occurred in the electron dense pseudotori (black arrow); a weak signal was found in the pit membrane region between pseudotorus caps (dark grey arrow). (d) Cell corner between fibers of *P. virginiana*, labeled with LM15. The antibody was mainly located in the region of the cell corner adjacent to the secondary cell wall (scw). Scale bars are 0.2 μm .

5.8 REFERENCES

- Alder N.N., Pockman W.T., Sperry J.S. & Nuismer S. (1997) Use of centrifugal force in the study of xylem cavitation. *Journal of Experimental Botany*, **48**, 665-674.
- Baier M., Goldberg R., Catesson A.-M., Liberman M., Bouchemal N., Michon V. & Penhoat C.H. (1994) Pectin changes in samples containing poplar cambium and inner bark in relation to the seasonal cycle. *Planta*, **193**, 446-454.
- Boyce C.K., Zwieniecki M.A., Cody G.D., Jacobsen C., Wirick S., Knoll A.H. & Holbrook N.M. (2004) Evolution of xylem lignification and hydrogel transport regulation. *Proceedings of the National Academy of Sciences of the United States of America*, **101**, 17555-17558.
- Braun H.J. (1970) *Funktionelle Histologie der sekundären Sprossachse. I. Das Holz*. Gebrüder Borntraeger, Berlin.
- Brodersen C.R., McElrone A.J., Choat B., Matthews M.A. & Shackel K.A. (2010) The dynamics of embolism repair in xylem: In vivo visualizations using high-resolution computed tomography. *Plant Physiology*, **154**, 1088-1095.
- Caffall K.H. & Mohnen D. (2009) The structure, function, and biosynthesis of plant cell wall pectic polysaccharides. *Carbohydrate Research*, **344**, 1879-1900.
- Carlquist S. (1986) Terminology of imperforate tracheary elements - a reply. *IAWA Bulletin*, **7**, 168-170.
- Cassab G.I. (1998) Plant cell wall proteins. *Annual Review of Plant Physiology and Plant Molecular Biology*, **49**, 281-309.
- Chaffey N.J. (2002) Conventional (chemical-fixation) transmission electron microscopy and cytochemistry of angiosperm trees. In: *Wood formation in trees: cell and molecular biology techniques* (ed N.J. Chaffey), pp. 41-64. Taylor & Francis, London.
- Chaffey N.J., Barnett J.R. & Barlow P.W. (1997) Cortical microtubule involvement in bordered pit formation in secondary xylem vessel elements of *Aesculus hippocastanum* L. (Hippocastanaceae): A correlative study using electron microscopy and indirect immunofluorescence microscopy. *Protoplasma*, **197**, 64-75.
- Choat B., Cobb A.R. & Jansen S. (2008) Structure and function of bordered pits: new discoveries and impacts on whole-plant hydraulic function. *New Phytologist*, **177**, 608-625.
- Choat B., Jansen S., Zwieniecki M.A., Smets E. & Holbrook N.M. (2004) Changes in pit membrane porosity due to deflection and stretching: the role of vested pits. *Journal of Experimental Botany*, **55**, 1569-1575.
- Cochard H., Herbette S., Hernandez E., Holtta T. & Mencuccini M. (2010) The effects of sap ionic composition on xylem vulnerability to cavitation. *Journal of Experimental Botany*, **61**, 275-285.

- Cybulska J., Zdunek A. & Konstankiewicz K. (2011) Calcium effect on mechanical properties of model cell walls and apple tissue. *Journal of Food Engineering*, **102**, 217-223.
- Czaninski Y. (1972) Ultrastructural observations on hydrolysis of primary walls of vessels in *Robinia pseudo-acacia* L. and *Acer pseudoplatanus* L. *Comptes Rendus Hebdomadaires Des Seances De L Academie Des Sciences Serie D*, **275**, 361-363.
- De Boer A.H. & Volkov V. (2003) Logistics of water and salt transport through the plant: structure and functioning of the xylem. *Plant Cell and Environment*, **26**, 87-101.
- Dute R., Hagler L. & Black A. (2008) Comparative development of intertracheary pit membranes in *Abies firma* and *Metasequoia glyptostroboides*. *IWA Journal*, **29**, 277-289.
- Ermel F.F., Follet-Gueye M.L., Cibert C., Vian B., Morvan C., Catesson A.M. & Goldberg R. (2000) Differential localization of arabinan and galactan side chains of rhamnogalacturonan I in cambial derivatives. *Planta*, **210**, 732-740.
- Evert R.F. (2006) *Esau's plant anatomy: meristems, cells, and tissues of the plant body: their structure, function, and development*. (3rd ed.). John Wiley & Sons, Inc., New Jersey.
- Funada R. & Catesson A.M. (1991) Partial cell wall lysis and the resumption of meristematic activity in *Fraxinus excelsior* cambium. *IWA Bulletin*, **12**, 439-444.
- Gasco A., Nardini A., Gortan E. & Salleo S. (2006) Ion-mediated increase in the hydraulic conductivity of Laurel stems: role of pits and consequences for the impact of cavitation on water transport. *Plant Cell and Environment*, **29**, 1946-1955.
- Gortan E., Nardini A., Salleo S. & Jansen S. (2011) Pit membrane chemistry influences the magnitude of ion-mediated enhancement of xylem hydraulic conductance in four Lauraceae species. *Tree Physiology*, **31**, 48-58.
- Guglielmino N., Liberman M., Jauneau A., Vian B., Catesson A.M. & Goldberg R. (1997) Pectin immunolocalization and calcium visualization in differentiating derivatives from poplar cambium. *Protoplasma*, **199**, 151-160.
- Guillemin F., Guillon F., Bonnin E., Devaux M.F., Chevalier T., Knox J.P., Liners F. & Thibault J.F. (2005) Distribution of pectic epitopes in cell walls of the sugar beet root. *Planta*, **222**, 355-371.
- Hacke U.G. & Jansen S. (2009) Embolism resistance of three boreal conifer species varies with pit structure. *New Phytologist*, **182**, 675-686.
- Hacke U.G. & Sperry J.S. (2003) Limits to xylem refilling under negative pressure in *Laurus nobilis* and *Acer negundo*. *Plant Cell and Environment*, **26**, 303-311.
- Hacke U.G., Sperry J.S., Wheeler J.K. & Castro L. (2006) Scaling of angiosperm xylem structure with safety and efficiency. *Tree Physiology*, **26**, 689-701.

- Hafren J., Daniel G. & Westermark U. (2000) The distribution of acidic and esterified pectin in cambium, developing xylem and mature xylem of *Pinus sylvestris*. *IWA Journal*, **21**, 157-168.
- Harrak H., Chamberland H., Plante M., Bellemare C., Lafontaine J.G. & Tabaeizadeh Z. (1999) A proline-, threonine-, and glycine-rich protein down-regulated by drought is localized in the cell wall of xylem elements. *Plant Physiology*, **121**, 557-564.
- Herbette S. & Cochard H. (2010) Calcium is a major determinant of xylem vulnerability to cavitation. *Plant Physiology*, **153**, 1932-1939.
- Imamura Y. & Harada H. (1973) Electron-microscopic study on development of bordered pit in coniferous tracheids. *Wood Science and Technology*, **7**, 189-205.
- Jansen S., Choat B. & Pletsers A. (2009) Morphological variation of intervessel pit membranes and implications to xylem function in angiosperms. *American Journal of Botany*, **96**, 409-419.
- Jansen S., Gortan E., Lens F., Lo Gullo M.A., Salleo S., Scholz A., Stein A., Trifilo P. & Nardini A. (2011) Do quantitative vessel and pit characters account for ion-mediated changes in the hydraulic conductance of angiosperm xylem? *New Phytologist*, **189**, 218-228.
- Jansen S., Sano Y., Choat B., Rabaey D., Lens F. & Dute R.R. (2007) Pit membranes in tracheary elements of Rosaceae and related families: New records of tori and pseudotori. *American Journal of Botany*, **94**, 503-514.
- Jarbeau J.A., Ewers F.W. & Davis S.D. (1995) The mechanism of water-stress-induced embolism in two species of chaparral shrubs. *Plant Cell and Environment*, **18**, 189-196.
- Knox J.P., Linstead P.J., King J., Cooper C. & Roberts K. (1990) Pectin esterification is spatially regulated both within cell walls and between developing tissues of root apices. *Planta*, **181**, 512-521.
- Lens F., Sperry J.S., Christman M.A., Choat B., Rabaey D. & Jansen S. (2011) Testing hypotheses that link wood anatomy to cavitation resistance and hydraulic conductivity in the genus *Acer*. *New Phytologist*, **190**, 709-723.
- Li Y.Y., Sperry J.S., Taneda H., Bush S.E. & Hacke U.G. (2008) Evaluation of centrifugal methods for measuring xylem cavitation in conifers, diffuse- and ring-porous angiosperms. *New Phytologist*, **177**, 558-568.
- Liese W. (1965) The fine structure of bordered pits in softwoods. In: *Cellular ultrastructure of woody plants* (ed W.A. Cote), pp. 271-290. Syracuse University Press, Syracuse.
- Lopez-Portillo J., Ewers F.W. & Angeles G. (2005) Sap salinity effects on xylem conductivity in two mangrove species. *Plant, Cell & Environment*, **28**, 1285-1292.
- MacDougall A.J., Brett G.M., Morris V.J., Rigby N.M., Ridout M.J. & Ring S.G. (2001a) The effect of peptide-pectin interactions on the gelation behaviour of a plant cell wall pectin. *Carbohydrate Research*, **335**, 115-126.
- MacDougall A.J., Rigby N.M., Ryden P., Tibbitts C.W. & Ring S.G. (2001b) Swelling behavior of the tomato cell wall network. *Biomacromolecules*, **2**, 450-455.

- Marcus S.E., Verhertbruggen Y., Herve C., Ordaz-Ortiz J.J., Farkas V., Pedersen H.L., Willats W.G.T. & Knox J.P. (2008) Pectic homogalacturonan masks abundant sets of xyloglucan epitopes in plant cell walls. *BMC Plant Biology*, **8**, 60.
- Micheli F. (2001) Pectin methylesterases: cell wall enzymes with important roles in plant physiology. *Trends in Plant Science*, **6**, 414-419.
- Micheli F., Ermel F.F., Bordenave M., Richard L. & Goldberg R. (2002) Cell walls of woody tissues: cytochemical, biochemical and molecular analysis of pectins and pectin methylesterases. In: *Wood formation in trees: cell and molecular biology techniques* (ed N.J. Chaffey), pp. 179-200. Taylor & Francis, London.
- Morrow A.C. & Dute R.R. (1998) Development and structure of pit membranes in the rhizome of the woody fern *Botrychium dissectum*. *IAWA Journal*, **19**, 429-441.
- Nardini A., Grego F., Trifilo P. & Salleo S. (2010) Changes of xylem sap ionic content and stem hydraulics in response to irradiance in *Laurus nobilis*. *Tree Physiology*, **30**, 628-635.
- Nardini A., Lo Gullo M.A. & Salleo S. (2011) Refilling embolized xylem conduits: Is it a matter of phloem unloading? *Plant Science*, **180**, 604-611.
- O'Brien T.P. (1970) Further observations on hydrolysis of the cell wall in the xylem. *Protoplasma*, **69**, 1-14.
- O'Neill M.A. & William S.Y. (2003) The composition and structure of plant primary walls. In: *The Plant Cell Wall, Annual Plant Reviews* (ed J.K.C. Rose), pp. 1-54. Blackwell Publishing Ltd, Oxford, UK.
- Parre E. & Geitmann A. (2005) Pectin and the role of the physical properties of the cell wall in pollen tube growth of *Solanum chacoense*. *Planta*, **220**, 582-592.
- Petty J.A. (1972) Aspiration of bordered pits in conifer wood. *Proceedings of the Royal Society of London Series B-Biological Sciences*, **181**, 395-406.
- Pittermann J., Choat B., Jansen S., Stuart S.A., Lynn L. & Dawson T.E. (2010) The relationships between xylem safety and hydraulic efficiency in the Cupressaceae: The evolution of pit membrane form and function. *Plant Physiology*, **153**, 1919-1931.
- Pittermann J., Sperry J.S., Hacke U.G., Wheeler J.K. & Sikkema E.H. (2005) Torus-margo pits help conifers compete with angiosperms. *Science*, **310**, 1924-1924.
- Plavcová L., Hacke U.G. & Sperry J.S. (2011) Linking irradiance-induced changes in pit membrane ultrastructure with xylem vulnerability to cavitation. *Plant, Cell and Environment*, **34**, 501-513.
- Proseus T.E. & Boyer J.S. (2008) Calcium pectate chemistry causes growth to be stored in *Chara corallina*: a test of the pectate cycle. *Plant Cell and Environment*, **31**, 1147-1155.
- R Development Core Team (2009) R: A language and environment for statistical computing. R Foundation for Statistical Computing, Vienna, Austria. ISBN 3-900051-07-0

- Rabaey D., Lens F., Huysmans S., Smets E. & Jansen S. (2008) A comparative ultrastructural study of pit membranes with plasmodesmata associated thickenings in four angiosperm species. *Protoplasma*, **233**, 255-262.
- Ryden P., MacDougall A.J., Tibbits C.W. & Ring S.G. (2000) Hydration of pectic polysaccharides. *Biopolymers*, **54**, 398-405.
- Salleo S., Trifilo P., Esposito S., Nardini A. & Lo Gullo M.A. (2009) Starch-to-sugar conversion in wood parenchyma of field-growing *Laurus nobilis* plants: a component of the signal pathway for embolism repair? *Functional Plant Biology*, **36**, 815-825.
- Sauter J.J., Iten W. & Zimmermann M.H. (1973) Studies on the release of sugars into the vessels of sugar maple (*Acer saccharum* Marsh.). *Canadian Journal of Botany*, **51**, 1-8.
- Sauter J.J. & Van Cleve B. (1992) Seasonal variation of amino acids in the xylem sap of "*Populus x canadensis*" and its relation to protein body mobilization. *Trees-Structure and Function*, **7**, 26-32.
- Schmid R. (1965) The fine structure of pits in hardwoods. In: *Cellular ultrastructure of woody plants* (ed W.A. Cote), pp. 291-304. Syracuse University Press, Syracuse.
- Schmid R. & Machado R.D. (1968) Pit membranes in hardwoods - Fine structure and development. *Protoplasma*, **66**, 185-204.
- Schmitz N., Jansen S., Verheyden A., Kairo J.G., Beeckman H. & Koedam N. (2007) Comparative anatomy of intervessel pits in two mangrove species growing along a natural salinity gradient in Gazi Bay, Kenya. *Annals of Botany*, **100**, 271-281.
- Slocum R.D. & Roux S.J. (1982) An improved method for the sub-cellular localization of calcium using a modification of the anitmonate precipitation technique. *Journal of Histochemistry & Cytochemistry*, **30**, 617-629.
- Sperry J.S. & Hacke U.G. (2004) Analysis of circular bordered pit function - I. Angiosperm vessels with homogenous pit membranes. *American Journal of Botany*, **91**, 369-385.
- Sperry J.S., Saliendra N.Z., Pockman W.T., Cochard H., Cruiziat P., Davis S.D., Ewers F.W. & Tyree M.T. (1996) New evidence for large negative xylem pressures and their measurement by the pressure chamber method. *Plant, Cell and Environment*, **19**, 427-436.
- Sperry J.S. & Tyree M.T. (1988) Mechanism of water stress-induced xylem embolism. *Plant Physiology*, **88**, 581-587.
- Sun Q.A., Greve L.C. & Labavitch J.M. (2011) Polysaccharide compositions of intervessel pit membranes contribute to Pierce's disease resistance of grapevines. *Plant Physiology*, **155**, 1976-1987.
- Tibbits C.W., MacDougall A.J. & Ring S.G. (1998) Calcium binding and swelling behaviour of a high methoxyl pectin gel. *Carbohydrate Research*, **310**, 101-107.
- Tyree M.T. & Zimmermann M.H. (2002) *Xylem structure and the ascent of sap*. (2nd ed.). Springer Verlag, Berlin.

- Valentin R., Cerclier C., Geneix N., Aguié-Beghin V., Gaillard C., Ralet M.C. & Cathala B. (2010) Elaboration of extensin-pectin thin film model of primary plant cell wall. *Langmuir*, **26**, 9891-9898.
- van Ieperen W. (2007) Ion-mediated changes of xylem hydraulic resistance in planta: fact or fiction? *Trends in Plant Science*, **12**, 137-142.
- Wardrop A.B. (1954) The mechanism of surface growth involved in the differentiation of fibres and tracheids *Australian Journal of Botany*, **2**, 165-175.
- Wick S.M. & Hepler P.K. (1980) Localization of Ca⁺⁺ -containing antimonate precipitates during mitosis. *Journal of Cell Biology*, **86**, 500-513.
- Willats W.G.T., McCartney L., Mackie W. & Knox J.P. (2001) Pectin: cell biology and prospects for functional analysis. *Plant Molecular Biology*, **47**, 9-27.
- Wisniewski M. & Davis G. (1995) Immunogold localization of pectins and glycoproteins in tissue of peach with reference to deep supercooling. *Trees*, **9**, 253-260.
- Wisniewski M., Davis G. & Arora R. (1991) Effect of macerases, oxalic acid, and EGTA on deep supercooling and pit membrane structure of xylem parenchyma of peach. *Plant Physiology*, **96**, 1354-1359.
- Zwieniecki M.A., Melcher P.J. & Holbrook N.M. (2001) Hydrogel control of xylem hydraulic resistance in plants. *Science*, **291**, 1059-1062.

6. General Discussion and Conclusions

6.1 The scope of the thesis

The research presented in this thesis focused on the structure and function of xylem. Xylem is the primary water-conducting system in plants and its function is closely coupled with nutrient acquisition and leaf gas exchange. As plant growth and survival depend on efficient and unimpaired xylem functioning (McDowell, Pockman, Allen *et al.*, 2008, Tyree, 2003b), a thorough understanding of xylem physiology is a valuable prerequisite for various practical applications in forestry, agriculture and plant conservation.

The water transport capacity of xylem is mainly driven by the number and size of functional conduits. Following the Hagen-Poiseuille equation (Eqn. 1-1), sapwood hydraulic conductivity scales positively with the sum of conduit diameters to the fourth power. However, a significant fraction of all available conduits may be permanently or temporarily blocked for water transport due to xylem embolism. It is well known that the structural and functional properties of xylem, including xylem-specific hydraulic conductivity and xylem vulnerability to embolism, vary greatly across different species (Wheeler, Baas & Rodgers, 2007). Studies focusing on this interspecific variability have been very useful in shaping our understanding of the functional and ecological significance of various xylem traits (Hacke, Sperry, Wheeler *et al.*, 2006, Jansen, Choat & Pletsers, 2009, Maherali, Pockman & Jackson, 2004). By comparison, much less research has been conducted at the intraspecific level, although such studies can provide additional valuable insights (Fichot, Barigah, Chamaillard *et al.*, 2010, Holste, Jerke & Matzner, 2006, Lamy, Bouffier, Burlett *et al.*, 2011, Martinez-Vilalta, Cochard, Mencuccini *et al.*, 2009, Sperry & Hacke, 2002).

The **first objective** of my PhD research, therefore, was to enhance our knowledge of within-species variability in the anatomical and hydraulic traits of xylem. In my thesis, I assessed the phenotypic plasticity of xylem traits using 3-month old saplings of hybrid poplar (*Populus trichocarpa* × *deltooides*, clone H11-11) subjected to experimental drought, fertilization and shading. Furthermore, I discussed the functional and ecological implications of these changes for plant acclimation. I also studied patterns in gene expression that were associated with the different xylem phenotypes.

The **second objective** of my PhD project was to expand our knowledge about intervessel pits, which are the cellular structures that presumably lie at the heart of xylem vulnerability to cavitation. While the prominent role of pits in xylem cavitation has been widely accepted (Choat, Cobb & Jansen, 2008, Sperry & Tyree, 1988), there are still a number of unresolved questions regarding the exact mode of their functioning. In this thesis, I used electron microscopy to study the structure and chemical composition of pit membranes in hybrid poplar, balsam poplar and three other hardwood species. Observed differences in pit membrane structure and chemical composition were linked with differences in xylem vulnerability. This provided novel insights into how these peculiar safety valves operate in protecting the transpiration stream against drought-induced cavitation.

6.2 Variability in xylem traits in hybrid poplar saplings

The results of my experiments showed that xylem anatomical and hydraulic parameters in hybrid poplar saplings change in response to experimental drought, fertilization and shading (Chapter 2, Chapter 3, Chapter 4). Considerable variability in two of the most important hydraulic traits, xylem-specific hydraulic conductivity and vulnerability to drought-induced cavitation, was observed. The changes in xylem hydraulic function were paralleled by changes in the dimensions of vessels and fibers as well as in their cell wall reinforcement. Such adjustments in xylem structure and function may be important for the ability of trees to optimize their performance under prevailing environmental constraints (Beikircher & Mayr, 2009, Sperry & Hacke, 2002) and for their ability to cope with variable and changing climate conditions (Bonan, 2008). It is not likely that the plasticity of xylem alone would be enough to mitigate the impacts of reduced water availability on plant performance. Nevertheless, changes in xylem transport safety and efficiency in conjunction with adjustments in root-to-shoot and leaf-to-xylem area ratios as well as changes in leaf gas exchange and water use efficiency (Fichot, Chamaillard, Depardieu *et al.*, 2011, Martinez-Vilalta *et al.*, 2009, Wikberg & Ögren, 2007) may contribute to the overall plant hydraulic acclimation.

Based on the results presented in this thesis, however, it is difficult to draw more specific conclusions about the potential effects of xylem acclimation on the performance of this hybrid poplar genotype under field conditions. In my studies, young saplings grown under controlled conditions in a growth chamber were used, and the experimental treatments were imposed one at a time and for a relatively short period of time (30-40 days). This situation is very different from

the complex and variable network of biotic and abiotic factors which shapes the performance of trees potentially growing for several decades in natural and commercial stands. Nonetheless, knowledge of how a single environmental cue affects xylem structure and function is an essential prerequisite for understanding the more complex situations common in nature. In order to assess intraspecific variability in the field, future studies could take advantage of poplar genotypes growing in common gardens (Schreiber, Hacke, Hamann *et al.*, 2011, Soolanayakanahally, Guy, Silim *et al.*, 2009). A number of common garden field sites have been established as part of a reciprocal transplant series planted across Canada and the United States (Schreiber *et al.*, 2011, Soolanayakanahally *et al.*, 2009). Such experimental design provides an excellent opportunity to study intraspecific variability because it allows separating the contributions of genetic adaptation and phenotypic plasticity to the overall trait variability at the intraspecific level.

The results of my experiments should also be interpreted with caution when the behavior of other species grown under similar experimental conditions is predicted. Poplars are fast-growing pioneer species characterized by a high demand for water and nutrients (Blake, Sperry, Tschaplinski *et al.*, 1996, Rennenberg, Wildhagen & Ehrling, 2010). It has been argued that phenotypic plasticity is particularly high in species with exploitative resource-use strategies (Crick & Grime, 1987, Grassein, Till-Bottraud & Lavorel, 2010). It is therefore possible that some of the changes in xylem structure and function described in this thesis, or the magnitude of these changes, are specific to poplar or species with a similar ecological strategy.

6.3 Changes in gene expression underlying different xylem phenotypes

Because clonally propagated plant material was used in my experiments, the observed variability in xylem traits was solely a result of phenotypic acclimation as opposed to genetic adaptation. With genotype being the same, it can be concluded that the differences in the xylem phenotype exhibited by the saplings in response to experimental treatments were driven by changes in gene expression. Using microarray analysis, I have detected almost 400 differentially expressed genes (fold change ± 1.5 , $P < 0.05$) in the developing xylem of fertilized and control saplings (Chapter 3). By analyzing transcriptional changes in conjunction with observed differences in xylem phenotype, I identified potential gene candidates that may underlie particular xylem traits, such as vessel diameter or cell wall thickness. Clearly, an in-depth functional characterization of specific

genes is now required in order to confirm their proposed functions. Nevertheless, studies like mine conveniently complement work using reverse genetic approaches and contribute to the ongoing efforts to unravel the molecular basis of wood formation in trees. In 2005, Andrew Groover, one of the pioneers in the molecular biology of forest trees, called the vascular cambium “the least understood plant meristem” (Groover, 2005). I think this label is still valid despite the substantial amount of work that has been done following the release of the *Populus* genome sequence in 2006 (Tuskan, DiFazio, Jansson *et al.*, 2006). Research combining molecular biology with traditional xylem functional anatomy holds great potential for many exciting discoveries (Lens, Smets & Melzer, 2012, Spicer & Groover, 2010). I therefore hope that studies bringing together the fields of wood physiological anatomy and molecular biology will be more common in the future.

6.4 The role of intervessel pits in xylem vulnerability

My research greatly enhanced our knowledge of mechanisms that underlie xylem vulnerability to cavitation by providing novel information about intervessel pits. In this thesis I demonstrated that xylem vulnerability in hybrid poplar saplings i) changes in response to growing conditions (Chapter 2, 3, 4), ii) changes along a developmental gradient (Chapter 2), and iii) is correlated with wood density (Chapter 2). Furthermore, I have shown that vulnerability increases after the perfusion with a calcium chelating agent in three out of four angiosperm species (Chapter 5). According to the air-seeding hypothesis, the difference in xylem vulnerability should be associated with differences in the permeability of pit membranes to air. Consequently, I could harness the observed differences in xylem vulnerability to better understand the factors potentially influencing the cavitation threshold.

6.4.1 Chemical properties of pit membranes

In my opinion, poor knowledge of the chemical composition of pit membranes has been the major limitation in our understanding of pit membrane function in terms of water transport. My research provided novel information on the chemical composition of pits (Chapter 4, Chapter 5). I showed that homogalacturonans, which are the most abundant type of pectins in plant cell walls, are not distributed homogeneously in the membrane of intervessel pits. While the main portion of the membrane did not contain detectable amounts of homogalacturonans, these pectic polysaccharides were specifically enriched

around the edge of the pit membrane, called the annulus. I consistently detected the same pattern in homogalacturonan distribution in four different species of woody angiosperms by two independent detection methods. I also showed that calcium co-localizes with homogalacturonans in the pit membrane annulus. To my knowledge, these results are the first to show the distribution of homogalacturonans in pit membranes with such high spatial resolution, and the first to describe the localization of calcium within pit membranes.

The heterogeneous distribution of homogalacturonans and calcium within pit membranes has ramifications for xylem vulnerability. Two studies previously showed that calcium removal leads to increased xylem vulnerability (Herbette & Cochard, 2010, Sperry & Tyree, 1988). Both studies speculated that this increased vulnerability is a result of the disruption of calcium-pectin cross-links within the pit membranes. However, my results demonstrated that calcium accumulates exclusively in the pit membrane annulus. This led me to speculate that the properties of the annulus may affect the cavitation threshold, likely by influencing pit membrane deflection and stretching (Chapter 5). Consistent with the circular orientation of cellulose microfibrils, the annulus may serve as a ring of springs that dissipate the impacts of the pressure difference, thereby preventing enlargement of pores in the main portion of the membrane. Alternatively, the annulus may influence the magnitude of membrane deflection, in turn affecting whether and when a pit membrane aspirates to the pit border. These hypotheses are novel and need to be tested. The effect of calcium removal on pit membrane aspiration could be conveniently studied in conifers in which pit aspiration is associated with decreasing hydraulic conductance due to the sealing action of pit membrane tori (Cochard, Hoelttae, Herbette *et al.*, 2009). Thus, it would be possible to test if a lower pressure difference, induced as a pressurized water flow through a stem segment, is sufficient to induce pit aspiration in stems treated with a calcium chelating agent, in comparison with control stems in which calcium was not removed.

My findings on the distribution of homogalacturonan also have substantial implications for the hypothesis that xylem hydraulic conductivity is affected by the putative hydrogel properties of pit membranes (Zwieniecki, Melcher & Holbrook, 2001). Assuming that pectins are major components of pit membranes, this hypothesis proposes that changes in hydraulic conductivity in response to varying ionic strength of xylem sap are a result of changes in pit porosity. The change in porosity has been attributed to the swelling and shrinking of pit

membrane pectins (Gasco, Nardini, Gortan *et al.*, 2006, Jansen, Gortan, Lens *et al.*, 2011, Zwieniecki *et al.*, 2001). This hypothesis seems questionable in the light of some previous findings (Nardini, Gasco, Cervone *et al.*, 2007) and my current results showing that homogalacturonans are restricted to a very limited region of the pit membrane (Chapter 4, Chapter 5). Indeed, alternative hypotheses to explain ion-mediated increases in xylem conductivity have been recently offered (Espino & Schenk, 2011, van Doorn, Hiemstra & Fanourakis, 2011). While van Doorn *et al.* (2011) suggested that the ion-mediated changes in conductivity may be linked with polyelectrolyte properties of other cell wall polymers such as lignin and hemicelluloses, Espino and Schenk (2011) highlighted potential methodological problems with the hydraulic measurements.

More research on the chemical composition of pit membranes is clearly required. Further studies examining pit membrane chemistry in a broad array of species with a wide taxonomical and ecological coverage should be conducted. Differences in the membrane chemical composition can be anticipated considering the conspicuously different appearance of membranes in different species (Jansen *et al.*, 2009, Schmitz, Koch, Schmitt *et al.*, 2008). Immunolabeling and specialized histological methods, such as ruthenium red staining or antimonate precipitation techniques (Chapter 5), carried out at the electron microscopy level represent powerful ways to examine the chemical composition of pit membranes. In addition, modern imaging methods such as atomic force microscopy (Pesacreta, Groom & Rials, 2005), Fourier transform infrared spectroscopy (Gorzsas, Stenlund, Persson *et al.*, 2011) and UV microspectrophotometry (Schmitz *et al.*, 2008) might be extremely useful as soon as reliable protocols for sample preparation are developed.

If pectic homogalacturonans are not abundant in pit membranes of (at least) some species, then what are the main components of the membrane matrix? Pectins other than homogalacturonans, hemicelluloses and lignins are obvious candidates (van Doorn *et al.*, 2011). Using immuno-gold labeling, I detected a weak and variable signal for rhamnogalacturonan I (pectin) and xyloglucan (hemicellulose) in some pit membranes (Chapter 5), indicating that these polymers might be present. However, more research corroborating these findings is needed. In addition, a future study investigating the distribution of cell wall proteins would be very interesting. To my knowledge, there is only one study demonstrating that cell wall proteins are present in the pit membranes of tomato plants (Harrak, Chamberland, Plante *et al.*, 1999). Structural proteins are

important for the mechanical properties of cell walls (Cosgrove, 1999, Lamport, Kieliszewski, Chen *et al.*, 2011). Hence, they may also influence the stretching and deflection of pit membranes.

6.4.2 Structural properties of pits

Aside from their chemical composition, the structural properties of pit membranes may also substantially influence the cavitation threshold. It is likely that thinner and more porous pit membranes are more susceptible to air-seeding. In Chapter 3, I showed that pit membranes in shaded poplar saplings were significantly thinner than in control plants grown under full-light conditions. The thinner membranes of shaded plants also showed increased porosity when water-dried wood samples were used to carry out the porosity measurements. These differences in pit membrane structure might provide an explanation for the greater vulnerability of shaded plants. My results clearly demonstrate that pit membrane structure changes in response to growing conditions. However, more research is needed to test whether differences in the thickness and porosity of pit membranes always result in altered xylem vulnerability, or whether additional mechanisms influence vulnerability at the intraspecific level.

Future studies could also assess pit border geometry in addition to measurements conducted on the pit membranes. Differences in pit border geometry translating into shallower or deeper pit chambers have recently been linked with differences in xylem vulnerability at the interspecific level (Hacke & Jansen, 2009, Lens, Sperry, Christman *et al.*, 2011), suggesting that the pit chamber depth affects vulnerability by controlling pit membrane deflection. It is possible that the secondary cell wall deposition during pit border formation is relatively easily modified by external and internal factors. Indeed, the secondary cell wall deposition underlying overall vessel wall thickness is highly variable and responsive to growing conditions (Fichot *et al.*, 2010, Junghans, Polle, Duchting *et al.*, 2006).

In Chapter 2, a very tight correlation between P50 and wood density was shown. This finding is consistent with similar results obtained from interspecific comparisons (Hacke, Sperry, Pockman *et al.*, 2001a, Jacobsen, Agenbag, Esler *et al.*, 2007). Such a strong association between these two traits is rather surprising considering their seemingly unrelated underpinnings. While xylem vulnerability is presumably determined by pit membrane permeability to air, wood density is mainly driven by the structural properties of xylem fibers. It has been proposed

that strong mechanical reinforcement is required to prevent the implosion of xylem conduits (Hacke *et al.*, 2001a). According to this hypothesis, cavitation resistant plants that experience highly negative xylem pressures tend to have thicker cell walls in order to prevent conduit collapse. In contrast, strong vessel reinforcement is not needed in vulnerable species because their conduits cavitate before reaching a xylem pressure capable of inducing vessel implosion. Such reasoning may explain the association between xylem mechanical strength and cavitation resistance on an evolutionary scale.

However, the close association between P50 and wood density found in my study using a single clone of hybrid poplar (Chapter 2) may suggest a more direct link between these two traits. First, it is possible that primary and secondary cell wall thickness are correlated, and because primary cell wall thickness translates into pit membrane thickness, this relationship could result in a correlation between wood density and P50. Some support for such an explanation has been provided at the interspecific level (Jansen *et al.*, 2009). Alternatively, I hypothesize that the mechanical support measured by wood density could be proportional to the probability of pit membranes suffering irreversible damage. Delicate pit membranes may be prone to tearing if pit fields are not sufficiently stabilized by a strong cell wall. r-shaped vulnerability curves measured in the distal segments of fertilized plants support this hypothesis. r-shaped curves have been previously measured for drought-stressed (Hacke, Stiller, Sperry *et al.*, 2001b) and senescent poplar xylem (Sperry, Perry & Sullivan, 1991) in which pit membrane damage was expected or even documented by SEM (Sperry *et al.*, 1991). In order to study the structural basis of the high vulnerability observed in distal stem segments, I examined their xylem under SEM; however, I could not detect any intact pit membranes. The observation that the majority of pit membranes were damaged in the distal segment is likely an artifact associated with sample preparation; however, it also highlights the fragile nature of pit membranes and the fact that strong mechanical reinforcement from the bulk xylem tissue is important to prevent their damage. While preparing the samples for SEM observations, I noticed that the wood specimens curled and deformed as the samples were drying out, which likely caused the pit membranes to rupture. This situation observed during sample dehydration is an extreme and artificial case. Nonetheless, it is possible that the integrity of pit membranes can be, to a certain extent, compromised by natural mechanical perturbations such as wind, hail or herbivore attack. A future study examining pit membranes in species that characteristically show r-shaped vulnerability curves (e.g., oak, grape vine) would

be interesting. Such work could test whether there is an increased number of membranes that appear torn or contain extremely porous regions. More broadly, further research is needed to determine whether leaky pits are intrinsic developmental mistakes (Jansen, Lamy, Burlett *et al.*, 2012) or whether they result from induced damage (Sperry *et al.*, 1991).

Taken together, my findings contribute to a growing body of literature linking qualitative characteristics of intervessel pits with cavitation resistance. In order to explain differences in cavitation resistance, more emphasis has previously been placed on quantitative parameters of intervessel pitting such as the total pit membrane area per vessel (Hargrave, Kolb, Ewers *et al.*, 1994, Wheeler, Sperry, Hacke *et al.*, 2005). However, it now becomes increasingly apparent that the differences in pit porosity, thickness and chemical composition are equally, if not even more, important (Jansen *et al.*, 2009, Lens *et al.*, 2011). A number of noteworthy studies on pits (e.g., Christman, Sperry & Adler, 2009, Christman, Sperry & Smith, 2012, Jansen *et al.*, 2009, Jansen *et al.*, 2011, Lens *et al.*, 2011, Pittermann, Choat, Jansen *et al.*, 2010) have been published over the course of my PhD program, indicating that it is a very timely and attractive topic. However, considerably more work will need to be done to fully understand these minute safety valves that are critical for preventing and mitigating the detrimental effects of xylem cavitation.

6.5 Conclusion and outlook

The research that I carried out during my PhD program has provided novel insight into the phenotypic plasticity of xylem traits and mechanisms that underlie drought-induced xylem cavitation. I demonstrated that xylem anatomy and hydraulic function in hybrid poplar saplings vary considerably in response to experimental drought, nitrogen fertilization and shading. Furthermore, I described patterns in gene expression associated with contrasting xylem phenotypes of fertilized versus control plants. This work expanded our understanding of molecular mechanisms that underlie xylogenesis. Finally, my work substantially enhances our knowledge of the structure and chemical composition of pit membranes, which is a prerequisite for deciphering how they function in preventing xylem cavitation and modifying hydraulic conductivity. The findings of my research have raised a number of interesting questions for future investigations.

Xylem is a fascinating and truly unique plant tissue, and the mechanisms of xylem transport are unparalleled in other biological transport systems. It is staggering to think about all the physical, anatomical and physiological features that enable the transport of large amounts of water under metastable conditions (Tyree, 2003a). Aside from the areas tackled in this thesis, a number of other unresolved issues in the area of long-distance xylem transport and wood physiology remain to be addressed. I have recently become intrigued with the living cells that are present in wood. Living parenchyma cells are intimately associated with xylem conduits and have several important and well recognized functions such as storage of carbohydrates, nitrogen compounds, water, and special defense metabolites (Evert, 2006, Spicer & Holbrook, 2007). Other functions, such as their involvement in the refilling of embolised conduits, are less understood despite their putative significance. In this thesis, I studied the conspicuous pits (Chapter 5) that occur at the interface between ray and vessel cells. The ultrastructure and chemical composition of vessel-ray pits may play an important role in the dynamics of refilling (Brodersen, McElrone, Choat *et al.*, 2010, Salleo, Lo Gullo, Trifilo *et al.*, 2004). I have shown that the membranes of vessel-ray pits are structurally and chemically very different from the extensively hydrolyzed intervessel pit membranes. In the future, I would like to study the role of living cells in xylem transport in more detail.

6.6 References

- Beikircher B. & Mayr S. (2009) Intraspecific differences in drought tolerance and acclimation in hydraulics of *Ligustrum vulgare* and *Viburnum lantana*. *Tree Physiology*, **29**, 765-775.
- Blake T.J., Sperry J.S., Tschaplinski T.J. & Wang S.S. (1996) Water relations. In: *Biology of Populus and its implications for management and conservation* (eds R.F. Stettler, H.D. Bradshaw, P.E. Heilman, & T.M. Hinckley), pp. 401-442. NRC Research Press, National Research Council of Canada, Ottawa, ON.
- Bonan G.B. (2008) Forests and climate change: Forcings, feedbacks, and the climate benefits of forests. *Science*, **320**, 1444-1449.
- Brodersen C.R., McElrone A.J., Choat B., Matthews M.A. & Shackel K.A. (2010) The dynamics of embolism repair in xylem: In vivo visualizations using high-resolution computed tomography. *Plant Physiology*, **154**, 1088-1095.
- Choat B., Cobb A.R. & Jansen S. (2008) Structure and function of bordered pits: new discoveries and impacts on whole-plant hydraulic function. *New Phytologist*, **177**, 608-625.

- Christman M.A., Sperry J.S. & Adler F.R. (2009) Testing the 'rare pit' hypothesis for xylem cavitation resistance in three species of *Acer*. *New Phytologist*, **182**, 664-674.
- Christman M.A., Sperry J.S. & Smith D.D. (2012) Rare pits, large vessels and extreme vulnerability to cavitation in a ring-porous tree species. *New Phytologist*, **193**, 713-720.
- Cochard H., Hoelttae T., Herbette S., Delzon S. & Mencuccini M. (2009) New insights into the mechanisms of water-stress-induced cavitation in conifers. *Plant Physiology*, **151**, 949-954.
- Cosgrove D.J. (1999) Enzymes And Other Agents That Enhance Cell Wall Extensibility. *Annual Reviews of Plant Physiology and Plant Molecular Biology*, **50**, 391-417.
- Crick J.C. & Grime J.P. (1987) Morphological plasticity and mineral nutrient capture in 2 herbaceous species of contrasted ecology. *New Phytologist*, **107**, 403-414.
- Espino S. & Schenk H.J. (2011) Mind the bubbles: achieving stable measurements of maximum hydraulic conductivity through woody plant samples. *Journal of Experimental Botany*, **62**, 1119-1132.
- Evert R.F. (2006) *Esau's Plant Anatomy: meristems, cells, and tissues of the plant body: their structure, function, and development*. (3rd ed.). John Wiley & Sons, Inc., New Jersey.
- Fichot R., Barigah T.S., Chamaillard S., Le Thiec D., Laurans F., Cochard H. & Brignolas F. (2010) Common trade-offs between xylem resistance to cavitation and other physiological traits do not hold among unrelated *Populus deltoides* x *Populus nigra* hybrids. *Plant, Cell and Environment*, **33**, 1553-1568.
- Fichot R., Chamaillard S., Depardieu C., Le Thiec D., Cochard H., Barigah T.S. & Brignolas F. (2011) Hydraulic efficiency and coordination with xylem resistance to cavitation, leaf function, and growth performance among eight unrelated *Populus deltoides*x*Populus nigra* hybrids. *Journal of Experimental Botany*, **62**, 2093-2106.
- Gasco A., Nardini A., Gortan E. & Salleo S. (2006) Ion-mediated increase in the hydraulic conductivity of Laurel stems: role of pits and consequences for the impact of cavitation on water transport. *Plant Cell and Environment*, **29**, 1946-1955.
- Gorzsas A., Stenlund H., Persson P., Trygg J. & Sundberg B. (2011) Cell-specific chemotyping and multivariate imaging by combined FT-IR microspectroscopy and orthogonal projections to latent structures (OPLS) analysis reveals the chemical landscape of secondary xylem. *Plant Journal*, **66**, 903-914.
- Grassein F., Till-Bottraud I. & Lavorel S. (2010) Plant resource-use strategies: the importance of phenotypic plasticity in response to a productivity gradient for two subalpine species. *Annals of Botany*, **106**, 637-645.
- Groover A.T. (2005) What genes make a tree a tree? *Trends in Plant Science*, **10**, 210-214.

- Hacke U.G. & Jansen S. (2009) Embolism resistance of three boreal conifer species varies with pit structure. *New Phytologist*, **182**, 675-686.
- Hacke U.G., Sperry J.S., Pockman W.T., Davis S.D. & McCulloh K.A. (2001a) Trends in wood density and structure are linked to prevention of xylem implosion by negative pressure. *Oecologia*, **126**, 457-461.
- Hacke U.G., Sperry J.S., Wheeler J.K. & Castro L. (2006) Scaling of angiosperm xylem structure with safety and efficiency. *Tree Physiology*, **26**, 689-701.
- Hacke U.G., Stiller V., Sperry J.S., Pittermann J. & McCulloh K.A. (2001b) Cavitation fatigue. Embolism and refilling cycles can weaken the cavitation resistance of xylem. *Plant Physiology*, **125**, 779-786.
- Hargrave K.R., Kolb K.J., Ewers F.W. & Davis S.D. (1994) Conduit diameter and drought-induced embolism in *Salvia mellifera* Greene (Labiatae). *New Phytologist*, **126**, 695-705.
- Harrak H., Chamberland H., Plante M., Bellemare C., Lafontaine J.G. & Tabaeizadeh Z. (1999) A proline-, threonine-, and glycine-rich protein down-regulated by drought is localized in the cell wall of xylem elements. *Plant Physiology*, **121**, 557-564.
- Herbette S. & Cochard H. (2010) Calcium is a major determinant of xylem vulnerability to cavitation. *Plant Physiology*, **153**, 1932-1939.
- Holste E.K., Jerke M.J. & Matzner S.L. (2006) Long-term acclimatization of hydraulic properties, xylem conduit size, wall strength and cavitation resistance in *Phaseolus vulgaris* in response to different environmental effects. *Plant Cell and Environment*, **29**, 836-843.
- Jacobsen A.L., Agenbag L., Esler K.J., Pratt R.B., Ewers F.W. & Davis S.D. (2007) Xylem density, biomechanics and anatomical traits correlate with water stress in 17 evergreen shrub species of the Mediterranean-type climate region of South Africa. *Journal of Ecology*, **95**, 171-183.
- Jansen S., Choat B. & Pletsers A. (2009) Morphological variation of intervessel pit membranes and implications to xylem function in angiosperms. *American Journal of Botany*, **96**, 409-419.
- Jansen S., Gortan E., Lens F., Lo Gullo M.A., Salleo S., Scholz A., Stein A., Trifilo P. & Nardini A. (2011) Do quantitative vessel and pit characters account for ion-mediated changes in the hydraulic conductance of angiosperm xylem? *New Phytologist*, **189**, 218-228.
- Jansen S., Lamy J.B., Burlett R., Cochard H., Gasson P. & Delzon S. (2012) Plasmodesmatal pores in the torus of bordered pit membranes affect cavitation resistance of conifer xylem. *Plant, Cell & Environment*, **35**, 1109-1120.
- Junghans U., Polle A., Duchting P., Weiler E., Kuhlman B., Gruber F. & Teichmann T. (2006) Adaptation to high salinity in poplar involves changes in xylem anatomy and auxin physiology. *Plant Cell and Environment*, **29**, 1519-1531.
- Lampert D.T.A., Kieliszewski M.J., Chen Y. & Cannon M.C. (2011) Role of the extensin superfamily in primary cell wall architecture. *Plant Physiology*, **156**, 11-19.

- Lamy J.-B., Bouffier L., Burlett R., Plomion C., Cochard H. & Delzon S. (2011) Uniform selection as a primary force reducing population genetic differentiation of cavitation resistance across a species range. *Plos One*, **6**, 1-12.
- Lens F., Smets E. & Melzer S. (2012) Stem anatomy supports *Arabidopsis thaliana* as a model for insular woodiness. *New Phytologist*, **193**, 12-17.
- Lens F., Sperry J.S., Christman M.A., Choat B., Rabaey D. & Jansen S. (2011) Testing hypotheses that link wood anatomy to cavitation resistance and hydraulic conductivity in the genus *Acer*. *New Phytologist*, **190**, 709-723.
- Maherali H., Pockman W.T. & Jackson R.B. (2004) Adaptive variation in the vulnerability of woody plants to xylem cavitation. *Ecology*, **85**, 2184-2199.
- Martinez-Vilalta J., Cochard H., Mencuccini M., Sterck F., Herrero A., Korhonen J.F.J., Llorens P., Nikinmaa E., Nole A., Poyatos R., Ripullone F., Sass-Klaassen U. & Zweifel R. (2009) Hydraulic adjustment of Scots pine across Europe. *New Phytologist*, **184**, 353-364.
- McDowell N., Pockman W.T., Allen C.D., Breshears D.D., Cobb N., Kolb T., Plaut J., Sperry J., West A., Williams D.G. & Yezzer E.A. (2008) Mechanisms of plant survival and mortality during drought: why do some plants survive while others succumb to drought? *New Phytologist*, **178**, 719-739.
- Nardini A., Gasco A., Cervone F. & Salleo S. (2007) Reduced content of homogalacturonan does not alter the ion-mediated increase in xylem hydraulic conductivity in tobacco. *Plant Physiology*, **143**, 1975-1981.
- Pesacreta T.C., Groom L.H. & Rials T.G. (2005) Atomic force microscopy of the intervessel pit membrane in the stem of *Sapium sebiferum* (Euphorbiaceae). *IAWA Journal*, **26**, 397-426.
- Pittermann J., Choat B., Jansen S., Stuart S.A., Lynn L. & Dawson T.E. (2010) The relationships between xylem safety and hydraulic efficiency in the Cupressaceae: The evolution of pit membrane form and function. *Plant Physiology*, **153**, 1919-1931.
- Rennenberg H., Wildhagen H. & Ehling B. (2010) Nitrogen nutrition of poplar trees. *Plant Biology*, **12**, 275-291.
- Salleo S., Lo Gullo M.A., Trifilo P. & Nardini A. (2004) New evidence for a role of vessel-associated cells and phloem in the rapid xylem refilling of cavitated stems of *Laurus nobilis* L. *Plant Cell and Environment*, **27**, 1065-1076.
- Schmitz N., Koch G., Schmitt U., Beekman H. & Koedam N. (2008) Intervessel pit structure and histochemistry of two mangrove species as revealed by cellular UV microspectrophotometry and electron microscopy: Intraspecific variation and functional significance. *Microscopy and Microanalysis*, **14**, 387-397.
- Schreiber S.G., Hacke U.G., Hamann A. & Thomas B.R. (2011) Genetic variation of hydraulic and wood anatomical traits in hybrid poplar and trembling aspen. *New Phytologist*, **190**, 150-160.

- Soolanayakanahally R.Y., Guy R.D., Silim S.N., Drewes E.C. & Schroeder W.R. (2009) Enhanced assimilation rate and water use efficiency with latitude through increased photosynthetic capacity and internal conductance in balsam poplar (*Populus balsamifera* L.). *Plant Cell and Environment*, **32**, 1821-1832.
- Sperry J.S. & Hacke U.G. (2002) Desert shrub water relations with respect to soil characteristics and plant functional type. *Functional Ecology*, **16**, 367-378.
- Sperry J.S., Perry A.H. & Sullivan J.E.M. (1991) Pit membrane degradation and air-embolism formation in ageing xylem vessels of *Populus tremuloides* Michx. *Journal of Experimental Botany*, **42**, 1399-1406.
- Sperry J.S. & Tyree M.T. (1988) Mechanism of water stress-induced xylem embolism. *Plant Physiology*, **88**, 581-587.
- Spicer R. & Groover A. (2010) Evolution of development of vascular cambia and secondary growth. *New Phytologist*, **186**, 577-592.
- Spicer R. & Holbrook N.M. (2007) Parenchyma cell respiration and survival in secondary xylem: does metabolic activity decline with cell age? *Plant Cell and Environment*, **30**, 934-943.
- Tuskan G.A., DiFazio S., Jansson S., Bohlmann J., Grigoriev I., Hellsten U., Putnam N., Ralph S., Rombauts S., Salamov A., Schein J., Sterck L., Aerts A., Bhalerao R.R., Bhalerao R.P., Blaudez D., Boerjan W., Brun A., Brunner A., Busov V., Campbell M., Carlson J., Chalot M., Chapman J., Chen G.-L., Cooper D., Coutinho P.M., Couturier J., Covert S., Cronk Q., Cunningham R., Davis J., Degroeve S., Dejardin A., dePamphilis C., Detter J., Dirks B., Dubchak I., Duplessis S., Ehlting J., Ellis B., Gendler K., Goodstein D., Gribskov M., Grimwood J., Groover A., Gunter L., Hamberger B., Heinze B., Helariutta Y., Henrissat B., Holligan D., Holt R., Huang W., Islam-Faridi N., Jones S., Jones-Rhoades M., Jorgensen R., Joshi C., Kangasjarvi J., Karlsson J., Kelleher C., Kirkpatrick R., Kirst M., Kohler A., Kalluri U., Larimer F., Leebens-Mack J., Leple J.-C., Locascio P., Lou Y., Lucas S., Martin F., Montanini B., Napoli C., Nelson D.R., Nelson C., Nieminen K., Nilsson O., Pereda V., Peter G., Philippe R., Pilate G., Poliakov A., Razumovskaya J., Richardson P., Rinaldi C., Ritland K., Rouze P., Ryaboy D., Schmutz J., Schrader J., Segerman B., Shin H., Siddiqui A., Sterky F., Terry A., Tsai C.-J., Uberbacher E., Unneberg P. (2006) The genome of black cottonwood, *Populus trichocarpa* (Torr. & Gray). *Science*, **313**, 1596-1604.
- Tyree M.T. (2003a) The ascent of water. *Nature*, **423**, 923-923.
- Tyree M.T. (2003b) Hydraulic limits on tree performance: transpiration, carbon gain and growth of trees. *Trees-Structure and Function*, **17**, 95-100.
- van Doorn W.G., Hiemstra T. & Fanourakis D. (2011) Hydrogel regulation of xylem water flow: an alternative hypothesis. *Plant Physiology*, **157**, 1642-1649.
- Wheeler E.A., Baas P. & Rodgers S. (2007) Variations in dicot wood anatomy: a global analysis based on the insidewood database. *IAWA Journal*, **28**, 229-258.

- Wheeler J.K., Sperry J.S., Hacke U.G. & Hoang N. (2005) Inter-vessel pitting and cavitation in woody Rosaceae and other vesselled plants: a basis for a safety versus efficiency trade-off in xylem transport. *Plant, Cell and Environment*, **28**, 800-812.
- Wikberg J. & Ögren E. (2007) Variation in drought resistance, drought acclimation and water conservation in four willow cultivars used for biomass production. *Tree Physiology*, **27**, 1339-1346.
- Zwieniecki M.A., Melcher P.J. & Holbrook N.M. (2001) Hydrogel control of xylem hydraulic resistance in plants. *Science*, **291**, 1059-1062.